

Descriptive Models, Grade-Tonnage Relations, and Databases for the Assessment of Sediment- Hosted Copper Deposits—With Emphasis on Deposits in the Central African Copperbelt, Democratic Republic of the Congo and Zambia



Scientific Investigations Report 2010–5090–J

This page intentionally left blank.

Global Mineral Resource Assessment

Michael L. Zientek, Jane M. Hammarstrom, and Kathleen M. Johnson, editors

Descriptive Models, Grade-Tonnage Relations, and Databases for the Assessment of Sediment-Hosted Copper Deposits—With Emphasis on Deposits in the Central African Copperbelt, Democratic Republic of the Congo and Zambia

By Cliff D. Taylor, J. Douglas Causey, Paul D. Denning, Jane M. Hammarstrom, Timothy S. Hayes, John D. Horton, Michael J. Kirschbaum, Heather L. Parks, Anna B. Wilson, Niki E. Wintzer, and Michael L. Zientek

Scientific Investigations Report 2010–5090–J

U.S. Department of the Interior

KEN SALAZAR, Secretary

U.S. Geological Survey

Suzette M. Kimball, Acting Director

U.S. Geological Survey, Reston, Virginia: 2013

For more information on the USGS—the Federal source for science about the Earth, its natural and living resources, natural hazards, and the environment—visit <http://www.usgs.gov> or call 1–888–ASK–USGS

For an overview of USGS information products, including maps, and publications, visit <http://www.usgs.gov/pubprod>

Suggested citation:

Taylor, C.D., Causey, J.D., Denning, P.D., Hammarstrom, J.M., Hayes, T.S., Horton, J.D., Kirschbaum, M.J., Parks, H.L., Wilson, A.B., Wintzer, N.E., and Zientek, M.L., 2013, Descriptive models, grade-tonnage relations, and databases for the assessment of sediment-hosted copper deposits—With emphasis on deposits in the Central African Copperbelt, Democratic Republic of the Congo and Zambia: U.S. Geological Survey Scientific Investigations Report 2010–5090–J, 154 p. and data files.

Any use of trade, firm, or product names is for descriptive purposes only and does not imply endorsement by the U.S. Government.

Although this information product, for the most part, is in the public domain, it also may contain copyrighted materials as noted in the text. Permission to reproduce copyrighted items must be secured from the copyright owner.

Contents

Abstract.....	1
Chapter 1. Overview of a New Descriptive Model for Sediment-Hosted Stratabound Copper Deposits.....	2
Introduction.....	2
Concise Description	2
Synonyms	2
Commodities (byproducts)	2
Importance.....	2
Associated Deposit Types.....	2
Ore System Components	2
Permissive Tract Delineation	3
Selected References.....	3
Detailed Description.....	3
Types of Sediment-Hosted Stratabound Copper Deposits	3
Global Distribution	3
Regional Geologic Setting and Age Distribution	3
Tectonic Settings	3
Depositional Environment	4
Age Range.....	4
Timing of Mineralization.....	4
Characteristics of Sediment-Hosted Stratabound Copper Deposits	4
Dimensions.....	4
Host Rocks	5
Structural Control	5
Ore Mineralogy.....	5
Ore Textures.....	5
Ore Mineral Zonation	5
Hypogene Gangue Minerals	13
Hypogene Alteration	13
Weathering and Supergene Ore	13
Geochemical Guides	13
Geophysical Guides.....	13
Genesis	14
Exploration and Resource Assessment Guides.....	14
Copper Source Rocks	14
Brines.....	14
Fluid Flow and Pathways	14
Organic Matter	15
Confining Beds and Containment Structures.....	15
Acknowledgments.....	15

Glossary.....	16
Chapter 2. Grade and Tonnage Relations for Sediment-Hosted Stratabound Copper Deposits.....	17
Introduction.....	17
Definition of SSC Deposit Types	17
Reduced-Facies—Nonbrecciated (n.b.) Deposits	19
Reduced-Facies—Carbonate Écaille Deposits	23
Sandstone Copper Deposits	23
Deposit Definition.....	23
Mineral Endowment	32
Cutoff Grade.....	32
Exploration	32
Spatial Rules for Aggregation.....	32
Data Quality Assessment.....	33
Exploratory Data Analysis	33
Grade and Tonnage Model for Sediment-Hosted Stratabound Copper Deposits.....	36
Grade and Tonnage Model for Sediment-Hosted Stratabound Copper Deposits in the Central African Copperbelt.....	36
Grade and Tonnage Model for Reduced-Facies—Nonbrecciated (n.b.) Deposits	36
Grade and Tonnage Model for Reduced-Facies—Carbonate Écaille Deposits.....	41
Grade and Tonnage Model for Sandstone Copper Deposits.....	44
Grade and Tonnage Model for Sandstone Copper—Roan Arenite.....	44
Missing Data.....	51
Silver	51
Cobalt.....	54
Relations Among Surface Area, Tonnage, and Contained Copper.....	55
Equations for Sandstone Copper Deposits.....	55
Equations for Reduced-Facies—Carbonate Écaille Deposits	55
Discussion and Conclusions	56
Acknowledgments.....	58
Chapter 3. Sediment-Hosted Structurally Controlled Replacement and Vein Copper Deposits in the Central African Copperbelt, Democratic Republic of the Congo and Zambia	60
Introduction.....	60
Concise Description	60
Commodities (byproducts)	60
Importance.....	60
Associated Deposit Types	63
Distribution.....	63
Age Range.....	63
Representative Deposits in the CACB	63
Kansanshi, Zambia.....	63
Kalengwa, Zambia	70
Dikulushi, DRC	70
Kikonkula, DRC	72

Kapulo Area, DRC.....	72
Frontier, DRC.....	72
Kipoi Project Area, DRC.....	74
Kipoi Central.....	74
Kileba	76
Lonshi, DRC.....	76
Tilwezembe, DRC.....	77
Other SCRV Deposits and Occurrences	77
Cashin, Colorado, United States.....	79
General Characteristics of SCRV Copper Deposits	81
Dimensions.....	81
Host Rocks	81
Ore Controls	81
Mineralogy.....	83
Alteration and Weathering.....	83
Geochemical Signature	83
Geophysical Signature.....	83
Genesis	83
Exploration and Resource Assessment Guidelines for SCRV Deposits	83
Grade and Tonnage Models for SCRV Deposits	84
Acknowledgments	84
References Cited (Chapters 1, 2, and 3).....	86
Appendix A. Relational Database of Sediment-Hosted Copper Deposits, Resources, and Production in the Central African Copperbelt, Democratic Republic of the Congo and Zambia	103
Introduction.....	103
Data Discussion and Methodology.....	103
Comparison of Total Endowment with Previously Published Values	108
Sources of Information	108
Database Design.....	108
Tables.....	109
Data Tables	109
Look-up Tables	113
Junction Tables	115
Internally Generated Table for Switchboard.....	115
Queries.....	115
Deposit_SumTons_qry Query	121
Deposit_TonsxGrade_qry Query	121
Deposit_SumGradexTons_qry Query	121
Deposit_WgtAvg_qry Query	121
Queries and Calculations Performed on Groups of Deposits.....	121
Group_SumTons_qry Query	121
Group_TonsxGrade_qry Query	128
Group_SumGradexTons_qry Query	128

Group_WgtAvg_qry Query	128
Queries Used to Provide Lists of References	128
DepRef_qry Query	128
ResRef_qry Query	128
Forms.....	128
Database Identification	128
Splashscreen Form.....	128
Switchboard Form	128
1_Deposittbl_frm Form.....	128
2_Resourcestbl_frm Form	128
Deposit_WgtAvg_qry_subform Form	128
Source Reference Forms.....	129
DepRef_MM_Subform Form and ResRef_MM_Subform form	129
Macros.....	129
Users' Guide.....	129
How to use the Access Database.....	129
Open Access Database	129
Browse Database	138
Identification Information in 1_Deposittbl_frm	139
Resource Information in 2_Resourcestbl_frm and 1_Deposits_frm	139
Reference Information	139
Calculating Resource Endowments.....	139
Print Records	139
Frequently Asked Questions (FAQs)	139
Acknowledgments	143
References Cited	144
Appendix B. Spatial Databases for Sediment-Hosted Stratabound and Structurally Controlled Replacement and Vein Copper Deposits and Prospects, Central African Copperbelt, Democratic Republic of the Congo and Zambia	145
Introduction.....	145
Overview of Spatial Databases	145
Deposits and Prospects.....	145
Ore Bodies.....	149
Open-Pit Mines.....	149
Acknowledgments	154
References Cited.....	154

Figures

1-1. Index maps showing the global distribution of sedimentary rocks hosting sediment-hosted stratabound copper deposits.....	6
1-2. Stratigraphic columns showing the position of reduced-facies type copper mineralization	8

1-3. Stratigraphic columns showing the position of sandstone-type copper mineralization	10
2-1. Distribution of log-transformed values for copper grade of sediment-hosted copper deposits.....	18
2-2. Chart illustrating the relations among types of sediment-hosted copper deposits.....	18
2-3. Variation in log ore, tonnage, and log copper grade by basin for reduced-facies copper deposits.....	20
2-4. Variation in log ore, tonnage, and log copper grade by basin for sandstone copper deposits	21
2-5. Distribution of log-transformed values of copper grade and ore tonnage between the sediment-hosted stratabound copper deposits in the Central African Copperbelt and all other areas in the world	22
2-6. Map showing the distribution of the Ore Shale Formation of the Roan Group in Zambia	24
2-7. Stratigraphic column of the Roan Group exposed in the Zambian portion of the Central African Copperbelt.....	25
2-8. Stratigraphic column of the Katangan system, illustrating the location of mineralized strata	26
2-9. Stratigraphic columns showing distribution of reduced-facies-carbonate écaïlle copper mineralization in the Mines Subgroup	27
2-10. Map and cross section of the Kamoto-Oliveira-Virgule (KOV) ore body	28
2-11. Map of the Tenke-Fungurume area showing exposures of Roan gigabreccia and megabreccia in the Central African Copperbelt.....	29
2-12. Stratigraphic column of the Roan Group exposed in the Zambian part of the Central African Copperbelt showing the stratigraphic distribution of reduced-facies (argillite-hosted and mixed argillite-arenite) and sandstone (arenite-hosted) mineralization	30
2-13. Distribution of distance and log (distance) between the edges of sediment-hosted copper ore bodies/open pits in the Central African Copperbelt.....	34
2-14. Bivariate plot of ore tonnage versus ore body area, projected to the surface.....	34
2-15. Bivariate plots of log copper grade versus log ore, in metric tons.....	35
2-16. Distribution of log-transformed values for tonnage, grade, and contained copper of 170 sediment-hosted stratabound copper deposits	39
2-17. Cumulative frequency plots of grade and tonnage for 170 sediment-hosted stratabound copper deposits	40
2-18. Distribution of log-transformed values for tonnage, grade, and contained copper of 77 sediment-hosted stratabound copper deposits in the Central African Copperbelt.....	42

2-19. Cumulative frequency plots of grade and tonnage for 77 sediment-hosted stratabound copper deposits in the Central African Copperbelt.....	43
2-20. Distribution of log-transformed values for tonnage, grade, and contained copper of 50 reduced-facies—n.b. copper deposits.....	44
2-21. Cumulative frequency plots of grade and tonnage for 50 reduced-facies—n.b. copper deposits	45
2-22. Distribution of log-transformed values for tonnage, grade, and contained copper of 50 reduced-facies—carbonate-écaille copper deposits.....	46
2-23. Cumulative frequency plots of grade and tonnage for 50 reduced-facies—carbonate-écaille deposits.....	47
2-24. Graph showing the variation of copper grade by year for 6 for sediment-hosted stratabound copper deposits in the Central African Copperbelt.....	48
2-25. Distribution of surface area of Roan gigabreccia fragments on the Likasi and Kolwezi geologic maps	49
2-26. Surface area of Roan gigabreccia fragments on the Likasi and Kolwezi geologic maps.....	49
2-27. Distribution of log-transformed values of ore tonnage, copper grade, cobalt grade, and contained copper of reduced-facies—carbonate écaille deposits in different tectonic settings, Central African Copperbelt.....	50
2-28. Distribution of log-transformed values for tonnage, grade, and contained copper of 70 sandstone copper deposits	51
2-29. Cumulative frequency plots of grade and tonnage for 50 sandstone deposits	52
2-30. Distribution of log-transformed values for tonnage, grade, and contained copper of 20 sandstone copper—Roan arenite deposits.....	53
2-31. Cumulative frequency plots of grade and tonnage for sandstone copper—Roan arenite deposits.....	53
2-32. Graphs showing the relative value of metal prices with time	54
2-33. Bivariate graphs of ore body area plotted against ore tonnage and contained copper metal for sediment-hosted stratabound copper deposits	56
2-34. Bivariate graphs of ore body area plotted against ore tonnage and contained copper metal for sandstone copper deposits.....	57
2-35. Bivariate graphs of ore body area plotted against ore tonnage and contained copper metal for reduced-facies—carbonate-écaille copper deposits.....	58
2-36. Box plots, normal quantile plots, and comparison circles for log-transformed values of ore, metric tons, copper grade, and contained copper illustrating differences between reduced facies—carbonate-écaille, reduced-facies—n.b., and sandstone copper deposits	59
3-1. Map showing the geology and major tectonic features of the Central African Copperbelt.....	61

3-2. Stratigraphic nomenclature and stratigraphy of the Katanga Supergroup throughout the Central African Copperbelt	62
3-3. Index map showing the distribution of structurally controlled replacement and vein deposits and prospects in the Central African Copperbelt	67
3-4. Kansanshi mine, Zambia	68
3-5. Map and cross-section of the Dikulushi structurally controlled replacement and vein deposit	71
3-6. Map showing location of deposits in the Kapulo area and their distribution along the Kapulo Fault	73
3-7. Simplified geological map of the Kipoi Central deposit	75
3-8. Geologic map of the Lonshi deposit	78
3-9. Generalized stratigraphic section of southeastern Utah and southwestern Colorado	80
3-10. Map showing fault patterns in the Cashin Mine area	81
3-11. Northwest-southeast cross section perpendicular to the Cashin Fault showing the distribution of copper	82
3-12. Distribution of log-transformed values for tonnage and copper grade for 11 structurally controlled replacement and vein copper deposits	85
3-13. Cumulative frequency plots of grade and tonnage for 11 structurally controlled replacement and vein copper deposits	85
A1. Relations among the 11 Access data tables	119
A2. List of tables in the database	120
A3. Deposit_SumTons_qry query design view and SQL	123
A4. Deposit_TonsxGrade_qry query design view and SQL	124
A5. Deposit_SumGradexTons_qry query design view and SQL	125
A6. Deposit_WgtAvg_qry query design view and SQL	126
A7. Group_SumTons_qry query design view and SQL	127
A8. Group_TonsxGrade_qry query design view and SQL	130
A9. Group_SumGradexTons_qry query design view and SQL	131
A10. Group_WgtAvg_qry query design view and SQL	132
A11. DepRef_qry query design view and SQL	133
A12. ResRef_qry query design view and SQL	134
A13. View of the splashscreen form	135
A14. View of the switchboard form showing data entry and query options	135
A15. Form view of the deposit data-entry form	136
A16. View of the resource data-entry form 2_Resourcestbl_frm	137
A17. View of the deposit tonnage and grade form, Deposit_WgtAvg_qry_subform	137
A18. View of the deposit references form DepRef_MM_Subform	137
A19. View of the resources references form ResRef_MM_Subform	138
A20. Design View of the macro Macro1	138
A21. Deposit entry form, 1_Deposittbl_frm	140
A22. Upper part of data entry form, 1_Deposit_frm	141
A23. Lower part of the main 1_Deposittbl_frm	141
A24. Record for the Konkola Deposit	142

B1. Map showing deposits, grouped deposits, ore bodies, and open pits in the northwestern part of the Central African Copperbelt in the Democratic Republic of the Congo.....	146
B2. Landsat image showing the areal extent of ore bodies and open pits in the northwestern part of the Central African Copperbelt in the Democratic Republic of the Congo	147
B3. Landsat image showing deposits, grouped deposit, and areal extent of ore bodies for the Konkola-Mutushi area in the Central African Copperbelt in the Democratic Republic of the Congo and Zambia	148

Tables

1-1. Copper minerals in sediment-hosted stratabound copper (SSC) deposits.....	4
1-2. Representative examples of sediment-hosted stratabound copper deposits.....	12
2-1. Tonnage and grade information for sediment-hosted stratabound copper deposits Title doesn't appear on file copy for this table (This table is on line only)	
2-2. Sediment-hosted stratabound copper deposits containing more than two million metric tons of copper.....	31
2-3. Summary statistics for sediment-hosted stratabound copper deposits.....	37
2-4. Goodness of fit statistics for sediment-hosted copper deposit types	38
2-5. Numbers of deposits reporting cobalt and silver, by deposit type.....	38
2-6. Summary of tonnage and grade distributions for sediment-hosted stratabound copper deposits recommendations for their use in resource modeling	41
2-7. Comparison of grades of oxidized ore formed on reduced-facies—carbonate <i>écaillé</i> subtype deposits mined early in the 20th century with grades reported for the same deposit area in this compilation.....	48
3-1. Selected characteristics of sediment-hosted copper deposits.....	64
3-2. Structurally controlled replacement and vein deposits in the Central African Copperbelt	66
3-3. Summary statistics for tonnage and grade of structurally controlled replacement and vein copper deposits	85
A1. Summary of grade, tonnage, and total endowment (pre-mining) of the sediment-hosted copper deposits of the Central African Copper and Vein	104
A2. Comparison of copper production and total copper endowment with previously reported values	109
A3. List and description of files in the database	110
A4. Source tables, queries, and fields for data displayed on the forms as well as any controls or type of data that should be entered	111

A5. Design and table structure of mineral deposits data table, 1_Deposittbl.....	112
A6. Design and table structure of mineral resources data table, 2_Resourcestbl	114
A7. Design and table structure of reference data table, 3_Referencetbl.....	114
A8. Structure and content of deposit-type look-up table, DepositType LU table	115
A9. Structure and content of deposit-subtype look-up table, DepositSubtype_LU	115
A10. Structure and content of the province and country look-up table, Province_LU	116
A11. Structure, content, and description of terms in the mineral resource categories look-up table, ResourceCat_LU	117
A12. Structure, content, and description of terms in the mineral resource standards look-up table, ResourceStd_LU	118
A13. Structure, content, and description of terms in the site activity look-up table, SiteActivity_LU.....	118
A14. Structure and content of the deposit reference junction table, DepRef_MM.....	119
A15. Structure and content of the resource reference junction table, ResRef_MM	119
A16. Structure and content of the Switchboard Items table.....	121
A17. List of queries and brief description of output and use in other queries	122
A18. Description of the forms in the Central African Copperbelt (CACB) database	129
A19. Description of operations that can be performed using the Switchboard form.....	129
B1. Description of digital data files for spatial databases (GIS)	149
B2. Examples of the types of sources used to compile the CACB_deposits_prospects shapefile	150
B3. Definitions of user-defined fields in the attribute table for the shapefile CACB_deposits_prospects	151
B4. Description of Katangan lithologies used in the “Unit” field.....	152
B5. Definitions of user-defined attribute fields in the shapefile CACB_orebodies.shp	153
B6. Definitions of user-defined attribute fields in the shapefile CACB_open_pits.shp.....	153

Conversion Factors

Inch/Pound to SI

Multiply	By	To obtain
Length		
inch (in.)	2.54	centimeter (cm)
inch (in.)	25.4	millimeter (mm)
foot (ft)	0.3048	meter (m)
mile (mi)	1.609	kilometer (km)
mile, nautical (nmi)	1.852	kilometer (km)
yard (yd)	0.9144	meter (m)
Area		
acre	4,047	square meter (m ²)
acre	0.4047	hectare (ha)
acre	0.4047	square hectometer (hm ²)
acre	0.004047	square kilometer (km ²)
square foot (ft ²)	929.0	square centimeter (cm ²)
square foot (ft ²)	0.09290	square meter (m ²)
square inch (in ²)	6.452	square centimeter (cm ²)
section (640 acres or 1 square mile)	259.0	square hectometer (hm ²)
square mile (mi ²)	259.0	hectare (ha)
square mile (mi ²)	2.590	square kilometer (km ²)
Mass		
ounce, avoirdupois (oz)	28.35	gram (g)
pound, avoirdupois (lb)	0.4536	kilogram (kg)
ton, short (2,000 lb)	0.9072	megagram (Mg)
ton, long (2,240 lb)	1.016	megagram (Mg)
ton per day (ton/d)	0.9072	metric ton per day
ton per day (ton/d)	0.9072	megagram per day (Mg/d)
ton per day per square mile [(ton/d)/mi ²]	0.3503	megagram per day per square kilometer [(Mg/d)/km ²]
ton per year (ton/yr)	0.9072	megagram per year (Mg/yr)
ton per year (ton/yr)	0.9072	metric ton per year

SI to Inch/Pound

Multiply	By	To obtain
Length		
centimeter (cm)	0.3937	inch (in.)
millimeter (mm)	0.03937	inch (in.)
meter (m)	3.281	foot (ft)
kilometer (km)	0.6214	mile (mi)
kilometer (km)	0.5400	mile, nautical (nmi)
meter (m)	1.094	yard (yd)
Area		
square meter (m ²)	0.0002471	acre
hectare (ha)	2.471	acre
square hectometer (hm ²)	2.471	acre
square kilometer (km ²)	247.1	acre
square centimeter (cm ²)	0.001076	square foot (ft ²)
square meter (m ²)	10.76	square foot (ft ²)
square centimeter (cm ²)	0.1550	square inch (in ²)
square hectometer (hm ²)	0.003861	section (640 acres or 1 square mile)
hectare (ha)	0.003861	square mile (mi ²)
square kilometer (km ²)	0.3861	square mile (mi ²)
Mass		
gram (g)	0.03527	ounce, avoirdupois (oz)
kilogram (kg)	2.205	pound avoirdupois (lb)
megagram (Mg)	1.102	ton, short (2,000 lb)
megagram (Mg)	0.9842	ton, long (2,240 lb)
metric ton per day	1.102	ton per day (ton/d)
megagram per day (Mg/d)	1.102	ton per day (ton/d)
megagram per day per square kilometer [(Mg/d)/km ²]	2.8547	ton per day per square mile [(ton/d)/mi ²]
megagram per year (Mg/yr)	1.102	ton per year (ton/yr)
metric ton per year	1.102	ton per year (ton/yr)

Temperature in degrees Celsius (°C) may be converted to degrees Fahrenheit (°F) as follows:

$$^{\circ}\text{F}=(1.8\times^{\circ}\text{C})+32$$

Temperature in degrees Fahrenheit (°F) may be converted to degrees Celsius (°C) as follows:

$$^{\circ}\text{C}=(^{\circ}\text{F}-32)/1.8$$

Vertical coordinate information is referenced to the World Geodetic System (WGS84).

Horizontal coordinate information is referenced to the World Geodetic System (WGS84).

Altitude, as used in this report, refers to distance above the vertical datum.

Acronyms and Abbreviations Used in This Report

A.D.	Anno Domini—a designation used to label or number years used with the Gregorian calendar.
ANOVA	analysis of variance
ASCII	American Standard Code for Information Interchange
B.C.	Before Christ—a designation used to label or number years used with the Gregorian calendar.
CACB	Central African Copperbelt
CRIRSCO	Committee for Mineral Reserves International Reporting Standards
DRC	Democratic Republic of the Congo
Esri	a software development and services company providing geographic information system software and geodatabase management applications
FAQ	frequently asked questions
g/t	grams per metric ton
Gécamines	La Générale des Carrières et des Mines, a state-owned mining company in the Democratic Republic of the Congo
GIS	geographic information system
GUI	graphical user interface
IOCG	iron oxide-copper-gold
Ma	mega-annum or millions of years before the present
MRDS	Mineral Resources Data System
SCRV	structurally controlled replacement and vein
SHRIMP	sensitive high-resolution ion microprobe
SQL	Structured Query Language
SSC	sediment-hosted stratabound copper
SSIB	small-scale digital internal boundaries
USGS	United States Geological Survey
UTM	Universal Transverse Mercator
$\delta^{13}\text{C}$	a measure of the ratio of stable isotopes ^{13}C : ^{12}C , reported in parts per thousand

Descriptive Models, Grade-Tonnage Relations, and Databases for the Assessment of Sediment-Hosted Copper Deposits—With Emphasis on Deposits in the Central African Copperbelt, Democratic Republic of the Congo and Zambia

By Cliff D. Taylor, J. Douglas Causey, Paul D. Denning, Jane M. Hammarstrom, Timothy S. Hayes, John D. Horton, Michael J. Kirschbaum, Heather L. Parks, Anna B. Wilson, Niki E. Wintzer, and Michael L. Zientek

Abstract

The Central African Copperbelt (CACB) is one of the most important copper-producing regions of the world. The majority of copper produced in Africa comes from this region defined by the Neoproterozoic Katanga sedimentary basin of the southern Democratic Republic of the Congo (DRC) and northern Zambia. Copper in the CACB is mined from sediment-hosted stratabound copper deposits associated with red beds and includes the giant deposits in the Kolwezi and Tenge-Fungurume districts in the DRC and the Konkola-Musoshi and Nchanga-Chingola districts in Zambia. In recent years, sediment-hosted structurally controlled replacement and vein (SCRV) copper deposits, such as the giant Kansanshi deposit in Zambia have become important exploration targets in the CACB region.

In 2011, the CACB accounted for 7.2 percent of the estimated global mine production of copper. Global production of copper is principally derived from porphyry and sediment-hosted copper deposits (57, and 23 percent, respectively). Almost 50 percent of the copper known to exist in sediment-hosted deposits (past production plus identified resources) is contained in the CACB, 25 percent is contained in the Zechstein Basin of northern Europe, and the remainder is contained in an additional 29 sedimentary basins distributed around the globe.

The U.S. Geological Survey (USGS) led an assessment of undiscovered copper resources in the CACB as part of a global mineral resource assessment for undiscovered resources of potash, copper, and platinum-group elements in selected mineral deposit types. As part of the assessment process, available data for the CACB were compiled

and evaluated. This report describes the results of that work, including new descriptive mineral-deposit and grade and tonnage models and spatial databases for deposits and occurrences, ore bodies and open pits.

Chapter 1 of this report summarizes a descriptive model of sediment-hosted stratabound copper deposits. General characteristics and subtypes of sediment-hosted stratabound copper deposits are described based upon worldwide examples. Chapter 2 provides a global database of 170 sediment-hosted copper deposits, along with a statistical evaluation of grade and tonnage data for stratabound deposits, a comparison of stratabound deposits in the CACB with those found elsewhere, a discussion of the distinctive characteristics of the subtypes of sediment-hosted copper deposits that occur within the CACB, and guidelines for using grade and tonnage distributions for assessment of undiscovered resources in sediment-hosted stratabound deposits in the CACB. Chapter 3 presents a new descriptive model of sediment-hosted structurally controlled replacement and vein (SCRV) copper deposits with descriptions of individual deposits of this type in the CACB and elsewhere. Appendix A describes a relational database of tonnage, grade, and other information for more than 100 sediment-hosted copper deposits in the CACB. These data are used to calculate the pre-mining mineral endowment for individual deposits in the CACB and serve as the basis for the grade and tonnage models presented in chapter 2. Appendix B describes three spatial databases (Esri shapefiles) for (1) point locations of more than 500 sediment-hosted copper deposits and prospects, (2) projected surface extent of 86 selected copper ore bodies, and (3) areal extent of 77 open pits, all within the CACB.

Chapter 1. Overview of a New Descriptive Model for Sediment-Hosted Stratabound Copper Deposits

By Michael L. Zientek, Timothy S. Hayes, and Jane M. Hammarstrom

Introduction

Sediment-hosted stratabound copper deposits that are associated with red beds have been mined since the 4th millennium B.C. in the Middle East (Weisgerber, 2006) and A.D. 1199 in the Kupferschiefer in central Europe (Beck, 1905, p. 492). At present, these deposits are mined in the Democratic Republic of the Congo and in Zambia, Poland, Kazakhstan, China, and the United States. The global distribution of sediment-hosted stratabound copper deposits and related sedimentary rocks are shown in figure 1-1.

Sediment-hosted stratabound copper deposits are the world's second most important source of copper (Cu), behind porphyry copper deposits, and account for more than 20 percent of the copper that has been discovered (Singer, 1995). Sediment-hosted stratabound copper deposits also represent the world's main source of cobalt (Co) production and rank third among all deposit types in silver (Ag) that has been discovered. Copper production from sediment-hosted stratabound copper deposits forms the basis of the economies of Poland, Zambia, and the Democratic Republic of the Congo (DRC).

This chapter is a brief overview of a mineral deposit model for sediment-hosted stratabound copper deposits that updates previous descriptive models for such deposits (Cox and others, 2003). The first descriptive model for this deposit type, then called "sediment-hosted Cu", was prepared by Cox (1986). This overview describes key attributes of the deposit type that are necessary for completing a mineral resource assessment, first in a concise format and then in greater detail.

Concise Description

Sediment-hosted stratabound copper mineralization consists of fine-grained copper- and copper-iron-sulfide minerals that occur as stratabound to stratiform disseminations in siliciclastic or dolomitic sedimentary rocks. Ore minerals occur as cements and replacements, and less commonly, as veinlets. The concentration of sulfide minerals conforms closely, but not exactly, with the stratification of the host rocks. Typically, the ore zones comprise chalcocite and bornite. These deposits are characterized by zoning of ore minerals laterally along and across bedding, from pyrite to chalcopyrite to bornite to chalcocite to hematite. Deposits are hosted in black, gray, green, or white (reduced) sedimentary strata within or above a thick section of red (oxidized) beds.

Synonyms

Continental red bed copper, copper-shale, Kupferschiefer-type copper, Mansfeld-type copper, marine paralic copper, red bed copper, reduced-facies copper, Revett copper, sandstone copper, sediment-hosted copper, sediment-hosted stratiform copper, shale-hosted copper, stratiform copper.

Commodities (byproducts)

Copper, silver (cobalt, lead, and zinc; rarely gold, platinum-group elements, uranium, and vanadium).

Importance

Sediment-hosted stratabound copper deposits account for approximately 20 percent of the world's past production and known resources of copper (Singer, 1995). Although such deposits are common throughout the world, economically significant deposits are rare (Hitzman and others, 2005).

Associated Deposit Types

Sediment-hosted stratabound copper deposits are transitional to volcanic red bed copper deposits (Kirkham, 1996b) and tabular sandstone-hosted uranium deposits. Genetically related deposit types include flood basalt-hosted native copper deposits as in the Keweenaw Native Copper District of northern Michigan (White, 1968), and massive carbonate replacement copper deposits at Kennecott, Alaska (MacKevett and others, 1997).

Spatially associated deposit types include evaporites, iron oxide-copper-gold (IOCG) deposits, sediment-hosted structurally controlled vein and replacement copper deposits, and Kipushi carbonate-hosted deposits (Cox and Burnstein, 1986).

Ore System Components

1. Source rocks for copper, typically oxidized (hematite-stable) siliciclastic sediment or mafic subaerial volcanic rocks.
2. Hematite-stable (oxidized) subsurface sedimentary brines capable of dissolving and transporting copper in solution.

3. The presence of brines moving generally in the direction of dewatering of a sedimentary basin.
4. Containment structures such as confining beds, stratigraphic pinchouts, and/or anticlinal traps.
5. A significant organic-rich sequence of sedimentary rocks capable of serving as an in situ reductant or of generating mobile reductants (natural gas, oil, and H_2S) that would cause the precipitation of copper from an oxidized subsurface sedimentary brine.

Permissive Tract Delineation

Mineral-resource-assessment geologists use descriptive information on ore deposit types to delineate areas, termed “permissive tracts,” in which the presence of as yet undiscovered deposits of a given type is possible. Each deposit type has certain fundamental characteristics related to ore system components that can be analyzed in concert with map data to define units that can in turn be used to delineate permissive tracts. The fundamental unit for delineation of a permissive tract for sediment-hosted stratabound copper deposits in a sedimentary basin is the presence of (1) a **flood-ing surface**¹ (typically a disconformity) that has carbonaceous and/or pyritic beds characteristic of a deeper water depositional environment, (2) reservoir facies rocks that contained trapped petroleum, or (3) fluvial reservoir facies rocks that contain detrital plant fragments that immediately overlie or are stratigraphically above and within 10 kilometers (km) from a section of sandy or grainy red beds, which are more than 300 meters (m) thick, from a fluvial or shallow-water depositional environment. Flood basalts may be associated with the red beds.

Selected References

Kirkham (1989); Brown (1997); Cox and others (2003); Hitzman and others (2005); Hitzman and others (2010).

Detailed Description

Sediment-hosted stratabound copper deposits are **pene-conformable** concentrations of copper minerals (table 1-1) in black, gray, green, or white sedimentary rocks within, or overlying, a succession of red beds that may be hundreds to thousands of meters thick. The disseminated copper minerals occur as cements and replacements, along with some veinlets. These deposits are characterized by zoning of the ore minerals laterally along and across bedding, from pyrite to chalcopyrite to bornite to chalcocite to hematite. Chalcocite and bornite typically comprise the ore zones; ores with

chalcopyrite as the major sulfide reach economic grades at places in the Central African Copperbelt (CACB).

Types of Sediment-Hosted Stratabound Copper Deposits

Host lithology and the nature of organic material in the host rock are used to distinguish three types of sediment-hosted stratabound copper deposits:

1. Reduced-facies copper deposits (Cox, 2003a): black to gray to green marine or lacustrine shale, siltstone, mudstone, or carbonaceous dolosiltstone/siliceous dolomite containing solid amorphous organic matter (fig. 1-2);
2. Sandstone copper deposits (Cox, 2003b): gray, well-sorted, fine- to coarse-grained sandstone which contained petroleum, probably as sour gas in most cases (fig. 1-3); and
3. Red bed copper deposits (Lindsey and Cox, 2003): gray, poorly to moderately sorted, commonly conglomeratic fluvial sandstone containing carbonized plant fragments ranging in size from silt to whole logs.

Representative examples of these types of deposits are listed and described in table 1-2.

Global Distribution

Sediment-hosted stratabound copper deposits have been found on every continent except Antarctica (fig. 1-1). Two areas, however, the Kupferschiefer in the Zechstein Basin in northern Europe and the CACB in the Katanga Basin in Zambia and the Democratic Republic of the Congo, account for more than 80 percent of the currently known resources in such deposits.

Regional Geologic Setting and Age Distribution

Tectonic Settings

Many of the largest sediment-hosted stratabound copper deposits are found in failed rifts that subsequently became major intracratonic basins, such as the Zechstein Basin in northern Europe and the Katanga Basin in central Africa (fig. 1-1; Hitzman and others, 2010). A few copper deposits of this type are found in other extensional settings, including trans-tensional and intermontane basins (Cox and others, 2003). Some are found within the bounds of a former intracratonic extensional basin but in coarse, **molassic** sedimentary host rocks deposited during or after the subsequent collisional stage of a complete **Wilson cycle** (Wilson, 1966; Cox and others, 2003). Intracontinental rift basins that formed within 20 to 30 degrees of the equator are ideal settings for sediment-hosted stratabound copper deposits because these basins contain thick packages of red beds that formed in hot dry climates, which also produce evaporites (Kirkham, 1989).

¹Words or phrases presented in this bold typeface are defined in the Glossary at the end of this chapter. Additional definitions of geologic terminology can be found in the American Geosciences Institute (AGI) Glossary of Geology online at <http://www.agiweb.org/pubs/glossary/>.

Depositional Environment

The stratigraphic record of rift basins records episodic pulses of extension that allowed sediment accumulation at fast rates followed by longer periods of tectonic quiescence when sediment supply exceeded subsidence (Martins-Neto and Catuneanu, 2010; Prosser, 1993). The early stage of rift initiation is represented by subaerial fluvial and alluvial deposits. These deposits are overlain by a major transgression (a flooding surface) that begins a depositional sequence that displays overall progradational trends and upward coarsening vertical stacking sequences (Martins-Neto and Catuneanu, 2010). Repeated episodes of extension will form vertically repeated cycles of a flooding surface overlain by a shale-turbidite sequence that grades upward into shallow water and coastal systems, which in turn grade upwards into alluvial facies (Martins-Neto and Catuneanu, 2010).

Host beds for many reduced-facies deposits occur at or just above the flooding surface that marks the transgression between an upward coarsening sag basin depositional sequence and underlying synrift, nonmarine red beds. Depositional environments that host reduced-facies mineralization above the transgressive surface include open-marine-shelf black shale, coastal sabkha deposits, and subtidal shelf carbonate rocks. Host rocks for sandstone copper deposits form in subtidal nearshore, beach, eolian, and fluvial settings, all of which make up the upper part of coarsening upwards depositional cycles. Mineralization is commonly found in well-sorted, fine- to coarse-grained, locally conglomeratic sandstone that exhibits cross bedding, parallel lamination, mud rip-up clasts, and ripple marks. The host rocks of red bed deposits are fluvial or, rarely, deltaic sandstones, which typically are conglomeratic, commonly with scour-and-fill features and cross bedding.

Age Range

Sediment-hosted stratabound copper deposits are limited to sedimentary or metasedimentary formations younger than 2,300 Ma, when free oxygen first appeared in Earth’s atmosphere (Bekker and others, 2004; Canfield, 2005), and the earliest red beds formed (Chandler, 1988; Bekker and others, 2005). Red bed deposits (Lindsey and Cox, 2003) are Silurian or younger, after vascular land plants first appeared.

Timing of Mineralization

The ages of the copper deposits are difficult to determine because of a lack of datable minerals that are related to the mineralizing event. Isotopic methods that have been applied include Re-Os dating of chalcopyrite and bornite, K-Ar dating of illite, and U-Pb dating of xenotime overgrowths on detrital zircon. Paleomagnetic dating of hematitic alteration (Rote Fäule of the Polish Kupferschiefer system) has also been attempted (Jowett and others, 1987; Nawrocki, 2000). Large uncertainties, inconsistencies, and large ranges of ages, as well as protracted or multistage ore-forming events,

Table 1-1. Copper minerals in sediment-hosted stratabound copper (SSC) deposits.

[Primary ore minerals are listed in order of decreasing copper oxidation state; *, most common minerals in SSC deposits]

Mineral	Formula
Primary copper ore minerals	
Chalcopyrite*	CuFeS ₂
Covellite	CuS
Bornite*	Cu ₅ FeS ₄
Anilite	Cu ₇ S ₄
Digenite	Cu ₉ S ₅
Djurleite	Cu ₃₁ S ₁₆
Chalcocite*	Cu ₂ S
Copper	Cu ^o
Primary copper-cobalt ore minerals	
Carrollite	Cu(Co,Ni) ₂ S ₄
Secondary copper minerals	
Cuprite	Cu ₂ O
Malachite*	Cu ₂ (CO ₃)(OH) ₂
Azurite	Cu ₃ (CO ₃) ₂ (OH) ₂
Chrysocolla	(Cu,Al) ₂ H ₂ Si ₂ O ₅ (OH) ₄ nH ₂ O
Planchéite	Cu ₈ Si ₈ O ₂₂ (OH) ₄ H ₂ O
Tenorite	CuO
Brochantite*	Cu ₄ (SO ₄)(OH) ₆

preclude precise dating of most deposits. Some, but not all, of the dating studies indicate that the age of mineralization postdates the deposition of the host rocks (Jowett and others, 1987; Nawrocki, 2000; Aleinikoff and others, 2012). This is consistent with petrologic and geochemical studies that indicate that ore deposition occurred during host rock diagenesis (Bartholomé, 1962; Brown, 1971; Hayes and Einaudi, 1986; Sweeney and Binda, 1989; Bechtel and others, 2001).

Characteristics of Sediment-Hosted Stratabound Copper Deposits

Dimensions

Lateral dimensions are large relative to deposit thickness, and deposit morphology varies by deposit type. Reduced-facies deposits have sheet-like geometry with lateral dimensions from hundreds to thousands of times greater than thicknesses. For example, strike lengths may be on the order of 3,000 to 5,000 m, widths from 500 to 2,000 m, and ore body thicknesses ranging from a few meters to 50 m. Sandstone copper deposits are tabular to lens-like; lateral dimensions are from 20 to 100 times their thicknesses. Red

bed copper deposits form lenses of copper-bearing rock. They are smaller than the other types of sediment-hosted stratabound copper deposits, with lengths and widths of a few tens of meters to a few hundred meters and typical thicknesses of ten meters or less. For all types of sediment-hosted stratabound copper deposits, bodies of mineralized rock typically are contained within a broader zone of anomalously high copper values (Lefebure and Alldrick, 1996). **Cutoff grades** are used to define ore bodies.

Host Rocks

Host rocks for reduced-facies deposits include black shale; dark gray to black siltstone; dark gray dolosiltstone, silty dolomite, and dolomite; gray shale; or locally, green shale or siltstone that contain solid organic material (various **macerals**) (Cox and others, 2003; Hitzman and others, 2005; Hitzman and others, 2010).

Sandstone copper deposit host rocks are typically well-sorted siliciclastic sandstones from a variety of deltaic topset environments. These rocks were probably reservoir rocks for petroleum when copper minerals were deposited. For many sandstone copper deposits, the petroleum was probably present as **sour gas** (Cox and others, 2003; Hitzman and others, 2005; Hitzman and others, 2010; Hayes and others, 2012).

Host rocks for red bed deposits are fluvial sandstone, commonly conglomeratic and containing carbonized vascular plant fragments (Cox and others, 2003).

Structural Control

Structural traps that enable the accumulation of hydrocarbons in sedimentary basins may also localize deposition of sediment-hosted copper mineralization. These include anticlines, and complex combination traps produced by pre-ore folding and faulting. Faults at high angles to the host beds are found at many sediment-hosted stratabound copper deposits. Evidence for syndepositional fault movement includes changes in net sand thickness across structures (Boleneus and others, 2005) or the offset of underlying red beds but not the slightly younger reduced-facies package (Kulick and others, 1986, p. 34; Selley and others, 2005, p. 972). Fold structures, some of which are fault- or salt-cored, localize sediment-hosted copper mineralization in the Chu-Sarysu (Syusyura and Tyugay, 2008) and Paradox (Hahn and Thorson, 2006) Basins.

Salt tectonics are associated with brine migration (Warren, 2000) and the development of structural traps that localize some sediment-hosted copper deposits such as at Canfield Creek, Maritimes Basin (O'Sullivan, 2006); and Blinman, Adelaide Geosyncline, South Australia (Selley, 2000; Dyson, 2004; Cowley and others, 2009). However, salt tectonics can disrupt earlier formed stratabound mineralization, such as the reduced-facies deposits associated with the Mines Subgroup of the CACB in the Katanga Basin (Jackson and others, 2003; François, 2006).

Ore Mineralogy

The principal copper ore minerals are chalcocite, bornite, and chalcopyrite; less common ore minerals include digenite, djurleite, covellite, sulfur-rich bornite=carrollite, Co-rich pyrite, and native silver. Pyrite is present in rocks outside the ore zones. Galena and sphalerite are found in the zones that separate copper ore from pyritic zones. Silver also may be present in solid solution in chalcocite, digenite, and/or bornite.

Uranium- and vanadium-oxide and silicate minerals may be present in some red bed deposits, for example, those in the Colorado Plateau region, United States. Uranium (U) in coffinite and vanadium (V) in illite or chlorite is typically present in pyritic assemblages (Brookins, 1976; Foster, 1959; Rackley, 1976; Riese, 1980). Uranium in uraninite and vanadium in montroseite are more typically found in chalcocite-bearing assemblages (Isachsen and Evenson, 1956; Evans, 1959; Trites and others, 1959).

Ore Textures

Copper sulfide minerals are fine grained and occur as disseminations concentrated along bedding, particularly the coarser grained fractions of the host rocks, and as intergranular cement interstitial to detrital silicates or carbonate **allochems** (Lefebure and Alldrick, 1996). Sharp-walled cracks or veinlets (< 1 centimeter, cm, thick; < 1 meter in length) of chalcopyrite, bornite, chalcocite, galena, sphalerite, or barite with quartz and/or calcite occur in some deposits, but are not an important component of the ore (Jowett, 1987; Lefebure and Alldrick, 1996). Pyrite can be **framboidal** or **colloform**.

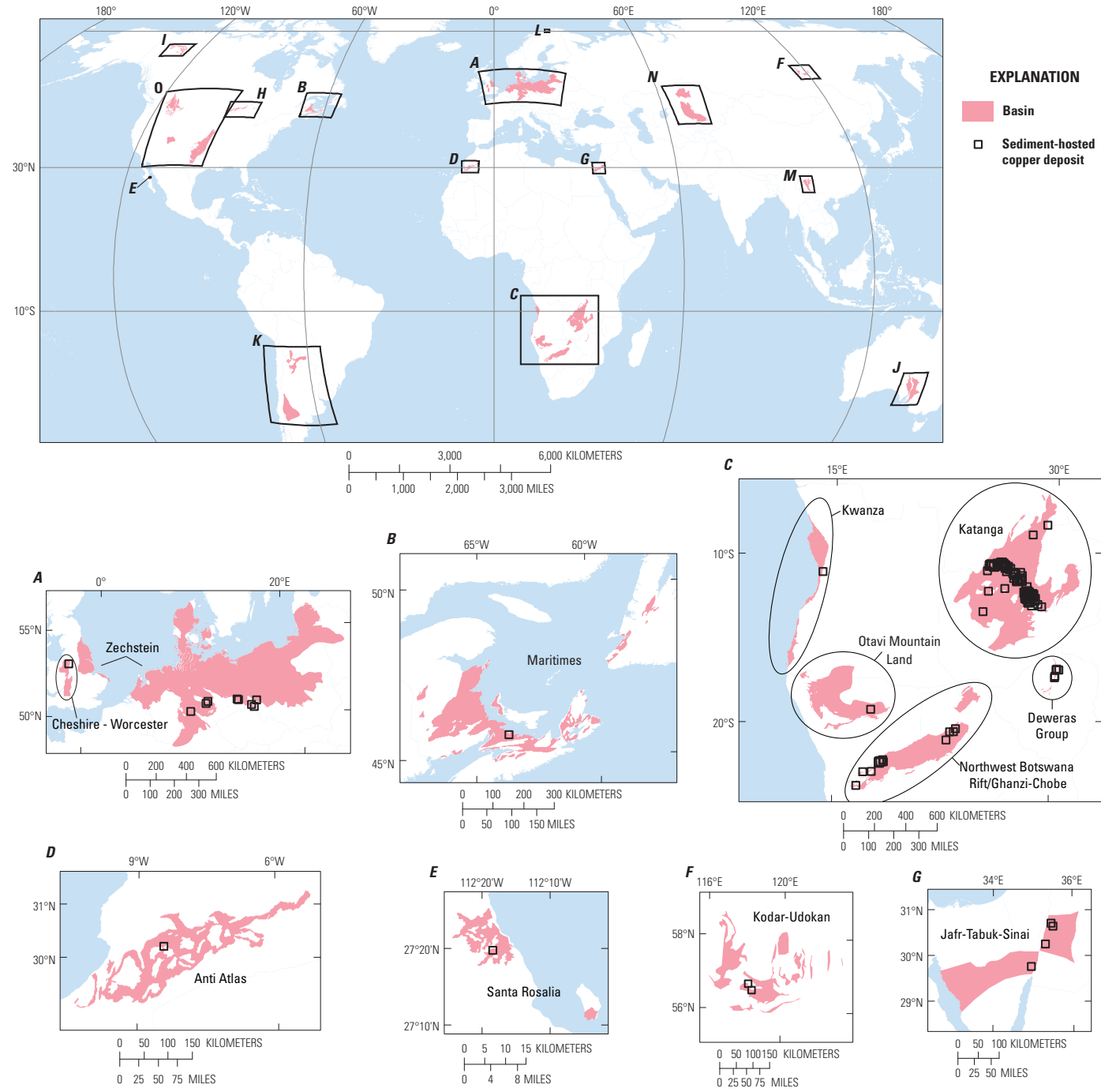
Copper sulfide minerals replace carbonaceous materials in the sedimentary host rocks at every scale. Where organic matter or organic carbon compounds were not directly replaced by the copper sulfides, the organic materials were altered both chemically and physically, by changing from predominantly **alginite** to bitumen, or by oxidizing to dissolved carbonate species and precipitating as carbonates.

Copper minerals also replace pre-ore diagenetic minerals in the host rocks, such as pyrite grains, framboids and nodules; in some host rocks, they form pseudomorphs of sulfate nodules or blade-shaped gypsum/anhydrite grains (Lefebure and Alldrick, 1996).

In unmetamorphosed sediment-hosted stratabound copper deposits, pyrite is replaced by chalcopyrite, which is replaced in turn by bornite, then by chalcocite. Further, pyrite is replaced by magnetite (rarely) or hematite (commonly).

Ore Mineral Zonation

Mineral zonation both laterally and vertically from pyrite to chalcopyrite to bornite to chalcocite to hematite is characteristic of reduced-facies and sandstone copper deposits. In many deposits, galena and sphalerite may occur with chalcopyrite or between the chalcopyrite and pyrite zones. The same minerals are found in red bed deposits, but with telescoped zonation.



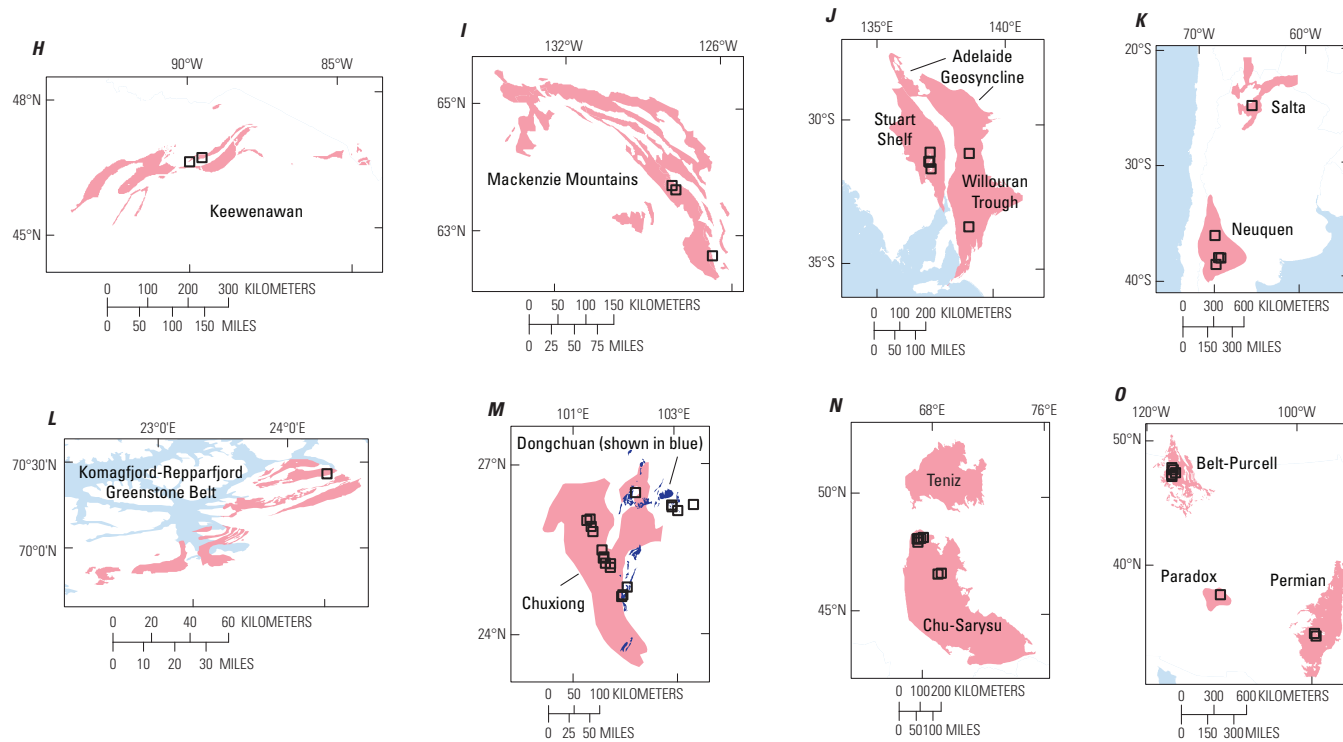


Figure 1-1. Index maps showing the distribution of sedimentary rocks hosting sediment-hosted stratabound copper deposits in basins discussed in chapters 1 and 2. (A) Extent of the Cheshire-Worcester Basin, United Kingdom, (Fugro Robertson, Ltd., 2008) and distribution of the Permian Zechstein Z1 unit in the Northern and Southern Permian Basins, northern Europe (Bavarian Geological State Office, 2004; Doornenbal and Stevenson, 2010; Federal Institute for Geosciences and Natural Resources, 1993; Vejrbæk and Britze, 1994; Zagorodnykh, 2000); (B) distribution of Paleozoic sedimentary rocks associated with the Maritimes Basin, Canada (Garrity and Soller, 2009); (C) extent of the Mesozoic Kwanza Basin (Fugro Robertson, Ltd., 2008), and distribution of Proterozoic sedimentary rocks associated with the Otavi Mountain Land, the Northwest Botswana Rift, the Katanga Basin, and the Dewaras Group, Africa (Andritzky, G., 1998; Haddon, 2001; Key, 1998; Laghmouch, 2008; Schreiber, 1980; Veselinovic-Williams and Frost-Killian, 2003 [2007]; Zimbabwe Geological Survey, 1985); (D) distribution of Paleozoic sedimentary rocks in the Anti Atlas Mountains, Morocco (Veselinovic-Williams and Frost-Killian, 2003 [2007]); (E) distribution of Cenozoic sedimentary rocks associated with the Santa Rosalia Basin, Mexico (Servicio Geológico Mexicano, 1997); (F) distribution of Proterozoic sedimentary rocks associated with the Kodar-Udokan trough, Russia (Konnikov and others, 1984; Lagzdina and others, 1978); (G) the extent of Cambrian carbonate-facies sedimentary rocks of the Araba, Burj, and Timna Formations in the Jafr-Tabuk-Sinai Basins, Egypt, Israel, and Jordan, extended to a depth of 2 kilometers (km) (Rybakov and Segev, 2004; Bender, 1975; Dardir, 1998; Guiraud, 1999; Khalifa and others, 2006; Klitzsch and others, 1987; Pollastro and others 1997; and Sneh and others 1998); (H) distribution of Proterozoic sedimentary rocks associated with the Keewenawan Rift, Canada and USA (Garrity and Soller, 2009); (I) distribution of Proterozoic sedimentary rocks associated with the Redstone Copperbelt, Mackenzie Mountains, Canada (Garrity and Soller, 2009); (J) distribution of Proterozoic sedimentary rocks associated with the Stuart Shelf and the Wilbourn Trough, Australia (Department of Primary Industries and Resources South Australia, 2006); (K) extent of the Mesozoic and Cenozoic Salta Basin (Marquillas and others, 2005) and Neuquen Basin, Argentina (Fugro Robertson, Ltd., 2008); (L) distribution of Proterozoic rocks associated with the Komagfjord-Repparfjord Greenstone Belt, Norway (NGU, written commun., 2006); (M) extent of the Mesozoic Chuxiong Basin (Fugro Robertson, Ltd., 2008) and distribution of Proterozoic sedimentary rocks associated with the Dongchuan area, China (Bureau of Geology and Mineral Resources of Yunnan Province, 1990); (N) extent of the Paleozoic and Mesozoic Chu-Sarysu and Teniz Basins, Kazakhstan (Fugro Robertson, Ltd., 2008); and (O) distribution of the sedimentary rocks associated with the Paleozoic Permian Basin (Garrity and Soller, 2009) and Proterozoic Belt-Purcell Basin (Garrity and Soller, 2009) and the extent of the Paleozoic and Mesozoic Paradox Basin (American Association of Petroleum Geologists, 1996).

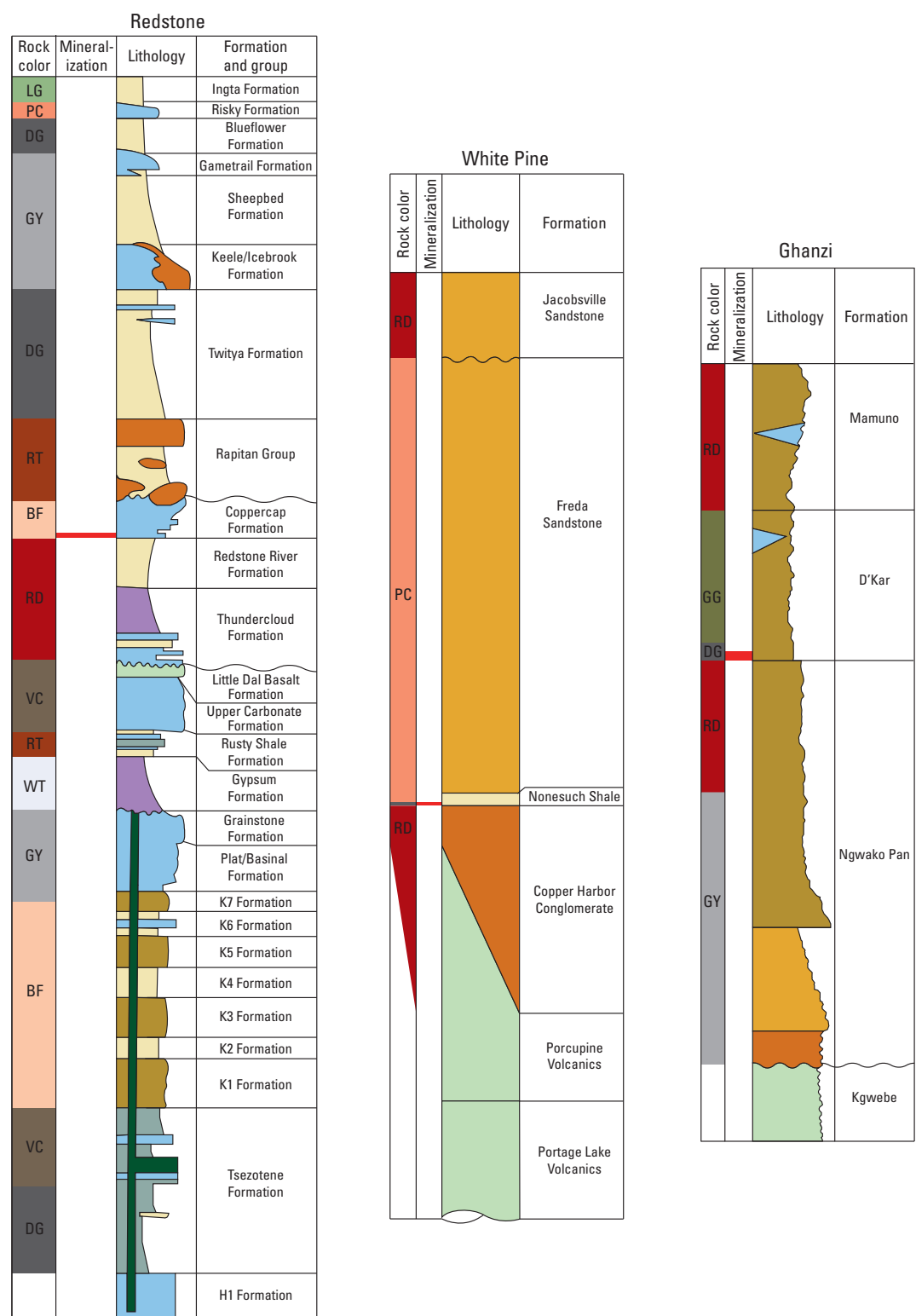


Figure 1-2. Stratigraphic columns showing the position of reduced-facies type copper mineralization in the Redstone Copper Belt, Mackenzie Mountains, Canada (Rainbird and others, 1996); the White Pine area, Keweenawan Rift, United States (Nicholson and others, 1997); the Ghanzi area, Northwest Botswana Rift, Botswana (Kampunzu and others, 1998); the Kupferschiefer, Zechstein Basin, Poland (Nawrocki, 1997); the Cuanza Basin, Angola (Brognon and Verrier, 1966), and the Central African Copperbelt (CACB), Democratic Republic of the Congo (François, 2006) and Zambia (Selley and others, 2005).

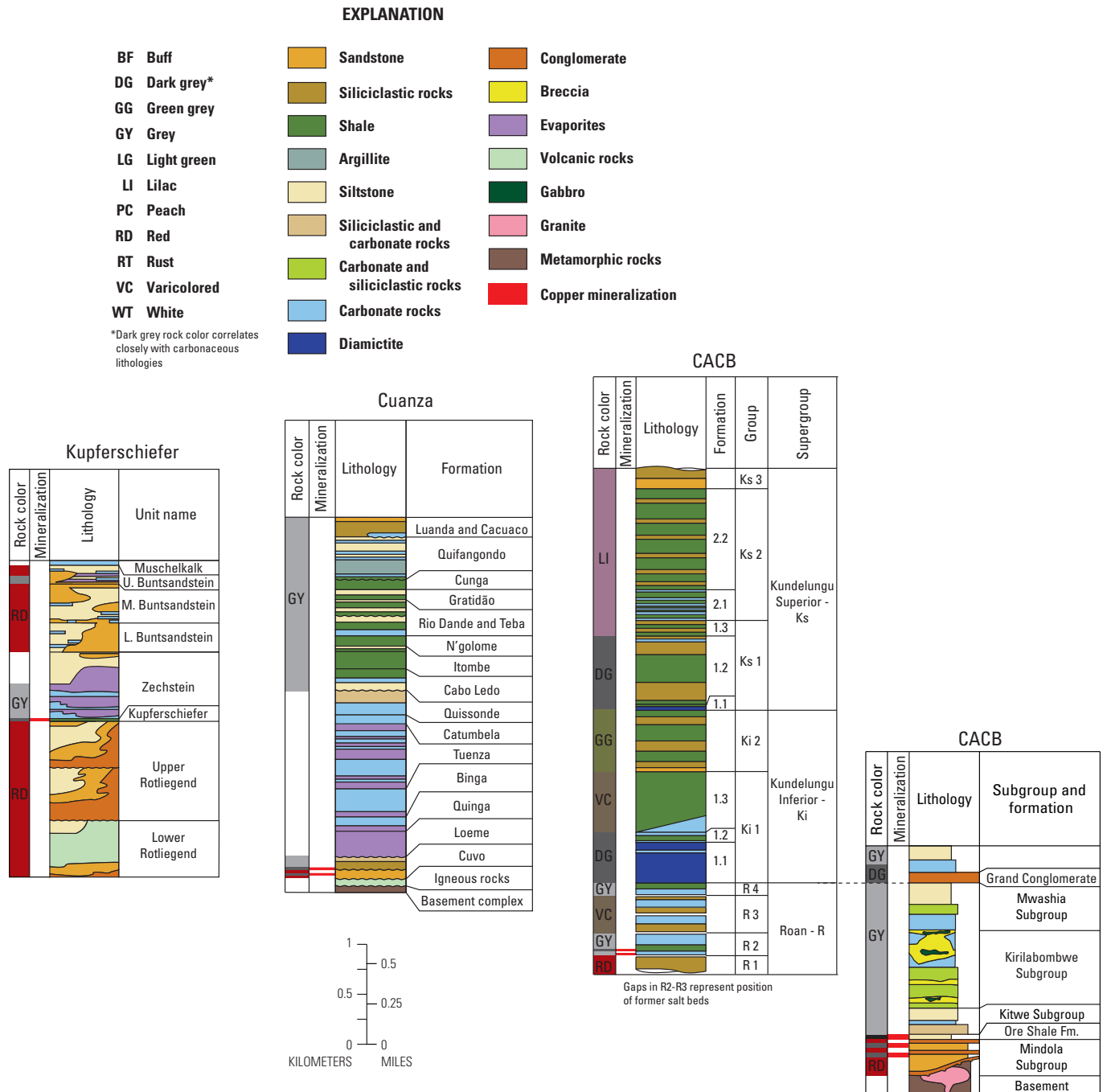


Figure 1-2.—Continued

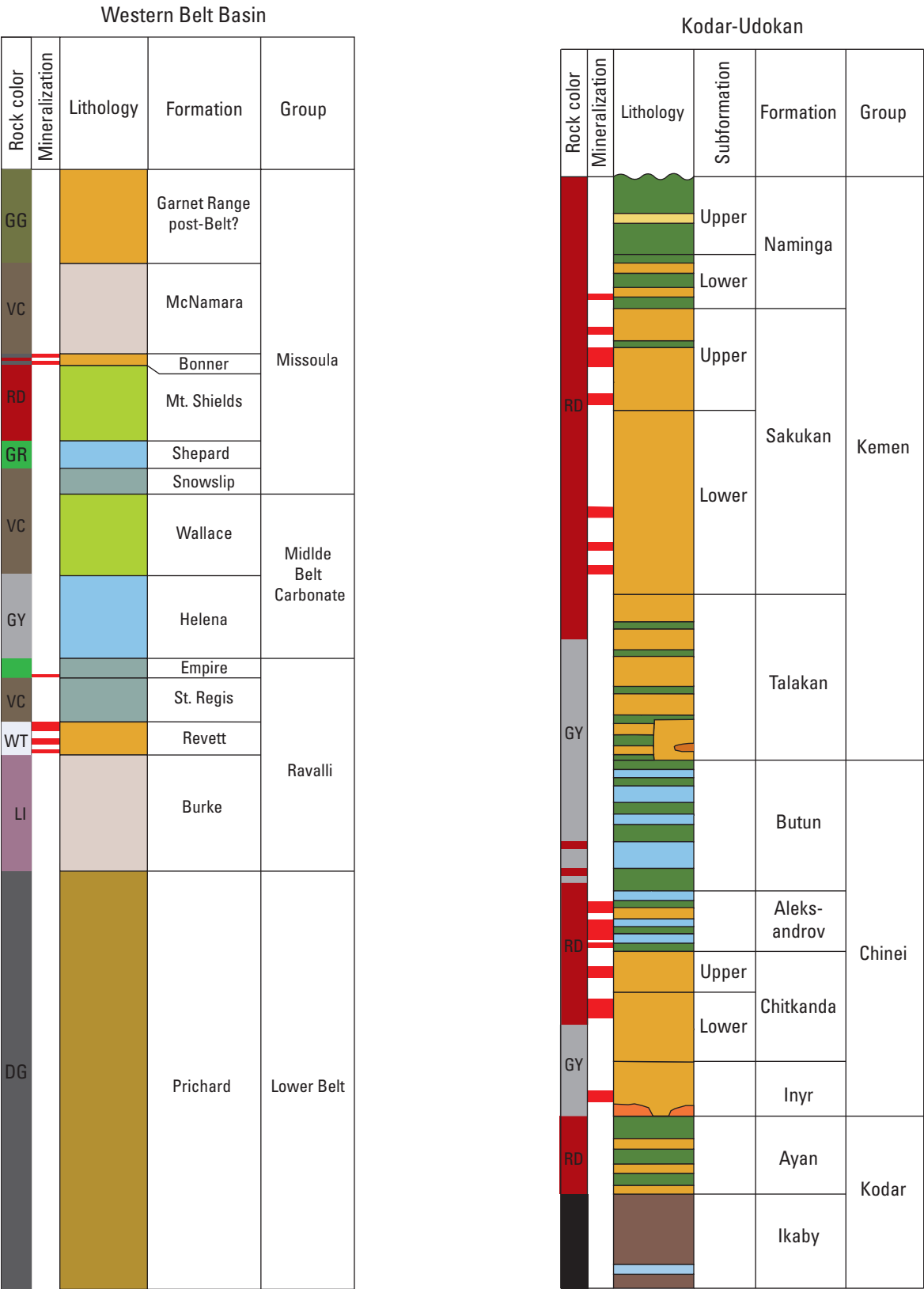
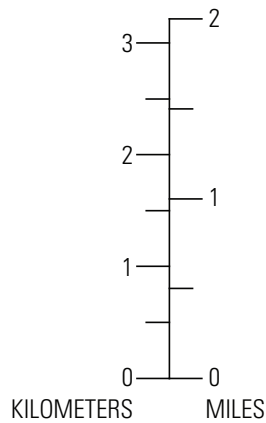


Figure 1-3. Stratigraphic columns showing the position of sandstone-type copper mineralization in the Belt Basin, United States (Cressman, 1990); the Kodar-Udokan area, Russia (Bogdanov and others, 1966); and the Chu-Sarysu Basin, Kazakhstan (Box and others, 2012).



EXPLANATION















DG	Dark grey		Sandstone		Evaporites
GG	Green grey		Siliciclastic rocks		Volcanic rocks
GR	Green		Shale		Granite
GY	Grey		Argillite		Quartzite and argillite
LI	Lilac		Carbonate and siliciclastic rocks		Metamorphic rocks
RD	Red		Carbonates		Copper mineralization
VC	Varicolored		Conglomerate		Unconformity
WT	White				

Figure 1-3.—Continued

Table 1-2. Representative examples of sediment-hosted stratabound copper deposits.

[SSC, sediment-hosted stratabound copper; Mt, million metric tons; %, percent; g/t, grams per metric ton; Ma, mega-annum—a period of one million years; km, kilometers; *, grades for hand-sorted ore]

Name	Location	Subtype	Geologic setting	Age	Grade and Tonnage	Comment	References
Lubin-Sieroszowice (Malomice, Lubin, Sieroszowice, Polkowice, Rudna, Glogow Gleboki-Przemyslowy, Bytom Odrzanski, Retkow, Gaworzyce, Radwanice Zachod)	Poland	reduced-facies copper	Southern flank of the Zechstein Basin	Permian, probably 240±3.8 Ma in host rocks deposited from 258 to 260.4 Ma	3,612.5 Mt, 1.99% Cu, 56.5 g/t Ag	Lubin-Sieroszowice is the largest sediment-hosted stratabound copper deposit in the world.	Jowett (1987), Oszczepalski (1989), Michalik (2001), Nowak and others (2001), Bechtel and others (2002), Piestrzyński and others (2002), Oszczepalski and others (2002), Kirkham and Broughton (2005)
Kolwezi Klippe (Kamoto-KOV-Musonie-Mupine)	Democratic Republic of the Congo	reduced-facies copper	Lufilian Arc in Neoproterozoic Katangan (meta) sedimentary rocks	Neoproterozoic, probably 816±62 Ma in host rocks deposited between 893 and 746 Ma	416.2 Mt, 4.49% Cu, 0.39% Co	Probably supergene enriched. World's largest known resource of cobalt.	Demesmaecker and others (1963), Bartholomé (1974), Bartholomé and others (1976), Hoy and Ohmoto (1989), Cailteux and others (2005), Dewaele and others (2006), El Desouky and others (2009)
Creta	Oklahoma, United States	reduced-facies copper	Northern flank of the Permian Hollis Basin	Unknown; late Permian host rocks	5.4 Mt, 1.9% Cu, 5.5 g/t Ag	Creta is underlain by more than 1,000 m of Permian rock, mostly red beds.	Hagni and Gann (1976), Johnson (1976), Kidwell and Bower (1976), Lockwood (1972)
Udokan	Transbaikalia Russia	sandstone copper	Southern margin of the Archean Aldan Shield	Proterozoic	1,528 Mt, 1.45% Cu, 12.6 g/t Ag	Udokan is the second largest known sandstone copper deposit in the world	Bakun and others (1966), Bogdanov and others (1966), Volodin and others (1994), Abramov (2008), V. Chechetkin (oral commun., 2010)
Spar Lake (Troy mine)	Montana, United States	sandstone copper	Belt Basin	Proterozoic; 1409±8 Ma in host rocks deposited between 1468 and 1443 Ma	80.6 Mt, 0.63% Cu, 46 g/t Ag	Silver is present in solid solution in copper sulfide minerals. Unmetamorphosed analogue is the Dzhhezka-zgan district, Kazakhstan.	Hayes and Einaudi (1986), Hayes and others (1989), Hayes (1990), Boleneus and others (2005), Hayes and others (2012)
Juramento	Argentina	sandstone copper	Folded Mesozoic sediments in the foreland between the Andean continental arc and the Rio de la Plata craton	Unknown; late Cretaceous host rocks	44.7 Mt, 0.80% Cu, 21.8 g/t Ag	Similar deposits occur within Cretaceous sandstones in the Neuquén Basin, several hundred km south of Juramento.	Durieux and Brown (2007), Alexander Mining (2005)
Corocoro	Bolivia	red-bed copper	Bolivian altiplano between eastern and western Andean Cordillera. Intermontane basin in hyperarid climate	Unknown; middle Tertiary host rocks	7.8 Mt, 7.1% Cu, 106 g/t Ag *	Corocoro is best characterized example of more than 20 deposits and districts on a NNW trend of salt diapirs with related SSC deposits that extends for 200 km.	Singewald and Berry (1922), Ljunggren and Meyer (1964), Entwistle and Bouin (1955), Flint (1989), Cox and others (1992)
Nacimiento	New Mexico, United States	red-bed copper	Flank between the Nacimiento Precambrian-cored uplift and the San Juan Basin	Unknown; middle Triassic host rocks; likely pre-Tertiary	10.0 Mt, 0.67% Cu, 2.4 g/t Ag	Supergene malachite and chrysocolla cements form halos around sulfidized logs and other sulfides in very porous sandstones.	Lindgren and others (1910), Soulé (1956), Elston (1967), Woodward and others (1974)

Hypogene Gangue Minerals

Gangue minerals include the common rock-forming minerals that make up the siliciclastic and carbonate sedimentary rocks that host the sulfide mineralization. Gangue also includes ore-stage minerals that form cements and replacements of earlier detrital and cementing minerals. Examples include authigenic K-feldspar, chlorite, and hematite. Authigenic quartz, tourmaline, manganese carbonate or oxide minerals, and barite are common gangue minerals in some deposits.

Hypogene Alteration

The mineralogical and textural changes that result from rock-fluid interactions that form sediment-hosted stratabound copper deposits are similar to those produced by normal diagenesis in a sedimentary basin. The alteration involves the intergranular replacement of earlier detrital minerals or cements or the formation of mineral overgrowths and cements. As such, this “alteration” is not distinguished in appearance, unless it forms nearly total replacements of the other minerals of the rock or occurs in strongly disconformable bodies.

Where it has been studied, the volumes of altered rock that are part of the mineralizing system are large, extending tens of kilometers and possibly up to 100 km laterally, and commonly affecting greater than 1 km of sedimentary rock thickness (Hitzman and others, 2005; Hitzman and others, 2010).

Alteration gangue minerals of sediment-hosted stratabound copper deposits are zonally arranged, with their zone boundaries parallel to the zonation of sulfide minerals. Authigenic hematite lining and filling pores is present in chalcocite zones of most deposits. Authigenic K-feldspar occurs as overgrowths on pre-existing detrital K-feldspar grains and as cements and replacements in ore zones of some reduced-facies and sandstone copper deposits. Other sodium-rich alteration phases include the sodic amphibole riebeckite and sodium-sulfate minerals. Chlorite is found as an authigenic mineral in many deposits, commonly in association with copper sulfide minerals. Iron-rich and manganese-rich calcite cements are found within fringing pyritic zones of sandstone copper deposits at Spar Lake, Belt Basin, Montana, and Dzhezkazgan, Chu-Sarysu Basin, Kazakhstan (Hayes, 1984, 1990; Lur’ye and Gablina, 1972).

All mineral zones of sediment-hosted stratabound copper deposits contain leucoxene pseudomorphs of the ilmenite in exsolved ilmeno-magnetite or ilmeno-hematite of formerly detrital grains.

Weathering and Supergene Ore

Weathered surfaces of rocks containing sediment-hosted copper mineralization are commonly coated by oxidized copper and iron minerals. During weathering, primary copper sulfide minerals are changed to sulfates, oxides, carbonates,

or silicates. Oxidized copper and iron minerals include cuprite, malachite, azurite, chrysocolla, planch  ite, tenorite, native copper, brochantite, and limonite. Malachite is typically most abundant. However, hypogene mineral zonation will affect weathering products. For example, brochantite is found in many places instead of malachite in weathered zones of bornite- and chalcocite-bearing rock. In others, “beer-bottle” limonite pseudomorphs develop from primary copper sulfide minerals (chalcocite, digenite, bornite, or chalcopyrite), whereas brown earthy goethite pseudomorphs replace pyrite.

In most climates, copper remains fixed in the weathering zone and copper grades are not enriched by weathering processes. In some situations, however, copper released by weathering reactions can be reprecipitated as the sulfide minerals, chalcocite and covellite, where oxidized fluids developed by weathering encounter a reducing environment at or below the water table, creating a zone of supergene enrichment (Taylor, 2011).

Geochemical Guides

Metasomatic effects from sediment-hosted stratabound copper mineralizing systems can be documented on the basis of the major-element compositions of mineralized rocks and country rocks. Potassium and barium enrichment accompany copper deposition (Hayes, 1990; Sutton and Maynard, 2005). The altered hematitic source rocks associated with the Western Montana Copper Sulfide Belt show depletion of copper, sodium metasomatism, and extreme calcium leaching (Hayes, 1990).

Copper is an excellent pathfinder element in soils and stream sediment geochemical surveys in many different weathering and climatic conditions. Additional pathfinder elements are silver and cobalt; however, no cases of anomalous silver have been documented without anomalous copper. Other potentially anomalous elements associated with sediment-hosted stratabound copper deposits include lead, zinc, antimony, arsenic, mercury, barium, and rarely uranium, vanadium, molybdenum, selenium, and germanium.

Soil gas analysis for methane, hydrogen, sulfur dioxide, carbon disulfide, and mercury might be a powerful exploration tool for sandstone copper deposits, where oxidizing, metals-transporting brines mixed and reacted with hydrogen-sulfide (H_2S)-bearing natural gas (McCarthy and Reimer, 1986; Hayes and others, 2012).

Geophysical Guides

Geologic framework studies—Gravity, magnetic and electromagnetic surveys can be used to map basement topography, bedrock geology, and basin and subbasin margins. Seismic reflection or refraction surveys can identify basin and subbasin margins, anticlines, stratigraphic traps, and combination traps.

Alteration studies—In basins hosting major sediment-hosted stratabound copper deposits, significant fluid flow

occurred and should have produced mappable alteration effects. Remote sensing of colors using Landsat imagery or remote sensing of ferric oxides using Landsat, ASTER, or AVIRIS imagery can be used to map bleaching of red beds (Beitler and others, 2003).

Directly targeting mineralization—The sulfide minerals of sandstone copper deposits or metamorphosed reduced-facies deposits are mildly conductive and may be detected with induced polarization and resistivity surveys providing that the local section does not contain highly carbonaceous or pyritic shales (Lindsey and others, 1995).

Genesis

Sediment-hosted stratabound copper mineralization is derived from hydrothermal fluids generated during diagenesis and lithification in sedimentary basins. On the basis of ore and gangue mineral zoning and alteration, mineral paragenesis, fluid inclusion studies, and stable isotope geochemistry, the metal bearing fluids are low temperature (75–220 degrees Celsius, °C), hematite-stable (oxidized), chloride-rich, subsurface sedimentary brines. These brines leach copper and other metals from synrift red beds and mafic volcanic rocks. The brines move upward toward a hydrologic seal where the primary cause of base-metal sulfide precipitation is the reduction of sulfate in the brine by organic material for reduced-facies or red bed deposits or is direct precipitation by the sour gas hydrogen sulfide (H_2S) in sandstone copper deposits. Thermochemical sulfate reduction probably adds additional sulfides to all three sediment-hosted stratabound copper deposit types (Hoy and Ohmoto, 1989; Bechtel and others, 2001; Hayes and others, 2012).

Exploration and Resource Assessment Guides

The starting point for exploration and resource assessment of sediment-hosted stratabound copper deposits is recognition of a basin that contains both copper source rocks and suitable sedimentary host rocks. Factors critical to exploration and assessment are described below.

Copper Source Rocks

The basin must contain some minimum thickness, perhaps at least 300 m, of oxidized, hematite-stable, permeable source rocks with slightly elevated copper content, probably continental red beds. The nearly universal spatial association of sediment-hosted stratabound copper deposits with continental red beds indicates that these rocks are necessary for the formation of this deposit type. Continental red beds are first-cycle, immature sediments that are deposited under oxidizing conditions and owe their red coloration to the early diagenetic development of hematite (Metcalf and others, 1994). Copper in red beds may be adsorbed on goethite and hematite. Subaerial basaltic

or other mafic volcanic rocks are an alternative source of copper. The red bed and/or volcanic source rock may be distant from the site of ore deposition.

Brines

Hematite-stable (oxidized) subsurface sedimentary brines leach copper from labile detrital and authigenic minerals (for example, copper adsorbed onto iron-oxide coatings on detrital particles) during diagenesis. The association of sediment-hosted stratabound copper mineralization with basins that contain significant thickness (probably several hundred meters) of sulfate- and halite-bearing evaporites suggest that dissolution of evaporites may be part of the ore-forming process. Brines capable of dissolving and transporting copper in solution could be pore fluids developed within the basin (evolved seawater brines, residual bittern brines, brines from evaporite dissolution, aqueous fluids derived from dehydration reactions during diagenesis) or meteoric waters whose high salinities are generated through dissolution of evaporites (Hitzman and others, 2005). Relative to the copper mineralized unit, evaporites can occur down section within the red bed sequence or in overlying marine or lacustrine sequences. Evidence of occult evaporites may include concordant and cross-stratal megabreccia zones, diapiric structures, breccia-cored and breached anticlines, and the presence of chlorine-rich minerals such as chlorine-bearing illite or marialitic scapolite (Beales and Hardy, 1977; Michalik, 1997; Hitzman and others, 2005; Jackson and others, 2003).

Fluid Flow and Pathways

The basin must have undergone subbasin-scale fluid flow that allowed for partial to total evaporite dissolution, brine formation, and upwards cross-stratal brine migration. Possible causes for brine migration include compaction-driven fluid flow (Swenson and others, 2004), topographically driven fluid flow (White, 1971; Garven, 1985; Brown, 2005, 2009), thermohaline (buoyancy)-driven convection induced by salt dissolution (Evans and Nunn, 1989), and thermally driven free convection (Jowett, 1986; Cathles and others, 1993). Tectono-thermal events, such as the emplacement of magmatic rocks, halokinesis, and basin inversion, are capable of initiating convection of subsurface sedimentary brines (Hitzman and others, 2005), but time association with magmatic events has not been demonstrated for any sediment-hosted stratabound copper deposit.

A flow system for transport of copper from source rocks to host rocks by sedimentary brines must have existed. Various types of flow systems and hydrologic drivers may have served as transport avenues, but the aquifers, at the time of mineralization, would have been confined so that brines migrated upward relative to stratigraphy. Transport/migration of copper must occur under artesian heads (by confined aquifer flow), because in almost all cases where it has been possible to determine, the zoning and paragenesis indicate that copper-rich, hematite-stable brines have entered the host rocks from below. Synsedimentary and postdepositional

faults were probably critical for many systems in providing focused cross-stratal fluid flow (Hitzman and others, 2005).

Most reduced-facies copper deposits and many of the other two deposit types appear to have formed on basin edges or where irregularities in the geometry of the basin focused fluid flow through the red bed package and upward into the host beds. Such focusing could be due to thinning of the red bed sequence on a basin margin, faults, permeability contrasts within specific sedimentary units, paleotopography within the basin itself (for example, basement highs, and anticlines), or enhanced fluid flow along the margins of salt walls or diapirs as in the Paradox Basin (Hahn and Thorson, 2006) and in the CACB in the DRC (Jackson and others, 2003).

Patterns of alteration mark pathways of metalliferous brine migration (hematite, albite, riebeckite, sodium sulfate minerals, epidote in volcanic rocks, sodium- and chlorine-bearing illite). Hematite- and albite-rich assemblages found in the ore bodies may extend many kilometers into surrounding rock layers; altered rocks depleted in copper, where known, extend for kilometers from ore-bearing zones.

Burial histories derived from petroleum exploration with methods such as **Lopatin modeling** (Lopatin, 1971) can subdivide permissive tracts into more favorable and less favorable areas. Only those areas within and adjacent to parts of the tract that underwent rapid sedimentation, subsidence, and burial are considered favorable.

Organic Matter

The basin must contain some form of organic matter that acted as a reductant at the site of copper mineral deposition. Organic-rich, poorly permeable sedimentary beds characterize reduced-facies deposits. Permeable beds with carbonized plant fragments distinguish red bed deposits. The organic reductant in the sandstone-type deposits is thought to be a mobile reductant, or in other words, petroleum vapor or liquids that accumulated in reservoir (permeable) beds. Mobile reductants require source beds for hydrocarbons in the stratigraphic sequence and a basin history that allowed the maturation and migration of hydrocarbon fluids. Evidence for petroleum that previously charged

the permeable strata that host sandstone copper deposits includes petroleum-bearing fluid inclusions and dead oil that coats detrital grains, stains authigenic minerals, and may locally form cements.

Carbon isotope studies of ore-associated carbonate minerals from both reduced-facies deposits and sandstone copper deposits, include some quite low $\delta^{13}\text{C}$ values. The low- $\delta^{13}\text{C}$ carbonates reflect oxidation of solid organic matter or petroleum to provide C for deposition of the carbonates (Sweeney and Binda, 1989; Bechtel and others, 2001; Hitzman and others, 2005).

Confining Beds and Containment Structures

Containment structures, such as stratigraphic pinchouts and anticlinal features with confining beds, are required to focus fluid flow of the copper-bearing brines to rocks that contain organic material that will cause sulfide mineral precipitation.

For reduced-facies deposits, the confining beds could be the fine-grained, organic-rich sedimentary host rocks themselves (fig. 1-2). In other basins, confining beds could include evaporite layers or shales that overlie permeable units that could host sandstone copper deposits (fig. 1-3).

Many types of stratigraphic and structural traps that may accumulate hydrocarbons in sedimentary basins may also localize deposition of sediment-hosted copper mineralization. These include the onlap of favorable host rocks onto paleotopographic features (updip pinch-out stratigraphic trap), unconformity traps, facies changes, stratigraphic pinchouts, anticlines, and complex combination traps produced by pre-ore folding and faulting (Hitzman and others, 2005, 2010).

Acknowledgments

USGS colleagues James Bliss, Pamela Dunlap, and Daniel Mosier provided helpful and constructive technical reviews. Heather Parks, Cassandra Lindsey, and Hannah Campbell helped prepare illustrations.

Glossary

alginite Organic material, kerogen, of algal or bacterial origin.

allochem² A collective term introduced by Folk (1959, p. 4) for one of several varieties of discrete and organized carbonate aggregates that serve as the coarser framework grains in most mechanically deposited limestones, as distinguished from sparry calcite (usually cement) and carbonate-mud matrix (micrite). Important allochems include: silt-, sand-, and gravel-size intraclasts; ooids; pellets; lumps; and fossils or fossil fragments (carbonate skeletons, shells, and so on).

bitumen² A generic term applied to natural inflammable substances of variable color, hardness, and volatility, composed principally of a mixture of hydrocarbons substantially free from oxygenated bodies. Bitumens are sometimes associated with mineral matter, the nonmineral constituents being fusible and largely soluble in carbon disulfide, yielding water-insoluble sulfonation products. Petroleums, asphalts, natural mineral waxes, and asphaltites are all considered bitumens.

colloform² Said of the rounded, finely banded kidney-like texture formed by ultra-fine-grained rhythmic precipitation of minerals.

cutoff grade The lowest grade, or quality, of mineralized material that qualifies as economically mineable and available in a given deposit (Committee for Mineral Reserves and Reporting Standards, 2006).

flooding surface In sequence stratigraphy, a surface separating younger from older strata across which there is evidence of an abrupt increase in water depth. This deepening is commonly accompanied by minor submarine erosion or nondeposition. This is not accompanied by subaerial erosion due to stream rejuvenation or a basinward shift in facies, including abnormal subaerial exposure, with a minor hiatus indicated. The flooding surface has a correlative surface in the coastal plain and a correlative surface on the shelf (Van Wagoner and others, 1990).

flysch² A marine sedimentary facies characterized by a thick sequence of poorly fossiliferous, thinly bedded, graded deposits composed chiefly of marls and sandy and calcareous shales and muds, rhythmically interbedded with conglomerates, coarse sandstones, and graywackes.

framoid² A microscopic aggregate of pyrite grains in shale, often in spheroidal clusters resembling a raspberry. The texture is linked with the presence of organic materials; sulfide crystals fill chambers or cells in bacteria.

ture is linked with the presence of organic materials; sulfide crystals fill chambers or cells in bacteria.

kerogen² Fossilized insoluble organic material found in sedimentary rocks, usually shales, which can be converted to petroleum products by distillation.

Lopatin model An empirical relationship between vitrinite reflectance and petroleum formation developed by N.V. Lopatin (1971) to use both time and temperature to calculate the thermal maturity of organic matter in sediments.

maceral² One of the organic constituents that comprise the coal mass; all petrologic units seen in polished or thin sections of coal. Macerals are to coal as minerals are to inorganic rock. Maceral names bear the suffix “-inite” (vitrinite, liptinite, and so on).

molasse² A paralic (partly marine, partly continental or deltaic) sedimentary facies consisting of a very thick sequence of soft, ungraded, cross-bedded, fossiliferous conglomerates, sandstones, shales, and marls, characterized by primary sedimentary structures and sometimes by coal and carbonate deposits. It is more clastic and less rhythmic than the preceding flysch facies.

peneconformable Almost conformable. The adverb “pene” is Latin for almost, nearly, or practically.

salt tectonics Any tectonic deformation involving salt, or other evaporites, as a substratum or source layer (Jackson and Talbot, 1991).

sour gas Natural gas containing significant amounts of hydrogen sulfide.

stratabound² Said of a mineral deposit confined to a single stratigraphic unit. The term can refer to a stratiform deposit, to variously oriented ore bodies contained within the unit, or to a deposit containing veinlets and alteration zones that may or may not be strictly conformable with bedding.

stratiform² Said of a special type of *stratabound* deposit in which the desired rock or ore constitutes, or is strictly coextensive with, one or more sedimentary, metamorphic, or igneous layers; for example, beds of salt or iron oxide, or layers rich in chromite or platinum in a layered igneous complex.

Wilson cycle² A successive recurrence of plate-tectonic spreading and convergence with a period generally in the 100-million-year range. Named after J. Tuzo Wilson, Canadian geophysicist.

²American Geosciences Institute (AGI) Glossary of Geology online at <http://www.agiweb.org/pubs/glossary/>.

Chapter 2. Grade and Tonnage Relations for Sediment-Hosted Stratabound Copper Deposits

By Michael L. Zientek, Timothy S. Hayes, and Cliff D. Taylor

Introduction

The USGS methodology to assess undiscovered mineral resources has three essential parts: (1) frequency distributions of tonnages and average grades of well explored deposits that are used as grade and tonnage models of undiscovered deposits of the same type in geologically similar settings, (2) mineral resource maps that show tracts where geology permits the existence of deposits of one or more specified types, and (3) estimates of some fixed, but unknown, number of undiscovered deposits that exist in the delineated tracts (Singer, 1993; Singer and Menzie, 2010). This chapter describes grade and tonnage models developed for sediment-hosted stratabound copper (SSC) deposits.

Deposit models specific to mineral deposit types are an integral part of the assessment process because they summarize geologic criteria used for classifying the deposits by type and for delineating permissive geographic areas (tracts) for the occurrence of undiscovered deposits. Deposits of a given type have characteristic sizes and grades that can be expressed as frequency distributions of tonnage and average grade on the basis of thoroughly explored examples of each type of mineral deposit. These grade and tonnage models can be illustrated with cumulative frequency plots, as well as with histograms, quantile box plots, and normal quantile plots (fig. 2-1). The grade and tonnage distributions of known deposits are used to constrain the probable size and grade of undiscovered deposits of the same type—undiscovered deposits are expected to be comparable to those in the grade and tonnage model for the deposit type.

Grade and tonnage models for various types of SSC deposits have been previously published. Mosier and others (1986) used data for 57 deposits to create a tonnage and grade model for sediment-hosted copper (equivalent to SSC deposits as used in this report). The descriptive (Cox, 2003c) and tonnage and grade models (Cox and Singer, 2003a) were revised using data for 135 deposits. On the basis of geologic characteristics, those authors distinguished three types of sediment-hosted copper and published tonnage and grade models for (1) reduced-facies copper (Cox, 2003a), with 62 deposits (Cox and Singer, 2003c); (2) red bed copper (Lindsey and Cox, 2003), with 33 deposits (Cox and Singer, 2003b); and (3) Revett copper (Cox, 2003b), with 14 deposits (Cox and Singer, 2003d). Silver was included in the models for all three types of deposits; cobalt was included only in the reduced-facies type.

This study extends the work of Mosier and others (1986) and that of Cox (2003a,b), and Lindsey and Cox (2003). For this report, grade and tonnage information was collected for approximately 200 sediment-hosted copper deposits with published tonnage and grade information in about 30 sedimentary basins worldwide (fig. 1-1 and table 2-1) (table 2-1 of this report is seen online only). The data for the Central African Copperbelt (CACB) are based on Wilson and others (appendix A, this report) and Parks and others (appendix B, this report). After screening the data, 170 SSC copper deposits were selected for grade and tonnage modeling.

Definition of SSC Deposit Types

Mineral deposits must be clearly defined if they are going to be used for mineral resource modeling. For inclusion in a tonnage and grade model, a mineral deposit should: (1) have economic potential (Cox and others, 1986); (2) form by the same genetic process and be the same deposit type as other sites used to construct the same model (Barton and others, 1995); and (3) be developed using similar mining and processing methods as other sites in the model (Bliss and others, 1987).

According to Singer (1995), sediment-hosted copper deposits account for more than 20 percent of all copper that has been discovered. Production has come from a few large districts in the Democratic Republic of the Congo, Germany, Kazakhstan, Poland, and Zambia. SSC deposits are mined using a variety of mining (open pit, underground room and pillar) and beneficiation (pyro- and hydrometallurgy) methods.

Shared geologic characteristics form the basis for grouping deposits into types, such as SSC, that formed in the same geologic setting and through similar geological processes (fig. 2-2). SSC deposits are diagenetic in timing and epigenetic in origin (Zientek and others, this report, chapter 1). The deposits consist of fine-grained copper and copper-iron sulfide minerals that occur as stratabound to stratiform disseminations in siliciclastic or dolomitic sedimentary rocks. Ore minerals occur as cements and replacements, or rarely, as veinlets. The concentration of sulfide minerals conforms closely, but not exactly, with the stratification of the host rocks. These deposits are characterized by zoning of ore minerals laterally along and across bedding: from pyrite to chalcopyrite to bornite to chalcocite to hematite. Chalcocite- and bornite-rich rocks typically constitute the ore zones.

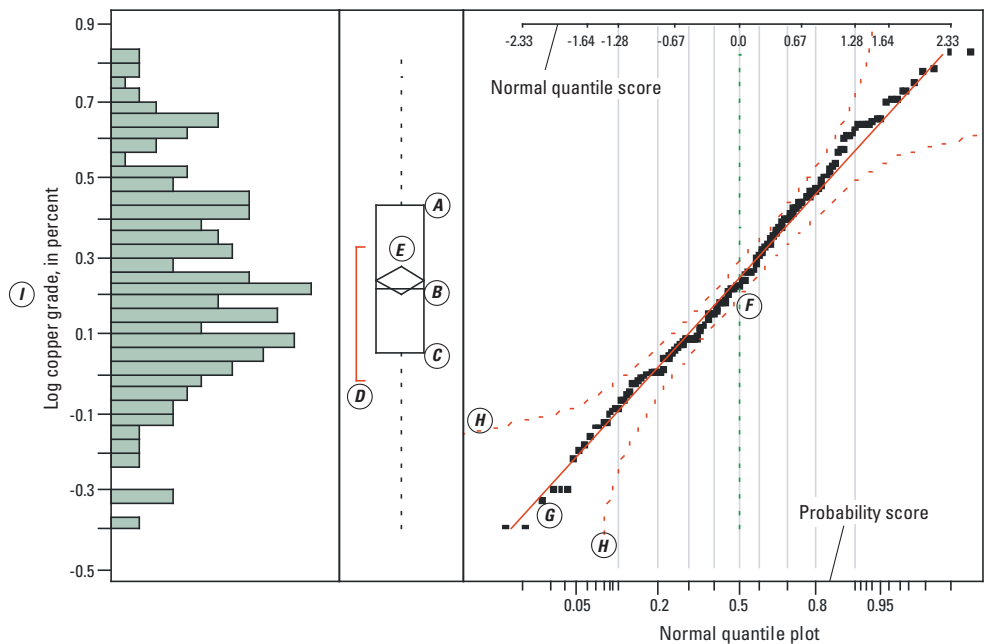
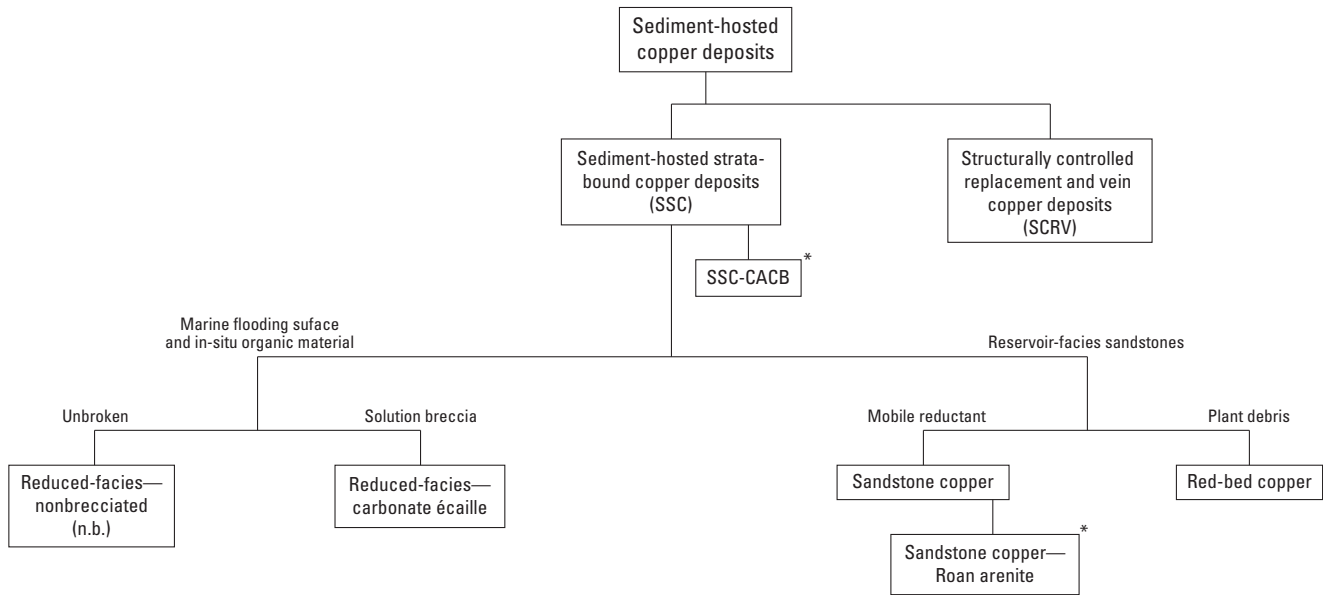


Figure 2-1. An example of histogram, box plot, and normal quantile plots illustrating the distribution of log-transformed values for copper grade of 187 sediment-hosted copper deposits. Shortest half is a bracket showing the densest 50 percent of the observations. The probability scale is the empirical cumulative probability for each value. The normal quantile scores are computed by the formula: $\phi^{-1}(r_i/(N+1))$, where ϕ is the cumulative probability distribution function for the normal distribution, r_i is the rank of the i^{th} observation, and N is the number of nonmissing observations.

EXPLANATION

- | | |
|--|---|
| A Upper quartile | F Mean is intersection of line with normal quantile score = zero |
| B Median | G Slope is standard deviation |
| C Lower quartile | H Confidence interval for normality |
| D Shortest half | I Data values |
| E Confidence interval on the mean | |



* Regional variant—Central African Copperbelt (CACB)

Figure 2-2. Chart illustrating the relations among types of sediment-hosted copper deposits.

Within a type, deposits can be further subdivided into smaller groups based on geology or distinct tonnage and grade characteristics. For example, the geologic setting between groups may be such that they would correspond to different areas on mineral potential maps. Previous workers distinguish two types of SSC deposits on the basis of the rocks hosting the deposits: (1) sandstones (Dzhezkazgan deposits of Bogdanov and others, 1973; continental red bed deposits of Kirkham, 1989 and Kirkham and others, 1994; and red bed deposits of Hitzman and others, 2005); and (2) shales and marls (copper shale deposits of Bogdanov and others, 1973; paralic marine deposits of Kirkham, 1989 and Kirkham and others, 1994; reduced-facies deposits of Cox and others, 2003; Kupferschiefer deposits of Hitzman and others, 2005; and reduced-facies—nonbrecciated deposits of this study).

The sandstone-hosted deposits have been divided still further into two additional types based on the nature of the organic material that localizes ore minerals in the rock: (1) patchy concentrations of plant remains (the Uralian deposits of Bogdanov and others, 1973; red bed deposits of Lindsey and Cox, 2003); and (2) a diffusely distributed reductant, probably a mobile hydrocarbon (Revelt deposits of Cox and others, 2003; sandstone copper, this study). Deposits of the red bed copper type of Lindsey and Cox (2003) were excluded from this study; although they are commonly found as mineral occurrences, few sites have formally reported tonnage and grade. Only 3 of the 20 deposits in the model developed by Lindsey and Cox (2003) contain more than 50,000 metric tons contained copper (a significant copper deposit as defined by Singer, 1995). Deposits of the red bed copper type of Lindsey and Cox (2003) are interesting because they indicate the presence of copper-bearing fluids in sedimentary basins, but their contribution to global mineral endowment is negligible and such deposits are not sought out by companies conducting minerals exploration.

Deposits of a given type also can be subdivided based on regional differences in their tonnage and grade distributions. This has been done for podiform chromite deposits (major and minor podiform chromite, Singer, Page, and Lipin, 1986; Singer and Page, 1986), volcanogenic massive sulfide deposits (kuroko massive sulfide and Sierran kuroko massive sulfide; Singer and Mosier, 1986; Singer, 1992), and porphyry copper deposits (all and giant porphyry copper deposits, Singer and others, 2008; Singer, Briske, and Cunningham, 2008). Deposit types with different grade and tonnage models probably have different economic values. Our colleagues in academia and industry suggest that SSC deposits in the CACB in the Katanga Basin have higher copper grades than deposits found elsewhere (figs. 2-3 and 2-4). The data set was divided into two groups—one for SSC deposits found in CACB (78 deposits) and those found elsewhere (92 deposits). Copper grade data (expressed in logarithms) for each group was tested for normality and variance homogeneity before being compared using a *t*-test. The results rejected the assumption that both groups have a same copper grade at the 1-percent confidence level (fig. 2-5). Median and mean copper grades

for the CACB deposits are 2.70 and 2.96 percent, respectively, compared to median and mean grades of 1.17 and 1.23 percent copper, respectively, for deposits elsewhere. Many deposits in the CACB contain cobalt, but few report data for silver grades; some deposits in other parts of the world contain elevated levels of silver but few report data for cobalt grades. Both reduced-facies- and sandstone-copper deposits are present in the CACB; two regional grade and tonnage models for SSC in the CACB were developed.

In this report, SSC deposits are subdivided into types (fig. 2-2) based on (1) host rocks, reductants, and the effect of salt tectonics on the deposit and (2) regional differences in copper grade as follows:

- Sediment-hosted stratabound copper deposits (all 170 deposits).
- Reduced-facies deposits that are not in salt solution breccias (50 of the 170 SSC deposits; 10 in the CACB and 40 elsewhere): reduced-facies—nonbrecciated, henceforth “reduced-facies—n.b.”
- Reduced-facies deposits that occur in salt dissolution breccias (49 of the 170 SSC deposits; 47 in the CACB and 2 in Australia): “reduced-facies—carbonate écaillé.”¹
- Sandstone copper deposits (70 of the 170 SSC deposits; 20 in the CACB and 50 elsewhere): “sandstone copper.”
- Sandstone copper deposits in the Roan Series, Zambia (20 of the 70 sandstone copper deposits): “sandstone copper—Roan arenite.”

Reduced-Facies—Nonbrecciated (n.b.) Deposits

Reduced-facies copper deposits are hosted by black to gray to green marine or lacustrine shale, siltstone, mudstone, or carbonaceous dolosiltstone/siliceous dolomite containing solid amorphous organic matter. Host beds for many reduced-facies deposits occur at or just above the flooding surface that marks the transgression between a marine, upward coarsening, sag basin depositional sequence and underlying synrift,

¹Breccias derived from specific stratigraphic units in the Roan Group in the Democratic Republic of the Congo are spectacular because the clasts range between 1 meter (m) and 10 kilometers (km) in size. For a “megabreccia,” the largest dimension of clasts is 100 to 400 m (American Geosciences Institute (AGI) Glossary of Geology online at <http://www.agiweb.org/pubs/glossary/>). Jackson and others (2003) coined the term “gigabreccia” for breccias in which the clasts are 1 km or more in size. In French geologic literature, these large breccia fragments are referred to as “écailles,” meaning “scales.”

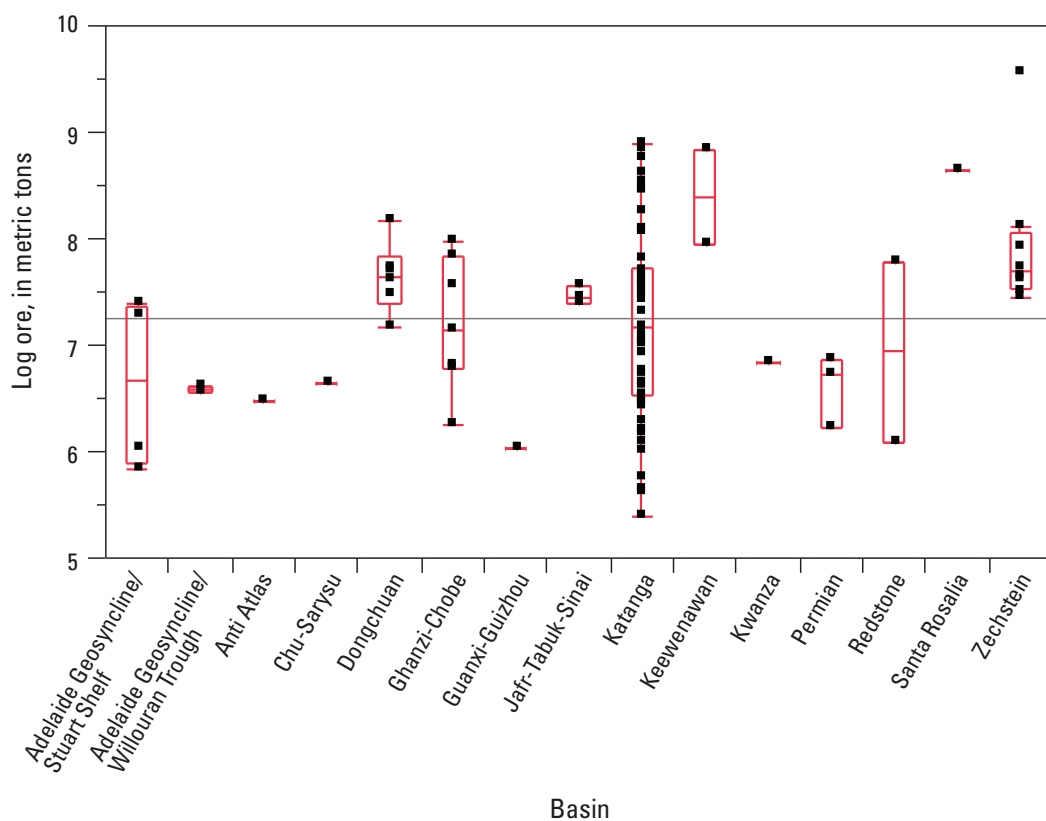
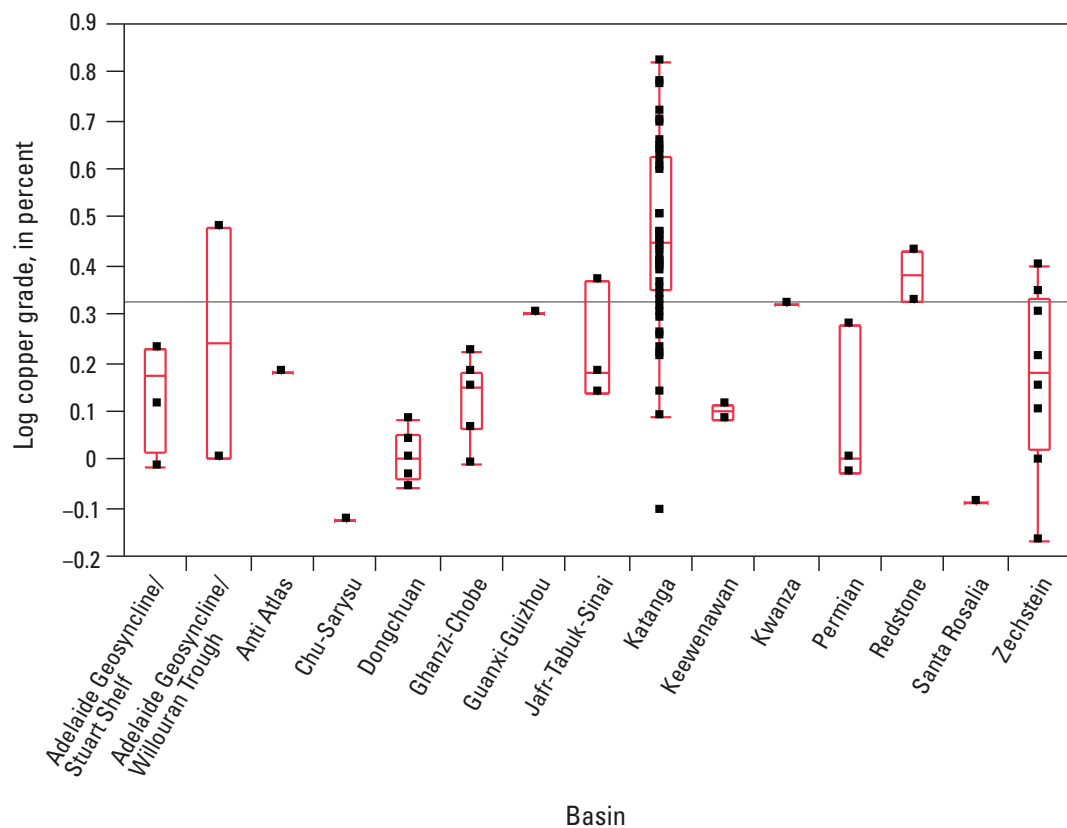


Figure 2-3. Quantile box plots showing the variation in log ore, tonnage, and log copper grade by basin for reduced-facies copper deposits.

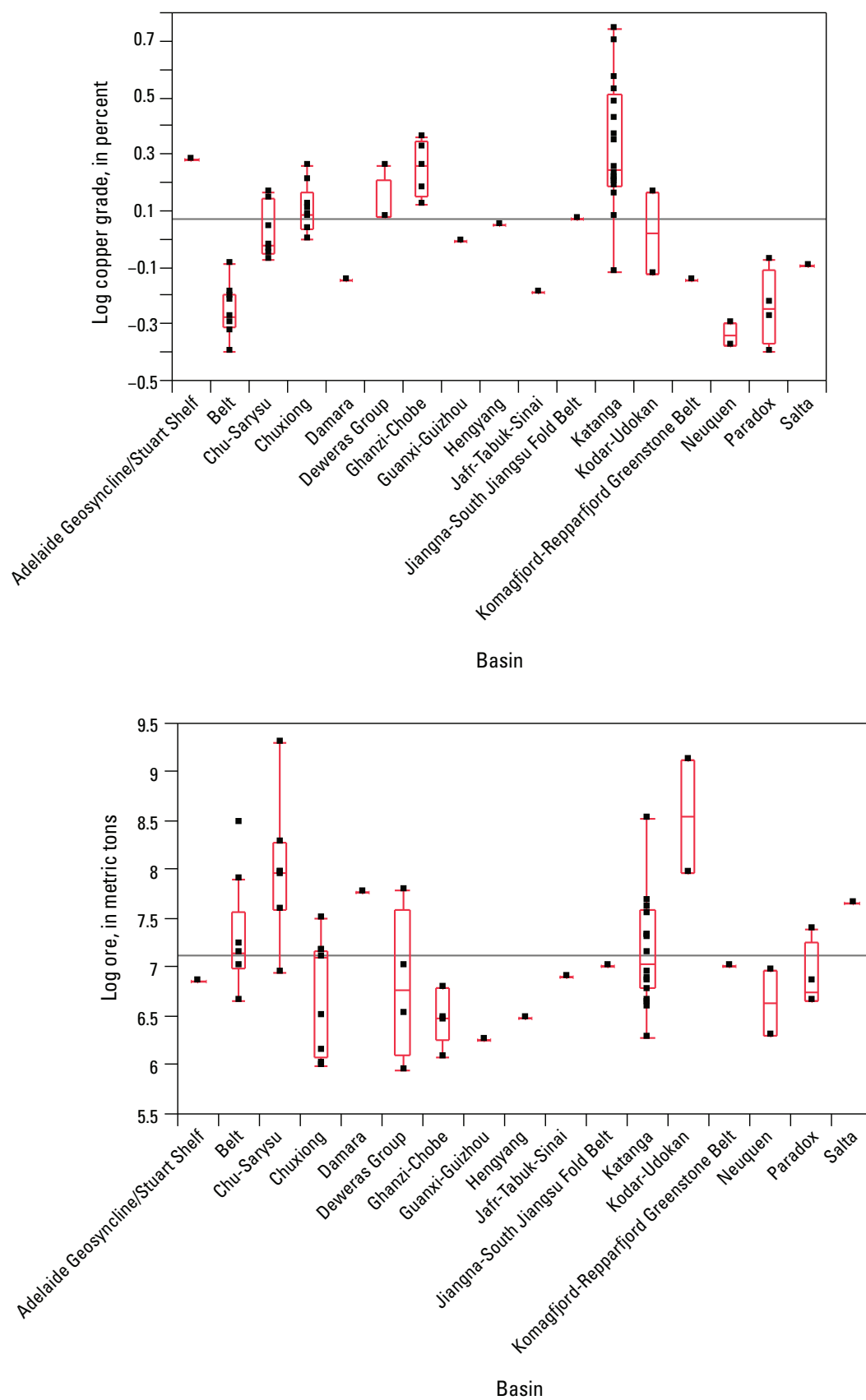


Figure 2-4. Quantile box plots showing the variation in log ore, tonnage, and log copper grade by basin for sandstone copper deposits.

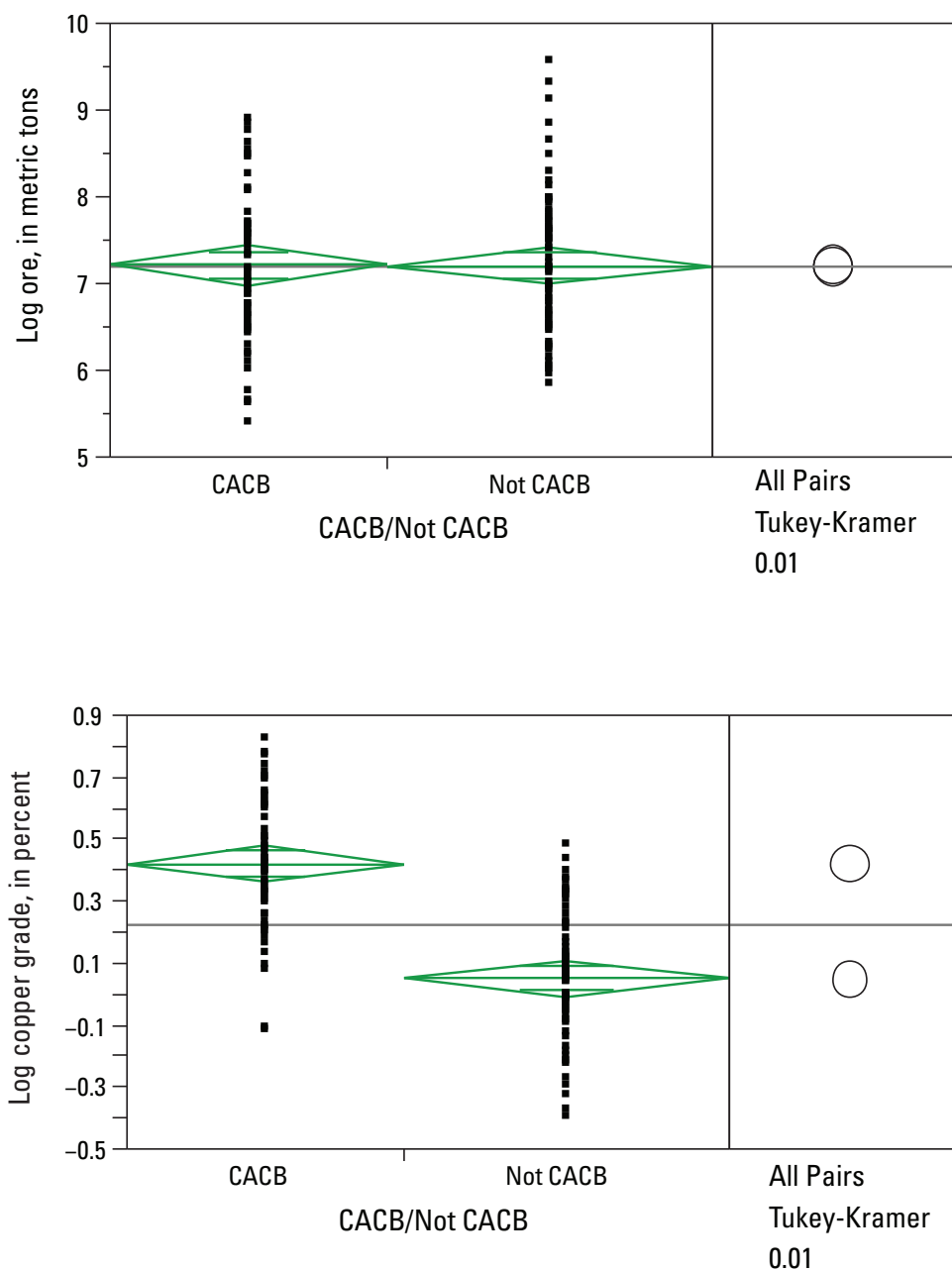


Figure 2-5. Plot showing mean diamonds and comparison circles for the distribution of log-transformed values of copper grade and ore tonnage between the sediment-hosted stratabound copper deposits in the Central African Copperbelt (CACB) and all other areas in the world. If the confidence intervals shown by the means diamonds do not overlap, the groups are significantly different. See Sall and others (2007) for explanation of comparison circles.

nonmarine red beds. Depositional environments hosting reduced-facies mineralization above the transgressive surface include open marine shelf black shale, coastal sabkhas, and subtidal shelf carbonates. Reduced-facies deposits have sheet-like geometry with lateral dimensions from hundreds to thousands of times greater than thicknesses. For example, strike lengths may be on the order of 3,000 to 5,000 meters (m), with widths of 500 to 2,000 m and ore thicknesses ranging from a few meters to 50 m. Examples of giant or world-class deposits are summarized in table 2-2. Permissive tracts for reduced-facies deposits should be based on the extent of a major flooding surface that immediately overlies red beds.

Reduced-facies deposits in the CACB occur in the Ore Shale Formation in the Zambian portion of the CACB (fig. 2-6; Annels, 1984 and 1989) and have elevated copper grades relative to many reduced-facies deposits in other sedimentary basins. These deposits occur in the Ore Shale Formation of the Kitwe Subgroup (fig. 2-7) and form large, continuous, high-grade deposits that have been affected by lower greenschist to upper amphibolite facies metamorphism and complex folding (Selley and others, 2005). Like other reduced-facies deposits, the deposits in Zambia are associated with the major flooding surface that deposited marine black shales on continental red beds and are localized at stratigraphic pinchouts, at basement highs, and in structural traps. A separate grade and tonnage model cannot be created because there are not enough examples of this style of mineralization. They are included in the reduced-facies—n.b. model.

Reduced-Facies—Carbonate Écaille Deposits

Reduced-facies deposits hosted by Kamoto, Dolomitic Shales, and Kambove Formations of the Mines Subgroup, of the Roan Group, CACB (figs. 2-8 and 2-9) occur in gigabreccia fragments ranging in size from about a meter to 10 kilometers (figs. 2-10 and 2-11; François, 1973; François and Cailteux, 1981; Jackson and others, 2003). In French, these gigabreccia fragments are referred to as “écailles”, meaning “scales”. The primary stratabound ore body geometry is preserved in the breccia fragments and pre-dates folding and brecciation.

The stratigraphic section hosting the mineralized layers appears to have been interlayered with salt beds (Jackson and others, 2003). After the copper-mineralizing event, deformation of the salt layers formed diapirs, salt walls, extrusions, thrust sheets, and fault-cored anticlines above a regional detachment surface produced by thrust faulting during the Lufilian orogeny (Garlick and Fleisher, 1972; Jackson and others, 2003). During halokinesis, rock units hosting the mineralized layers, dolomitic formations or other competent units, were broken into fragments and the salt was dissolved. The resulting dissolution breccias host the mineralized strata.

Compared to reduced-facies deposits outside the CACB, the reduced-facies deposits hosted by the Mines Subgroup breccias have higher copper grades. The occurrence of the deposits in gigabreccia fragments imparts a secondary control on the tonnage distribution of these reduced-facies deposits.

A separate reduced-facies grade and tonnage model, reduced-facies—carbonate écaille, was created for use in mineral resource assessment. These deposits are excluded from the reduced-facies—n.b. model. Examples of giant or world-class deposits are summarized in table 2-2.

Sandstone Copper Deposits

Sandstone copper deposits are hosted in gray, well-sorted, fine- to coarse-grained, locally conglomeratic sandstone, which is characterized by cross bedding, parallel lamination, mud rip-up clasts, and ripple marks. Sandstone copper host rocks are typically well-sorted siliciclastic sandstones from a variety of deltaic topset environments that make up the upper part of the coarsening upwards depositional cycles. Sandstone copper deposits are tabular to lens-like; lateral dimensions are from 20 to 100 times their thicknesses. These rocks were probably reservoir rocks for petroleum when the copper minerals were deposited. For many sandstone copper deposits, petroleum was probably present as sour gas (Hayes and others, 2012). Structural traps that allow the accumulation of hydrocarbons in sedimentary basins may localize deposition of sediment-hosted copper mineralization. Permissive tracts for sandstone copper deposits should delineate reservoir rocks within a basin hosting red beds, hydrocarbon source beds, and evaporites. World-class deposits include Dzhezkazgan and Zhaman-Aibat in Kazakhstan, Udokan in Russia, and Rock Creek/Montanore in Montana (table 2-2).

In the CACB, sandstone copper deposits are found in coarser-grained siliciclastic rocks above and below the Ore Shale Formation of the Kitwe Subgroup (fig. 2-12), and in dolomitic siltstone that is a lateral facies equivalent to the Ore Shale Formation. Like other sandstone copper deposits, they occur in reservoir facies rock types in stratigraphic and structural traps similar to those that collect oil and gas. Compared to other sandstone deposits outside the CACB, they have higher copper grades. A regional variant of the sandstone copper grade and tonnage model, sandstone copper—Roan arenite, was created for use in mineral resource assessment of undiscovered deposits in the Roan Series in Zambia. These deposits are not excluded from the sandstone copper model. Mufulira, Zambia, is the only giant or world-class deposit in this regional model (table 2-2).

Deposit Definition

For grade and tonnage models, the grade and tonnage data associated with a deposit should represent similar sampling units. The tonnage and grade data should (1) be an estimate of pre-mining, in-situ mineral endowment; (2) use a consistent cutoff grade; and (3) represent a well-explored deposit (Singer and Menzie, 2010). Finally, rules are used to consistently define how ore bodies are spatially grouped into

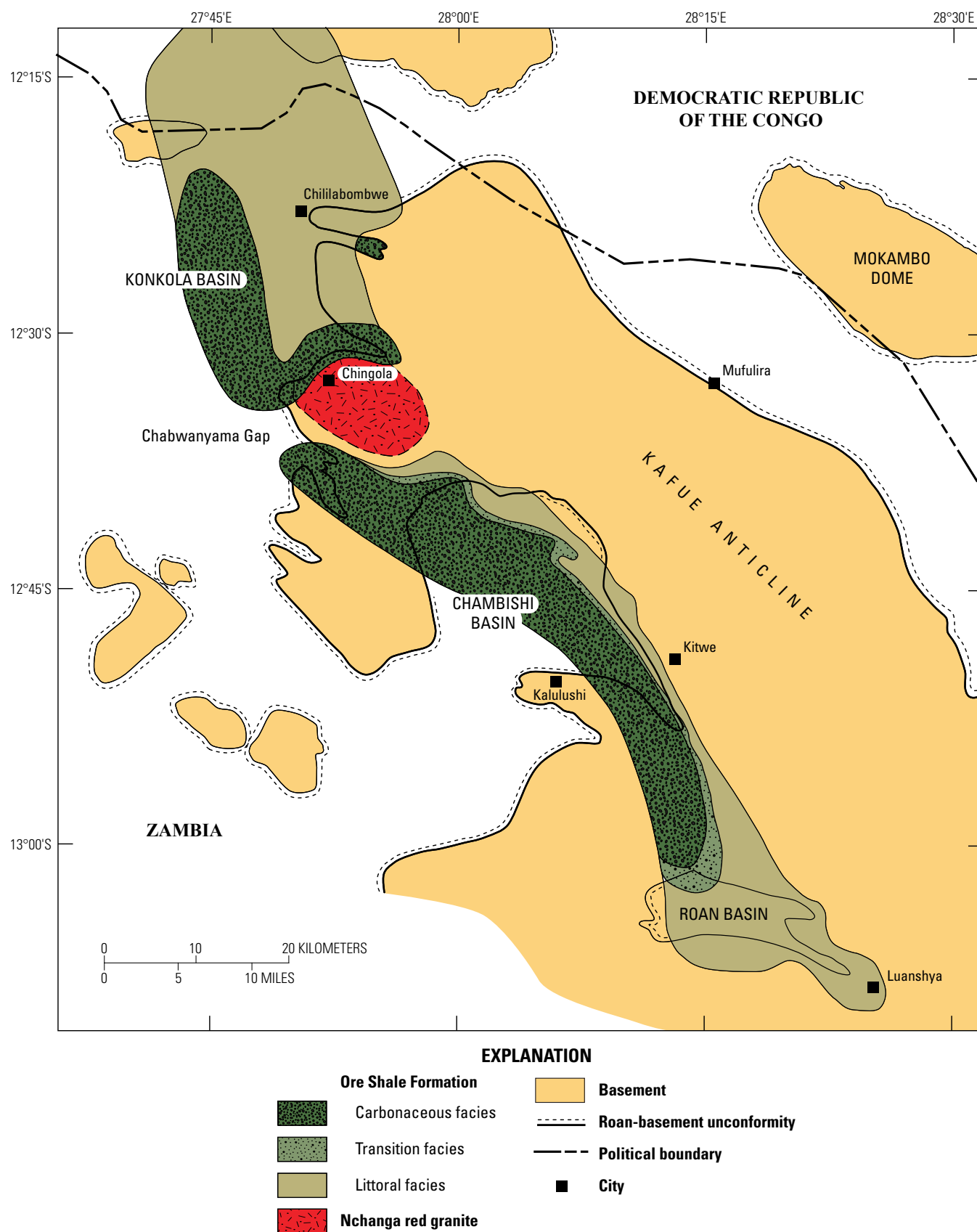


Figure 2-6. Geologic map showing the distribution of the Ore Shale Formation of the Roan Group in Zambia. Modified from Annels (1984).

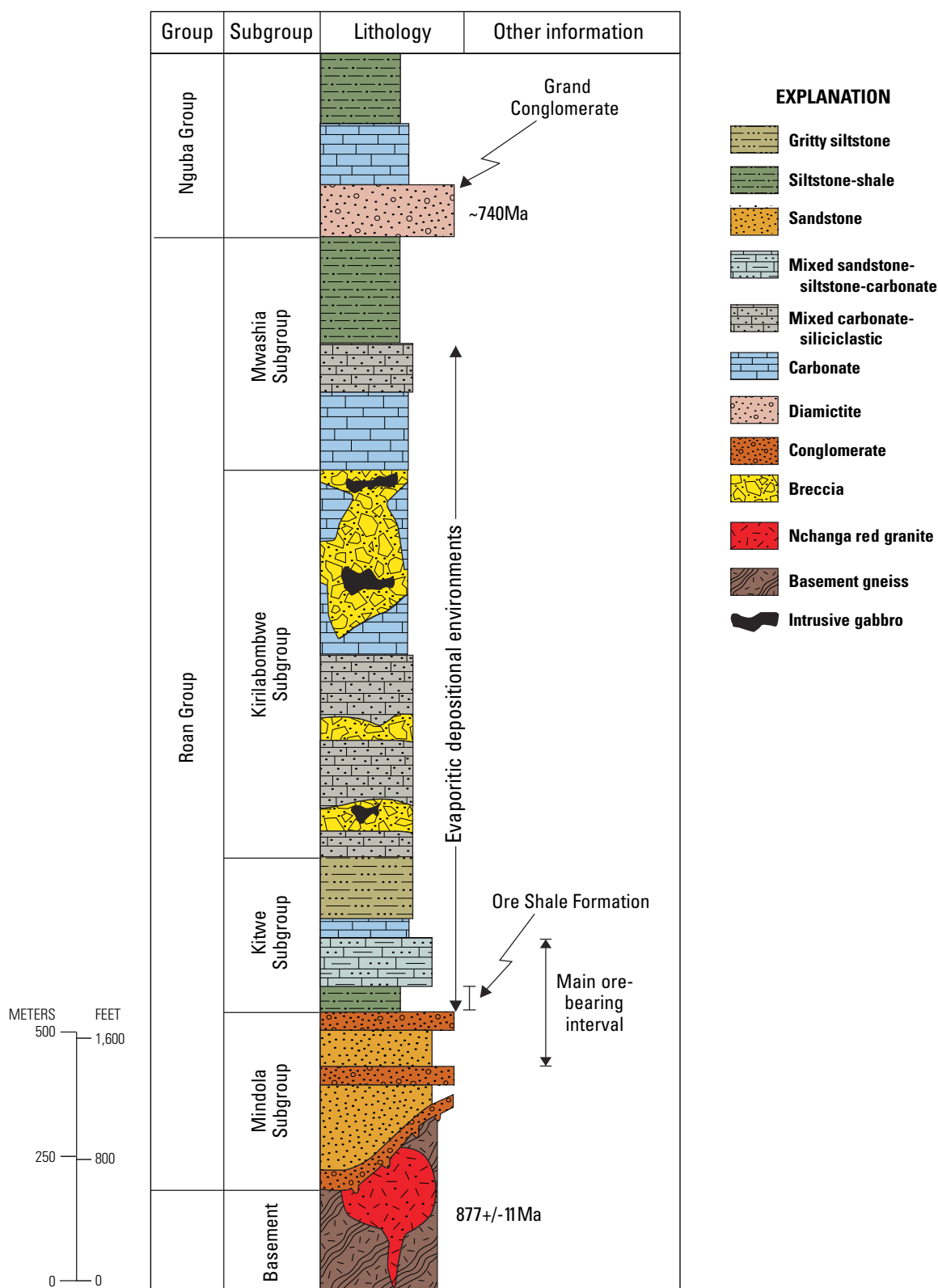


Figure 2-7. Stratigraphic column of the Roan Group exposed in the Zambian part of the Central African Copperbelt. Reduced-facies copper mineralization is associated with the Ore Shale Formation. Modified from Selley and others (2005).

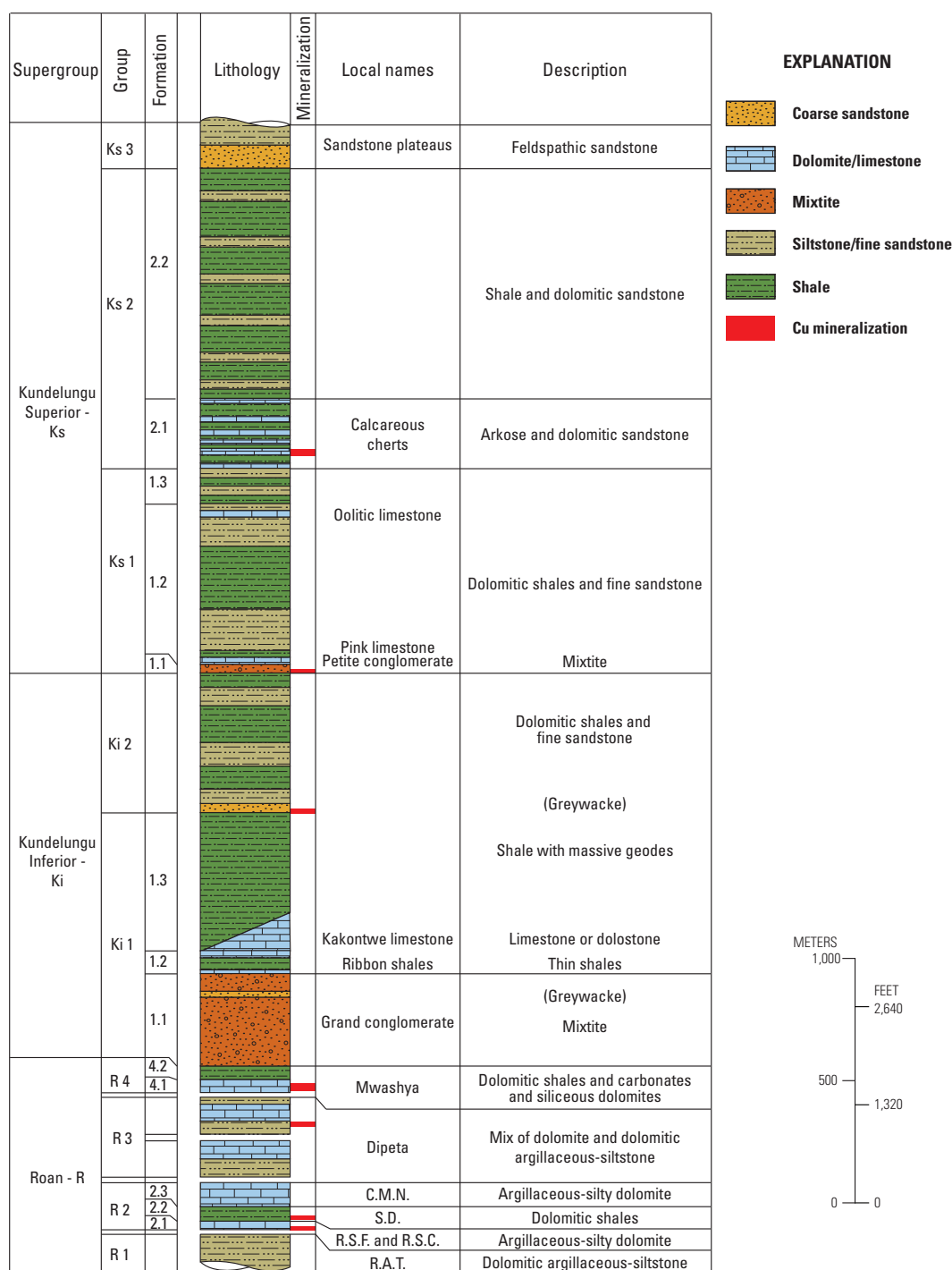


Figure 2-8. Stratigraphic column of the Katangan system, illustrating the location of mineralized strata. The reduced-facies-carbonate écaïlle mineralization is associated with the Mines Group (R2) in the Roan Supergroup. Gaps in the Roan section indicate where evaporate may have been present. Stratigraphic abbreviations: C.M.N.—“calcaire à minerais noirs” (black limestone ore); S.D.—“schistes Dolomitiques” (dolomitic shales); R.S.F.—“roches siliceuses feuilletées” (laminated siliceous rocks), and R.S.C.—“Roches Siliceuses Cellulaires” (cellular siliceous rocks), and R.A.T.—“roches argilo-talqueuses” (clayey talcose rocks). Modified from François (2006).

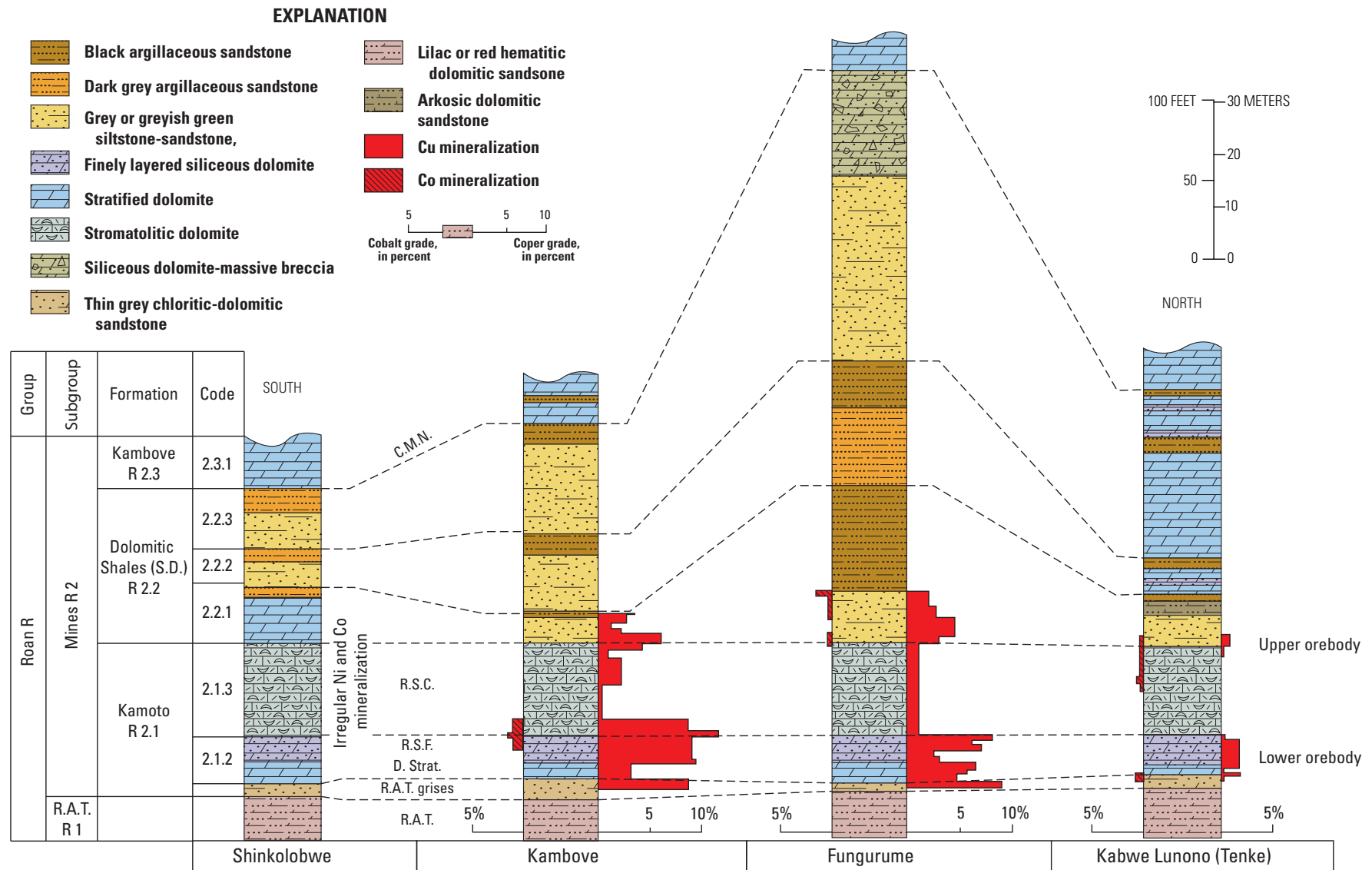


Figure 2-9. Stratigraphic columns showing distribution of reduced-facies-carbonate écaille copper mineralization in the Mines Subgroup into an upper and lower ore body in the Central African Copperbelt in the Democratic Republic of the Congo. Stratigraphic abbreviations: C.M.N.— “cálcaire á minerais noirs” (black limestone ore), R.S.C.— “Roches Siliceuses Cellulaires” (cellular siliceous rocks), R.S.F.— “roches siliceuses feuilletées” (laminated siliceous rocks), D. strat—“dolomies stratifiées” (laminated dolomites), R.A.T. grises—“roches argilo-talqueuses grises” (gray clayey talcose rocks), and R.A.T.— “roches argilo-talqueuses” (clayey talcose rocks). Modified from François (2006).

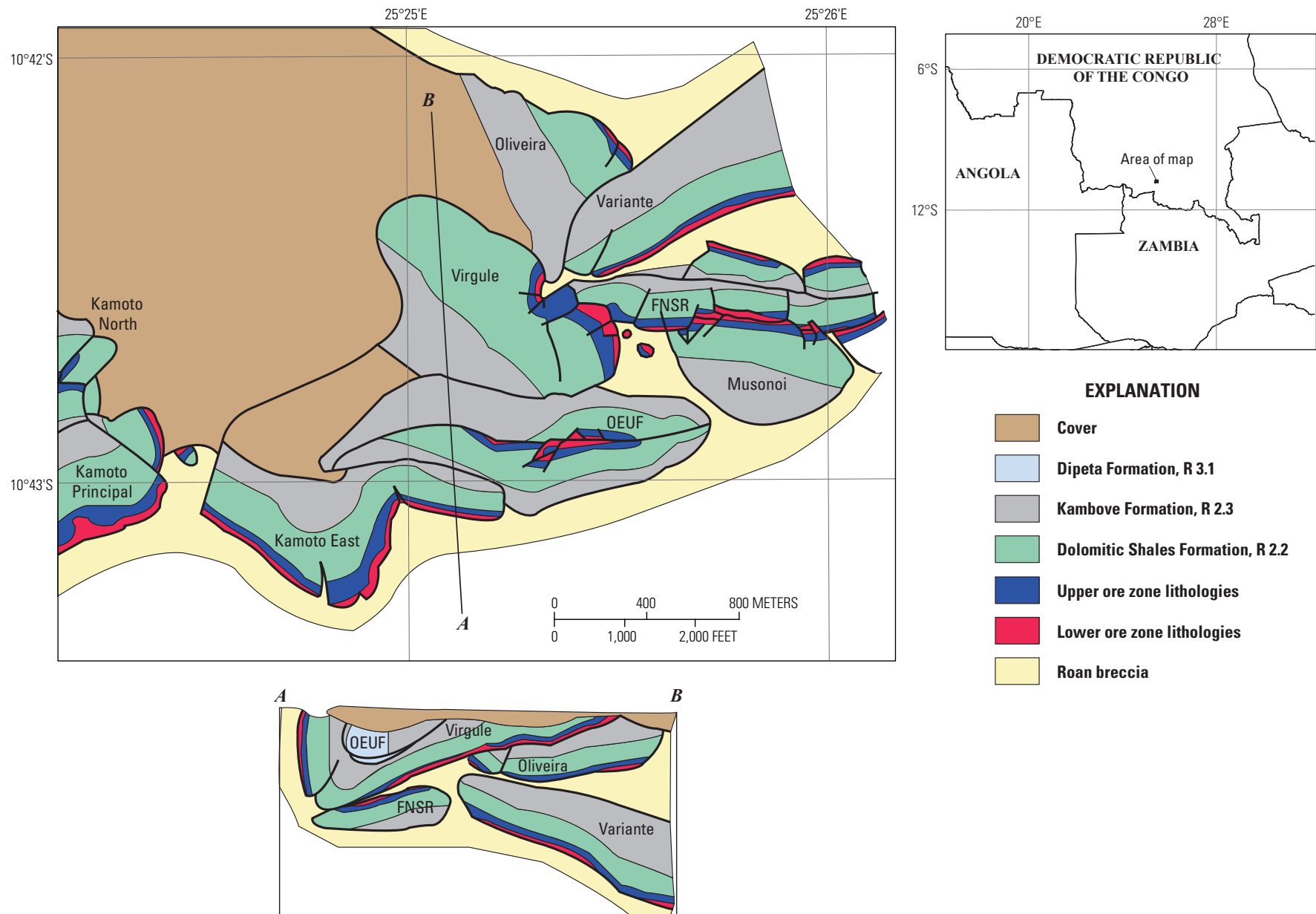
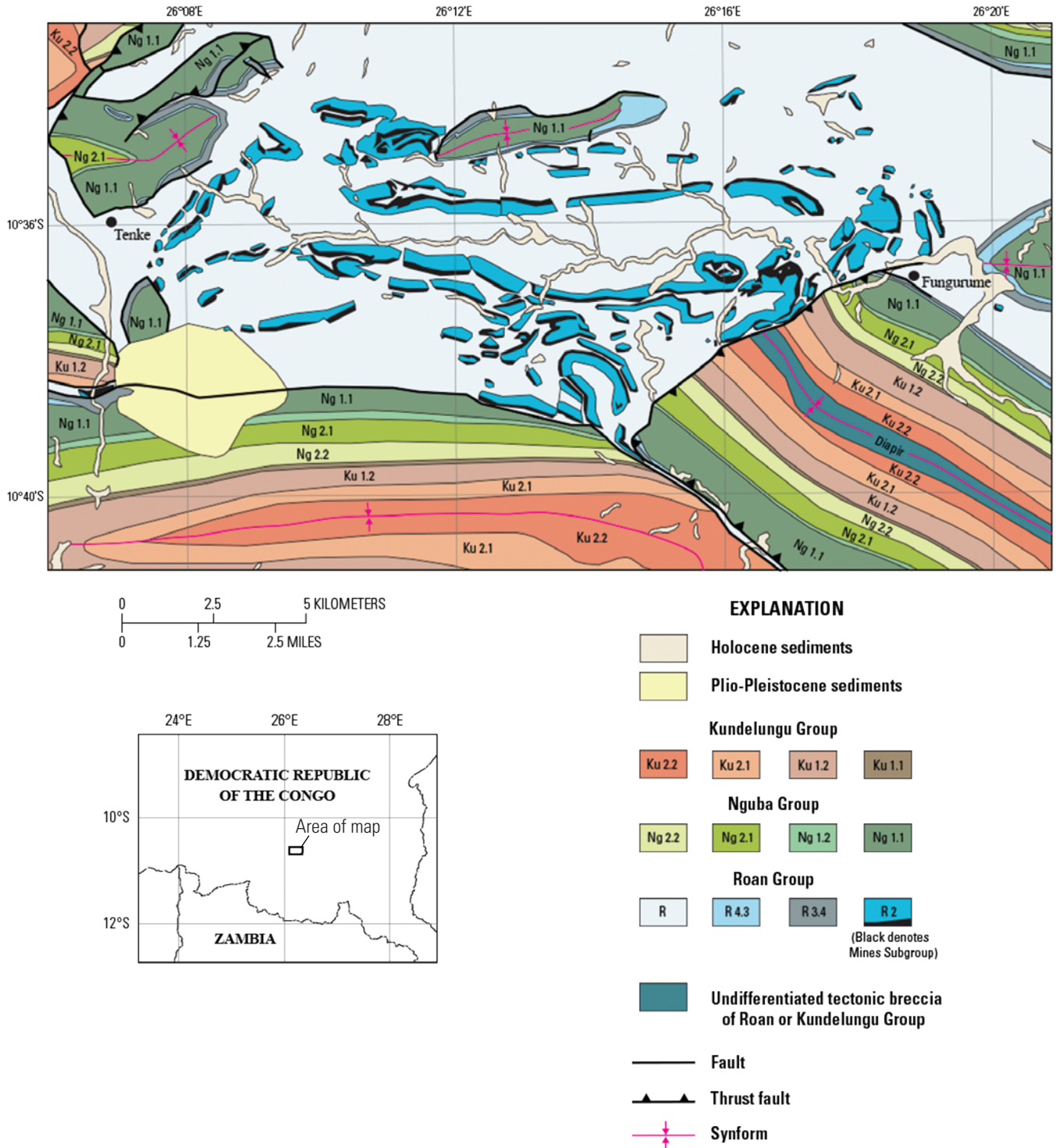


Figure 2-10. Geologic map and cross section of the Kamoto-Oliveira-Virgule (KOV) ore body that shows large gigabreccia fragments (écaïlle) of Roan Group strata that host reduced-facies mineralization. On the map and section, each fragment is named (for example, Musonoi or Virgule). See figure 2-7 for stratigraphic names and abbreviations. Modified from Dixon (2007).



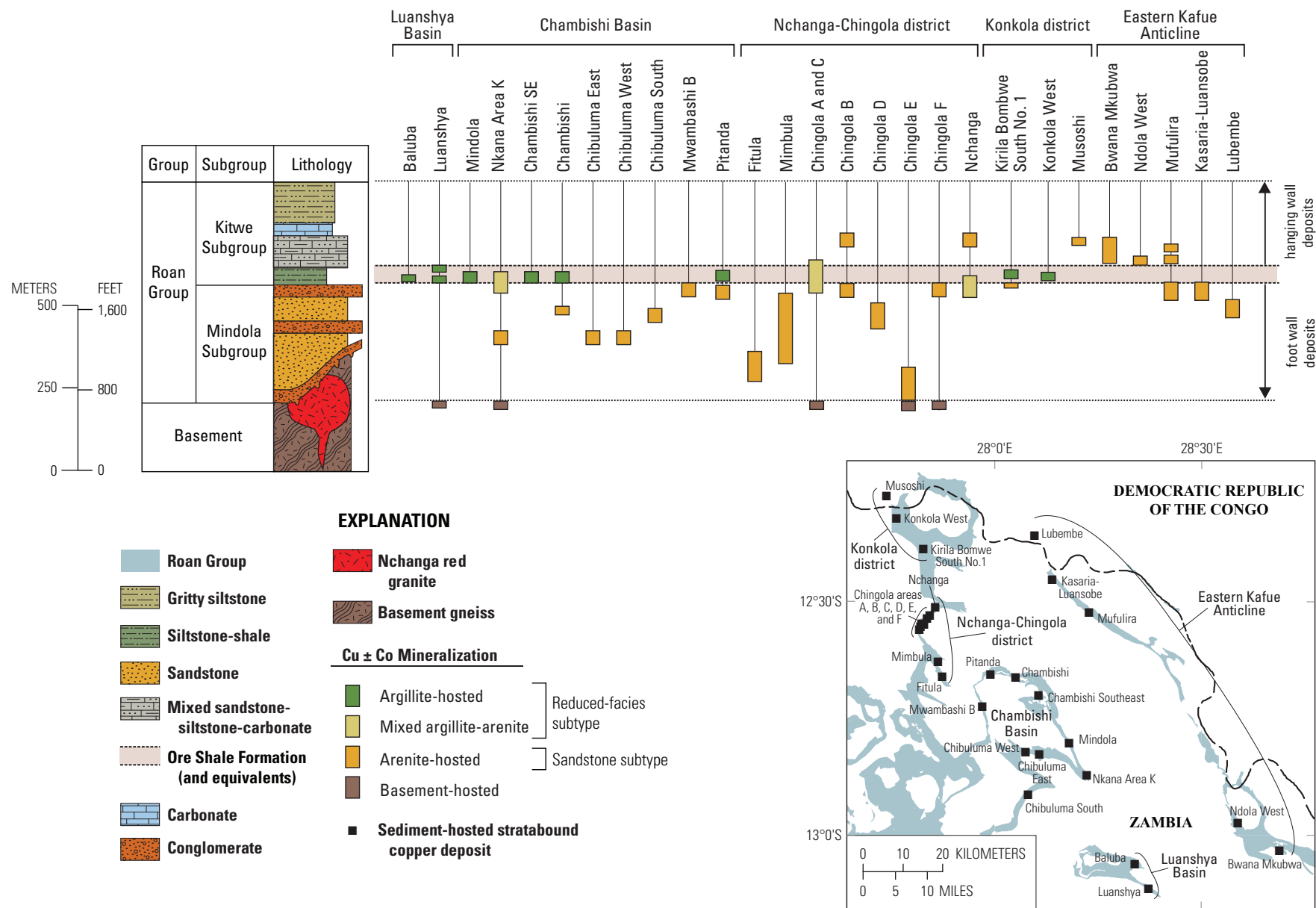


Figure 2-12. Stratigraphic column of the Roan Group exposed in the Zambian part of the Central African Copperbelt showing the stratigraphic distribution of reduced-facies (argillite-hosted and mixed argillite-arenite) and sandstone (arenite-hosted) mineralization. Modified from Selley and others (2005).

Table 2-2. Sediment-hosted stratabound copper deposits containing more than two million metric tons of copper (equivalent to giant deposit category of Singer, 1995).

[t, metric tons; DRC, Democratic Republic of the Congo; n.b., nonbrecciated]

Name	Basin	Country	Contained copper metal (t)
Reduced-facies—carbonate <i>écaille</i>			
DIMA	Katanga	DRC	7,800,000
Fungurume	Katanga	DRC	2,800,000
Kambove Principal-Kambove West	Katanga	DRC	3,100,000
Kamoto-KOV-Musonie-Mupine	Katanga	DRC	19,000,000
Kansalawile-Mambilima	Katanga	DRC	2,800,000
Kimbwe	Katanga	DRC	2,000,000
Kinsevere	Katanga	DRC	2,100,000
Kwatebala	Katanga	DRC	2,200,000
Mutanda Ya Mukonkota	Katanga	DRC	3,700,000
Tenke	Katanga	DRC	2,500,000
Reduced-facies—n.b.			
Baluba-Muliashi-Luanshya	Katanga	Zambia	10,000,000
Boleo (0.5 cutoff)	Santa Rosalia	Mexico	3,600,000
Chambishi Main and West	Katanga	Zambia	2,900,000
Chambishi Southeast	Katanga	Zambia	3,800,000
Chingola-Nchanga	Katanga	Zambia	16,000,000
Kalumbila	Katanga	Zambia	2,700,000
Konkola-Musoshi	Katanga	Zambia	22,000,000
Lubin-Sieroszowice,	Zechstein	Poland	72,000,000
Mansfeld	Zechstein	Germany	2,000,000
Mindola-Nkana N-S	Katanga	Zambia	15,000,000
White Pine	Keewenawan	United States	8,300,000
Sandstone copper			
Dzhezkazgan	Chu-Sarysu	Kazakhstan	22,000,000
Mufulira	Katanga	Zambia	8,900,000
Rock Creek/Montanore	Belt	United States	2,400,000
Udokan	Kodar-Udokan	Russia	19,000,000
Zhama-Aibat	Chu-Sarysu	Kazakhstan	2,700,000

a deposit for modeling purposes (Singer and Menzie, 2010). Unfortunately, data about mineral deposits rarely meet all of these requirements.

Mineral Endowment

For modeling purposes, the original mineral deposit size and grade is estimated by combining past production with estimates of remaining in-place mineral resources. Published production information includes data such as the mass of ore mined or processed, average grade, and/or total amount of material produced. Information on mining and beneficiation losses is seldom reported; therefore, the production information used to estimate pre-mining mineral endowment is not adjusted for these losses. Estimates of remaining, in-place mineral resources are based on reported mineral inventory for a deposit. The inventory is a formal quantification of naturally occurring materials, estimated by a variety of empirically or theoretically based procedures (Sinclair and Blackwell, 2006). These resources exist for a specified economic condition and currently feasible or near-feasible technology of production (Harris, 1984).

Mineral inventories reported before the late 1990s generally do not report the quality and quantity of data, the procedures used to make the estimate, or the economic assumptions. Beginning in the late 1990s, international standards require detailed reporting of the assumption and methods used in estimating mineral inventory (Committee for Mineral Reserves International Reporting Standards, 2006, or Securities and Exchange Commission Industry Guide 7 (http://web.cim.org/standards/documents/Block474_Doc32.pdf, accessed February 28, 2012). The data used in this compilation are a mix of historical information with little or no supporting material and modern, regulatory compliant reports that provide good documentation. For deposit data that conform to Committee for Mineral Reserves International Reporting Standards (CRIRSCO) standards, the weighted average is calculated using all exclusive reserve and resource categories, including inferred resources.

Cutoff Grade

Cutoff grade is the lowest grade, or quality, of mineralized material that qualifies as economically mineable and available in a given deposit (Committee for Mineral Reserves and Reporting Standards, 2006). Cutoff grade is used to separate two courses of action, to mine or to leave, to mill or to dump; also, cutoff grade is any of a series of grades used to truncate a frequency distribution, or to separate mineralized materials into graded fractions (Taylor, 1972). In order to economically evaluate mineral deposits, grades and tonnages may be reported at various cutoff grades. In addition, different mining methods based on different cutoff grades may be employed on the same deposit and will affect the production tonnages.

Ideally, estimates of deposit grades and tonnages used in models would be based on the same cutoff grade. Commonly, various values have been used for cutoff grade, which introduces ambiguity in model development. When possible, tonnage and grade at the lowest cutoff grade are used for modeling grade and tonnage distributions (Singer and Menzie, 2010).

For SSC deposits, the cutoff can be based on copper grade, silver grade, or net-smelter return (table 2-1). For most of the deposits where cutoff is reported, copper grade is used; values range from about 0.3 to greater than 1.0 weight percent copper. The Rock Creek/Montanore deposit in Montana uses a cutoff grade of 1 ounce per ton of silver. Other sites use cutoff grades based on the values of all metals, expressed either as copper equivalent values (Boleo, Mexico) or net-smelter return (Troy, Montana).

Exploration

The sites with modern CRIRSCO-compliant mineral inventories are well-explored by surface sampling and drilling. The historical resource numbers, before enhanced reporting requirements were established in the late 1990s, are probably based on drilling data. Most sites in the compilation probably have potential for reserve growth.

Spatial Rules for Aggregation

Grade and tonnage data are available to varying degrees for districts, deposits, mines, and shafts. Spatial aggregation rules are developed to try to insure that deposits in grade and tonnage and spatial density models correspond to deposits as geologic entities. These rules are essential in order to ensure an internally consistent assessment system in which the estimated number of undiscovered deposits is consistent with the grade and tonnage model (Singer and Menzie, 2010).

Spatial rules are used in the development of several grade and tonnage models. For the volcanogenic-massive sulfide deposit model, all mineralized rock within 500 m is combined into one deposit (Mosier and others, 2009). For the porphyry copper deposit and the sediment-hosted lead-zinc deposit models, all mineralized rock or alteration within 2 kilometers (km) is combined into one deposit (Singer and others, 2008; Singer and others, 2009). For the purposes of grade and tonnage modeling, Cox and other (2003) defined a sediment-hosted copper deposit as one or more separate ore bodies separated from its nearest neighbor by more than 2,000 m. However, these studies did not define what is meant by mineralized rock, alteration, or ore body, or explain how the value for spatial aggregation was determined.

The presence of mineralized rock and an associated alteration zone is a difficult criterion to apply to sediment-hosted copper deposits. Masses of rock for which mineral inventory has been reported are typically contained within broad zones of weakly mineralized rock that extend hundreds to thousands of meters away from the ore body. Alteration associated with sediment-hosted copper deposits affect large

volumes of the enclosing rocks and form systems that may extend tens of kilometers and possibly as much as 100 km laterally, and commonly affect more than 1 km of sedimentary rock thickness.

To determine spatial rules for aggregation, the ore body is defined as the volume of mineralized rocks for which a tonnage and grade has been determined. Using this definition, the shape of an ore body reflects geologic contacts, economic cutoff limits, and property boundaries. Maps showing the surface projection of the volume of rock associated with a given tonnage and grade estimate were found for approximately 30 percent of the deposits considered in this study; these sites are biased towards large deposits and those found in the CACB. Ore body outlines were found for approximately 40 sites in the CACB and approximately 20 sites in 6 other basins. For the remainder of the sites, a point is used to approximate the location of the deposit.

The spatial aggregation rule is constructed on the basis of deposits in the CACB, which has the highest density of sediment-hosted stratabound deposits in the world. The location of deposits was estimated from the spatial database of the surface projection of ore bodies (appendix B, this report). If an ore body was not specifically represented by a polygon in the GIS, open pit outlines were used as a surrogate (appendix B, this report). The nearest distance between the edges of all pairs of ore body/open pit polygons that occurred within a 5 kilometer radius of each other in the CACB was calculated using spatial analysis tools in ArcGIS. Histograms and normal quantile plots showed a maximum in the histogram and a slope break in the quantile plots that was used to select an aggregation distance of 500 m between ore body polygons (fig. 2-13). The same aggregation distance for ore body polygons is used in other sedimentary basins.

The diameter of the median ore body areas should provide a rough approximation for the aggregation distance between points representing a deposit location. The median area of deposits with ore body polygons is 1.27 square kilometers (km²). Using the positive correlation between ore tonnage and the area of an ore body, values for ore body area were imputed where that information is missing (fig. 2-14). Integrating the imputed values into the calculation lowers the median size of a sediment-hosted copper ore body to 0.38 km². If a circular ore body outline is assumed, the estimated median diameter is 700 m, similar to the 500-m value determined when measuring edge to edge of deposit polygons.

For the global dataset, the 500-m aggregation rule was used, measuring either from the edge of a deposit polygon or between points representing deposit locations. Aggregated locations were given a new point location for the group (see site status in table 2-1). The sensitivity of the aggregation process was tested by determining how many additional sites would be aggregated if a spatial rule of 700 m and 1,000 m was applied to the deposit points. At 700 m, no additional points would be aggregated. At 1,000 m, only one additional pair of deposits would be aggregated.

Data Quality Assessment

Just as 95% of research efforts are devoted to data collection, 95% of the time remaining should be spent ensuring that the data collected warrant analysis (Good and Hardin, 2009, p. 51).

The tonnage and grade database review includes (1) calculating the minimum and maximum values of the data to ensure that they are geologically feasible; (2) checking deposit type classification using descriptive information and geologic maps and excluding deposits that are not of the appropriate type; (3) eliminating duplicates from the database; (4) identifying sites that are explicitly described as being incompletely explored; and (5) verifying that the spatial aggregation rule of 500 m is correctly applied. Deposits that are not SSC deposits (for example, the Nama cobalt-copper deposits in the CACB, appendix A, this report) and sites that could not be characterized by type due to lack of information (such as Aynak, Afghanistan; Abdullah and others, 1980; Peters and Bawiec, 2007) were excluded. Two partially explored sites in the Kodar-Udokan area were excluded because the formal mineral inventory established by drilling and sampling (C category resources) was less than the predicted undiscovered mineral estimate (prognostic resource; Diatchkov, 1994; Jakubiak and Smakowski, 1994 Arkhangel'skaya and others, 2004).

Qieke and Yaojianzi (Yan and others, 2010); Lochaber Lake (Kirkham and others, 1994; Cox and others, 2003); Shangolowe, Etoile Extension, and Nundo (appendix A, this report); and the Kona Dolomite (Wilband, 1978) were identified as outliers that fell outside the 99th density ellipses on bivariate plots of log tonnage versus log copper grade (fig. 2-15). The most likely reasons that these points are outliers are incomplete delineation of resources or the use of a cutoff grade that is substantially different than that used for the rest of the deposits in the database. The Snowstorm deposit, a high-copper-grade outlier for the sandstone copper deposits, was also excluded because the limited information on this deposit suggests that high-grade material was selectively mined in the early 1900s (Timberline Resources, 2012; Boleneus and others, 2005).

Exploratory Data Analysis

Models are more likely to be stable if (1) data from at least 20 deposits are used in model construction, (2) tonnage and grades of commodities that constitute less than 10 percent of the ore are not significantly different from a lognormal distribution, (3) standard deviations for tonnage (expressed in logarithms) are less than 1.0, and (4) tonnage and grade are not significantly correlated (Singer and Menzie, (2010).

In order to prevent undue influence of one or more failures in the data, a large number of deposits in the models

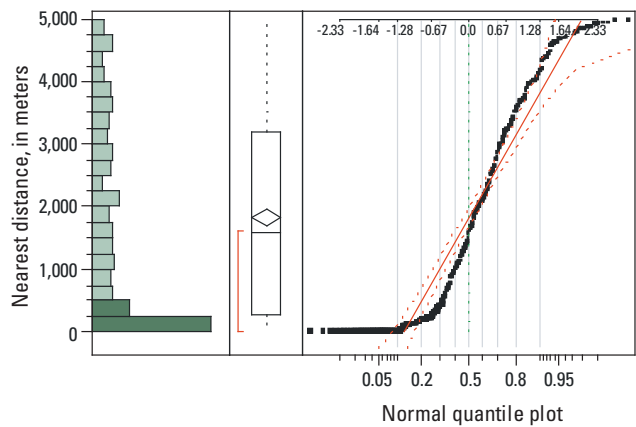


Figure 2-13. Histogram, box plot, and normal quantile plot illustrating the distribution of the nearest distance and log (nearest distance) between the edges of sediment-hosted copper ore bodies/open pits in the Central African Copperbelt. Highlighted histogram intervals and points show ore bodies that are within 500 meters of each other.

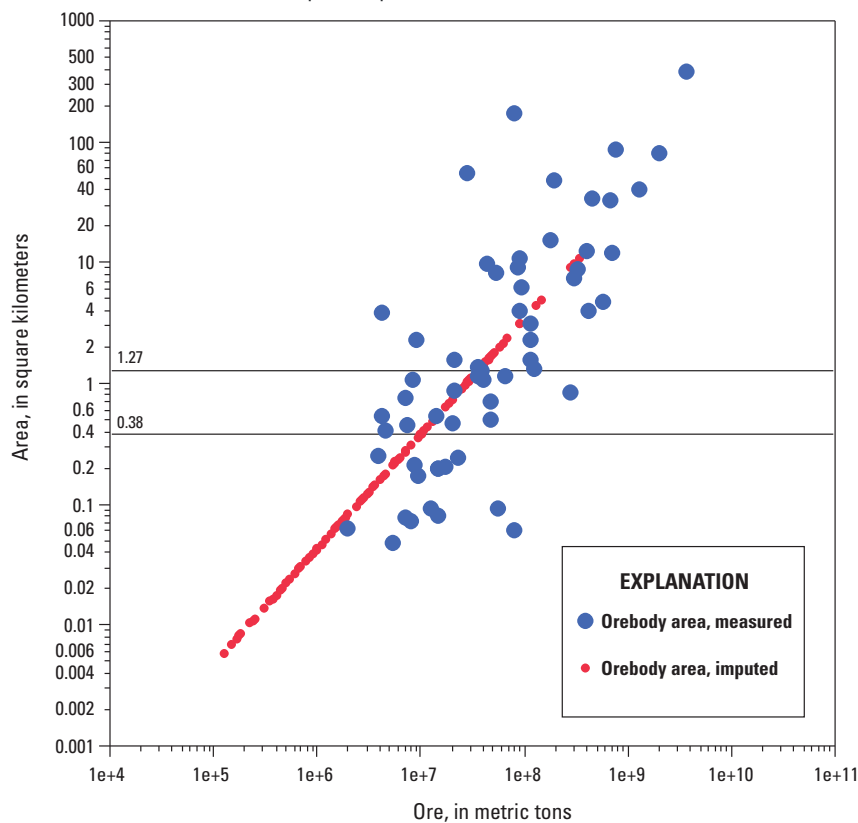
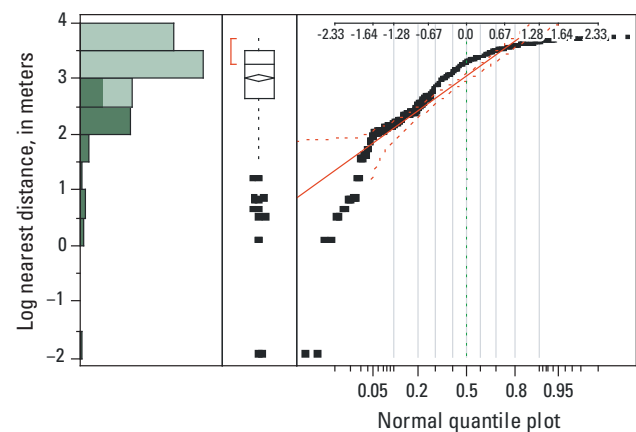


Figure 2-14. Bivariate plot of ore tonnage versus ore body area, projected to the surface. Median area of measured values is 1.27 square kilometers (km²); median area of measured and imputed values is 0.38 km².

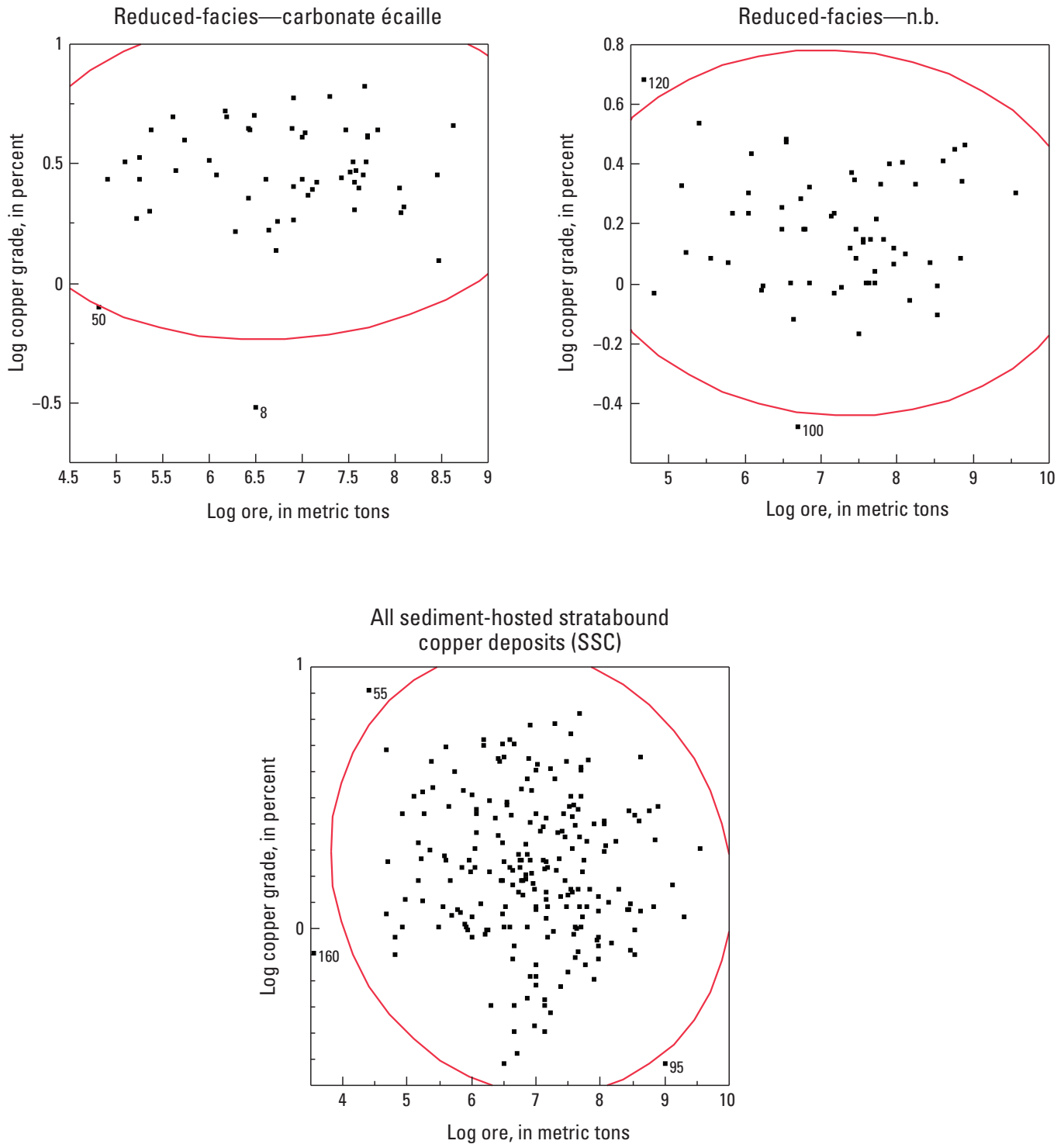


Figure 2-15. Bivariate plots of log copper grade versus log ore, metric tons for all sediment-hosted stratabound copper, reduced-facies—carbonate écaillé, and reduced-facies—n.b. deposits. Numbered points are outliers: 8, Etoile Extension (DRC); 50, Nundo (DRC); 55, Shangolowe (DRC); 95, Kona Dolomite (USA); 100, Locaber Lake (Canada); 120, Yaojianzi (China); 160, Qieke (China). The curved red lines are the 99th percentile density ellipses.

will help insure the sample mean and standard deviation are an unbiased estimate of the mean and standard deviation of the true population. At the minimum, a grade and tonnage model should be based on 20 deposits (Singer and Menzie, 2010).

Classical hypothesis tests assume that the observations are (1) independent; (2) come from populations with the same variance, and, for parametric tests; and (3) follow a normal distribution (Van Belle, 2008). Homogeneous populations of variables representing weights, lengths, volumes, and grades of trace quantities of a commodity (less than 10 percent) are positively skewed and usually deviate from a normal distribution. These variables can be represented with a lognormal distribution; in other words, log-transformed values of these variables follow a normal distribution (Singer, 2011). Log-transformed values of tonnage and grade were tested to determine if they are not significantly different than the normal distribution. If they were not, the distributions can be used in parametric statistical tests. Plots and statistics were used to discover if the data contained multiple populations or outliers and the data was screened to determine if tonnage and grade are significantly correlated.

After removing outliers, the standard deviation of log tonnage for all stratabound sediment-hosted deposits was 0.98. In order to reduce the standard deviation, deposits with less than 10,000 metric tons of contained copper were excluded. Most of the excluded sites belong to the sandstone copper deposit type. These small sites may not be fully explored or of economic interest in current market conditions. The standard deviation for the distribution of log tonnage of the remaining 170 SSC is 0.78.

For this report, five grade and tonnage models are described below. The distribution of values in each model is characterized by a histogram, an outlier box plot, a normal quantile plot, and cumulative frequency plots; summary statistics for each model are given in table 2-3.

Normal models were fit to each log-transformed distributions of tonnage and grade and goodness of fit tested using the Shapiro-Wilk test for the normal model (Scholtzhauer, 2007; table 2-4). Distributions of log-transformed values of ore tonnage, grade, and contained copper are not rejected at the 99th percent confidence limit and fall within the confidence interval for normality on normal quantile plots. For the purposes of comparing populations and testing correlations, log-transformed values of ore tonnage and grade will be used. Pearson correlation coefficients (r) were calculated between tonnage and grade; for all the sediment-hosted stratabound deposits, r values between tonnage and grade are low and not significant at the 99th percent confidence limit.

Histograms for some of the frequency distributions have multiple modes (a distribution with two modes is bimodal; multiple modes is multimodal). If the log-transformed data are normally distributed, they should follow a straight line on the normal quantile plots. The patterns of distributions with multiple modes on the corresponding quantile plots deviate from the straight line, forming curved patterns or line segments with different slopes. Multiple modes may indicate

that the sample is not homogeneous and that the observations are from two or more overlapping distributions. However, none of the multimodal distributions observed in this study were pronounced enough to cause the assumption of normality for log-transformed values to be rejected when using a Shapiro-Wilk goodness of fit test.

Grade and Tonnage Model for Sediment-Hosted Stratabound Copper Deposits

The grade and tonnage model is based on 170 SSC deposits (figs. 2-16 and 2-17); summary statistics are given in table 2-3. Median and mean values for (1) ore tonnage are 14 and 98 million metric tons and for (2) copper grades are 1.6 and 2.0 percent, respectively. Distributions of ore tonnage, copper grade, and contained copper are all positively skewed and consistent with a normal model (table 2-4). Cobalt and silver data are missing for 72 and 78 percent of the samples, respectively (table 2-5). The standard deviation of log-transformed value of deposit tonnage is less than one for this model (0.78). Log-transformed values of copper grades do not show significant correlation with log-transformed values of deposit tonnage (table 2-6).

Grade and Tonnage Model for Sediment-Hosted Stratabound Copper Deposits in the Central African Copperbelt

The grade and tonnage model is based on 77 SSC deposits in the CACB (figs. 2-18 and 2-19); summary statistics are given in table 2-3. Median and mean values for (1) ore tonnage are 14 and 72 million metric tons and for (2) copper grades are 2.7 and 3.0 percent, respectively. Distributions of ore tonnage, copper grade, and contained copper are all positively skewed and consistent with a normal model (table 2-4). Cobalt and silver data are missing for 48 and 99 percent of the samples, respectively (table 2-5). The standard deviation of log-transformed value of deposit tonnage is less than one for this model (0.79). Log-transformed values of copper grades do not show significant correlation with log-transformed values of deposit tonnage (table 2-6). Histograms for log tonnage and log copper are bimodal (fig. 2-18).

Grade and Tonnage Model for Reduced-Facies—Nonbrecciated (n.b.) Deposits

The grade and tonnage model is based on 50 reduced-facies—n.b. deposits (figs. 2-20 and 2-21); summary statistics are given in table 2-3. Median and mean values for (1) ore tonnage are 34 and 180 million metric tons and for (2) copper grades are 1.5 and 1.6 percent, respectively. Distributions

Table 2-3. Summary statistics for sediment-hosted stratabound copper deposit models.

[SSC, sediment-hosted stratabound copper; CACB, Central African Copperbelt; n.b., nonbrecciated; –, no data or not applicable]

Deposit type	Number of deposits	Mean	Quantile 5th	Quantile 10th	Quantile 25th	Median	Quantile 75th	Quantile 90th	Quantile 95th
Ore, million metric tons									
SSC	170	98	1.0	1.6	4.4	14	48	170	430
SCC in CACB	77	72	0.54	1.5	4.4	14	47	280	430
Reduced-facies—carbonate écaïlle	50	42	0.42	1.0	2.9	10	42	110	290
Reduced-facies—n.b.	50	180	1.1	1.6	6.2	34	97	550	730
Sandstone copper	70	77	1.1	1.9	4.5	10	39	91	310
Sandstone copper—Roan arenite	20	34	2.0	3.9	6	11	39	47	320
Copper grade, percent									
SSC	170	2.0	0.5	0.7	1.1	1.6	2.7	4.2	4.9
SCC in CACB	77	3.0	1.2	1.6	1.9	2.7	4.0	4.9	5.5
Reduced-facies—carbonate écaïlle	50	3.3	1.3	1.7	2.4	2.9	4.3	5.0	5.9
Reduced-facies—n.b.	50	1.6	0.8	0.9	1.0	1.5	2.1	2.5	2.8
Sandstone copper	70	1.4	0.5	0.5	0.8	1.2	1.7	2.6	3.7
Sandstone copper—Roan arenite	20	2.4	0.8	0.8	1.5	1.7	3.3	4.9	5.5
Silver grade, grams per metric ton									
SSC	38	35	5	7	12	22	52	73	110
SCC in CACB									
Reduced-facies—carbonate écaïlle	1	8.1	8.1	1.0	8.1	8.1	8.1	8.1	8.1
Reduced-facies—n.b.	19	33	2.4	5.0	10	17	45	110	140
Sandstone copper	18	38	8.0	11	13	32	64	73	93
Sandstone copper—Roan arenite	0	–	–	–	–	–	–	–	–
Cobalt grade, percent									
SSC	48	0.4	–	–	0.1	0.3	0.6	1.1	1.7
SCC in CACB	44	0.5	–	–	–	0.3	0.6	1.1	1.8
Reduced-facies—carbonate écaïlle	36	0.6	0.0	0.1	0.2	0.4	0.7	1.2	2.0
Reduced-facies—n.b.	9	0.1	–	–	0.03	0.1	0.1	0.3	0.3
Sandstone copper	3	0.1	–	–	–	–	0.2	0.2	0.2
Sandstone copper—Roan arenite	3	0.1	–	–	–	–	0.2	0.2	0.2
Contained copper metal, million metric tons									
SSC	170	1.8	0.017	0.25	0.023	0.067	0.94	2.8	9.5
SCC in CACB	77	2.0	0.021	0.051	0.11	0.34	1.4	4.6	15
Reduced-facies—carbonate écaïlle	50	1.3	0.016	0.031	0.077	0.36	1.3	2.8	5.5
Reduced-facies—n.b.	50	3.5	0.016	0.023	0.1	0.46	1.4	10	19
Sandstone copper	70	1.0	0.016	0.018	0.054	0.12	0.41	1.0	5.5
Sandstone copper—Roan arenite	20	0.81	0.059	0.062	0.11	0.28	0.54	1.8	8.5

38 Descriptive Models, Grade-Tonnage Relations, and Databases for the Assessment of Sediment-Hosted Copper Deposits

Table 2-4. Goodness of fit statistics (based on the Shapiro-Wilk *W* test) for stratabound sediment-hosted copper deposits.

[Log-transformed values; fitted normal. SSC, sediment-hosted stratabound copper deposits; CACB, Central African Copperbelt; n.b., nonbrecciated; –, no data or not applicable; Prob<*W*, probability less than *W* * indicates values of probability very close to zero that may indicate that the data are not a sample from a normal distribution]

Deposit subtype	Tonnage		Copper grade		Silver grade		Cobalt grade		Contained copper	
	<i>W</i>	Prob< <i>W</i>	<i>W</i>	Prob< <i>W</i>	<i>W</i>	Prob< <i>W</i>	<i>W</i>	Prob< <i>W</i>	<i>W</i>	Prob< <i>W</i>
All SSC	0.989488	0.2404	0.990006	0.2776	0.976119	0.5807	0.967535	0.2470	0.977633	0.0076*
All SSC—CACB	0.985722	0.5448	0.978185	0.2708			0.983795	0.8257	0.982705	0.3796
Reduced-facies—n.b.	0.981011	0.5953	0.971594	0.2684	0.983219	0.9730	—	—	0.980919	0.5913
Reduced-facies—carbonate écaillé	0.983658	0.7127	0.973828	0.3289	—	—	0.986108	0.9285	0.979055	0.5128
Sandstone copper	0.955071	0.0135*	0.0.980641	0.3515	0.919479	0.1266	—	—	0.952190	0.0095*
Sandstone copper—Roan arenite	0.942759	0.2702	0.959034	0.5247	—	—	—	—	0.922274	0.1096

Table 2-5. Numbers of deposits reporting cobalt (Co) and silver (Ag) by subtype.

[SSC, sediment-hosted stratabound copper deposits; CACB, Central African Copperbelt; n.b., nonbrecciated]

Deposit type or subtype	Number of deposits	Number of deposits reporting Co	Number of deposits reporting Ag	Co, percent missing	Ag, percent missing
All SSC deposits	170	48	38	72	78
SSC—CACB deposits	77	40	1	48	99
Reduced-facies—carbonate écaillé	50	36	1	28	98
Reduced-facies—n.b.	50	9	19	82	62
Sandstone copper	70	3	19	96	73
Sandstone copper—Roan arenite	20	3	0	85	100

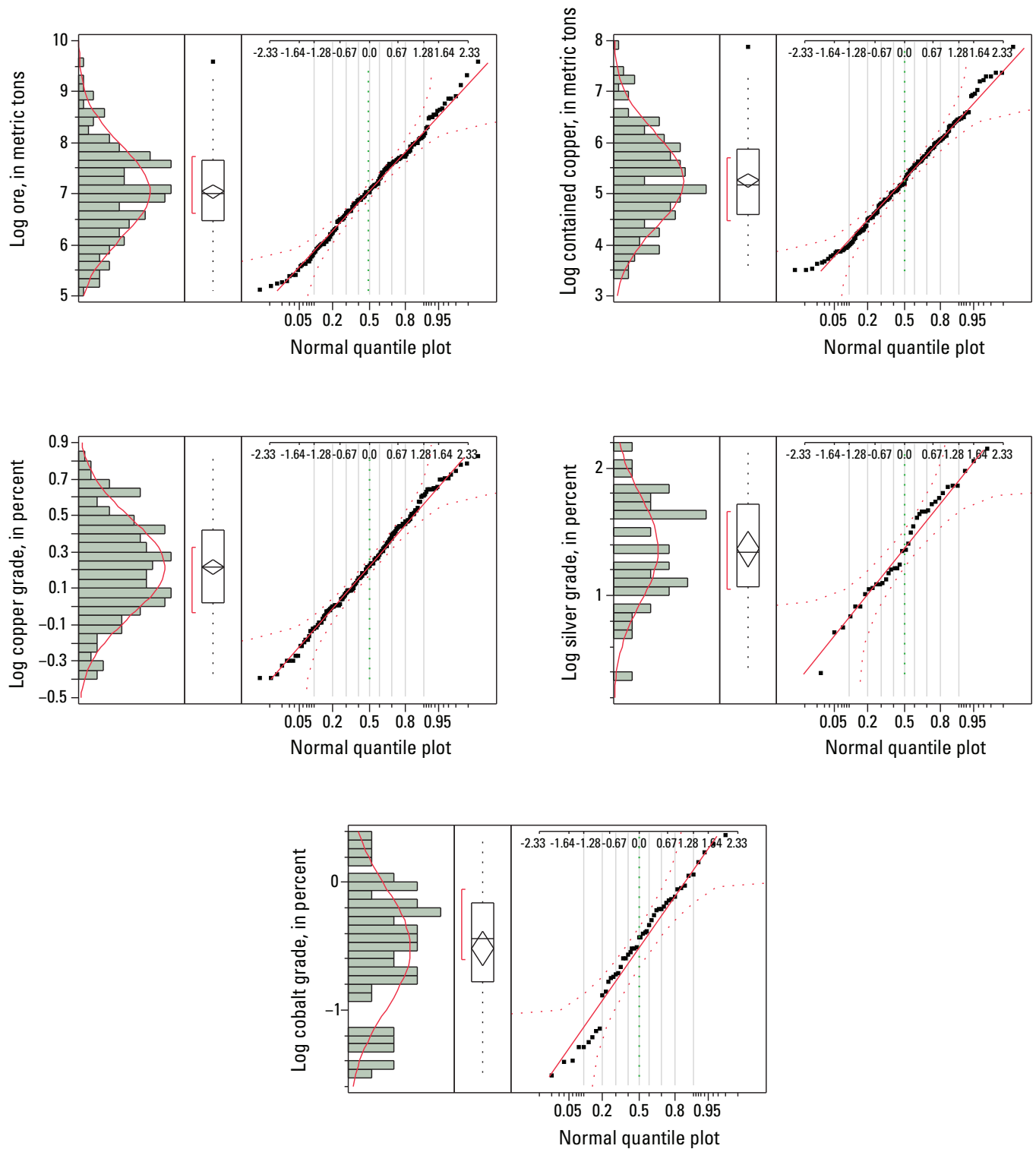


Figure 2-16. Histogram, box plot, and normal quantile plot illustrating the distribution of log-transformed values for tonnage, grade, and contained copper of 170 sediment-hosted stratabound copper deposits.

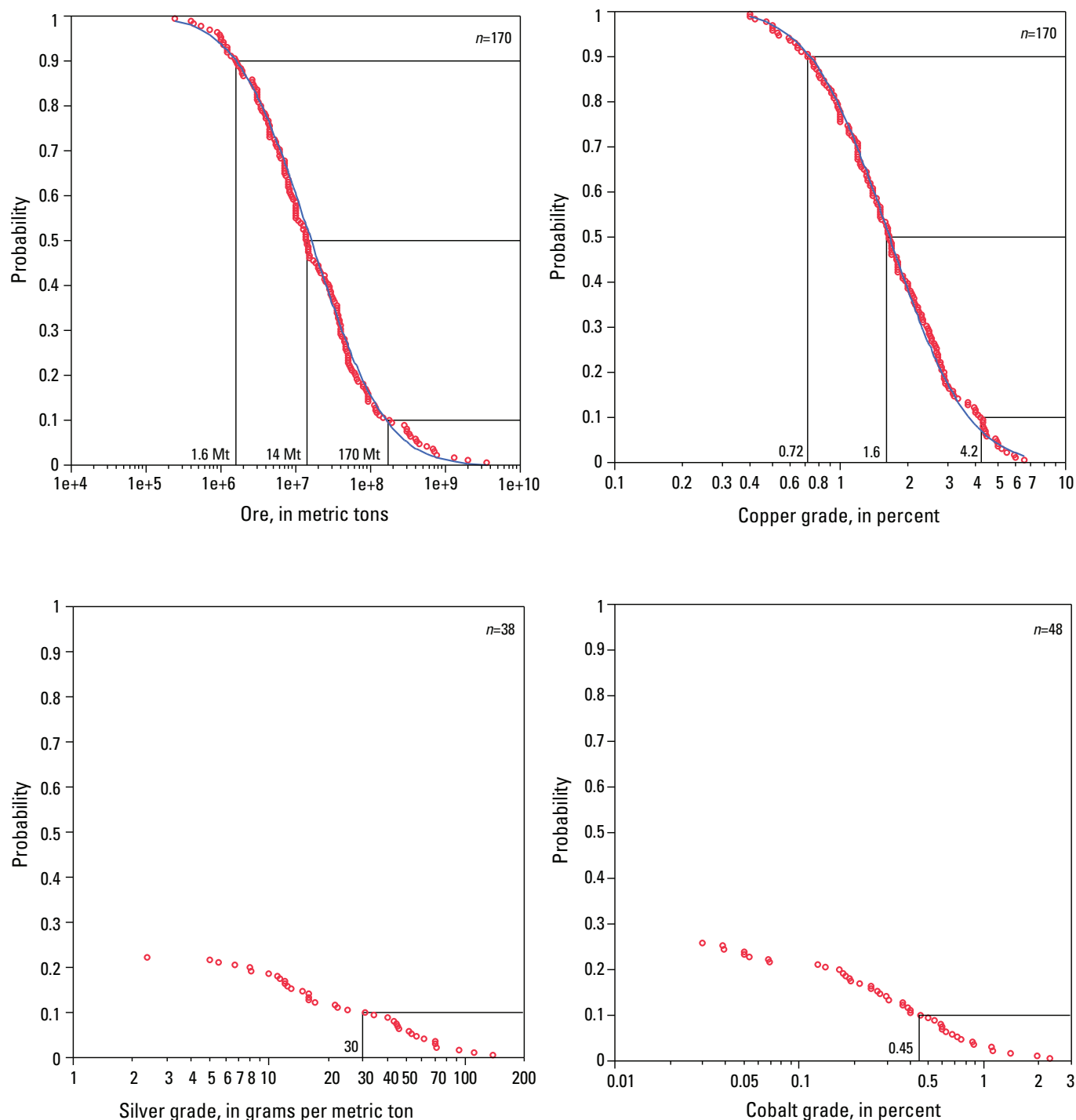


Figure 2-17. Cumulative frequency plots of grade and tonnage for 170 sediment-hosted stratabound copper deposits. Each red circle is a data point for a deposit; the blue curve is the calculated lognormal distribution based on the population parameters of the data. Values for tonnage and grade for the 90th, 50th, and 10th probability values of the distribution are illustrated by extending a horizontal line from the vertical axis to the data curve, then drawing a vertical line to the horizontal axis. The value for the point where the vertical line intersects the horizontal axis is labeled. For some deposits, values for some metals are not reported, resulting in a censored or truncated dataset. For these metals, only the probability values for the data points with reported values are illustrated. Mt, million metric tons.

Table 2-6. Summary of tonnage and grade distributions for sediment-hosted stratabound copper deposits with recommendations for their use in resource modeling.

[CACB, Central African Copperbelt; n.b., nonbrecciated]

Deposit type or subtype	Lognormal distribution	At least 20 deposits	Standard deviations for log tonnages less than 1.0	No significant correlation between log tonnage and log copper grade	Appropriate usage
Sediment-hosted stratabound copper deposits	yes	170	0.7844376	– 0.1002	A frequency distribution using all sediment hosted deposits. May overestimate copper outside CACB and underestimate copper within the CACB. Silver and cobalt numbers may also be biased.
Sediment-hosted stratabound copper in the CACB	yes	77	0.7935138	– 0.1602	A frequency distribution using all CACB sediment hosted deposits. For use in the Katanga Basin, where separate tracts for reduced-facies and sandstone-type copper deposits cannot be distinguished.
Reduced-facies—n.b.	yes	50	0.8627252	0.0533	Reduced-facies copper mineralization (nonbrecciated) in any sedimentary basin other than the Katanga
Reduced-facies—carbonate écaïlle	yes	50	0.7856822	– 0.1845	Katanga Basin, for reduced-facies deposits associated with salt dissolution breccias.
Sandstone copper	yes	70	0.6881622	– 0.0903	Sandstone copper deposits in sedimentary basins other than the Katanga
Sandstone copper—Roan arenite	yes	20	0.5215564	– 0.1469	Sandstone copper deposits in Katanga Basin

of ore tonnage, copper grade, and contained copper are all positively skewed and consistent with a normal model (table 2-4). Cobalt and silver data are missing for 82 and 62 percent of the samples, respectively (table 2-5). The standard deviation of log-transformed value of deposit tonnage is less than one for this model (0.86). Log-transformed values of copper and cobalt grades do not show significant correlation with log-transformed values of deposit tonnage (table 2-6).

Grade and Tonnage Model for Reduced-Facies—Carbonate Écaïlle Deposits

The grade and tonnage model is based on 50 reduced-facies—carbonate écaïlle deposits (figs. 2-22 and 2-23); summary statistics are given in table 2-3. Median and mean values for (1) ore tonnage are 10 and 42 million metric tons and for (2) copper grades are 2.9 and 3.3 percent, respectively. Distributions of ore tonnage, copper grade, and contained copper

are all positively skewed and consistent with a normal model (table 2-4). Cobalt and silver data are missing for 28 and 98 percent of the samples, respectively (table 2-5). The standard deviation of log-transformed value of deposit tonnage is less than one for this model (0.78). Log-transformed values of copper and cobalt grades do not show significant correlation with log-transformed values of deposit tonnage (table 2-6). The histogram for log copper is bimodal (fig. 2-22); log tonnage may have multiple modes, but more data is required to be sure.

The bimodal distribution of copper grades may reflect the difference in copper grade between primary (hypogene) and supergene-enriched ores. Supergene processes result in the replacement of bornite by chalcocite, at or near the water table. For deposits with carbonate-rich host rocks, such as those that make up the carbonate-écaïlle deposits, weathering may produce oxide ores that are substantially enriched in copper relative to hypogene or supergene sulfide ores. During the Pliocene, oxidation and leaching formed cobalt caps in lateritic profiles over the carbonate-écaïlle deposits (Decree and

others, 2010). The same event created dissolution voids in the carbonate-rich lithologies which were filled by malachite in the form of laminated crusts and speleothems (De Putter and others, 2010). These malachite-rich rocks developed on the carbonate-*écaille* deposits were the principal ore type mined up to the late 1950s (Theys and Lee, 1958). Grades ranging up to 16 percent copper are reported early in the history of development of this type of deposit (table 2-7). Weed (1907) reports grades of 10 to 14 percent copper for the Kolvezi (Kolwezi), Musonoi, and Dikurwe mines. By the 1970s, mines in this same area (Dikuluwe and Mashamba East) were producing ores with 5 to 9 percent copper (fig. 2-24); current grades are 3 to 6 percent copper (table 2-7).

The normal quantile plots of tonnage for the reduced-facies, carbonate *écaille* show linear segments characterized

by different slopes (fig. 2-22). The variation shown on the histograms and normal quantile plots may reflect size differences of gigabreccia fragments in different tectonic settings. The mineralized layer appears to have been interlayered with salt beds (Jackson and others, 2003). Halokinetic deformation of the salt layers occurred after the copper-mineralizing event and formed two distinct styles of structures—(1) salt welds³ along thrusts and (2) salt diapirs and walls (Garlick and Fleisher, 1972; Jackson and others, 2003). During halokinesis, the mineralized layer, in dolomitic formations or other competent units, was broken into fragments ranging in size from about 1 to 10 km. The breccia matrix is a pelite or a dolomitic, chloritic, talcose siltstone (François and Cailteux, 1981; Jackson and others, 2003). These breccia fragments are

³**salt weld** Surface or zone joining strata originally separated by salt. The weld is a negative salt feature resulting from the complete or nearly complete removal of the intervening salt. The weld consists of brecciated, insoluble residue containing halite pseudomorphs or salt too thin to be resolved in reflection seismic data. The weld is usually but not always marked by structural discordance. Another distinctive feature of welds is a structural inversion above them (Jackson and Talbot, 1991).

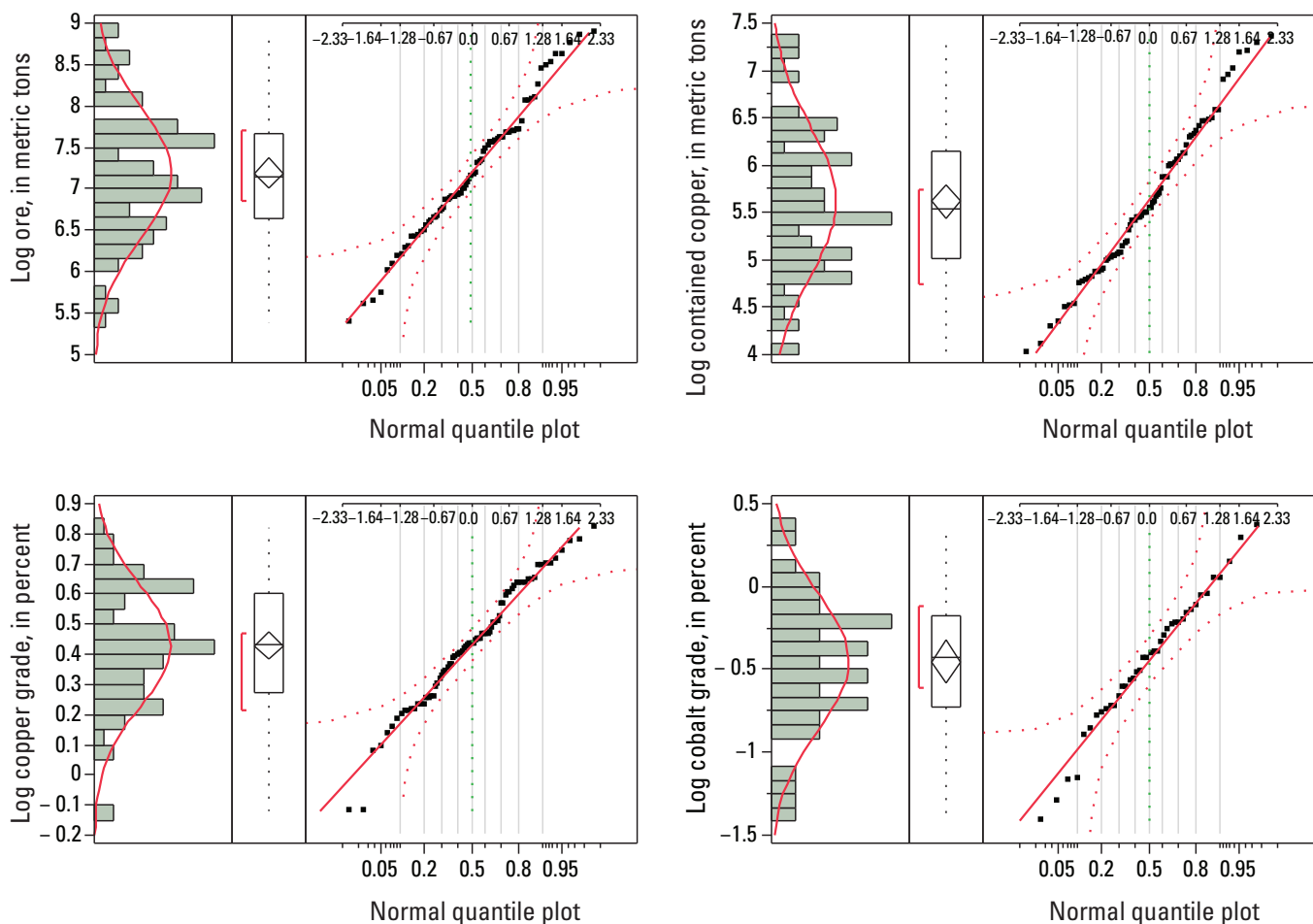


Figure 2-18. Histogram, box plot, and normal quantile plot illustrating the distribution of log-transformed values for tonnage, grade, and contained copper of 77 sediment-hosted stratabound copper deposits in the Central African Copperbelt.

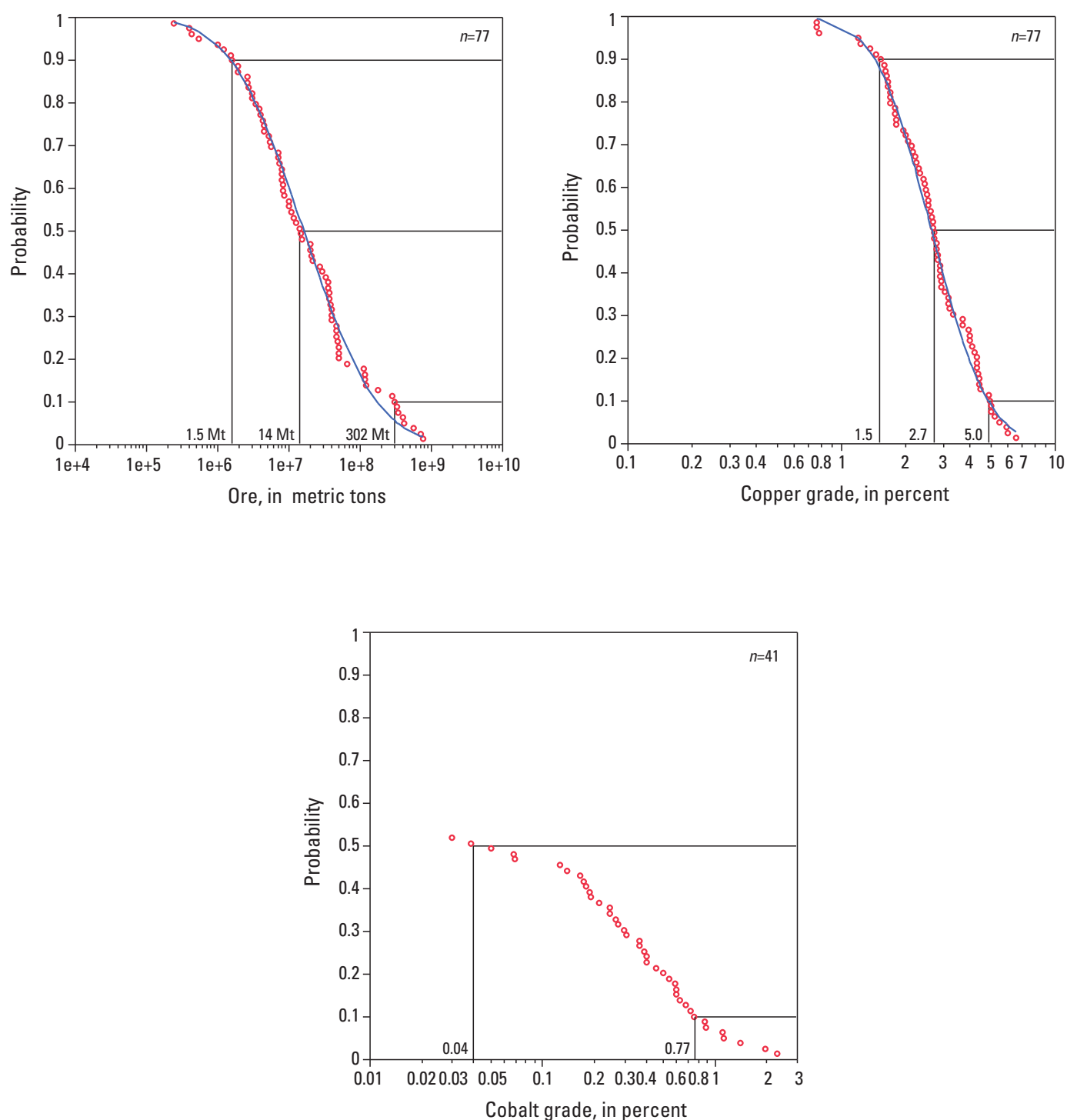


Figure 2-19. Cumulative frequency plots of grade and tonnage for 77 sediment-hosted stratabound copper deposits in the Central African Copperbelt. Each red circle is a data point for a deposit; the blue curve is the calculated lognormal distribution based on the population parameters of the data. Values for tonnage and grade for the 90th, 50th, and 10th probability values of the distribution are illustrated by extending a horizontal line from the vertical axis to the data curve, then drawing a vertical line to the horizontal axis. The value for the point where the vertical line intersects the horizontal axis is labeled. For some deposits, values for some metals are not reported, resulting in a censored or truncated dataset. For these metals, only the probability values for the data points with reported values are illustrated. Mt, million metric tons.

shown on the 1:100,000-scale geologic maps of the Likasi and Kolwezi areas (Musée Royal de l’Afrique Centrale, 2006a,b). Using GIS, the areas of the breccia fragments were measured. The large mineralized breccia fragments in the salt welds are larger than the fragments in the salt diapirs and salt walls (fig. 2-25). The size distribution of fragments associated with salt welds (thrust sheets) is statistically larger than fragments that occur in diapirs or anticlines (fig. 2-26). As a result, the larger breccias fragments in the salt welds can host larger tonnage deposits (fig. 2-27).

Grade and Tonnage Model for Sandstone Copper Deposits

The grade and tonnage model is based on 70 sandstone copper deposits (figs. 2-28 and 2-29; summary statistics are given in table 2-3. Median and mean values for (1) ore tonnage are 10 and 77 million metric tons, and (2) copper grades are 1.2 and 1.4 percent, respectively. Distributions

of ore tonnage, copper grade, and contained copper are all positively skewed and consistent with a normal model (table 2-4). Cobalt and silver data are missing for 96 and 73 percent of the samples, respectively (table 2-5). The standard deviation of log-transformed value of deposit tonnage is less than one for this model (0.69). Log-transformed values of copper and cobalt grades do not show significant correlation with log-transformed values of deposit tonnage (table 2-6). Log tonnage and log copper grade are still positively skewed after transforming the values using logarithms. The 5 giant sandstone copper deposits contribute to the positive skew for tonnage (table 2-2). The high copper grade values are associated with the CACB deposits.

Grade and Tonnage Model for Sandstone Copper—Roan Arenite

The grade and tonnage model is based on 20 sandstone copper deposits in the CACB (figs. 2-30 and 2-31); summary

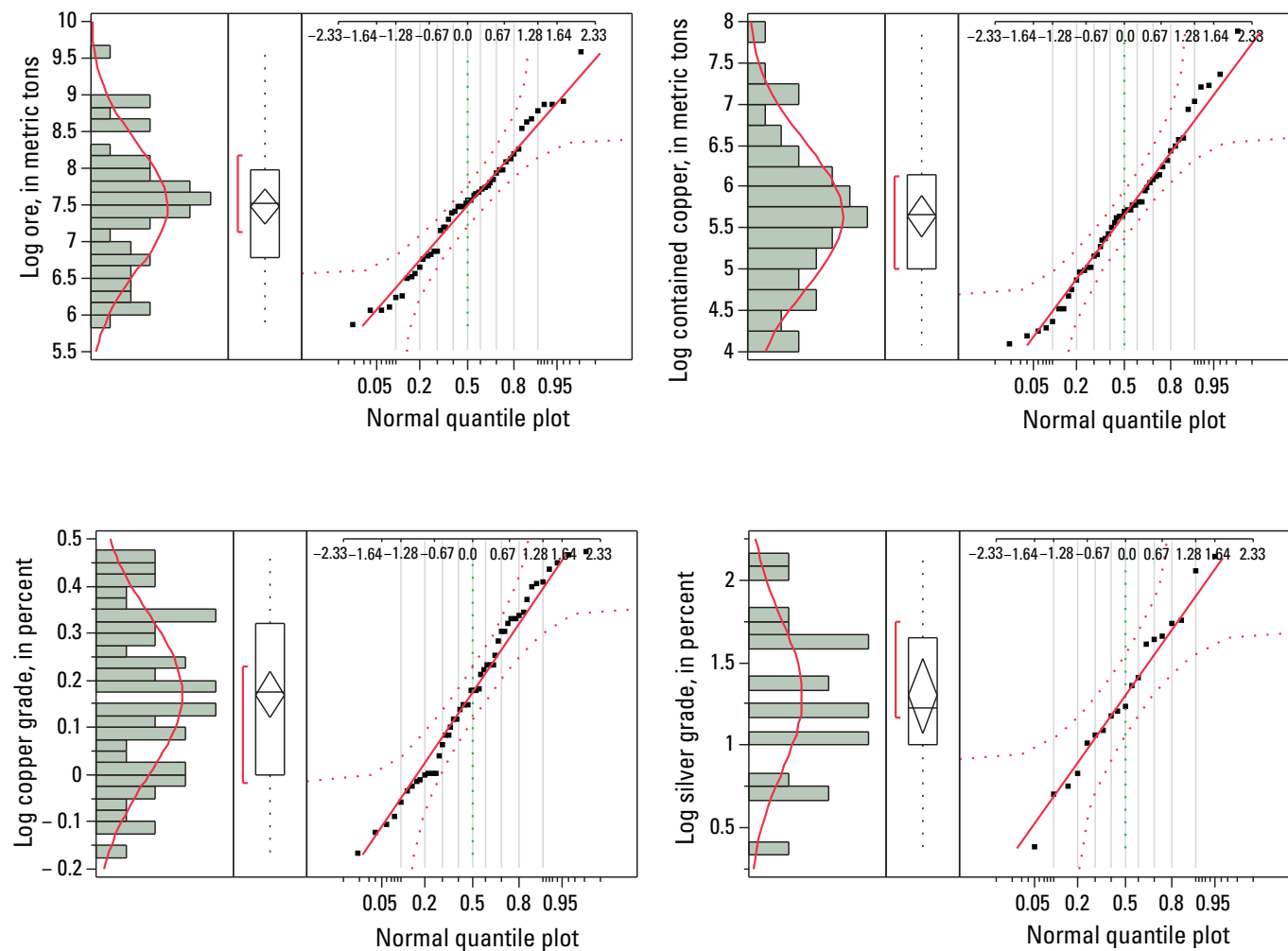


Figure 2-20. Histogram, box plot, and normal quantile plot illustrating the distribution of log-transformed values for tonnage, grade, and contained copper of 50 reduced-facies—n.b. copper deposits.

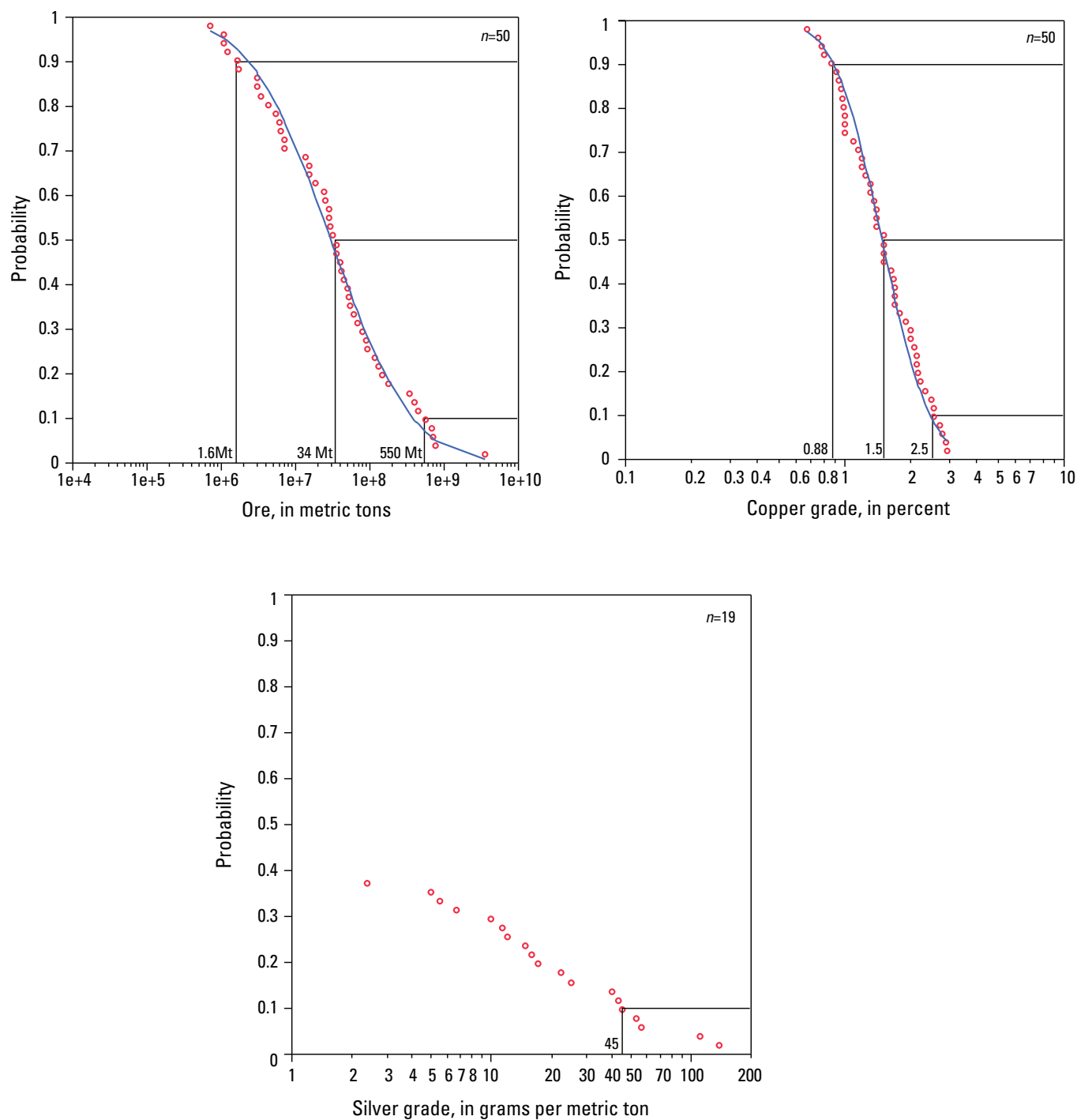


Figure 2-21. Cumulative frequency plots of grade and tonnage for 50 reduced-facies—n.b. copper deposits. Each red circle is a data point for a deposit; the blue curve is the calculated lognormal distribution based on the population parameters of the data. Values for tonnage and grade for the 90th, 50th, and 10th probability values of the distribution are illustrated by extending a horizontal line from the vertical axis to the data curve, then drawing a vertical line to the horizontal axis. The value for the point where the vertical line intersects the horizontal axis is labeled. For some deposits, values for some metals are not reported, resulting in a censored or truncated dataset. For these metals, only the probability values for the data points with reported values are illustrated. Mt, million metric tons.

statistics are given in table 2-3. Median and mean values for (1) ore tonnage are 11 and 34 million metric tons, and (2) copper grades are 1.7 and 2.4 percent, respectively. Distributions of ore tonnage, copper grade, and contained copper are all positively skewed and consistent with a normal model (table 2-4). Cobalt and silver data are missing for 96 and 73 percent of the samples, respectively (table 2-5). The standard deviation of log-transformed value of deposit tonnage is less than one for this model (0.52). Log-transformed values of copper and cobalt grades do not show significant correlation with log-transformed values of deposit tonnage (table 2-6).

Supergene processes result in the replacement of bornite by chalcocite at or near the water table in many sandstone copper deposits. Oxidation of the deposits in Zambia formed two zones, one in which copper has been leached to form a barren outcrop or gossan, and another in which there has been

nearly complete transformation of sulfide minerals to oxidized copper compounds, with grades similar to or slightly less than those of the original sulfide ores (Bateman, 1935). In the Zambian part of the CACB, supergene chalcocite is found in sandstone copper deposits such as Chibuluma West (Sweeney and Binda, 1994), Mufulira (Gray, 1932), and Bwana Mkubwa (Notebaart and Vink, 1972).

At Mufulira, the distribution of chalcocite shows an obvious relation to the surface and to horizons of deep leaching and oxidation (Gray, 1932). The grade of copper ores produced at Mufulira decreases from greater than 5 percent in the 1930s to slightly more than 2 percent in the 1990s. This trend probably reflects changing cutoff grades as the mine was developed but also records the mining of high grade supergene-enriched sulfide ores early in the production history of the mine (fig. 2-24).

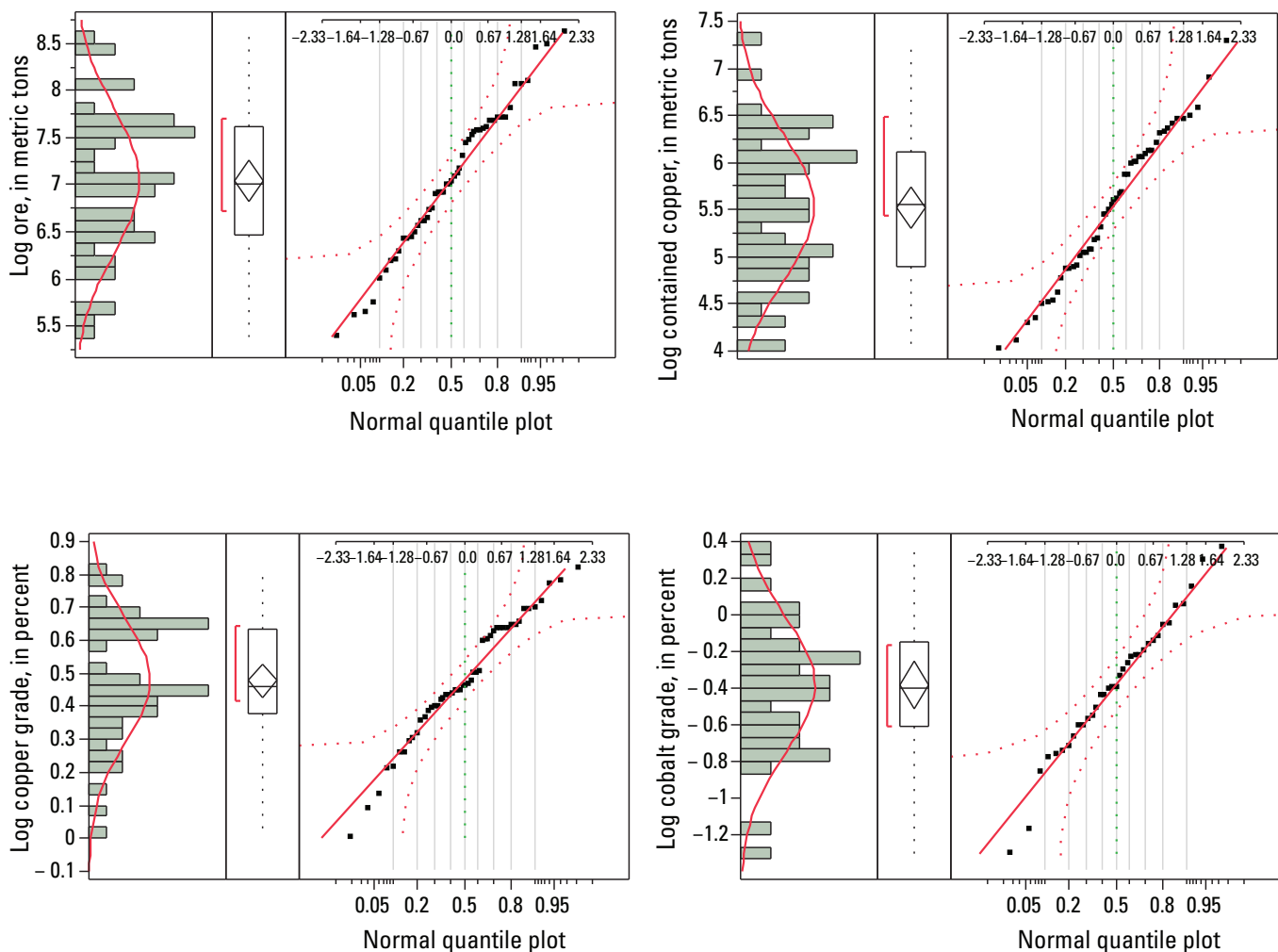


Figure 2-22. Histogram, box plot, and normal quantile plot illustrating the distribution of log-transformed values for tonnage, grade, and contained copper of 50 reduced-facies—carbonate-écaillé copper deposits.

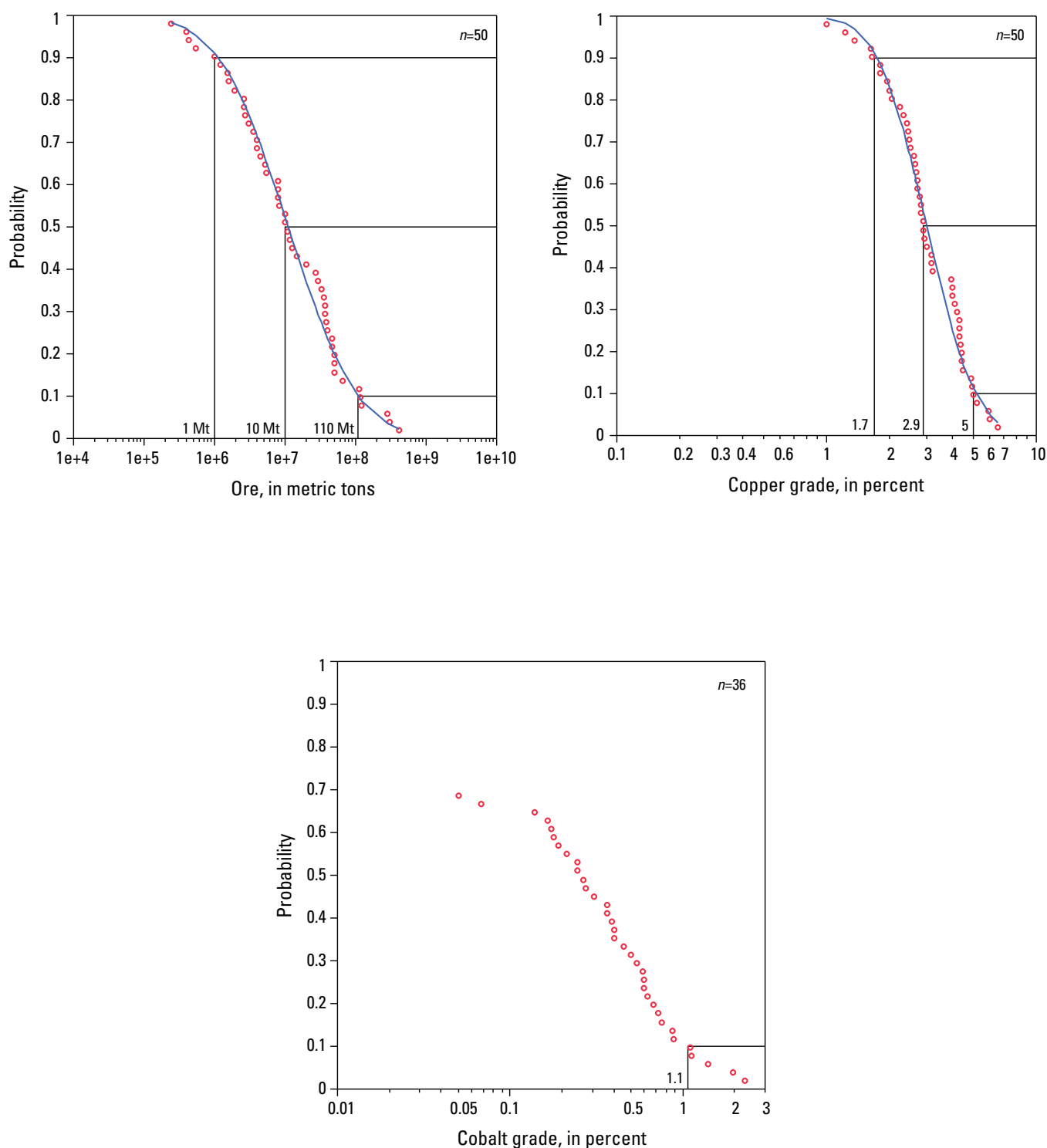


Figure 2-23. Cumulative frequency plots of grade and tonnage for 50 reduced-facies—carbonate-écaillé deposits. Each red circle is a data point for a deposit; the blue curve is the calculated lognormal distribution based on the population parameters of the data. Values for tonnage and grade for the 90th, 50th, and 10th probability values of the distribution are illustrated by extending a horizontal line from the vertical axis to the data curve, then drawing a vertical line to the horizontal axis. The value for the point where the vertical line intersects the horizontal axis is labeled. For some deposits, values for some metals are not reported, resulting in a censored or truncated dataset. For these metals, only the probability values for the data points with reported values are illustrated. Mt, million metric tons.

Table 2-7. Comparison of grades of oxidized ore formed on reduced-facies—carbonate *écaille* deposits mined early in the 20th century with grades reported for the same deposit area in this compilation.

Deposit	Copper, in percent, historic records	Material	Reference	Deposit in this compilation	Copper, in percent, this compilation
Kambove	14.8 to 16.0	Unsorted ore from shaly sandstone and high-grade carbonate ore	Weed (1907)	Kambove Principal-Kambove West	6.58
Kambove	11.80	Mill feed of oxidized ores (with malachite and chrysocolla) to Panda concentrator	Newton and Wilson (1942)		
Kolvezi, Musonoi, and Dikurwe	10.0 to 14.0	Quartz reefs and laminated sandstones	Weed (1907)	DIMA Kolwezi	2.78 6.0
Fungurume	6.0 to 8.0	Sandstone ore	Weed (1907)	Fungurume	4.32
Likasye	15 to 16.5		Weed (1907)	Likasi	Mined out

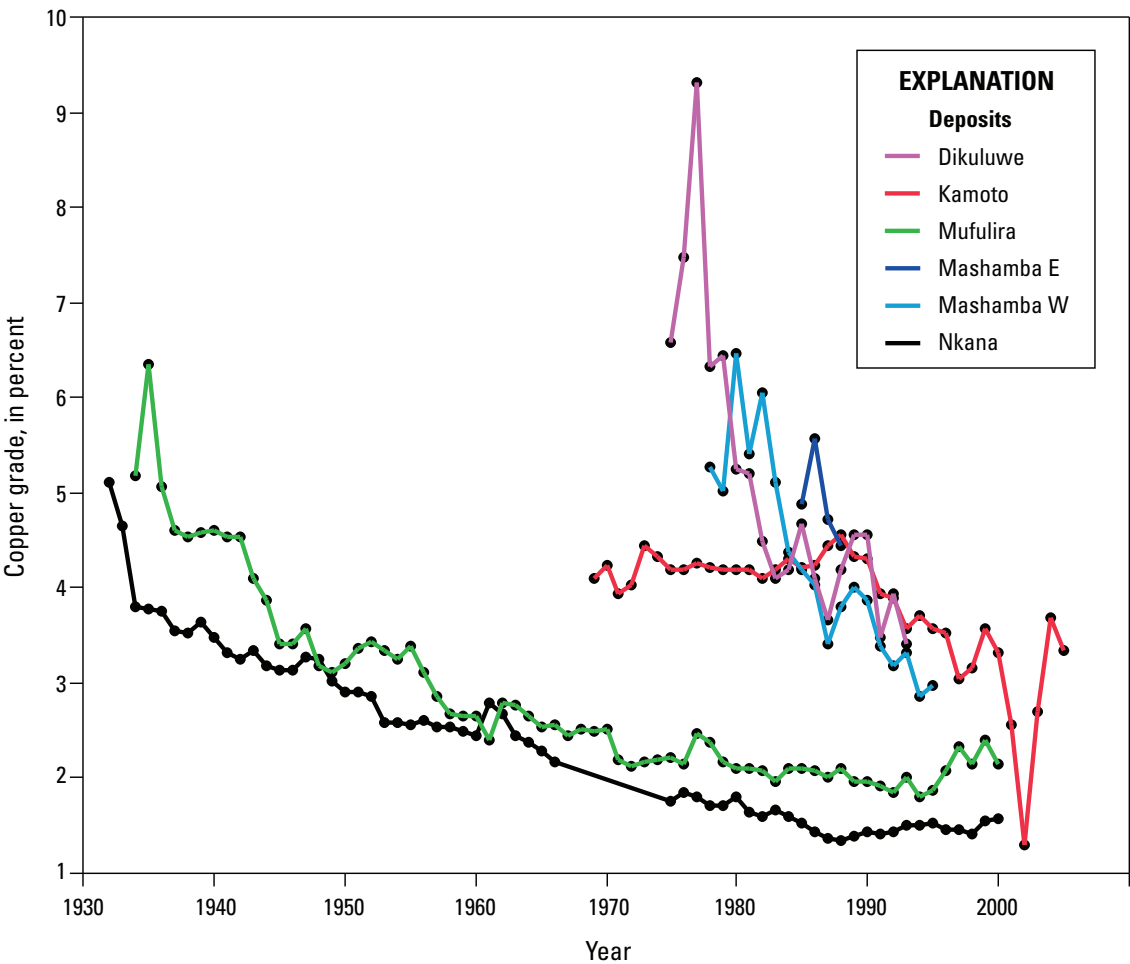


Figure 2-24. Graph showing the variation of copper grade by year for six sediment-hosted stratabound copper deposits in the Central African Copperbelt.

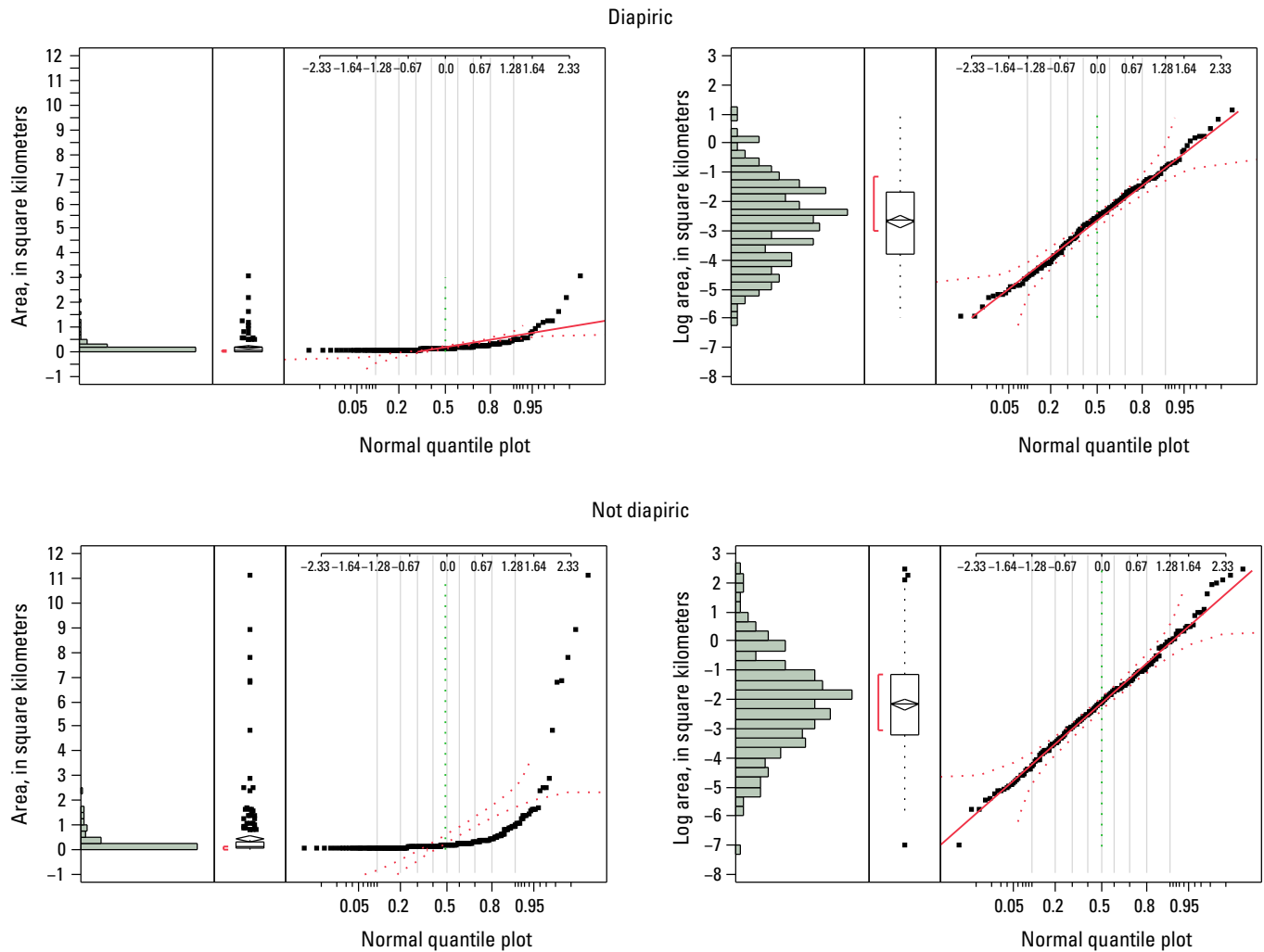


Figure 2-25. Histogram and normal quantile plots showing the distribution of surface area of Roan gigabreccia fragments on the Likasi and Kolwezi geologic maps. Classification of fragments into “diapiric” and “not diapiric” groups based on the polygons showing the limit of the diapir province illustrated on figure 12 of Jackson and others (2003).

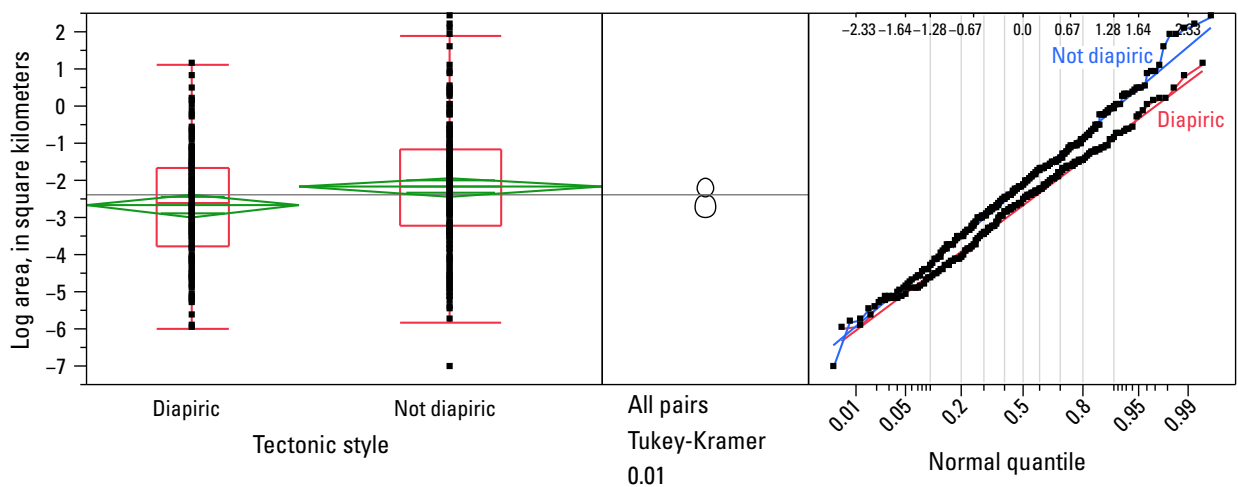


Figure 2-26. Quantile plots, comparison circles, and normal quantile plots comparing the surface area of Roan gigabreccia fragments on the Likasi and Kolwezi geologic maps. Classification of fragments into “diapiric” and “not diapiric” groups based on the polygons showing the limit of the diapir province illustrated on figure 12 of Jackson and others (2003).

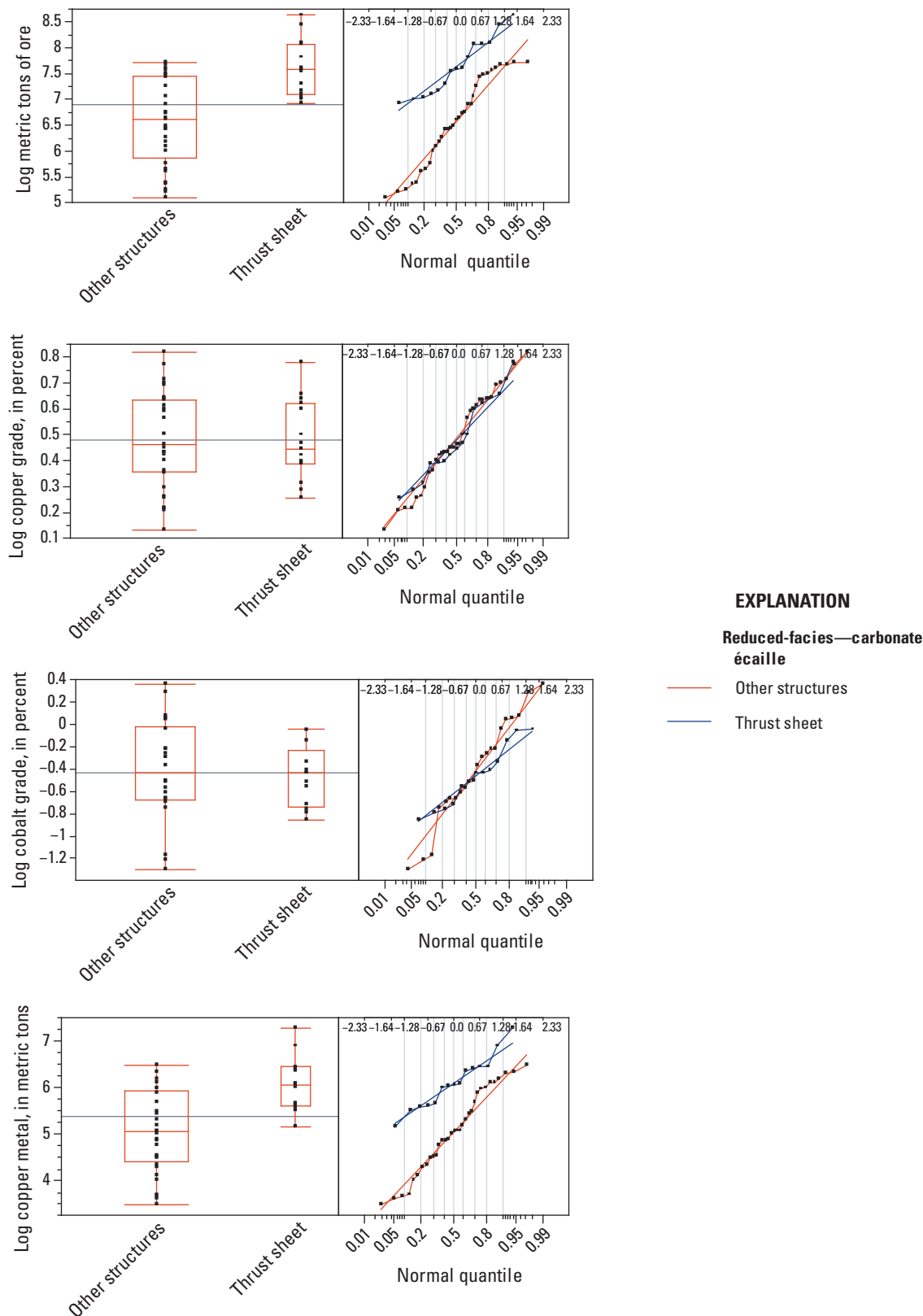


Figure 2-27. Box plot and normal quantile plot comparing the distribution of log-transformed values of ore tonnage, copper grade, cobalt grade, and contained copper of reduced-facies—carbonate écaïlle deposits in different tectonic settings, Central African Copperbelt. Thrust sheet includes salt welds; other structures includes salt diapirs and walls.

Missing Data

Missing data can cause bias to be introduced into studies, and statisticians note that missing data takes many forms (Schuenemeyer and Drew, 2011). When grade and tonnage models have been input into simulation software (Root and others, 1992; Bawiec and Spanski, 2012), missing grade data here have been coded as “zero.” This approach assumes that the data are not missing at random, but rather indicates little or no concentration of the metal of interest. However, the data could be missing for other reasons. In the following sections, possible reasons for missing data for cobalt and silver in the SSC models are discussed.

Cobalt and silver grades are reported for about 28 and 22 percent of SSC deposits, respectively (table 2-5). However, different types of SSC deposits have different proportions of missing data. Silver is rarely reported for all of the SSC deposits of the CACB. Most of the reported cobalt grades are associated with the reduced-facies—carbonate-*écaillé* deposits of the

CACB; cobalt is rarely reported for reduced-facies deposits outside the CACB or for any sandstone copper deposits.

Silver

Many other workers have noted the silver-poor character of the deposits in the CACB. The low concentration of silver, however, is hard to verify because few trace element analyses of CACB ores are published. The information that is available supports an interpretation that the missing values reflect low concentrations of silver in the mineralized rocks. Analyses of selected ore samples from the Bwana Mkubwa sandstone copper—Roan arenite deposit contain 5 to 9 grams per metric ton (g/t) silver (Pinaar, 1961). The silver grade of the reduced-facies deposit in the Konkola North area is 0.42 g/t, with a maximum single sample result of 14.62 g/t (Simposya and Hart, 2008). Three hundred seventy-five core composites from 35 boreholes in the Chambishi Southeast reduced-facies deposit were analyzed for silver. In 200 of those samples, the

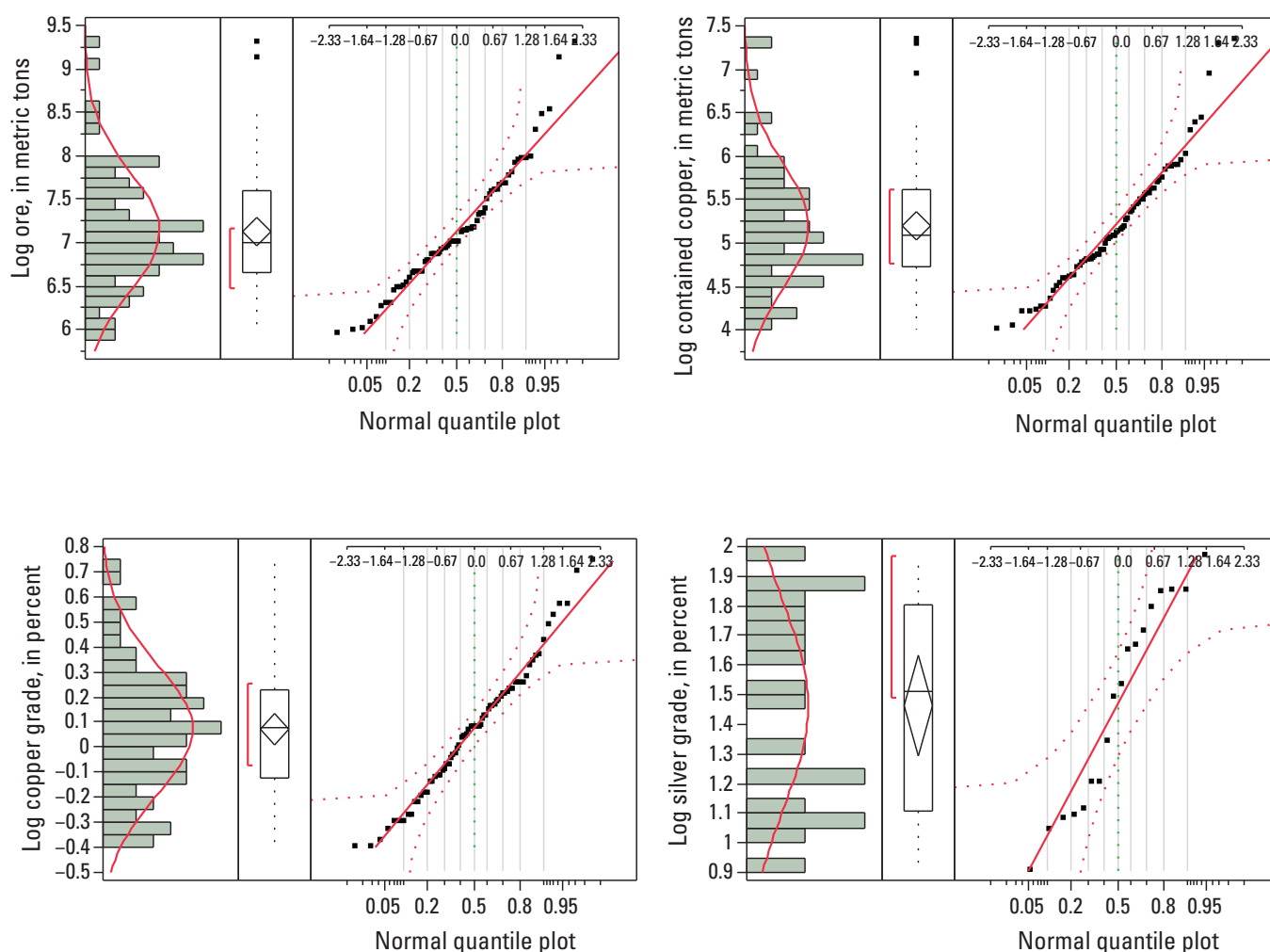


Figure 2-28. Histogram, box plot, and normal quantile plot illustrating the distribution of log-transformed values for tonnage, grade, and contained copper of 70 sandstone copper deposits.

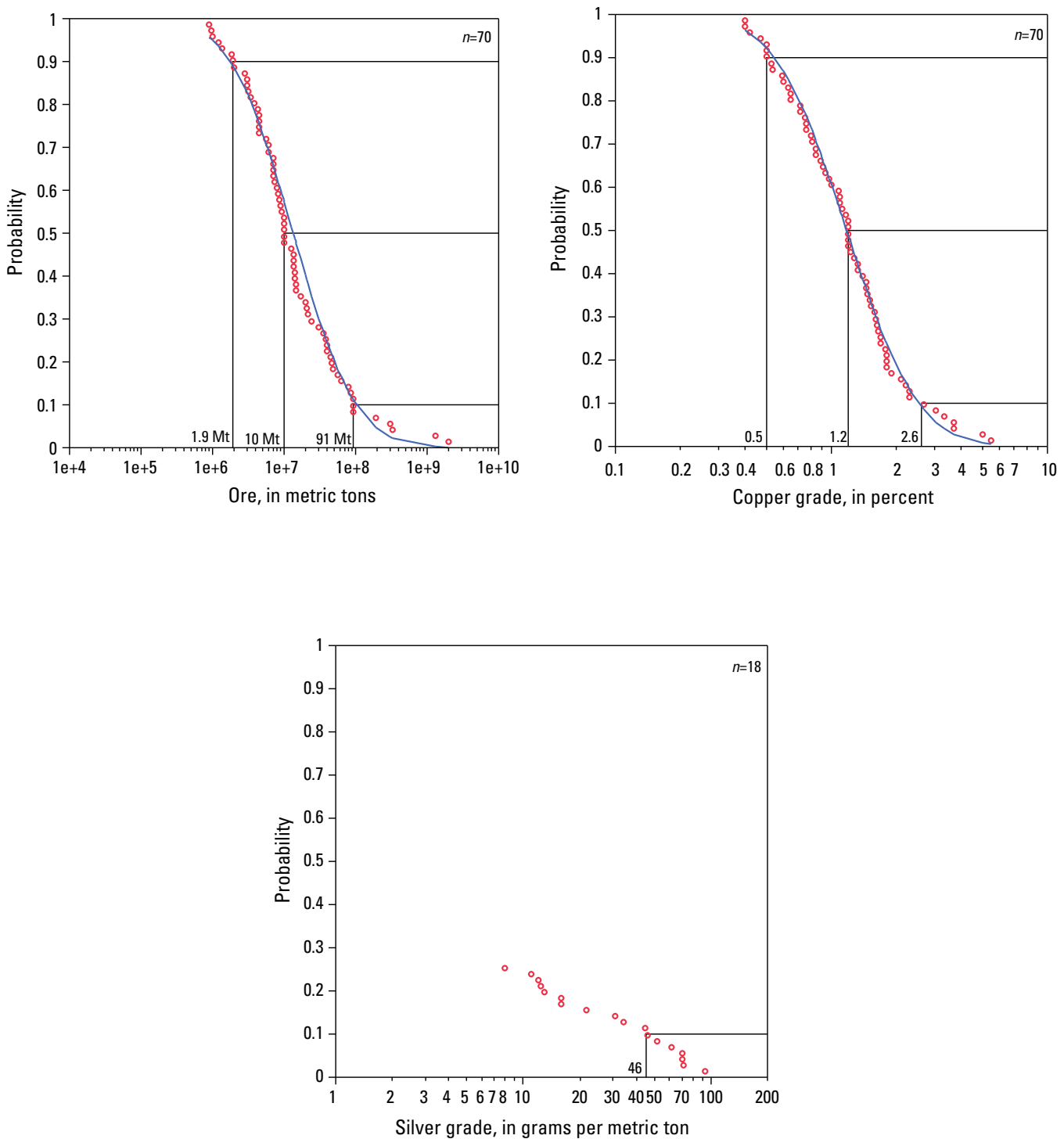


Figure 2-29. Cumulative frequency plots of grade and tonnage for 70 sandstone deposits. Each red circle is a data point for a deposit; the blue curve is the calculated lognormal distribution based on the population parameters of the data. Values for tonnage and grade for the 90th, 50th, and 10th probability values of the distribution are illustrated by extending a horizontal line from the vertical axis to the data curve, then drawing a vertical line to the horizontal axis. The value for the point where the vertical line intersects the horizontal axis is labeled. For some deposits, values for some metals are not reported, resulting in a censored or truncated dataset. For these metals, only the probability values for the data points with reported values are illustrated. Mt, million metric tons.

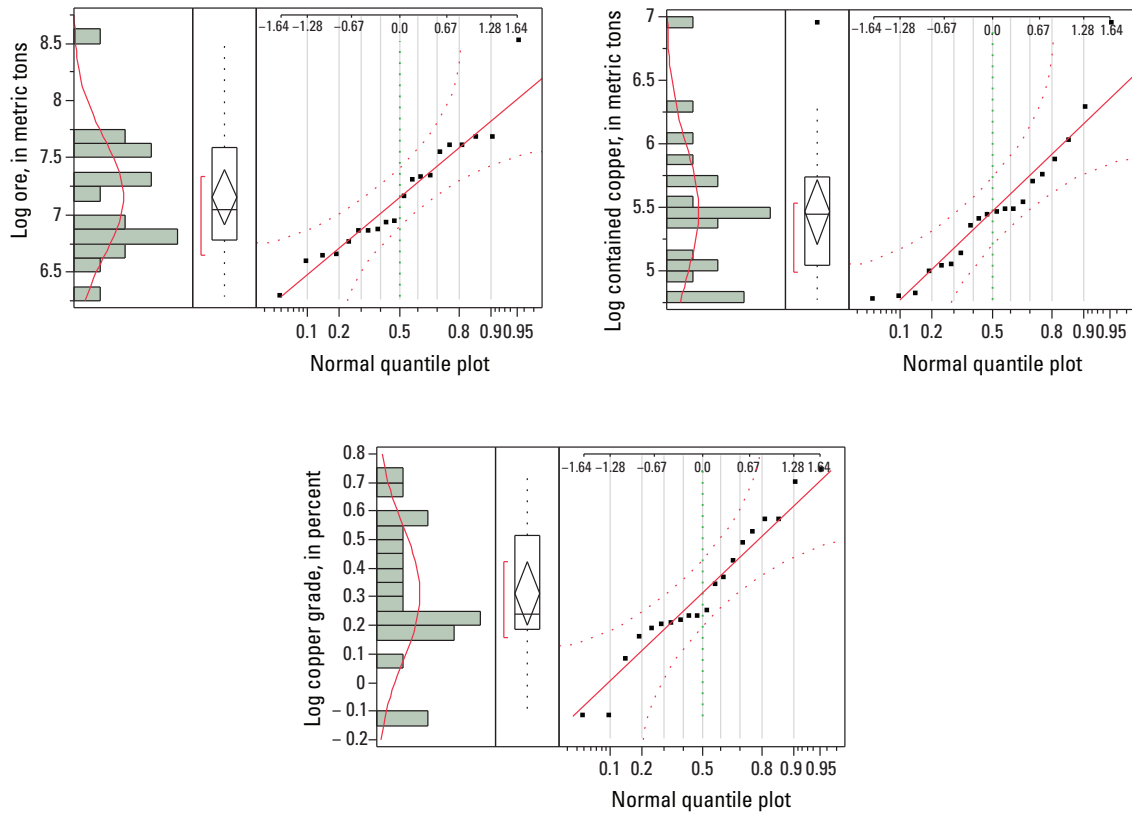


Figure 2-30. Histogram, box plot, and normal quantile plot illustrating the distribution of log-transformed values for tonnage, grade, and contained copper of 20 sandstone copper—Roan arenite deposits.

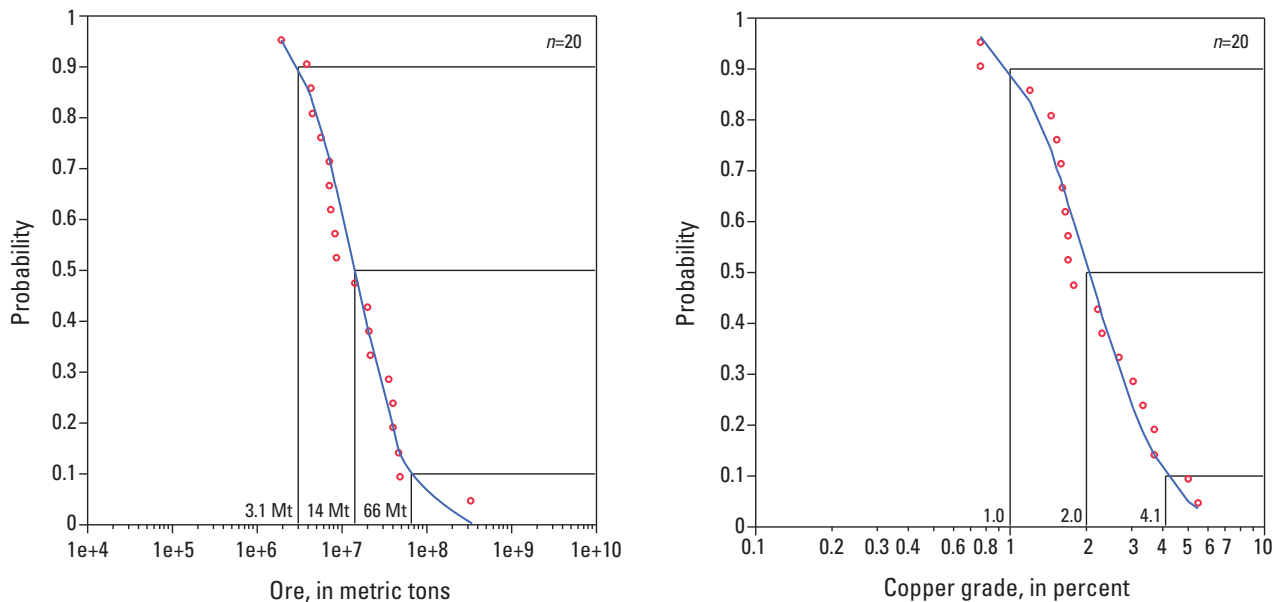


Figure 2-31. Cumulative frequency plots of grade and tonnage for sandstone copper—Roan arenite deposits. Each red circle is a data point for a deposit; the blue curve is the calculated lognormal distribution based on the population parameters of the data. Values for tonnage and grade for the 90th, 50th, and 10th probability values of the distribution are illustrated by extending a horizontal line from the vertical axis to the data curve, then drawing a vertical line to the horizontal axis. The value for the point where the vertical line intersects the horizontal axis is labeled. For some deposits, values for some metals are not reported, resulting in a censored or truncated dataset. For these metals, only the probability values for the data points with reported values are illustrated. Mt, million metric tons.

concentration of silver is below the detection limit of 0.5 g/t; an additional 125 samples have silver values below the detection limit of 5 g/t. Fifty samples had detectable silver; most values are less than 5 g/t; the highest value is 14 g/t (Japan International Cooperation Agency and Metal Mining Agency of Japan, 1996a, b). Kipoi North, a reduced-facies—carbonate écaïlle deposit, has a silver grade of 4.4 g/t (Reidy and others, 2009). In his monograph on the central part of the Katanga copper arc, François (2006) describes silver only once, where it occurs in trace amounts at the Kapulo copper occurrence in the Upper Kundelungu Supergroup. Silver minerals are not described in literature on the ore-mineralogy of the CACB deposits (GECO Project, 2009).

Silver is reported for about 30 to 35 percent of the deposits that make up the reduced-facies and sandstone copper deposits found outside the CACB. Although the percentage of missing data is high, missing values may represent not-reported data rather than no values. For some regions, silver data are available for part of the resource base, a group of deposits, or production, but cannot be partitioned to individual deposits. Examples include the Kupferschiefer in Germany and Poland; Chu Sarysu Basin, Kazakhstan; and the Redstone Copperbelt, Canada. In other cases, silver may not have been reported because of its value relative to copper. The relative value of silver to copper has fluctuated dramatically in the last 40 years (fig. 2-32). At current metal prices, silver represents about 20 to 30 percent of the value of the metal in reduced-facies—n.b. and sandstone copper deposits. At times when silver has relatively low value (as in the 1990s), it may not be reported. When it is worth more (as in the 1980s), silver is a significant part of the value of the deposit and is more likely to be reported. Although data are not available for each deposit in the grade and tonnage model, silver may be an important commodity for all reduced-facies—n.b. and sandstone copper deposits. However, the number of deposits with missing values is too high to make statistical inferences using imputation techniques. Schuenemeyer and Drew (2011) suggest that any inference made when the proportion of missing data is greater than 15 percent should be interpreted with great caution.

Cobalt

Economically significant quantities of cobalt are documented for the reduced-facies deposits of the CACB. Missing cobalt data for the reduced-facies—carbonate-écaïlle deposits, however, most likely represent nonreporting rather than low concentration. Techniques to estimate missing values would be appropriate to apply, particularly for the carbonate-écaïlle deposits. Cobalt grade typically is not reported for reduced-facies deposits in other parts of the world and sandstone copper deposits, in general. Missing values appear to reflect low concentrations of cobalt in these deposits. Reserves of the Boleo reduced-facies deposit in Mexico have cobalt grades of 0.07 percent, roughly an order of magnitude less than the mean values for reduced-facies—carbonate écaïlle

deposits (Dreisinger and others, 2010). Cobalt concentrations in mineralized sections of the reduced-facies Kupferschiefer range from 10 to 270 g/t (0.001 to 0.027 percent), with a mean of 125 g/t (0.0125 percent) (Wedepohl, 1964). These low values are consistent with the distribution of cobalt (generally <0.001 percent or 10 g/t) shown in the Dachow M24 drill hole (Oszczepalski, 1999) and the values of 28 to 140 g/t cobalt at Mansfeld (Knitzchke, 1995). In a study of minor and trace elements of the Spar Lake sandstone copper deposit, only a single sample out of 205 analyzed had cobalt exceeding the 10 g/t (0.001 percent) detection limit. Mineralized samples from the Kodar-Udokan sandstone copper deposits have less than 25 g/t (0.0025 percent) cobalt (Bakun and others, 1966; Boris Syusyura, Mining and Economic Consulting Ltd., written commun., 2009).

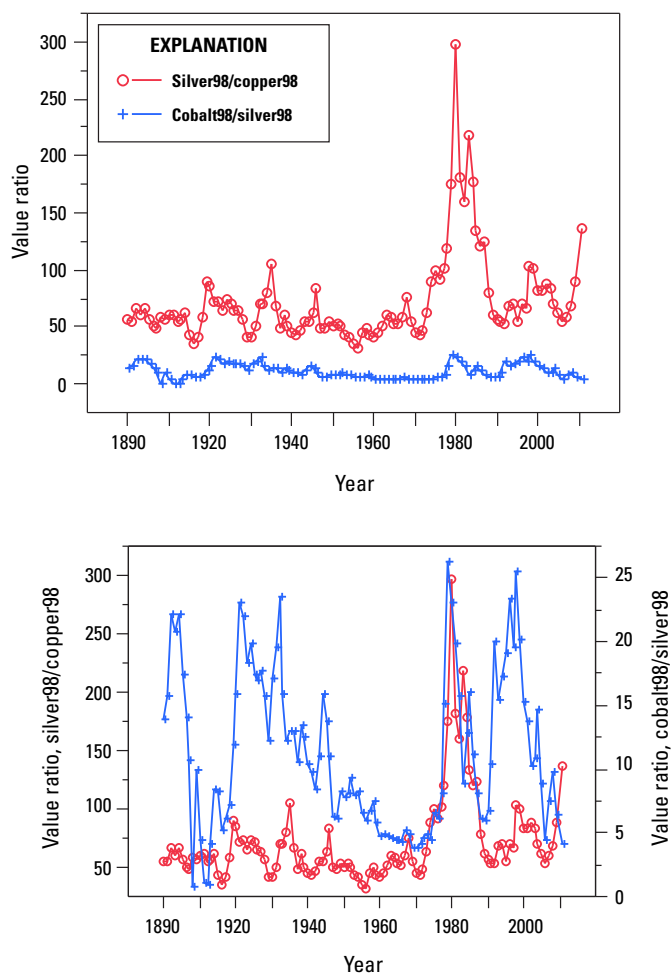


Figure 2-32. Graphs showing the relative value of metal prices with time. Upper graph shows the ratio of silver/copper and cobalt/silver prices, in constant 1998 dollars, using a uniform scale. Lower graph shows the ratio of silver/copper and cobalt/silver prices, in constant 1998 dollars, with independent scales.

Relations Among Surface Area, Tonnage, and Contained Copper

In USGS mineral assessments, geologists create mineral resource maps that show tracts where geology permits the existence of deposits of one or more specified types, and make estimates of the number of undiscovered deposits that exist in the delineated tracts. The undiscovered deposit estimates need to be consistent with the grade and tonnage models for the deposit type being assessed and not with the population of mineral occurrences (Singer and Menzie, 2010). Specifically, the estimated number of deposits must match the percentile values of the grade- and tonnage- model. Summary statistics can be derived from the grade and tonnage model to assist the assessment geologist in making deposit estimates that are consistent with the model. During assessments, knowing the area of deposits that comprise the grade and tonnage models is also useful. It helps in selecting a spatial rule for aggregation of deposits but also allows the assessment geologist to know the spatial constraints on how many deposits can fit inside of a tract. If the geologist knows the extent of the area that may correspond to a deposit, the relations between area and tonnage and contained metal allow undiscovered estimates to be made.

For this study, areas of deposits were measured and compiled along with tonnage and grade data. The area of the surface projection of ore bodies was measured for 55 of the 170 deposits in the grade and tonnage models. Areas range from 0.05 to 375 km², with mean and median values of 19.4 and 1.55 km², respectively. The distribution of values for area is positively skewed and the assumption that log-transformed data can be represented as a normal distribution was not rejected at the 1-percent confidence level. The dataset is biased: small deposits (less than 2 million metric tons of ore) are not well represented in the dataset (fig. 2-14) and deposits in the CACB are over-represented. CACB deposits make up about 45 percent of the deposits database (table 2-1) but constitute 69 percent of the deposits for which an area was estimated. Never-the-less, the data for all deposits show a positive correlation between area (square kilometers) and ore tonnage (metric tons) and contained copper (metric tons) for SSC deposits (fig. 2-14).

Regression equations can be used to estimate tonnage and contained copper from the deposit areas for 55 SSC deposits (fig. 2-33). The regression equation for tonnage is:

$$\log(\text{ore, metric tons}) = 7.51 + 0.78 \times \log(\text{area, km}^2),$$

where both tonnage and area have values for which the lognormal distribution was not rejected at the 99th percent confidence limit. The regression equation is significant at the 99th percent confidence limit and 77 percent of the variability in deposit tonnage can be explained given knowledge of deposit area. Contained copper can be estimated using the following equation:

$$\log(\text{contained copper, metric tons}) = 5.80 + 0.71 \times \log(\text{area, km}^2),$$

where both contained copper and area have values for which the lognormal distribution was not rejected at the 99th percent confidence limit. The regression equation is significant at the 99th percent confidence limit and 66 percent of the variability in contained copper can be explained given knowledge of deposit area.

Equations for Sandstone Copper Deposits

Regression equations can be used to estimate tonnage and contained copper from the deposit areas for 28 sandstone copper deposits (fig. 2-34). The regression equation for tonnage is:

$$\log(\text{ore, metric tons}) = 7.35 + 0.85 \times \log(\text{ore body area, km}^2),$$

where both tonnage and area have values for which the lognormal distribution was not rejected at the 99th percent confidence limit. The regression equation is significant at the 99th percent confidence limit and 78 percent of the variability in deposit tonnage can be explained given knowledge of deposit area. Contained copper can be estimated using the following equation:

$$\log(\text{contained copper, metric tons}) = 5.60 + 0.70 \times \log(\text{ore body area, km}^2),$$

where both contained copper and area have values for which the lognormal distribution was not rejected at the 99th percent confidence limit. The regression equation is significant at the 99th percent confidence limit and 66 percent of the variability in contained copper can be explained given knowledge of deposit area.

Equations for Reduced-Facies—Carbonate Écaille Deposits

Regression equations can be used to estimate tonnage and contained copper from the deposit areas for 12 reduced-facies—carbonate écaille deposits (fig. 2-35). The regression equation for tonnage is:

$$\log(\text{ore, metric tons}) = 7.79 + 0.81 \times \log(\text{ore body area, km}^2),$$

where both tonnage and area have values for which the lognormal distribution was not rejected at the 99th percent confidence limit. The regression equation is significant at the 99th percent confidence limit and 88 percent of the variability in deposit tonnage can be explained given knowledge of deposit area. Contained copper can be estimated using the following equation:

$$\log(\text{contained copper, metric tons}) = 6.22 + 0.96 \times \log(\text{ore body area, km}^2),$$

where both contained copper and area have values for which the lognormal distribution was not rejected at the 99th percent

confidence limit. The regression equation is significant at the 99th percent confidence limit, and 88 percent of the variability in contained copper can be explained given knowledge of deposit area.

The recently discovered Kamoa deposit in the CACB is a laterally extensive reduced-facies deposit (Broughton and Rogers, 2010a, b) for which mineral inventory information is not published. Broughton and Rogers (2010a, b) describe the geology and discovery history of the deposit and indicate that mineralization grading more than 1 percent copper over 3 meters extends over an area of 80 km². An independent NI 43-101 report completed in January 2011 defined indicated and inferred resources over an area of 35 km² (Ivanhoe Nickel & Platinum, 2011). Broughton and Rogers (2010b) consider an average grade-thickness of 20 meter-percent copper to be typical of reduced-facies deposits in Zambia and Poland. Using this estimate, each square kilometer would contain approximately 20

million metric tons of potential ore, containing approximately 0.5 million metric tons of copper. Using the area estimate of 35 km² and their approximations, the Kamoa deposit could contain 700 million metric tons of potential ore containing 18 million metric tons of copper. Using the same value for the area and the regression equation based on all SSC, the estimated tonnage for the Kamoa deposit is about 520 million metric tons of potential ore containing approximately 7.9 million metric tons of copper. Either approximation suggests Kamoa is a world-class or giant deposit (containing in excess of 2 million metric tons of contained copper).

Discussion and Conclusions

T-tests show that the SSC deposits in the CACB have significantly higher copper grades than deposits found in other basins (fig. 2-5). Supergene enrichment of the ore

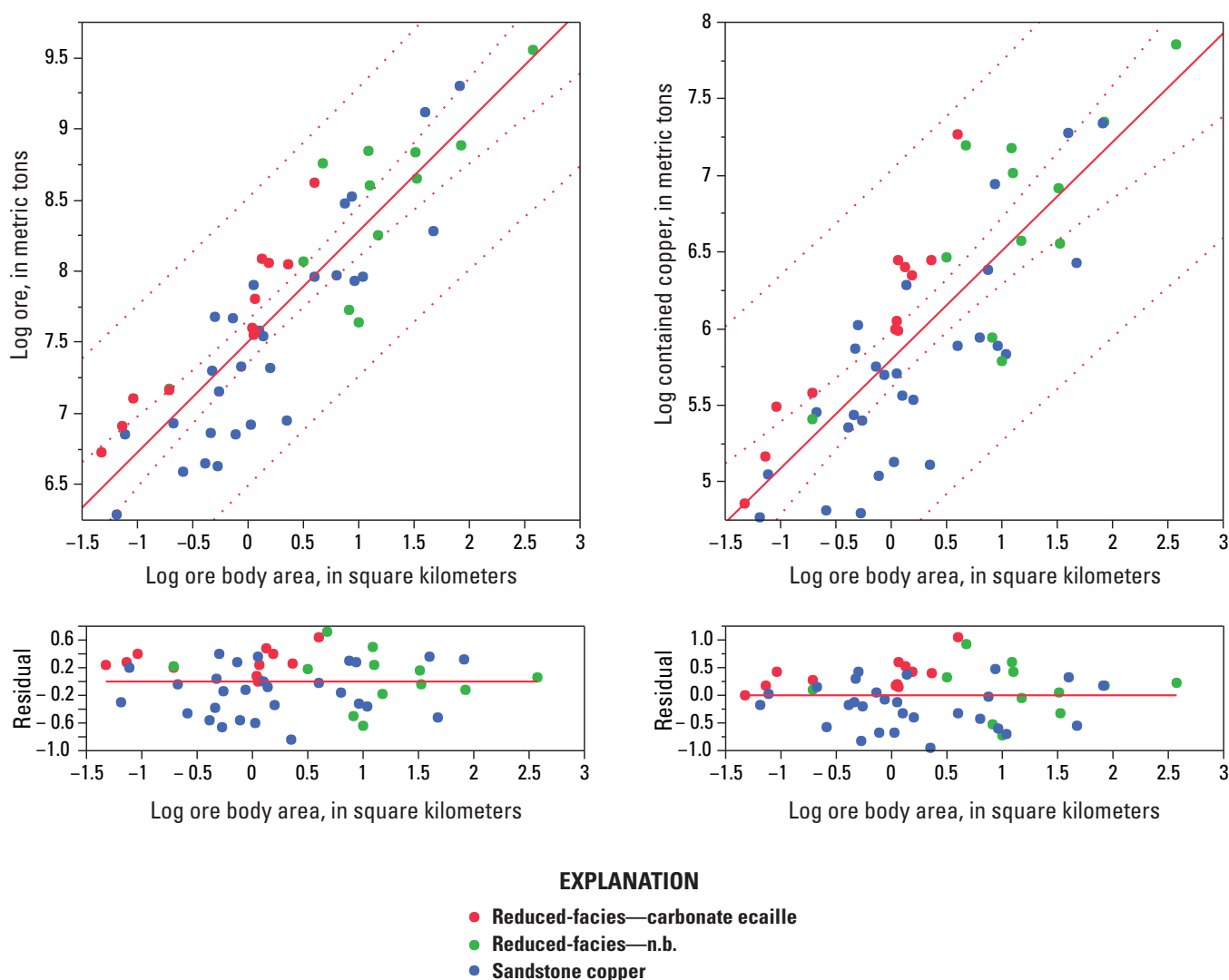


Figure 2-33. Bivariate graphs of ore body area plotted against ore tonnage and contained copper metal for sediment-hosted stratabound copper deposits. Regression line, confidence intervals, and a plot of residuals are also shown. n.b., nonbrecciated.

bodies in the CACB, and correspondingly higher cutoff grades, may account for some of this difference. As previously described, supergene-enrichment characterizes the reduced-facies—carbonate *écaille* and the sandstone copper—Roan arenite deposits. Supergene chalcocite is also described from reduced-facies deposits associated with the Ore Shale Formation in Zambia: Chambishi (Davidson, 1931), N’Changa-Chingola (Jackson, 1932; Notebaart and Vink, 1972), Roan Antelope (Davis, 1954; Notebaart and Vink, 1972), and Chililabombwe (Notebaart and Vink, 1972). Broughton and Rogers (2010a, b) describe a recently discovered reduced-facies deposit, Kamoia, in the DRC, that has an interval 50 to 200 m thick enriched in supergene chalcocite underlying a leached zone up to 50 m thick. The supergene zone contains 3 to 7 percent copper compared to grades of 2 to 4 percent copper that characterize the underlying hypogene mineralized rocks. More research is required to determine if this is the sole reason for the difference between deposits in the CACB and the rest of the world.

When compared using ANOVA tests, the various types of SSC deposits show these statistically significant differences using a 0.05 confidence limit (fig. 2-36): (1) the tonnage of the

reduced-facies—n.b. deposits is larger than reduced-facies—carbonate *écaille* and sandstone copper deposits; (2) the copper grade of reduced-facies—carbonate *écaille* deposits is higher than reduced-facies—n.b. deposit, which are both higher than sandstone copper deposits; (3) the contained copper of sandstone copper deposits is lower than reduced-facies deposits.

The characteristics of the deposit types and their suitability for grade and tonnage modeling in resource assessment are summarized in table 2-6, using the criteria of Singer and Menzie (2010, p. 93). All the distributions given in table 2-6 are consistent with the normal model after values for tonnage and grade are log-transformed and the standard deviation of log-transformed values of tonnage are less than 1.0. Log-transformed values of tonnage and metal grade do not show significant correlation.

Although the distribution of data for all SSC deposits meets all the criteria listed by Singer and Menzie (2010), as a grade and tonnage model, it will overestimate copper and cobalt in most basins and will overestimate silver and underestimate copper in the Katanga Basin.

In order to reduce bias in resource assessments of undiscovered copper, the CACB should be evaluated with

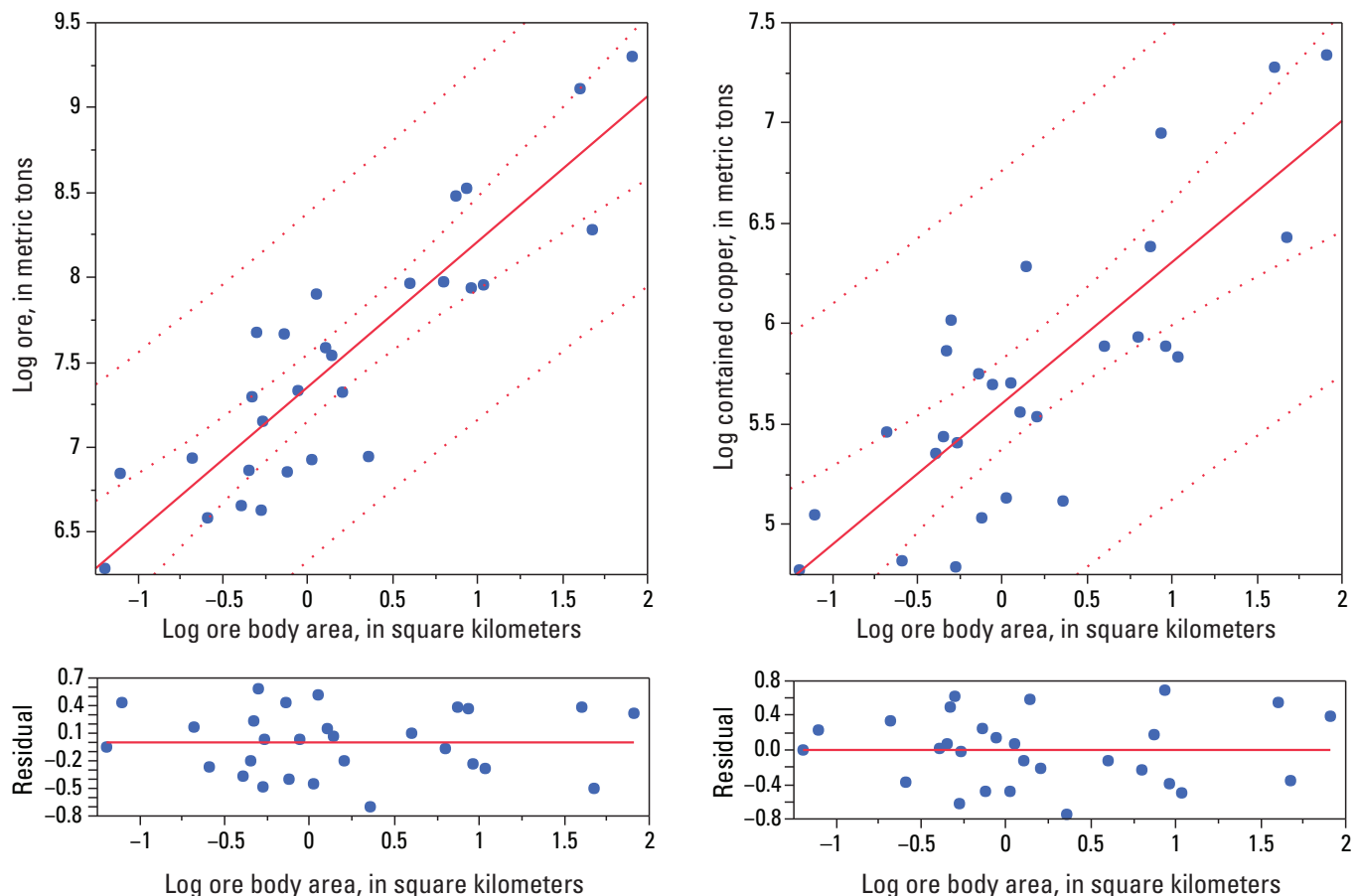


Figure 2-34. Bivariate graphs of ore body area plotted against ore tonnage and contained copper metal for sandstone copper deposits. Regression line, confidence intervals, and a plot of residuals are also shown.

its own grade and tonnage models. The distributions for reduced-facies, carbonate *écaillé* and sandstone copper Roan arenite, are good models for undiscovered deposits in the halokinetically deformed Mines Subgroup rocks in the Democratic Republic of the Congo and the Roan Group in Zambia, respectively. There are not enough reduced-facies deposits associated with the Ore Shale Formation to make a separate model; the reduced-facies—n.b. distribution should be used. A separate model that includes only SSC deposits in the CACB would be more appropriate to apply to the Katanga Basin where separate tracts for reduced-facies and sandstone copper deposits cannot be distinguished. One should be aware that using this distribution as a model presumes that the proportion of undiscovered deposit types will be the same as in the model. In other words, 66 percent of the undiscovered deposits would be like those associated with the Mines Subgroup, 23 percent would be like those in the Roan Group in Zambia, and 11 percent would be like those in the Ore Shale Formation in Zambia. Cobalt should not be modeled because it appears to be enriched only in the deposits in the Mines Subgroup.

The sandstone copper distribution is considered a good model for undiscovered deposits of this type in basins

throughout the world (excluding the Katanga Basin). The reduced-facies—n.b. distribution can be used for assessment of deposits of this type in any sedimentary basin. Further research is required on the silver and cobalt concentrations in SSC deposits. With the current dataset, cobalt enriched ores appear to be restricted to reduced-facies—carbonate *écaillé* deposits in the CACB. Silver appears to be enriched in both sandstone and reduced-facies—n.b. deposits, except in the CACB. Additional analyses of ores are needed to confirm these patterns.

Acknowledgments

Discussions with James Bliss and Donald Singer helped us understand many of the nuances of creating tonnage and grade models for resource assessment. Murray Hitzman and David Broughton gave us insights on how to classify deposit type in the CACB. Illustrations were prepared by Heather Parks, Kassandra Lindsey, and Joseph Miles. Jane Hammarstrom reviewed an early version of this report. James Bliss, Pamela Dunlap, and Daniel Mosier provided formal technical reviews.

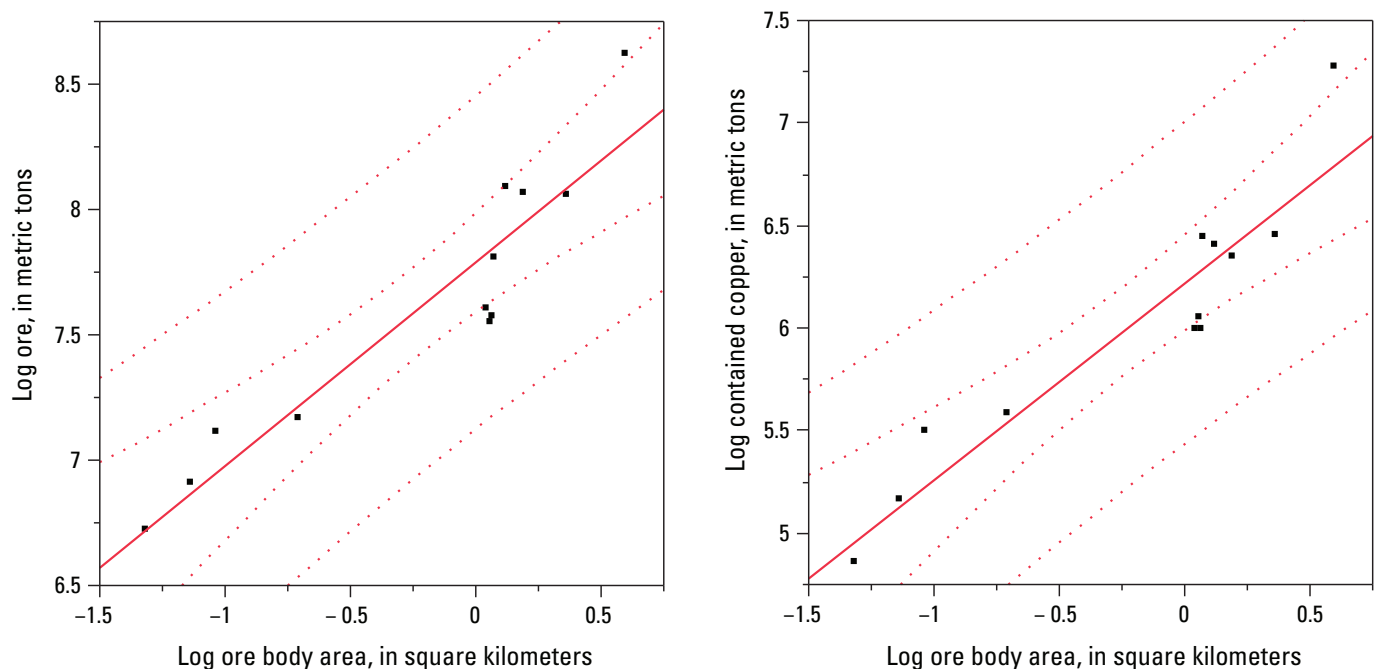


Figure 2-35. Bivariate graphs of ore body area plotted against ore tonnage and contained copper metal for reduced-facies—carbonate-*écaillé* copper deposits. Regression line, confidence intervals, and a plot of residuals are also shown.

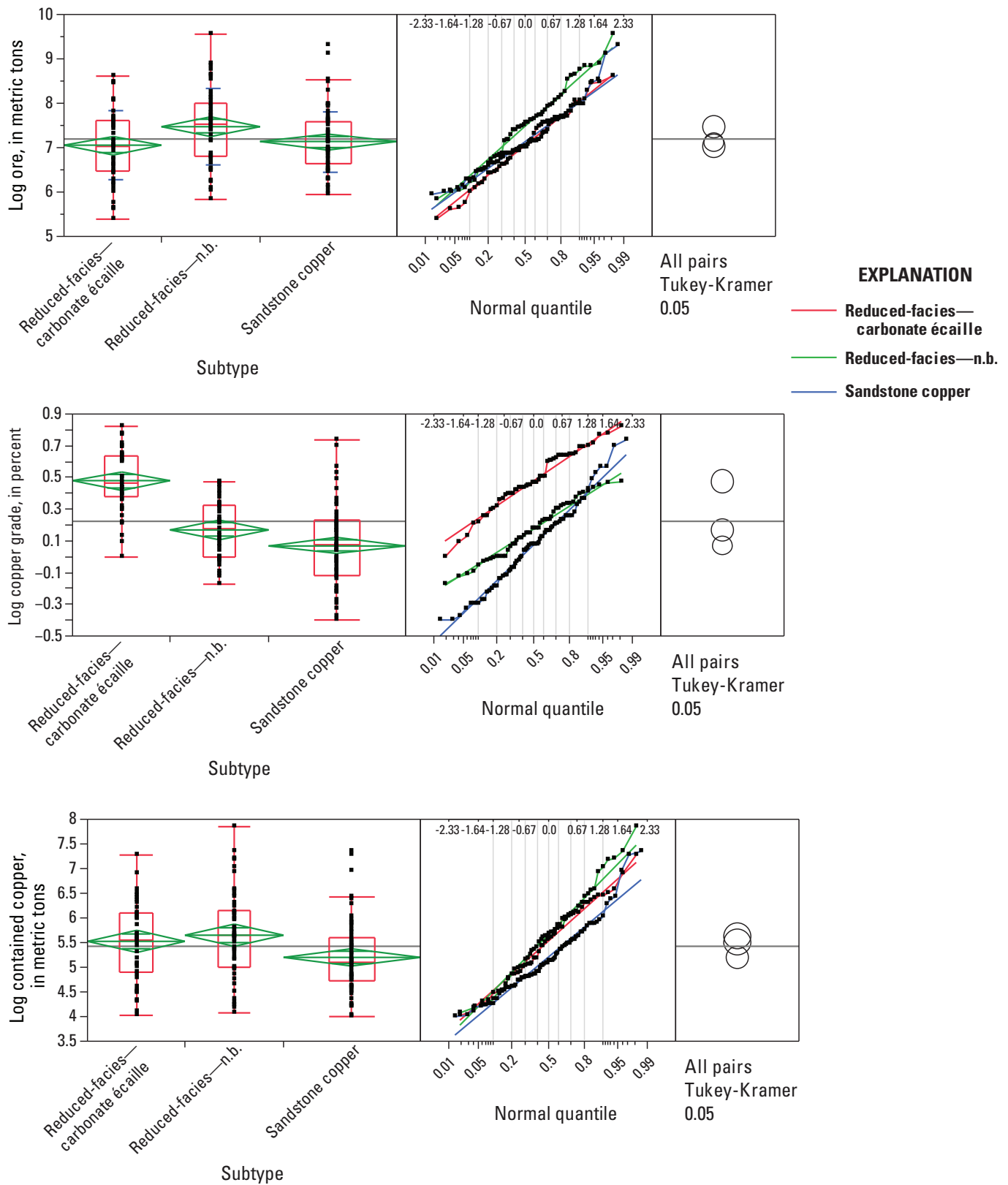


Figure 2-36. Box plots, normal quantile plots, and comparison circles for log-transformed values of ore, metric tons, copper grade, and contained copper illustrating differences among reduced-facies—carbonate-écaillé, reduced-facies—n.b., and sandstone copper deposits. n.b., nonbrecciated.

Chapter 3. Sediment-Hosted Structurally Controlled Replacement and Vein Copper Deposits in the Central African Copperbelt, Democratic Republic of the Congo and Zambia

By Cliff D. Taylor

Introduction

Sediment-hosted copper districts are the result of long-lived mineralizing systems that stayed active over several hundred-million years, from earliest continental rifting through basin inversion and orogeny (McGowan and others, 2003; Selley and others, 2005; Hitzman and others, 2005, 2010). Within sedimentary basins that host red beds, copper-dominant deposits have variable morphologies, and form diachronously, resulting in the array of stratabound sediment-hosted copper deposit subtypes described in this volume (see Zientek and others, this report, chapter 1) as well as a diverse subgroup of deposits that are referred to here as structurally controlled replacement and vein (SCRV) deposits. The various subtypes of sediment-hosted copper deposits have virtually similar mineralogy and metal endowments and owe their origins to the same red bed copper source rocks, transport of copper as a chloride complex in a brine, and redox precipitation mechanisms. Sediment-hosted copper deposits that are epigenetic SCRVR may have formed tens to hundreds of million years later than sediment-hosted stratabound copper deposits within the same rift-related sedimentary sequence.

Both stratabound and SCRVR copper deposits occur throughout the Neoproterozoic Katangan Basin that hosts the Central African Copperbelt (CACB). Historically, exploration has targeted stratabound deposits in the Lufilian Arc, an arcuate, Neoproterozoic to early Paleozoic orogenic fold and thrust belt between the Congo and Kalahari Cratons (fig. 3-1). The majority of copper production in the CACB has come from these stratabound deposits. Within this main portion of the CACB, deposits with the greatest production are hosted in the Mines Group rocks of the lower Katangan Supergroup. Lesser production has come from an array of smaller deposits of variable morphologies that occur in higher stratigraphic intervals of the Katangan Supergroup (fig. 3-2) and (or) from peripheral parts of the CACB such as the Lufilian Foreland, an underexplored foreland basin to the west, north, and east of the Lufilian Arc and the Domes region of the CACB in the inner portion of the arc. In the past, SCRVR copper deposits may have been overlooked due to genetic concepts that required sediment-hosted copper mineralization to occur syngenetically or during early diagenesis (Garlick, 1961; Annels, 1974; Rentzsch, 1974; van Eden, 1974; Sweeney and others, 1986; Mendelsohn,

1989) rather than after lithification of the host sediments. However, the presence of the giant Kansanshi SCRVR deposit in the Domes region and the development of the Dikulushi SCRVR deposit, the first producing copper mine in the Lufilian Foreland, has spurred exploration interest for SCRVR deposits higher in the Katangan stratigraphy and in peripheral portions of the CACB in recent years (El Desouky, 2008).

Many of the SCRVR deposits form massive, near-monomineralic veins of ore minerals such as chalcocite-bornite or chalcopyrite-bornite-covellite with highly variable amounts of quartz, carbonate, or feldspar gangue. Typically, the ore minerals are in direct contact with siliciclastic walls of faults or fractures, within brecciated rock between fault strands, or disseminated in more porous sandstones in the vicinity of structures that act as the plumbing system to bring the copper-rich brines into contact with reductant-bearing strata.

Chapter 1 of this report summarizes a deposit model for sediment-hosted stratabound copper deposits, which include the reduced-facies, sandstone Cu, and red bed subtypes. This chapter presents an overview of the characteristics of SCRVR deposits, another type of sediment-hosted copper deposit, which also occurs throughout the CACB.

Concise Description

Sediment-hosted structurally controlled replacements and veins of copper sulfide minerals are collocated in sedimentary basins that also host sediment-hosted stratabound copper deposits. The characteristics of the general class of sediment-hosted copper deposits are summarized in table 3-1.

Commodities (byproducts)

Copper (cobalt, gold, silver, uranium).

Importance

Most sediment-hosted structurally controlled replacement and vein deposits are small; notable exceptions are the Kansanshi deposit in Zambia and the Frontier deposit in the Democratic Republic of the Congo (figs. 3-1 and 3-3; table

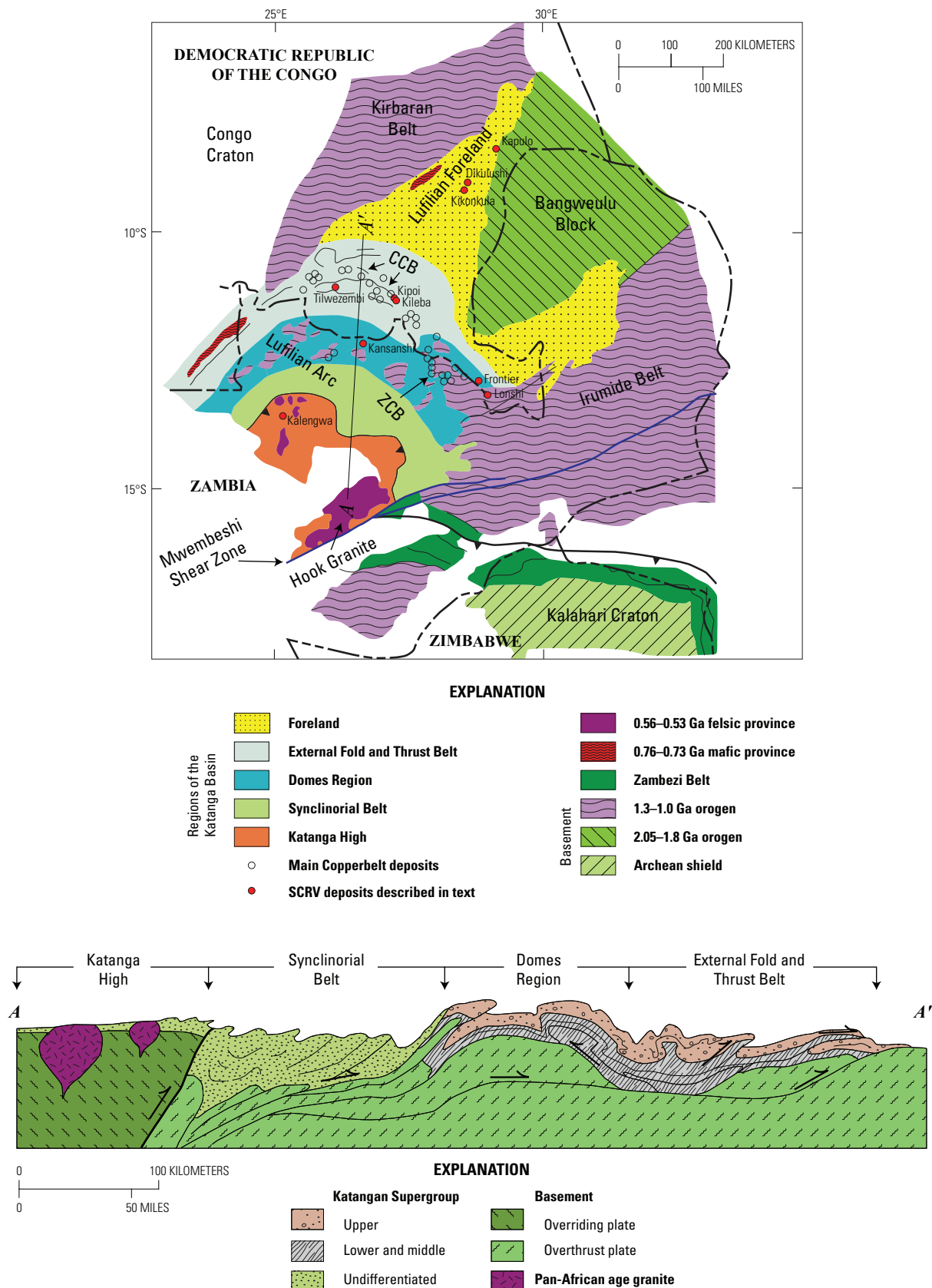


Figure 3-1. Map showing the geology and major tectonic features of the Central African Copperbelt (modified from Selley and others, 2005). ZCB and CCB refer to Zambian and Congolese copper belts, respectively. Ga, giga-annum.

Figure 3-2. Stratigraphic nomenclature and stratigraphy of the Katanga Supergroup throughout the Central African Copperbelt (modified from Cailteux and others, 2005b; 2007); structurally controlled replacement and vein (SCRV) mineralized intervals are shown in red. Ma, mega-annum.

SUPERGROUP					GROUP	SUBGROUP	FORMATION	Former nomenclature (François, 1987)	LITHOLOGY			SCRV Mineralized Intervals	
Katangan		± 500 Ma		Kundelungu - Ku (formerly Upper Kundelungu- Ks)		Biano - Ku 3		Ks 3	arkoses, conglomerates, argillaceous sandstones				
					Ngule - Ku 2	Sampwe - Ku 2.3		Ks 2.2	dolomitic pelites, argillaceous to sandy siltstones				
						Kiubo - Ku 2.2		Ks 2.1	dolomitic sandstones, siltstones and pelites				
						Mongwe - Ku 2.1		Ks 1.3	dolomitic pelites, siltstones and sandstones				
					Lubudi - Ku 1.4		Ks 1.2.4	pink oolitic limestone and sandy carbonate beds					
				Gombela - Ku 1	Kanianga - Ku 1.3		Ks 1.2.2 and 1.2.3	carbonate siltstones and shales					
					Lusele - Ku 1.2		Ks 1.2.1	pink to grey micritic dolomite					
					Kyandamu - Ku 1.1		Ks 1.1	Petit Conglomérat (glacial diamictite)					
		(± 620 Ma)			Monwezi - Ng 2.2		Ki 2	dolomitic sandstones, siltstones and pelites					
				Nguba - Ng (formerly Lower Kundelungu - Ki)	Bunkeya - Ng 2		Katete - Ng 2.1	Ki 1.3	dolomitic sandstones, siltstones and shales in northern areas; alternating shale and dolomite beds ("Série Récurrente") in southern areas				
					Muombe - Ng 1	Kipushi - Ng 1.4		Ki 1.2.2	dolomite with dolomitic shale beds in southern areas				
						Kakontwe - Ng 1.3			carbonates; Zn-Cu-Pb				
						Kaponda - Ng 1.2		Ki 1.2.1	carbonate shales and siltstones; "Dolomie Tigrée" at the base				
						Mwale - Ng 1.1		Ki 1.1	Grand Conglomérat (glacial diamictite)				
			± 750 Ma										
	DEMOCRATIC REPUBLIC OF THE CONGO								ZAMBIA				
		GROUP	SUBGROUP	FORMATION	Former nomenclature (François, 1987)	LITHOLOGY		LITHOLOGY		FORMATION	SUBGROUP		
		Roan R	Mwashya (formerly Upper Mwashya) - R4	Kanzadi - R 4.3	R 4.2	sandstones or alternating siltstones and shales		dolomitic shales, grey to black carbonaceous shales, quartzites	dolomites to arenitic dolomites interbedded with dolomitic shales; intrusive gabbros (formerly Carbonate Unit or Upper Roan)	Bancroft Kanwangungu RU 1 and RU 2	Mwashia		
				Kafubu - R 4.2		carbonaceous shales							
				Kamoya - R 4.1		dolomitic shales, siltstones, sandstones, including conglomeratic beds and cherts in variable position							
Dipeta - R 3		Kansuki - R 3.4	R 4.1	(formerly Lower Mwashya): dolomites including volcaniclastic beds; Cu-Co		shales with grit (Antelope Clastics)	Kibalongo RL 3	Kitwe					
		Mofya - R 3.3		dolomites, arenitic dolomites, dolomitic siltstones									
		R 3.2		argillaceous dolomitic siltstones with interbedded sandstone or white dolomite; intrusive gabbros									
		R.G.S. - R 3.1		argillaceous dolomitic siltstones ("Roches Gresol-Schisteuses")									
Mines - R 2		Kambove - R 2.3		stromatolitic, laminated, shaly or talcose dolomites; locally sandstone at the base; interbedded siltstones in the upper part; Cu-Co		dolomite, argillite beds at top	Chingola RL 4						
		Dolomitic shales - R 2.2		R 2.2.2 and 3: dolomitic shales containing carbonaceous horizons; occasional dolomite or arkose		arkoses, sandy to dolomitic argillites	Pelito-arkosic RL 5						
			Kamoto - R 2.1		R 2.2.1: arenitic dolomite at the top and dolomitic shale at the base; pseudomorphs after evaporite nodules and concretions; Cu-Co		arenites, argillaceous dolomites, argillites, dolomites, evaporites; Cu-Co	Ore Shale RL 6					
		R.A.T. - R 1	red argillaceous dolomitic siltstones, sandstones and pelites ("Roches Argilo-Talqueuses")				conglomerates, coarse arkoses and argillaceous siltstones	Mutonda	Mindola - RL 7				
		base of the R.A.T. sequence - unknown					quartzites	Kafufya					
	< 900 Ma basal pebble and cobble conglomerate					pebble and cobble conglomerate	Chimfunsi						
± 2,050 Ma KIBARAN and PRE-KIBARAN, respectively													

3-2), which contain 4.8 and 3.3 million metric tons contained copper, respectively. Kansanshi, the largest known SCR.V deposit, ranks 11th largest out of the 27 known giant (>2 million metric tons, Singer, 1995; based upon contained copper metal, see table 2-1, Zientek and others, this report, chapter 2) sediment-hosted stratabound and SCR.V copper deposits worldwide; Frontier ranks 15th.

Associated Deposit Types

Associated deposit types include sediment-hosted stratabound copper deposits, sediment-hosted uranium, sediment-hosted cobalt, unconformity uranium, basaltic copper, and Kipushi/Tsumeb-type lead-zinc-copper deposits (Unrug, 1989; Selley and others, 2005; Kampunzu and others, 2009). Halite, sylvite, gypsum, anhydrite and stratabound iron oxide deposits may be present within the same stratigraphic sequences; iron oxide-copper-gold-uranium deposits may occur within the same districts (Cox and others, 2003, rev. 2007).

Distribution

SCR.V deposits and occurrences are present throughout the CACB and throughout the Katangan stratigraphic sequence (figs. 3-1, 3-2, and 3-3).

Age Range

Like other sediment-hosted copper deposit subtypes, the SCR.V deposits are limited to sedimentary or metasedimentary formations younger than 2,300 mega-annum (Ma), when free oxygen accommodated formation of the earliest red beds (Chandler, 1988; Bekker and others, 2004, 2005).

Available constraints on the age of mineralization of SCR.V deposits in the CACB suggest that they may have formed during multiple periods associated with extension and basaltic volcanism just prior to the deposition of the Grand Conglomerate, from approximately 765–735 Ma (Key and others, 2001; Barron and others, 2003; Master and others, 2005), and during Lufilian orogenesis and metamorphism starting at approximately 580 Ma, with peak orogenesis and metamorphism occurring at approximately 540–510 Ma (Selley and others, 2005).

Crosscutting relationships and presence of mineralized clasts in the Grand Conglomerate at the Kipoi Central deposit suggest that both primary stratiform as well as structurally hosted breccia and vein mineralization hosted in the Mwashya Subgroup must be older than the Grand Conglomerate (~765 Ma; Reidy and others, 2009). The age of mineralization at Kansanshi has been established by a variety of geochronological techniques (Re-Os, molybdenite; U-Pb, monazite and brannerite) and is well constrained to about 513–501 Ma (Torrealday and others, 2000; Broughton and others, 2002). Geochemical and petrographic work at the Dikulushi deposit

and the Kikonkula, Lufukwe, and Mwitapile occurrences in the Lufilian Foreland suggest that mineralization occurred in two discrete stages. A polymetallic assemblage was deposited during the Lufilian orogeny from a saline fluid at moderate temperature. Remobilization of the polymetallic assemblage by low temperature fluids after the Lufilian orogeny resulted in deposition of a copper-silver assemblage along northeast-trending faults (El Desouky and others, 2008; Haest, Muchez, Dewaele, and others, 2009; Haest, Muchez, Petit, and Vanharccke, 2009). Lead isotopic constraints on the two assemblages suggest mineral-forming events at approximately 520 Ma followed by remobilization during a Cretaceous fluid-flow event between 100–80 Ma (Haest and others, 2010).

Representative Deposits in the CACB

The locations of currently known SCR.V deposits and prospects are shown on a map of the CACB in figures 3-1 and 3-3. The relative positions of these deposits within the Katangan lithostratigraphy are shown in figure 3-2. Reported tonnages and grades are listed in table 3-2, along with key references for each deposit.

Kansanshi, Zambia

The Kansanshi deposit (figs. 3-1 and 3-3) contains 412.5 million metric tons of ore at an average grade of 1.16 percent copper, and recoverable gold. The deposit, mined since before Europeans arrived in Africa, was one of the early and most important rediscoveries in the Zambian Copperbelt (Broughton and others, 2002). A giant deposit, with an estimated copper metal content of almost 4.8 million metric tons, it is also the largest of the eleven identified SCR.V deposits in the CACB.

Kansanshi is hosted in phyllites, schists, and marbles of the Nguba Group at a stratigraphic level that is tentatively correlated with the Grand Conglomerate (fig. 3-2). Rocks intersected by drilling suggest that the deposit is underlain by approximately 1,140 meters (m) of sedimentary rocks tentatively correlated with the Mwashya Subgroup through lower Roan Group strata (Broughton and others, 2002).

The Kansanshi deposit consists of a series of north-south striking, undeformed, high-angle veins and vein swarms, with associated alteration halos, that are distributed in an en echelon pattern along the axis of the northwest trending Kansanshi antiform (fig. 3-4A). Three stages of crosscutting veins are characterized by chalcopyrite-pyrrhotite-pyrite with minor to trace amounts of brannerite, monazite, uraninite, pitchblende, molybdenite and rare bornite (fig. 3-4B). Gangue minerals include quartz, ferroan carbonate minerals, rutile, and biotite. Gold occurs as native grains associated with chalcopyrite. The vein swarms have strike lengths of hundreds of meters to more than 1,200 m, widths as much as 200 m, and vertical dimensions as much as 300 m. Individual veins can

Table 3-1. Selected characteristics of sediment-hosted copper deposits.

[Based on Hitzman and others (2005, 2010), Cox and others (2003), Kirkham (1989, 1996a), and Brown (1992, 1997)]

Topic	Characteristics
Tectonic setting	Continental rift basins Failed rifts or aulacogens; less commonly rifted continental margins or passive margins Pull-apart basins, grabens Associated with periods of continental breakup Long-lived continental to epicontinental, basins closed to fluid flow Post-mineral enhancement during basin inversion and orogeny
Depositional settings	Arid environments at low latitudes during ore formation Thick continental clastic sequences (red beds) overlain by fine grained, organic-rich, marginal marine or lacustrine sedimentary rocks Fining upward siliciclastic to shale-evaporite or carbonate-evaporite cycles indicate rift-drift or rift-sag transgressive sedimentary sequences Evaporative lagoonal settings, sabkhas
Depth considerations	1 to 4 kilometers Areas of preserved continental sedimentary basins (consider likelihood that deposits have been eroded away or are not yet exposed) Systems may be intact and laterally continuous or folded and dismembered by post-mineralization deformation
Structural setting	Basement uplifts, pinchouts, and basin margin faults against stratigraphic seals (aquaculdes such as shale or salt horizons) important sites of mineralization Stratigraphic traps, anticlines, and oilfield structural geometries are favorable sites for mineralization Halokinesis, including the formation of dissolution breccias, diapirs, salt-walls and salt intrusions Extension related to gravitational collapse of the passive margin or halokinesis
Igneous petrology	No direct link to igneous activity Host sedimentary basins often contain rift-related bi-modal volcanic rocks and associated sills/dikes
Texture	Conglomerates and arkoses grading upsection into well rounded, mature sandstones, arenites, and aeolian sandstones. Fine grained, organic rich shales, siltstones, carbonate-rich siltstones, and shallow water carbonates Stratiform/stratabound style of ore includes pyrite framboids and disseminated sulfides, massive sulfides, breccias, and veins
Hydrothermal alteration	Vast areas of hydrothermally altered rock (hundreds of km ²) may indicate basins that were unusually hydrodynamically active Widespread hematite alteration with anhydrite and illite observed in some basins. Intense alteration can be destructive of sedimentary textures and extends well beyond ore limits. Complex paragenesis involving K, Na, and Mg mineral phases: feldspars, muscovite, chlorite, anhydrite, carbonate, quartz, tourmaline, scapolite, sodic amphiboles, and talc
Mineralogy	Primary sulfide minerals: native copper, chalcocite, bornite, chalcopyrite, galena, sphalerite, pyrite, carrollite, cobaltite, siegenite, tetrahedrite + others Supergene minerals: chalcocite, cuprite, covellite, malachite, azurite, pseudomalachite, chrysocolla, heterogenite + others

Table 3-1. Selected characteristics of sediment-hosted copper deposits.—Continued

[Based on Hitzman and others (2005, 2010), Cox and others (2003), Kirkham (1989, 1996a), and Brown (1992, 1997)]

Topic	Characteristics
Geophysical signature	<p>Self potential, induced polarization, electromagnetics, magnetotellurics, magnetics, gravity, radiometrics, and other methods extensively employed</p> <p>General lack of success in direct detection of ore due to subtle geophysical target, deep oxidation of sulfides, variable lateritization and weathering, and conductive overburden</p> <p>Host strata displays low density and low magnetic susceptibility, with anomalously high resistivity</p> <p>Potential for the delineation of favorable host rocks and basin architecture using gravity, resistivity, and seismic profiles</p> <p>Radiometrics helpful for mapping potassic alteration; K and Th track each other for many rock types, but Th is relatively immobile during potassic alteration. Positive U-Th anomalies coupled with negative potassium anomalies may be useful in locating SCR/V sub-type deposits due to presence of uranium-thorium veins and biotite-destructive alteration</p>
Remote sensing	<p>ASTER may be useful to delineate broad-scale patterns of oxidation and reduction (bleaching) in hematite-stable red beds discernable over large areas. Not useful for buried deposits or in heavily vegetated areas</p> <p>Landsat TM imagery can be used to delineate differences in vegetation patterns relating to underlying lithology and structures in heavily vegetated terrains</p>
Geochemical signature	<p>Copper is the best pathfinder element in stream sediments and soils. Cu, Co, Ag, Pb, Zn, Fe, (Mo, V, Ni, Mn, U, Re, Ge, Au and PGE's). Co, Ag, Au, U, and PGE's locally important byproducts. U-enrichments result in weak radioactivity</p> <p>Geochemistry is an essential exploration tool for shallow sediment-hosted copper deposits</p>
Weathering	<p>Deposits exposed to weathering may develop leached cappings and supergene enrichment profiles depending on tectonoclimatic controls. Secondary chalcocite enrichment along hydrogeologic gradients is common</p> <p>Optimal settings for supergene enrichment: low erosion rate, steep faults, uninterrupted weathering (0.5 to >5 million years), tectonic uplift/water table depression, and hot, semiarid to pluvial climate</p>
Associated deposit types	<p>Occurrence of deposits or prospects for the following deposit types may indicate likelihood of occurrence of sediment-hosted copper deposits: stratiform sediment-hosted and vein uranium deposits, Kipushi-type Cu-Pb-Zn deposits, Tsumeb-type Pb-Zn deposits, massive iron-oxide deposits, basalt-hosted copper deposits, bedded halite, potash, gypsum, and anhydrite (evaporite) deposits</p> <p>Continental rift or failed rift tectonic setting also likely to result in spatial-temporal association with iron oxide-copper-gold-uranium deposits and REE-U deposits in association with anorogenic intrusive rocks and alkaline granites. So-called five-element vein deposits may be present</p> <p>Presence, or evidence of the former presence, of hydrocarbon accumulations and (or) sour gas is very important</p> <p>Relation to Neoproterozoic global glacial events suggests association with Rapitan-type iron deposits</p>

Table 3-2. Structurally controlled replacement and vein deposits in the Central African Copperbelt.

[t, metric ton; %, percent; n.d., no data; DRC, Democratic Republic of the Congo; Contained Cu in metric tons is computed as tonnage (t) × Cu grade (%)]

Deposit	Country	Commodities	Latitude	Longitude	Ore (t)	Cu Grade (%)	Co Grade (%)	Contained Cu (t)	References	Host unit
Kansanshi	Zambia	Cu, Au, U	-12.097	26.433	412,472,600	1.16	n.d.	4,767,304	Arthurs (1992), Broughton and others (2002), Torrealday and others, 2000	Nguba Group phyllite, schist, marble (correlative with Grand Conglomerate)
Kalengwa	Zambia	Cu, Ag	-13.459	24.999	4,000,000	5.2	n.d.	208,000	Thieme and Johnson (1981), Broughton and others (2004), Ellis and McGregor (1967)	Upper Katangan undifferentiated
Dikulushi	DRC	Cu, Ag	- 8.892	28.274	3,114,104	4.45	0.17	138,591	Haest, Muchez, Dewaele, and others (2007); Haest, Muchez, Dewaele, and others (2009); Haest, Muchez, Petit, and Vanharccke (2009); Haest and others (2010); Lepersonne (1974)	Kundelungu Group
Frontier	DRC	Cu	-12.728	28.475	284,247,567	1.17	n.d.	3,313,797	Gregory and others (2006)	Grand Conglomerate
Kileba	DRC	Cu	-11.286	27.124	9,502,431	1.4	n.d.	133,034	Reidy and others (2009)	Mwashya
Kipoi Central	DRC	Cu, Co, Ag	-11.255	27.095	56,611,535	1.81	0.08	303,600	Reidy and others (2009)	Mwashya
Lonshi	DRC	Cu	-13.177	28.941	16,935,836	4.02	n.d.	680,838	Stephens and Newall (2003)	Kirilabombwe/Mwashia Sub-group contact
Tilwezembe	DRC	Cu, Co	-10.802	25.692	23,351,600	1.83	0.64	426,801	Dixon and others (2009)	Mwashya
Safari North and South	DRC	Cu, Ag	- 8.329	29.238	2,357,000	2.62	n.d.	61,794	Mawson West Limited (2006), Le Burn and Hayward (2011)	Kundelungu Group (Luapula beds)
Sase [Central]	DRC	Cu, Co	- 11.453	27.078	14,700,000	1.36	0.10	200,400	Tiger Resources Limited (2009)	Lower Kundelungu Group
Shaba	DRC	Cu, Ag	- 8.301	29.235	6,014,000	3.38	n.d.	203,192	Mawson West Limited (2006), Le Burn and Hayward (2011)	Kundelungu Group (Luapula beds)

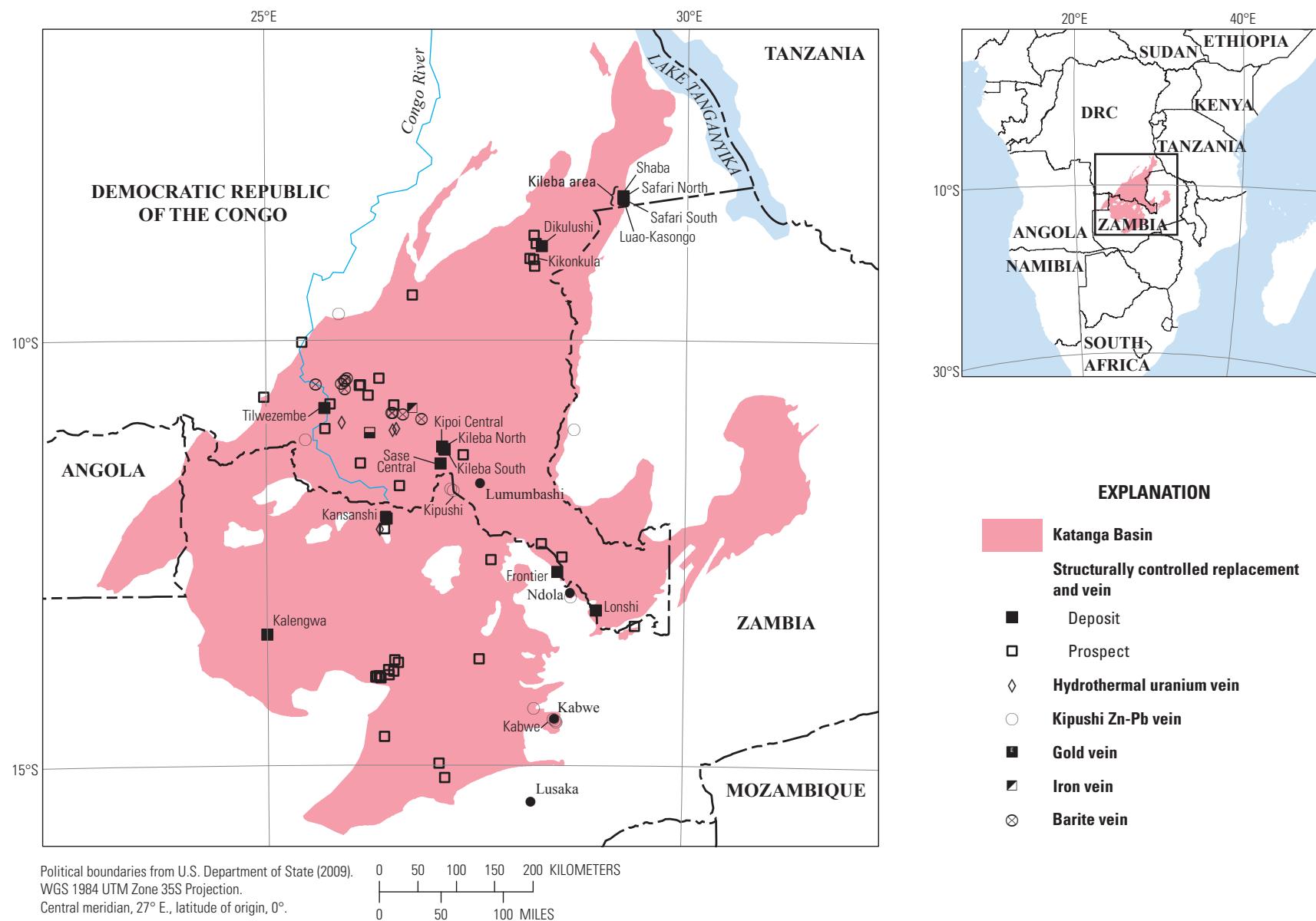


Figure 3-3. Index map showing the distribution of structurally controlled replacement and vein (SCRV) deposits and prospects in the Central African Copperbelt, in relation to the extent of the Katanga Basin.

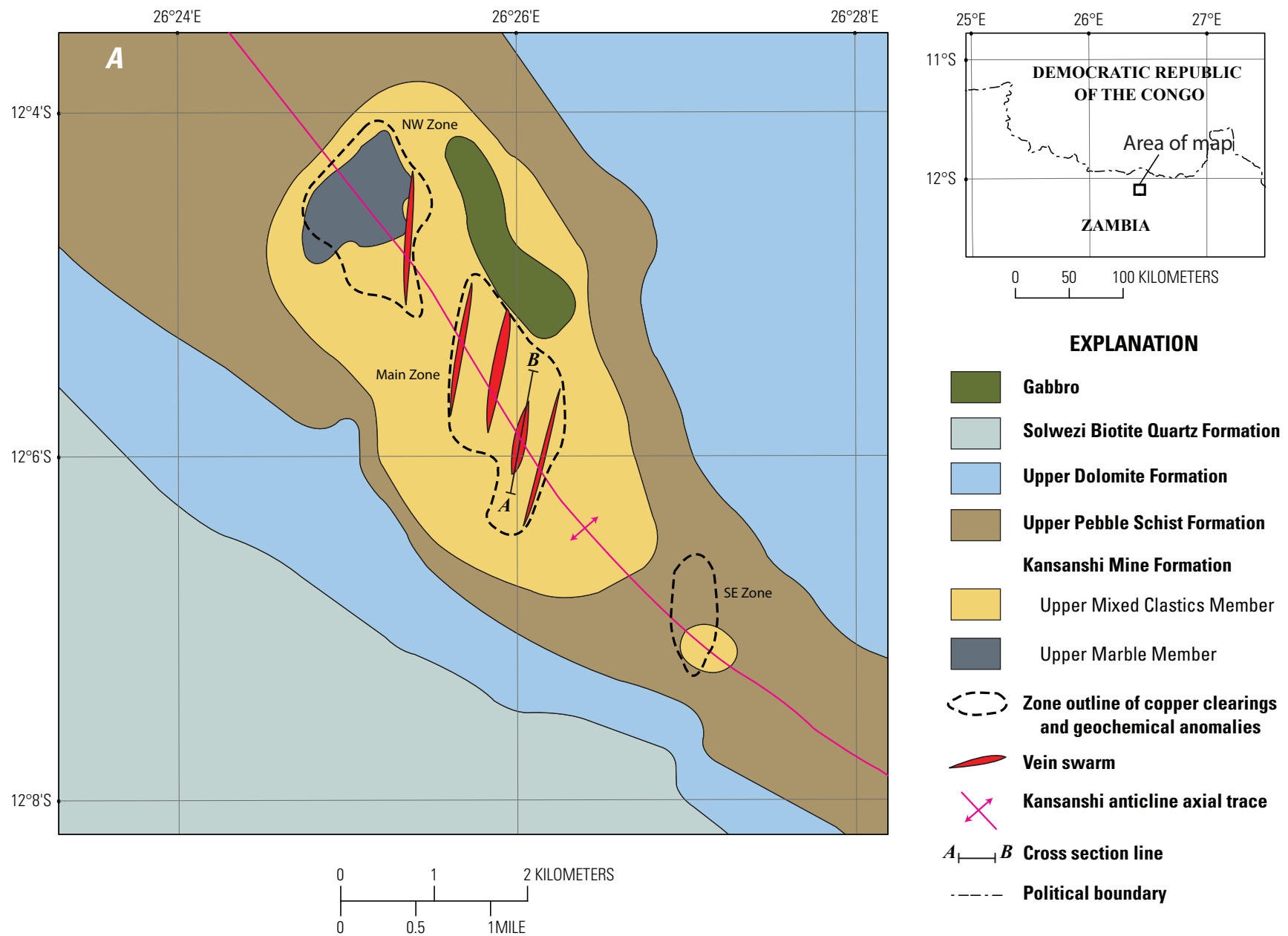


Figure 3-4 A, Kansanshi mine, Zambia. Plan view of the Kansanshi mine area, showing en-echelon distribution of major vein swarms along the axis of the Kansanshi anticline (modified from Broughton and others, 2002). NW, northwest, SE, southwest. B, Schematic illustration of different types of veins and associated alteration at Kansanshi mine (modified from Torrealday and others, 2000). Vein widths less than 1 centimeter to greater than 5 meters. The location of the deposit is shown on the index map, figure 3-3.

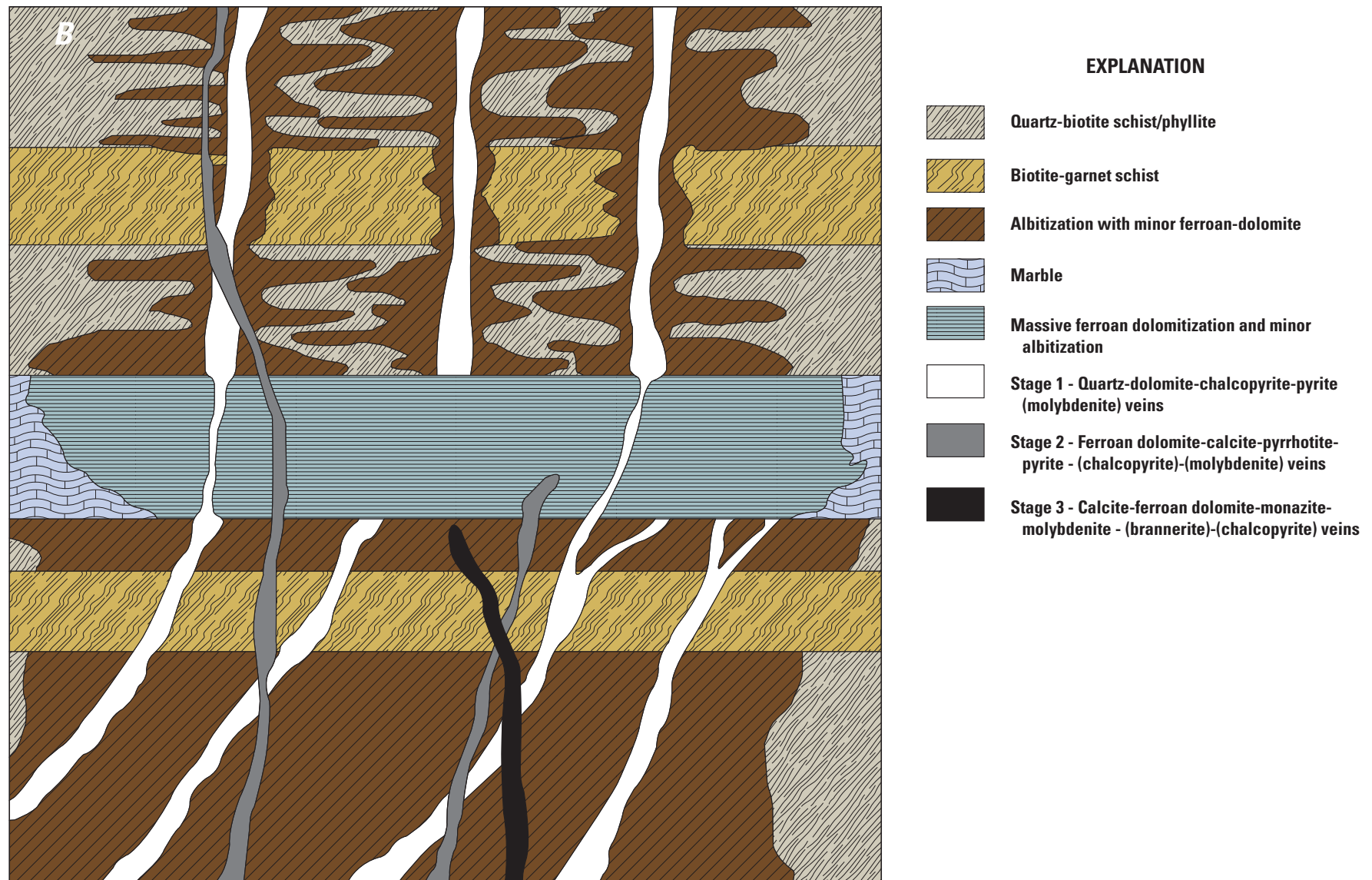


Figure 3-4.—Continued.

be traced for more than 400 m along strike and 50 m down dip, and have widths of <1 centimeter (cm) to >5 m. The veins and vein swarms are surrounded by alteration halos of albite, ferroan dolomite, ferroan calcite, quartz, green muscovite (V-rich roscoelite), and rutile. A fourth stage of mineralization occurs as brecciated veins and breccia zones of altered wall rock and vein fragments in a matrix of ferroan dolomite, calcite, albite, quartz, rutile and rare chalcocite. As mentioned above, the age of mineralization at Kansanshi is constrained to about 513–501 Ma (Torrealday and others, 2000; Broughton and others, 2002).

The copper at Kansanshi may have been deposited by basinal brines (like those that formed nearby stratiform copper deposits; figs. 3-1 and 3-3) that were heated during metamorphism (Hitzman and others, 2005).

Kalengwa, Zambia

The Kalengwa deposit (figs. 3-1 and 3-3) is a relatively small, high grade, supergene-enriched deposit hosted in undifferentiated upper Katangan low grade meta-sedimentary rocks (Thieme and Johnson, 1981). Host rocks include calcareous siltstones, sandstones, conglomerates, and thin marble beds (Broughton and others, 2004; Ellis and McGregor, 1967). The deposit is in the immediate footwall of a breccia zone described by Broughton and others (2004) as being similar to breccias in the Congolese part of the CACB that are thought to be produced by halokinesis and dissolution of evaporites. Ellis and McGregor (1967) describe a supergene-enriched ore body with a strike length of about 150 m and width of 25 m in subcrop 1–8 m below the present-day land surface. The supergene ore body dips steeply to the northwest and narrows with depth to less than a meter of chalcocite-bornite mineralization at a depth of 131 m. Moderate to intense sodic (calcic) and local potassic alteration of the breccia and underlying meta-sedimentary sequence appears to predate hypogene mineralization. The main ore minerals are supergene malachite and chalcocite replacements of the carbonate matrix of conglomerate (Ellis and McGregor, 1967). Primary sulfide minerals include chalcocite, bornite, and lesser pyrite replacing hematite and carbonate minerals. Ellis and McGregor (1967) noted that the richer concentrations of ore occur in the conglomerate, which varies in texture from a sedimentary breccia with slight displacement of fragments to a poorly sorted calcareous conglomerate. The Kalengwa deposit is most likely hosted in Nguba Group strata and, based on its relationship to a stratiform breccia horizon and the replacement nature of the hypogene mineralization, belongs to the SCR type of sediment-hosted copper deposits.

Dikulushi, DRC

The Dikulushi deposit is located about 300 km northeast of Lubumbashi in the Democratic Republic of the Congo (DRC) (figs. 3-1 and 3-3). The Dikulushi deposit is a small,

high grade, SCR deposit hosted in brecciated red sandstones, shales, and carbonate rocks that are tentatively correlated with the upper Gombela (Lubudi Formation) and lower Ngule (Mongwe Formation; fig. 3-2) subgroups of the Kundelungu Group. Northeast-directed shortening during the Lufilian orogeny resulted in the formation of several gently folded, north-west trending anticlines above subparallel detachment surfaces at depth (Dewaele and others, 2006; Haest and others, 2007). At Dikulushi, a north-northwest oriented thrust fault caused the upward displacement and ductile deformation of a shale unit against the base of a sandstone-dolomite sequence, causing brecciation and kink folding (fig. 3-5). A second period of structural disruption at Dikulushi is marked by the presence of cross-cutting, high angle, east-west and northeast oriented faults across the apex of the anticline, creating a structurally disrupted zone that was highly favorable for epigenetic styles of mineralization. Regionally, the contact between the Lubudi Formation carbonate rocks and the overlying Mongwe siltstones is characterized by broad-scale silicification, brecciation, and copper-mineralized veining, suggesting that there has been significant tectonic disruption and fluid flow within this stratigraphic interval of the Kundelungu Group (Anvil Mining Ltd., 2009).

The copper-lead-zinc-iron mineralization at Dikulushi is localized by a series of recurrently active, northeast trending fault zones that are present over a width of approximately 50 m. Within the fault-bounded zone, the sandstone unit and sandstone clasts within the breccia at the western end of the deposit are altered to a gray color with green clay, which diminishes gradually eastwards. The Dikulushi ore body is located in the relatively narrow zone (up to 25 m in thickness) between the Main and Northern Fault zones (fig. 3-5), dips 70° to the southeast, and is open at depth. The ore body is characterized by a variable mineral assemblage of early chalcocite, bornite, and chalcocite, with minor pyrite, arsenopyrite, sphalerite, tennantite, and galena associated with a gangue of dolomite, calcite, and quartz, and a later assemblage of silver-rich chalcocite with barite, calcite, and quartz gangue (Haest and others, 2007; Haest, Muchez, Dewaele, and others, 2009). The richest Dikulushi ore occurs as massive chalcocite with silver in solid solution that grades as high as 20 percent copper and 600 g/t silver (Dewaele and others, 2006). It occurs along the intersection of the Main and North Fault zones in the eastern portions of the mine and continues to depth where chalcocite surrounds remnant bornite mineralization. Supergene mineralization consists of malachite, chrysocolla, and azurite and occurs at the deepest levels of the mine (+905 m; Haest and others, 2007; Haest, Muchez, Dewaele, and others, 2009).

Fluid inclusion and isotopic studies indicate that mineralization at Dikulushi formed in two distinct episodes: (1) early deposition of subeconomic copper-lead-zinc-iron sulfides in a zone of crosscutting faults during the Lufilian orogeny, where chalcocite, bornite, chalcocite, and sphalerite precipitated from moderate temperature (~90 to 140 degrees Celsius, °C), saline H₂O-NaCl-CaCl₂ fluids in a reducing environment, and (2) post-orogenic remobilization of copper from the

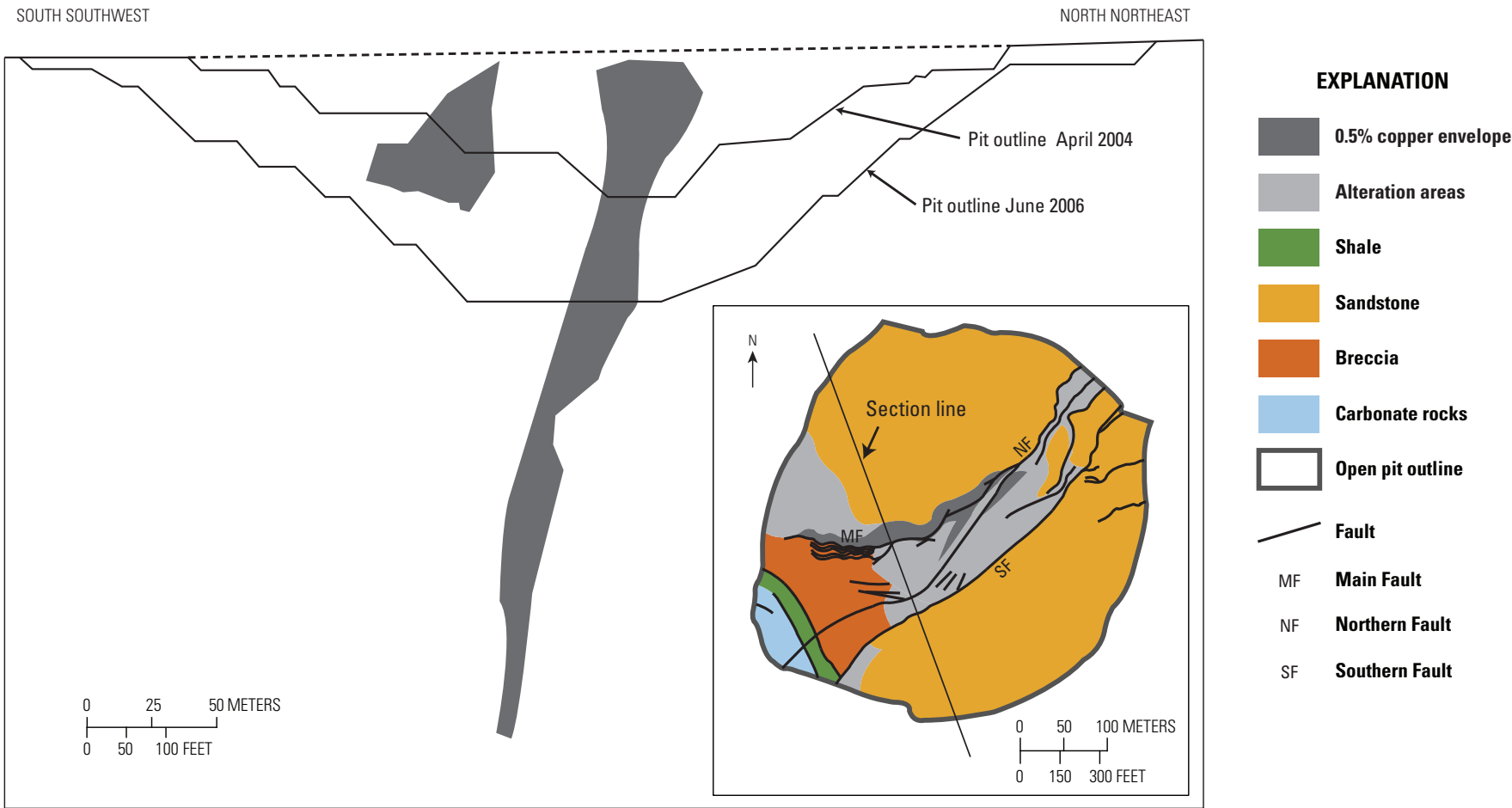


Figure 3-5. Map and cross-section of the Dikulushi structurally controlled replacement and vein (SCRV) deposit, Democratic Republic of the Congo, showing structurally controlled, steeply dipping envelopes of >0.5 percent copper around the major faults in the open pit (modified from Haest and others, 2007). The location of the deposit is shown on the index map, figure 3-3. %, percent.

upper parts of the polymetallic stage that formed chalcocite-dominant copper-silver ores from lower temperature ($\sim 70^\circ\text{C}$) H_2O - NaCl - KCl fluids in an oxidizing setting in reactivated and new faults along the eastern parts of the deposit (Haest, Muchez, Dewaele, and others, 2009; Haest, Muchez, Petit, and Vanharcke, 2009; Haest and others, 2010).

Kikonkula, DRC

The Kikonkula prospect is on the northern nose of the Kiaka Anticline 22 km southwest of the Dikulushi mine (fig. 3-3). It is hosted in upper Nguba and Kundelungu Group strata and exposed in gentle anticlinal structures along with stratiform copper prospects at Lufukwe and Mwitapile (Haest, Muchez, Dewaele, and others, 2009); therefore, all of the prospects are thought to be tectonically related to Lufilian or younger tectonic events. Mineralization at Kikonkula consists of disseminated chalcopyrite in the Lubudi Formation carbonate rocks along an east-west trending fault of Lufilian to post-Lufilian age (Haest, Muchez, Dewaele, and others, 2009). The chalcopyrite is associated with dolomite following early quartz. Subsequent remobilization has resulted in a digenite-bornite-covellite assemblage associated with barite.

Kapulo Area, DRC

The Kapulo-area copper-silver deposits and prospects are located approximately 130 km northeast of Dikulushi (figs. 3-1 and 3-3). The Kapulo deposits are (cumulatively) the largest sediment-hosted SCR type resource in the Lufilian Foreland (table 3-1). At Kapulo, deposits and prospects occur along a 3-km strike length of the Kapulo Fault and include, from north to south, the Shaba (Katanga), Safari North, and Safari South deposits, and the Luao-Kasongo prospect (fig. 3-6). Where exposed by artisanal workings, the Kapulo Fault generally dips steeply to the west. The Kapulo deposits are interpreted as hypogene, fault-controlled ore bodies with disseminated chalcopyrite and bornite in the sulfide zone and massive to nodular cuprite, malachite, and azurite in the oxide zone. The mineralization is hosted in shales and coarse-grained sandstones (the Luapula beds) of the Kundelungu Group and in basement granites of the Bangweulu Block (Kibaran basement on fig. 3-6) along the Kapulo Fault. Both the sedimentary rocks and granites exhibit varying degrees of brecciation and high grade zones are associated with bornite-chalcopyrite-filled matrix. The individual deposits are generally small, high grade, and range in thickness from 0-40 m (Mawson West Ltd., 2006).

The Shaba (Katanga) deposit is controlled by a north-northwest trending fault that dips 55° to the west and roughly separates sandstones and shales of the Kundelungu Group from granite in the footwall. The deposit occurs in the hanging wall of the fault and is located at the contact between a black shale and silicified sandstone interbedded with variably

granite-dominant and sedimentary rock-dominant polymictic breccias. The hanging wall sandstone is not mineralized and is in contact with variably brecciated and epidote-altered granite. Copper mineralization consists of a band of cuprite at the foot-wall contact of the black shale and a broad zone of supergene malachite and azurite near surface. The mineralized interval is characterized by disseminated chalcopyrite and minor chalcocite at depth with increasing bornite and native silver as the interval plunges to the south. Drilling at the Shaba deposit intersected primary ore at 125 m depth where the ore body is roughly 15 m wide and averages 4 percent copper.

The Safari North and South deposits (referred to as the Safari North and South Group for grade and tonnage modeling purposes due to their proximity; see appendix A, this report) are also located along the Kapulo Fault in coarse-grained gray sandstones with unmineralized shale and sandstone in the hanging wall. Mineralization occurs as chalcopyrite and bornite, which continues into brecciated footwall granite. Pyrite increases and chalcopyrite decreases as the granite becomes less fractured and more brecciated (Le Burn and Hayward, 2011).

Malachite occurs in two forms in the Kapulo area deposits, with the most abundant form occurring as light green disseminated malachite in shales and sandstones on the footwall side of the fault and the less abundant form as darker green fracture filling most typically in the shales. Azurite is present as nodules and layers in the shales and sandstones at both Shaba and Safari North and cuprite occurs in massive and nodular form within the shale unit and along its contacts, particularly the footwall contact. The main sulfide mineral at both Shaba and Safari North is chalcopyrite with lesser bornite and chalcocite. The chalcopyrite occurs as fine-grained disseminated sulfides, as more massive blebs up to 10 mm in size, and as replacement layers in sandstone. Paragenetic relationships suggest that chalcopyrite is early and that bornite and chalcocite occur as both hypogene and supergene phases. With increasing depth, chalcopyrite decreases and pyrite becomes the dominant sulfide. However, at the Shaba deposit a high-grade zone in which bornite is the dominant sulfide and is accompanied by native silver plunges to the south at 50 degrees. In this zone, bornite occurs as matrix to brecciated sandstone and granite at the footwall contact (Le Burn and Hayward, 2011).

Frontier, DRC

The Frontier deposit is located in the DRC, roughly 35 km northwest of Ndola, Zambia (figs. 3-1 and 3-3). The deposit is epigenetic, structurally controlled, and located within the Grand Conglomerate and underlying shales of the Mwashya Subgroup. The shales unconformably overlie a dolomite unit of the upper Roan (possibly the Bancroft Formation). The deposit is confined to the thickened fold nose of a shallowly southeastward-plunging, northeastward-dipping, overturned anticline. Deep drilling in the southern portion of the ore body indicates that the mineralized shale folds back

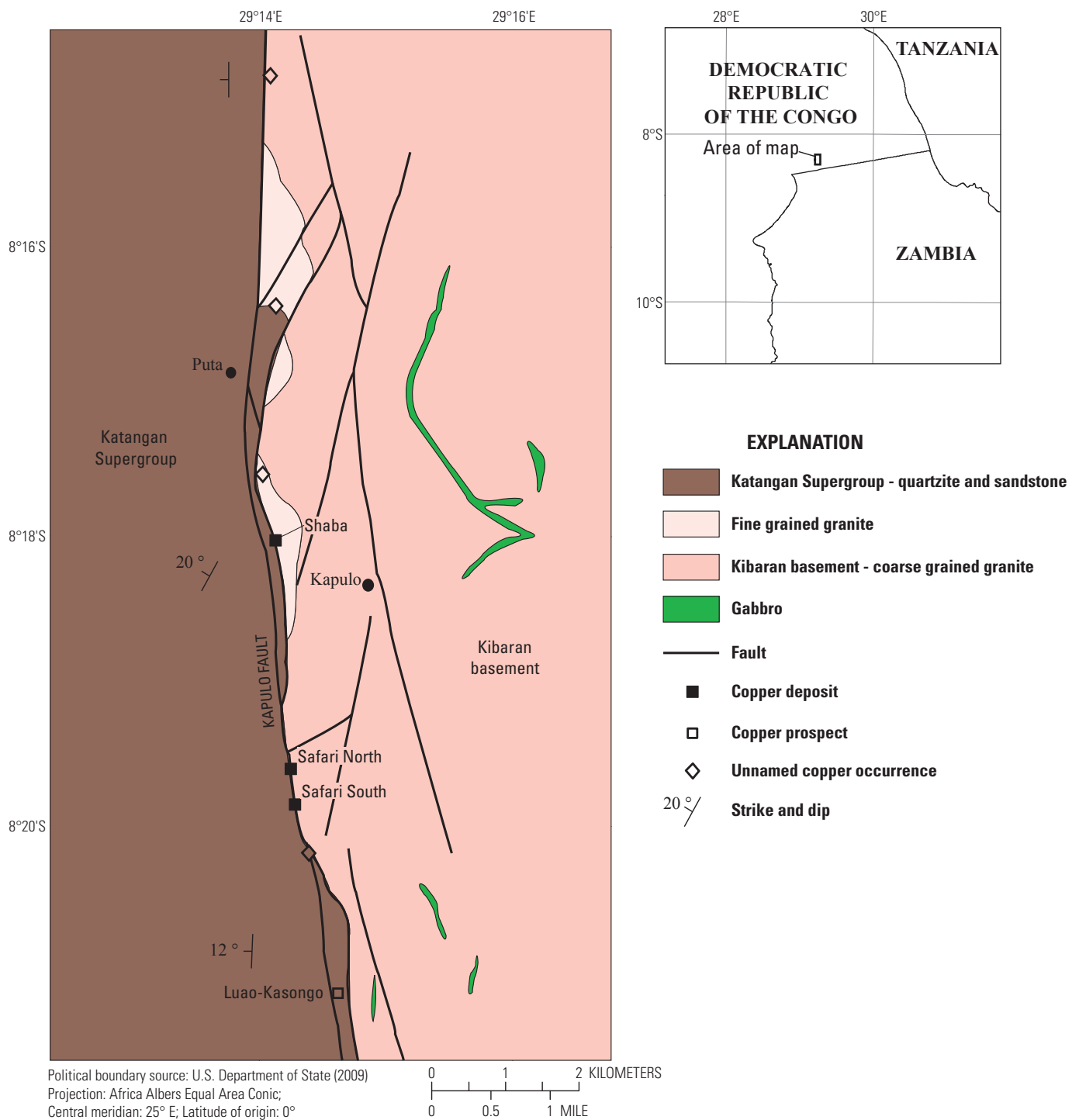


Figure 3-6. Map showing locations of deposits in the Kapulo area, Democratic Republic of the Congo, and their distribution along the Kapulo Fault (modified from Mawson West Ltd., 2006). The location of the Kapulo area is shown on the index map, figure 3-3.

on itself below the overturned anticline. Alteration associated with mineralization consists of sodic metasomatism, silicification, and dolomitization of the host rocks. Mineralization occurs as coarse-grained chalcopyrite with trace amounts of chalcocite, digenite, bornite, and covellite. Pyrite is the major gangue sulfide. The sulfide assemblage occurs in quartz-albite-carbonate stockworks, veins, veinlets, and breccias, and as foliation-parallel disseminations in altered shales and diamictites. Gangue minerals consist of plagioclase, carbonates, quartz, potassium feldspar, biotite and muscovite in decreasing order. Cobalt-rich areas within the ore body are present but are unevenly distributed. No discrete cobalt sulfides have been detected and scanning-electron-microscope studies have determined that pyrite is cobaltiferous (1.5 to 6.9 percent cobalt) and weakly arsenic bearing (0.2 to 1.7 percent arsenic; Gregory and others, 2006).

The Frontier deposit is bounded on the west by a fault zone that is oriented parallel to the ore body and vertically displaces the upper Roan dolomite. The ore body is primarily hosted by the (Mwashya) shale unit, which is sandwiched between the conformably overlying Grand Conglomerate and the unconformably underlying upper Roan dolomite. As of December, 2006, the ore body was closed to the north and west and open at depth to the south. The mineralized shale horizon has a strike length of 2 km and is at a depth of over 400 m below surface at the southwestern end (Gregory and others, 2006). The Frontier mine commenced production in November, 2007, and as of December, 2009, was projected to have a 15-year mine life (First Quantum Minerals Ltd., 2010).

Kipoi Project Area, DRC

Both the Kileba and Kipoi Central deposits are located in the Kipoi project area about 85 km northwest of Lubumbashi in the DRC (figs. 3-1 and 3-3). Kileba is approximately 6 km southeast of Kipoi Central (fig. 3-3). Host rocks in the project area consist of the Mwashya Subgroup (R4) unconformably overlain by tillites of the lower Nguba Group and discordantly underlain by talcose breccias (locally called the Breche Heterogene) of the R.A.T. and lowermost Mines Subgroups (R1 and R2.1). Throughout the project area the Mwashya Subgroup contains an interval of light green talc-chlorite rocks interpreted as altered mafic volcanic rocks. In drill core they are massive, with internal monomictic breccias of irregularly shaped and angular clasts. The hanging wall contact is commonly marked by a 1- to 3-meter-wide band of hematite and jasperoid iron formation. At Kipoi Central, the iron formation is overlain by dolomitic siltstones with at least two interbedded dolomite layers that are each about 20–30 m thick and strike northeast-southwest (fig. 3-7). The uppermost stratigraphic layer consists of thin-bedded, fine- to medium-grained dolomitic siltstone that is about 150 m thick. This Mwashya Subgroup siltstone hosts 70–80 percent of the mineralization (Reidy and others, 2009). Bedding measurements in the stratified portion of the Mwashya Subgroup indicate

that these rocks strike easterly to northeasterly and are dipping 60–90° to the southeast. In outcrop, the contact with the overlying Nguba Group tillites is a high-angle unconformity and the contact of the Mwashya Subgroup with the underlying Breche Heterogene is irregular and generally steeply dipping to vertical. This contact is interpreted as the surface of a diapir related to salt extrusion.

Kipoi Central

Observations of tectonic breccias at several locations at the Kipoi Central deposit indicate that the deposit is controlled by structural features. Artisanal workings expose structures that are mostly brittle faults subparallel, or at high angles, to bedding (fig. 3-7). Associated breccias are localized and separated by intervals of weakly deformed rocks cut by conjugate subvertical veins that are cross cut by late-stage subhorizontal veins. The most prominent brittle structure is located near the north end of the artisanal workings where it strikes nearly east-west, dips steeply to the west, and separates mineralized dolomitic siltstones from the mafic pyroclastic unit. The contact shows strong brittle deformation and a late-stage planar fault that is heavily overprinted by cobalt mineralization. The western portion of the Kipoi Central project area is thought to be separated from the Kipoi Central deposit by a north- to northeast-striking lineament that may consist of several minor subparallel faults. Where this lineament is exposed in the northwestern project area, it is characterized by strong brecciation and mineralization that separates Breche Heterogene from pyroclastic rocks. Southward, the presence of the lineament is inferred on the basis of a strong magnetic gradient and several minor subparallel splay-faults. This lineament may have exerted a control on the pattern of Mwashya Subgroup sedimentation to the east. An east-west trending brittle fault is mapped west of the lineament, terminates against it, and is marked by artisanal workings that exploit copper oxides. Structural interpretations suggest that the Kipoi Central project area represents a structurally dismembered (possibly diapiric) segment of Mwashya Subgroup sedimentary rocks that terminate eastward against Breche Heterogene and to the west is adjacent to an uplifted block of lower Mwashya Subgroup mafic volcanic rocks. The unconformable contact with overlying rocks and the presence of mineralized clasts in the tillite suggest that both brittle deformation and mineralization occurred before the deposition of the Nguba Group tillite (Grand Conglomerate).

Both primary sulfide and secondary oxide copper mineralization is observed at Kipoi Central, with the majority of the resource resulting from secondary enrichment and oxidation of primary sulfides in the weathering profile. In non-oxidized core, primary sulfides are present in cross-cutting and bedding-parallel veins and as matrix in crackle, mosaic, and rubble breccias of tectonic origin. The mineralogy of primary sulfide assemblages in late-stage veins consists of chalcopyrite and pyrite with quartz and calcite gangue. Paragenetically

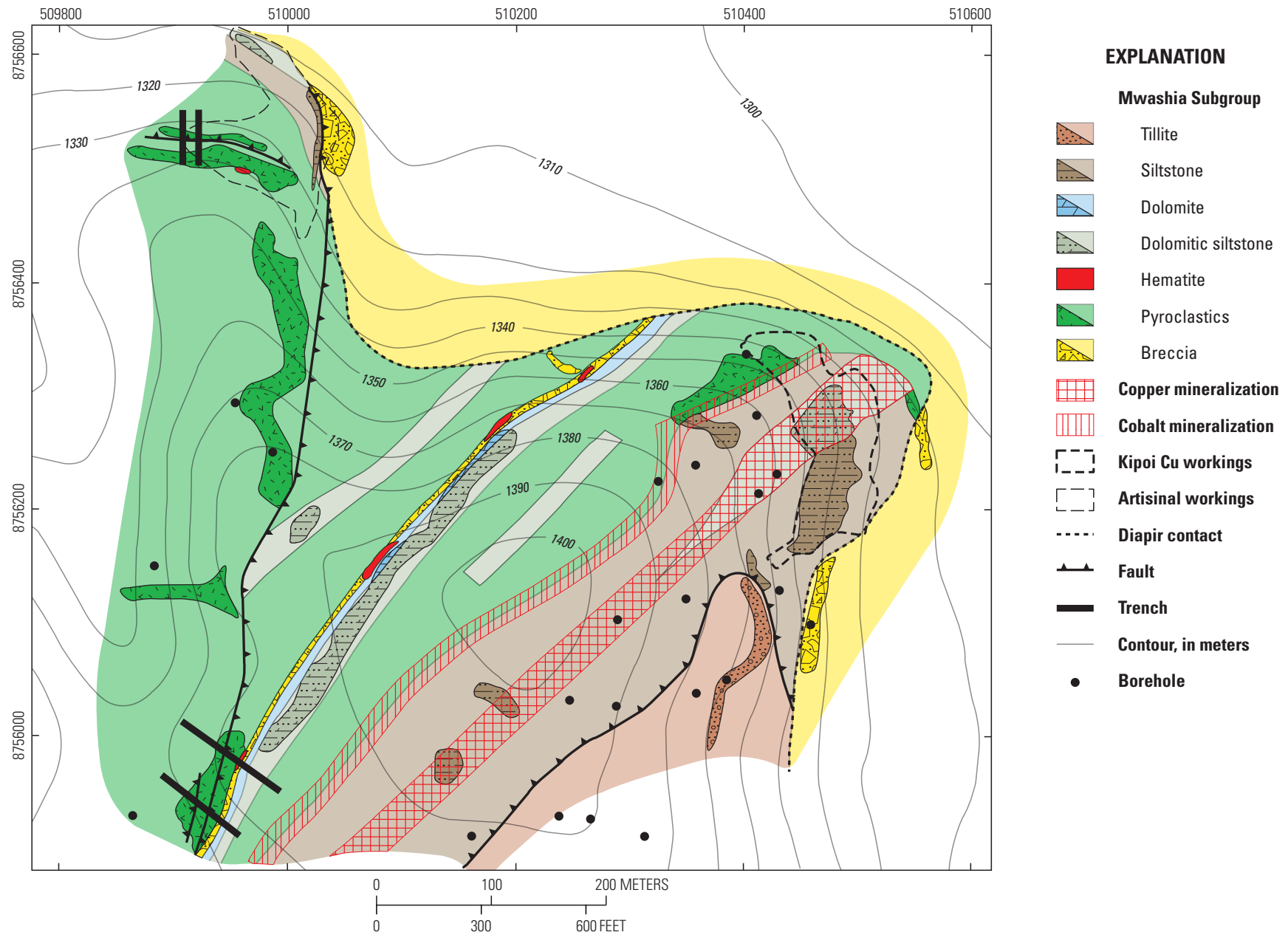


Figure 3-7. Simplified geological map of the Kipoi Central deposit, Democratic Republic of the Congo (modified from Reidy and others, 2009). Areas of outcrop within map units are shown with patterns and darker shades of color. UTM grid, zone 35.

earlier bedding-parallel veins contain chalcopyrite exclusively. Primary sulfide minerals at Kipoi Central are therefore epigenetic and are almost exclusively structurally controlled. Primary sulfides have been strongly affected by deep weathering and oxidation, resulting in redistribution of copper. The main copper oxide mineral at Kipoi Central is malachite, with minor azurite, chalcocite, and native copper. The oxide mineralization occurs as in-situ replacement of stratabound primary sulfides, as coatings on bedding, cleavage, and joint surfaces, and to a lesser degree as fillings in cavities. As a result, copper oxides are dispersed over a much larger volume of rock than the primary copper sulfides. Both a volumetric as well as a textural zonation of copper minerals is observed in the vicinity of faults, with strong copper enrichments in fault matrix giving way laterally to mosaic and then simple vein styles of mineralization. Cobalt enrichment is important at Kipoi Central but is less well constrained. Cobalt is most strongly concentrated near the contact between Mwashya Subgroup sedimentary and mafic volcanic rocks and occurs in a black, talc-rich, soft mass that is up to several tens of meters thick. No cobalt minerals have been identified; it is assumed that cobalt occurs in the mineral heterogenite (Reidy and others, 2009).

Copper mineralization has not been observed in the underlying Breche Heterogene. Copper oxide-bearing clasts are present in the sandy matrix of the overlying Nguba Group tillite, suggesting that primary copper sulfides were present at the time of deposition of the tillite. Copper oxide mineralization is also present in brittle fractures that crosscut the tillite suggesting that prolonged or repeated deformation occurred.

Kileba

The Kileba deposit is located along a topographical ridge-line that extends from the Judiera prospect in the northwest, through the Kipoi Central deposit to Kileba at the southeast end of the trend. The Kileba deposit is separated by a low gap in the ridge into northwestern and southeastern segments marked by artisanal workings that occur intermittently over a strike length of about 1,100 m (Reidy and others, 2009). Mineralization is hosted in Mwashya Subgroup rocks consisting of a package of steeply southwest dipping (75–80°) mafic volcanic, talcose dolomite, banded iron formation, siltstones, and pebble conglomerate rocks. The mineralization is primarily hosted in the talcose dolomites at the base of the iron formation; however, the mineralized zone is interpreted as an east-west zone of thickening oblique to strike and is thought to be either fold or fault related, with isoclinal folding observed in the artisanal workings. The iron formation is a laterally continuous and slightly discordant hematite lens about 2 m thick and subparallel to bedding that is located about 20 m above the mafic pyroclastic rocks. The iron formation is generally composed of laminated specular hematite with internal breccias observed in places. The contact between the mafic pyroclastic rocks and sedimentary rocks is strongly sheared in the main pit at the southeastern end of the trend. A similar package of sheared and deformed mafic pyroclastic rocks

to the northeast in contact with dolomitic siltstones to the southwest has been observed at the northwestern end of the prospect area.

Surface mapping augmented by regional magnetic data suggest that the Kileba deposit lies on the northeastern flank of a regional syncline. Whether this syncline is followed by an anticline or a thrust fault to the northeast has not been determined but is postulated based upon inferred contact-parallel shearing and incipient anticlinal geometry. Subvertical, north to northeast-trending brittle structures crosscut and therefore postdate northwest trending structures, suggesting that regional stress was variable over time or that progressive deformation developed secondary splay structures. An abrupt dip reversal from southwest to northeast is observed in association with a narrow northeast-trending brittle fault at the northwestern end of the main pit, and a second dip reversal related to late faulting is inferred to occur in the gap between the northwestern and southeastern ridges due to the observed southwest dipping strata observed in outcrop on the northwestern ridge (Reidy and others, 2009).

Copper mineralization at Kileba consists entirely of copper oxides, with malachite and minor azurite localized within a halo of brecciated and silicified rock surrounding the contact between mafic pyroclastic rocks and dolomitic siltstones. Copper oxides occur in veins and fractures extending up to 20 m from the contact. As at Kipoi Central, there is a strong empirical correlation between the volume of copper mineralization and proximity to epigenetic structural features (Reidy and others, 2009). The project area is divided by the gap in the ridgeline into two mineralized prospects, the Kileba North and South deposits, each with a different tenor of copper enrichment. The Kileba South deposit consists primarily of a supergene copper oxide body about 730 m long, 130 m wide and 120 m thick (depth to the base of the weathering profile) with copper sulfides extending below the oxidized zone. The majority of the inferred resources of 9.5 million metric tons at 1.4 percent copper (modeled at 0.5 percent copper cutoff) is located within the oxide body (Reidy and others, 2009). The Kileba North deposit is thought to be a continuation of the structural zone hosting the Kileba South deposit and consists of copper oxides along 650 m of strike length and extending to a depth of 110 m; however, a supergene body apparently did not develop here. Mineralization is reported to be open at depth and along strike to the northwest. Both of the deposits are thought to be connected by a continuous deep zone of mineralization (Reidy and others, 2009).

Lonshi, DRC

The Lonshi deposit is hosted in Kirilabombwe Subgroup rocks just below the contact with the Mwashia Subgroup in the DRC approximately 10 km southeast of Ndola, Zambia (figs. 3-1 and 3-3). The stratigraphic succession in the mine area consists of eastward dipping lower Roan clastic rocks overlain by upper Roan pelitic, carbonate, and minor clastic

rocks which are in turn overlain by Mwashya Subgroup shales. The Lonshi ore body is located along a thrust and sheared contact between the Lonshi conglomerate and an overlying dolomitic marble (fig. 3-8). Sulfide mineralization occurs primarily as chalcopyrite replacing carbonate clasts in the Lonshi conglomerate and as disseminations and rare veinlets in both the conglomerate and the dolomitic marble. Supergene enrichment and subsequent deep oxidation and weathering have resulted in complete dissolution of the carbonate rock to produce a residual silty black material called Terre Noir. Terre Noir is host to a major secondary oxide ore body consisting of chalcocite that has largely been weathered to malachite and black copper oxide minerals. At depth, dissolution of the dolomitic marble is incomplete and Terre Noir has formed only along the upper and lower contacts of the carbonate unit (Stephens and Newall, 2003).

Extensions of the Lonshi ore body have been traced over a strike length of 2.5 km and have been drilled to a maximum depth of 150 m. Oxide mineralization varies from 2 to 50 m in true thickness with ore grades and mineable thicknesses being confined to a synclinal fold flexure. In 2003, similar synclines were mapped to the north and south of the Lonshi deposit but were not drilled (Stephens and Newall, 2003). The Lonshi oxide ore body was depleted and mining operations ceased in August, 2008. As of December, 2009, no oxide resources remain at Lonshi. First Quantum Minerals is currently investigating the continuation of sulfide mineralization along the trend of the Lonshi horizon to a depth of 350 m below the base of the present pit (First Quantum Minerals Ltd., 2010).

Tilwezembe, DRC

The Tilwezembe deposit is located in the western portion of the CACB about 27 km east of Kolwezi (figs. 3-1 and 3-3). The deposit is near the western end of the Tilwezembe Anticline which extends eastward for more than 45 km before disappearing under recent alluvium. The crest of the anticline is marked by the trace of the north-verging Kamikongwa Thrust Fault that places older Mwashya Subgroup strata over younger lower Nguba Group strata. At least eight copper-cobalt prospects are located along the crest of the Tilwezembe Anticline and include the Tilwezembe deposit as well as the Kisanfu, Kalumbwe-Myunga, and Deziwa prospects (Dixon and others, 2009).

The deposit is primarily hosted in vuggy to massive, strongly brecciated siliceous dolomites and dolomitic shales beneath a prominent hanging wall marker horizon of hematitic iron formation and ferruginous dolomites of the Mwashya (R4) Subgroup (fig. 3-2). However, lesser mineralization in brecciated lower Nguba Group strata along the footwall of the thrust suggests that mineral deposition is younger than lower Nguba Group strata (Dixon and others, 2009). The Nguba Group strata include various massive, bedded and brecciated argillites and tillites, which are in turn thrust over younger maroon Kundelungu argillites (Dixon and others, 2009).

A Mwashya north-south cross-section perpendicular to the Kamikonwa Thrust Fault consists of basal Nguba Group tillite (the Grand Conglomerate) underlain by rocks of the Mwashya Subgroup, a secondary fault, and fragments of Nguba Group siltstones on the southern flank of the anticline above the trace of the thrust. The northern flank of the anticline below the thrust consists of shales and siltstones of the lower Nguba Group. The Mwashya Subgroup is 20–50 m thick, dips 40–50° to the south, and contains sporadic copper mineralization for a distance of 600 m and cobalt mineralization for 1,200 m along strike. Drilling has delineated mineralization to a depth of 250 m (Dixon and others, 2009).

Ore in the oxide zone above a depth of 60–100 m consists primarily of malachite, pseudomalachite, and heterogenite with traces of libethenite. Manganese oxide gangue is ubiquitous and occurs as psilomelane and manganite (Dixon and others, 2009). Toward the base of the oxide zone, native copper is locally common along with sphaerocobaltite and chrysocolla. Carrollite, chalcocite and some bornite with traces of chalcopyrite characterize most of the sulfide assemblage. Thin carbonaceous shale at the base of the Mwashya Subgroup is always enriched in bedded and breccia-hosted carrollite and chalcocite. Mineralization is strongly correlated with silicification of the dolomite and occurs as infilling of vugs and in fissures and open fractures associated with brecciation in all lithologies.

Other SCR Deposits and Occurrences

Examples of other districts that exhibit stratiform/stratabound disseminated to epigenetic structurally controlled replacement and vein type deposits in the same sedimentary sequence include the Paradox Basin of Colorado-Utah, United States where both stratiform (Lisbon Valley mine) and structurally controlled (Cashin Mine, Cliffdweller) copper deposits were mined from the same sedimentary sequence, and the Kupferschiefer of Germany, where Mansfeld-type deposits and Ruckel "vein" deposits are present within the Rotliegendes sandstone and Kupferschiefer shale Formations of the Southern Permian Basin. Although the Kupferschiefer deposit in Poland and Germany is the type example of the reduced-facies subtype of sediment-hosted stratabound copper deposit, crosscutting epigenetic mineralized veins have been described as a distinct, but related style of mineralization to explain the cobalt-nickel-bismuth veins along fault systems in contact with Zechstein sedimentary rocks at the Bieber deposit in Germany (Wagner and Lorenz, 2002). Within the Kupferschiefer itself, vertical sulfide-calcite veinlets and replacement textures are observed, where bedding plane sulfate and sulfide veinlets are cut by vertical sulfide veinlets. Jowett (1987) proposed that these vertical veinlets may have formed by hydrofracturing due to fluid overpressure from a temperature increase and generation of carbon dioxide (CO₂) and hydrocarbon gases from Kupferschiefer organic matter during rapid basin subsidence.

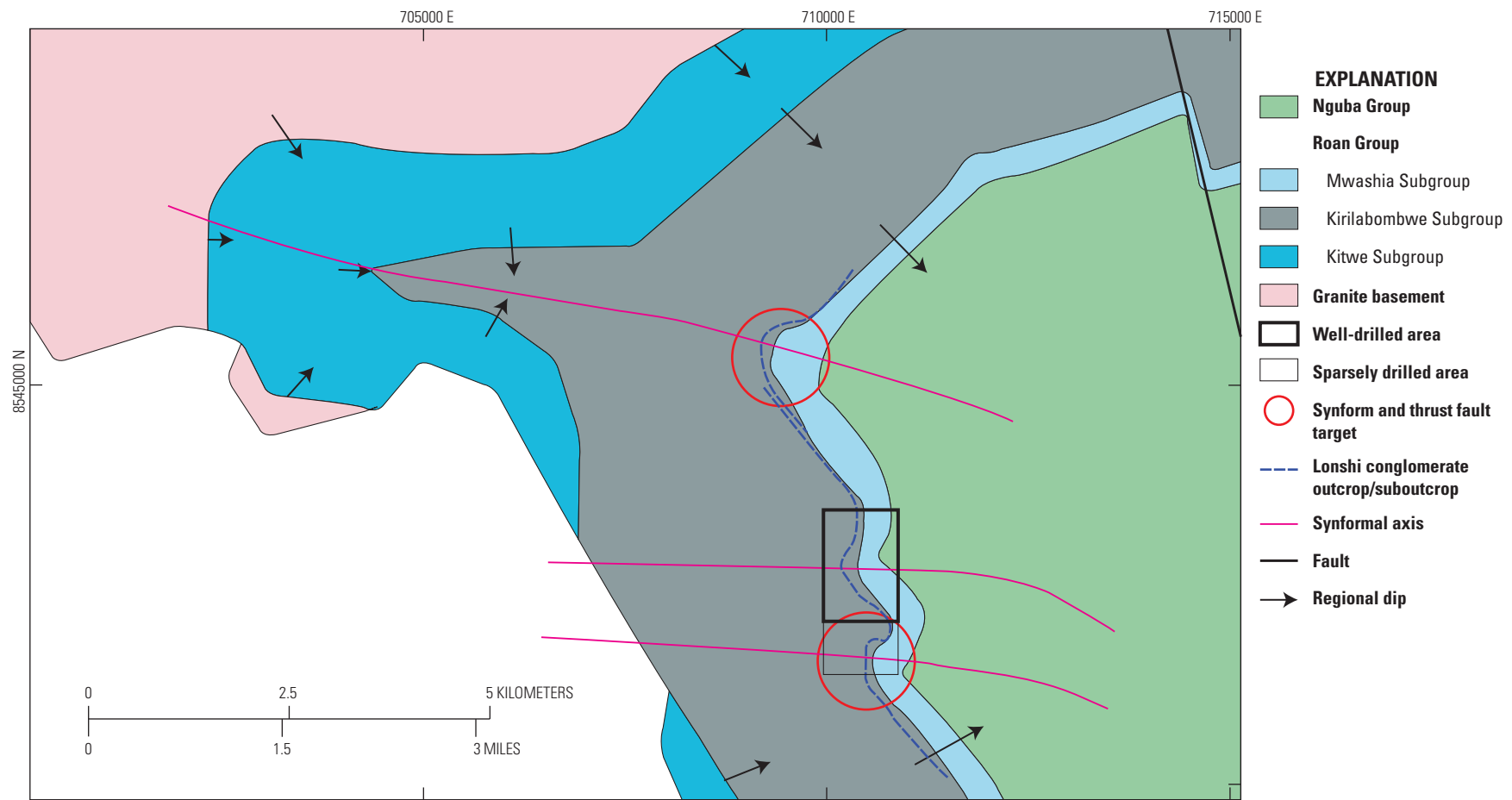


Figure 3-8. Geologic map of the Lonshi deposit, Democratic Republic of the Congo (based on Stephens and Newall, 2003). The location of the deposit is shown on the index map, figure 3-3. UTM grid, zone 35.

The sandstone-hosted deposits of the Chu-Sarysu Basin of Kazakhstan may be another example of a district containing both stratabound and SCR-type deposits and may be related to differences in stratal versus structurally controlled fluid flow (Gablina, 1981; Syusyura and others, 1986; Syusyura, 2008).

Cashin, Colorado, United States

The Cashin Mine is about 25 km northeast of the Lisbon Valley in Montrose County, southwestern Colorado. The Cashin deposit contains 11,750,000 metric tons of ore with an average copper grade of 0.52 percent. With 61,100 metric tons of contained copper, the Cashin deposit is smaller than any of the SCR deposits in the CACB (table 3-2).

Cashin is one of a number of epigenetic and structurally controlled sediment-hosted SCR prospects that are hosted within intracontinental, rift-related, terrestrial sandstones and restricted marine sedimentary rocks of the Paradox Basin (fig. 3-9). The basin initially received 600–900 m of evaporitic sediments of the Paradox Formation in Pennsylvanian time followed by as much as 3,500 m of mostly continental red beds and eolian sandstones during Permian through Jurassic time. The marine transgression of the Interior Seaway in the Early Cretaceous sealed the basin beneath 600–900 m of Mancos shale (fig. 3-9). Salt tectonics during the Permian, Triassic, Jurassic, and Tertiary have resulted in the formation of diapirs or salt walls over northwest trending basement faults that have folded or pierced the overlying stratigraphy. The Paradox Basin also is host to significant petroleum reserves generated from organic-rich siltstones of the Paradox Formation. Additional mineral deposit types present in the basin include sediment-hosted stratabound copper deposits such as the Lisbon Valley deposit, which contains 48 million metric tons at 0.514 percent copper hosted in the Jurassic-Cretaceous sandstones, and sandstone-hosted uranium-vanadium deposits in the late Jurassic Morrison Formation and uranium in the Triassic Chinle Formation (Thorson, 2005).

The Cashin deposit is localized in porous Jurassic Wingate eolian sandstone on either side of the Cashin Fault, about 1.5 km from the inferred southwestern edge of the Paradox Valley salt anticline (fig. 3-10). The Wingate sandstone is about 75 m thick and consists of fine-grained, red-orange, carbonate-cemented sandstone with dark red to black iron and manganese staining on outcrops. The Wingate is underlain by red-brown shale and siltstone of the Triassic Chinle Formation and conformably overlain by the irregularly bedded, red, buff, light gray, and lavender shale, siltstone, and fine- to coarse-grained sandstone of the Kayenta Formation (fig. 3-9).

Structural relationships at the Cashin Mine are relatively simple (fig. 3-10). The host sedimentary rocks strike northwesterly and dip about 5° to the southwest at the mine and steepen to about 18–20° near the edge of the salt diapir.

The Cashin Fault strikes about N45°E, dips 60–75° to the northwest, and has 12–18 m of normal, down to the northwest offset. Slickensides on the fault plane rake obliquely to the southwest. The similar Cliffdweller Fault is located about 450 m to the northwest of the Cashin Mine and creates a pie-shaped wedge of rock that slid down and away from the Paradox Anticline. In the mine area, the Cashin Fault is composed of two or more en echelon strands that are separated by horsetail zones of more intense fracturing. Several small subsidiary faults subparallel to the Cliffdweller Fault cross-cut the Cashin Fault and appear to control the location of the horsetail zones. Locally more intense fracturing and presence of copper veinlets within the horsetail zones create high grade zones in the “disseminated” deposit.

The most obvious alteration feature is a roughly 13 km long, 6.5 km wide, semicircular area centered on the mine area in which the Wingate and Navajo sandstones have been visibly altered from red to white. Within this bleached zone, an earlier fluid is suggested to have reduced hematite to pyrite and altered sodic plagioclase prior to carbonate cementation and copper mineralization. The significance of this relatively widespread fluid alteration event is that it served to convert otherwise unfavorable oxidized strata into a reducing, favorable host rock for later copper-silver bearing fluids (Thorson, 2004; MacIntyre and others, 2004, 2005). The presence of oil-bearing fluid inclusions in the Wingate sandstone suggests that the source of both fluids was probably organic-rich units in the Paradox Formation (MacIntyre and others, 2004; Thorson and MacIntyre, 2005). Petrographic evidence indicates quartz dissolution and replacement by bornite and chalcopyrite in mineralized areas.

Copper mineralization is localized along the strike of the Cashin Fault for greater than 1,000 m and extends through the complete vertical section of the Wingate sandstone (fig. 3-11). Copper grades are highest along the fault and in stratiform zones of higher permeability or higher concentrations of reductant. Disseminated zones of copper mineralization commonly extend 120 m and narrow zones of copper oxides have been traced as far as 550 m from the Cashin Fault. Disseminated sulfides consisting of chalcopyrite, bornite, covellite, and chalcocite replace pyrite, bituminous hydrocarbons, pore-filling dolomite, and occasionally quartz. Oxidation of this assemblage results in minor copper remobilization and creates thick supergene sequences of disseminated low-grade copper oxides consisting of malachite, azurite, copper-bearing neotocite, and supergene chalcocite. Oxidation becomes less pervasive at depth and commonly extends to depths of 30 m and 60 m along strike of the Cashin Fault.

Sulfide minerals along the Cashin Fault occur within a vein zone of crushed sandstone with veinlets and open-space fillings of pink saddle dolomite and white barite gangue. The vein also contains native copper and a complex assemblage of copper arsenides at depth. Filling temperatures of fluid inclusions in dolomite and barite from the Cashin vein are up to 105 °C (Gray and others, 1996; Thorson and MacIntyre, 2005).

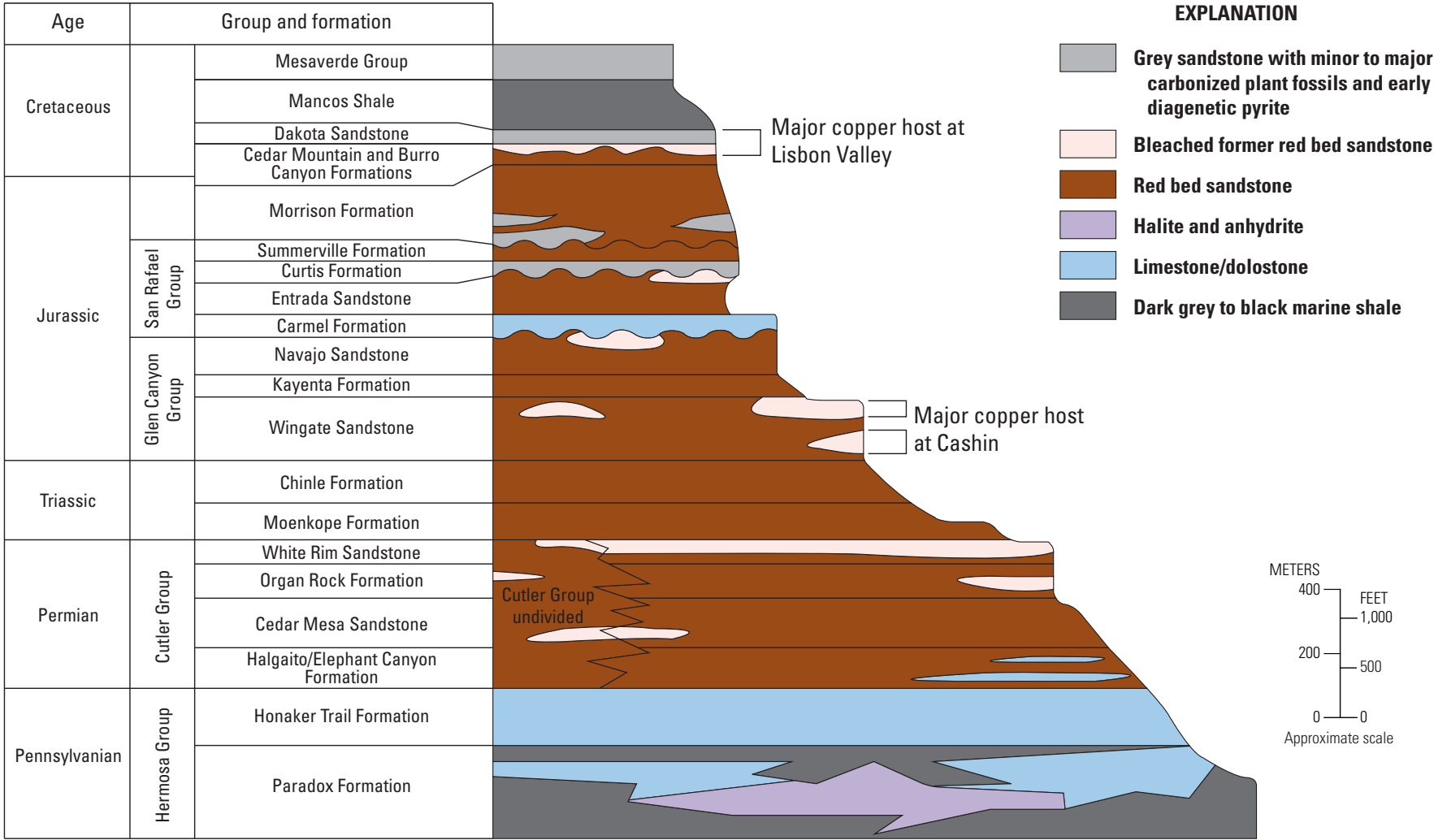


Figure 3-9. Generalized stratigraphic section of southeastern Utah and southwestern Colorado, United States (modified from Thorson, 2005).

General Characteristics of SCRV Copper Deposits

General characteristics of SCRV deposits are briefly described here, based on the limited number of deposits that have been described as sediment-hosted replacement and vein, rather than as stratabound deposits.

Dimensions

Vein swarms can have strike lengths of hundreds of meters to more than 1,200 m, widths up to 200 m, and vertical dimensions of up to 500 m. Individual veins at Kansanshi, for example, can be traced for more than 400 m along strike and 50 m down dip, and have widths of <1 cm to >5 m. The copper-lead-zinc-iron mineralization at Dikulushi is constrained by a series of northeast-trending fault zones that are present over a width of approximately 50 m. The Dikulushi ore body is located in a relatively narrow zone (up to 25 m thick) between fault zones and is open at depth. The mineralized shale horizon at the Frontier deposit has a strike length of 2 km and extends from surface to a depth of more than 400 m below surface at the southwestern end (Gregory and others, 2006). The Lonshi ore body has been traced over a strike length of 2.5 km along a thrust contact and has been drilled to a maximum depth of 150 m (Stephens and Newall, 2003).

Oxide mineralization varies from 2 to 50 m in true thickness (Stephens and Newall, 2003). The presence of sulfide mineralization along the trend of the Lonshi ore body to a depth of 350 m below the base of the present pit (First Quantum Minerals Ltd., 2010) may indicate a vertical extent of up to 500 m.

Host Rocks

Host rock lithologies include phyllites, schists, and marbles, calcareous siltstones, sandstones, conglomerates, and thin marble beds, shales, and carbonate rocks. In the CACB, SCRV deposits are present throughout the approximately 7-km-thick Katangan Supergroup (fig. 3-2). SCRV deposits occur in the lowermost Roan Group, at upper stratigraphic levels in the Mwashya Subgroup, throughout the Nguba Group and in the middle stratigraphic levels of the Kundelungu Group, and at contacts between contrasting lithologies (fig. 3-2). Mineralization crosses multiple lithologic units in many deposits.

Ore Controls

Fault intersections with permeable strata localize SCRV deposits by creating zones of increased permeability favorable for epigenetic styles of mineralization. Cross-cutting, high angle faults, and other structures developed during and subsequent to the Lufilian orogeny in the CACB provided conduits for copper-mineralizing fluids. Anticlines, detachment

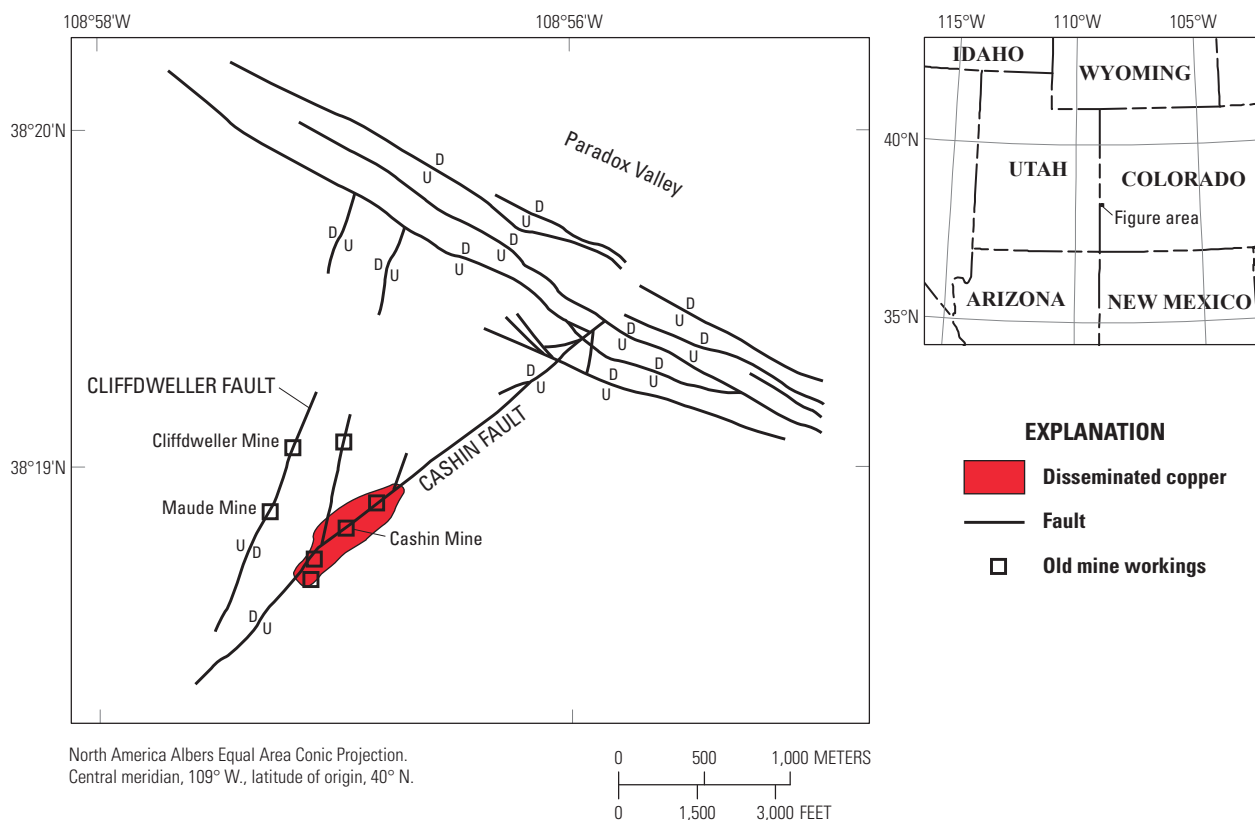


Figure 3-10. Map showing fault patterns in the Cashin Mine area, Colorado, United States (modified from Thorson and MacIntyre, 2005).

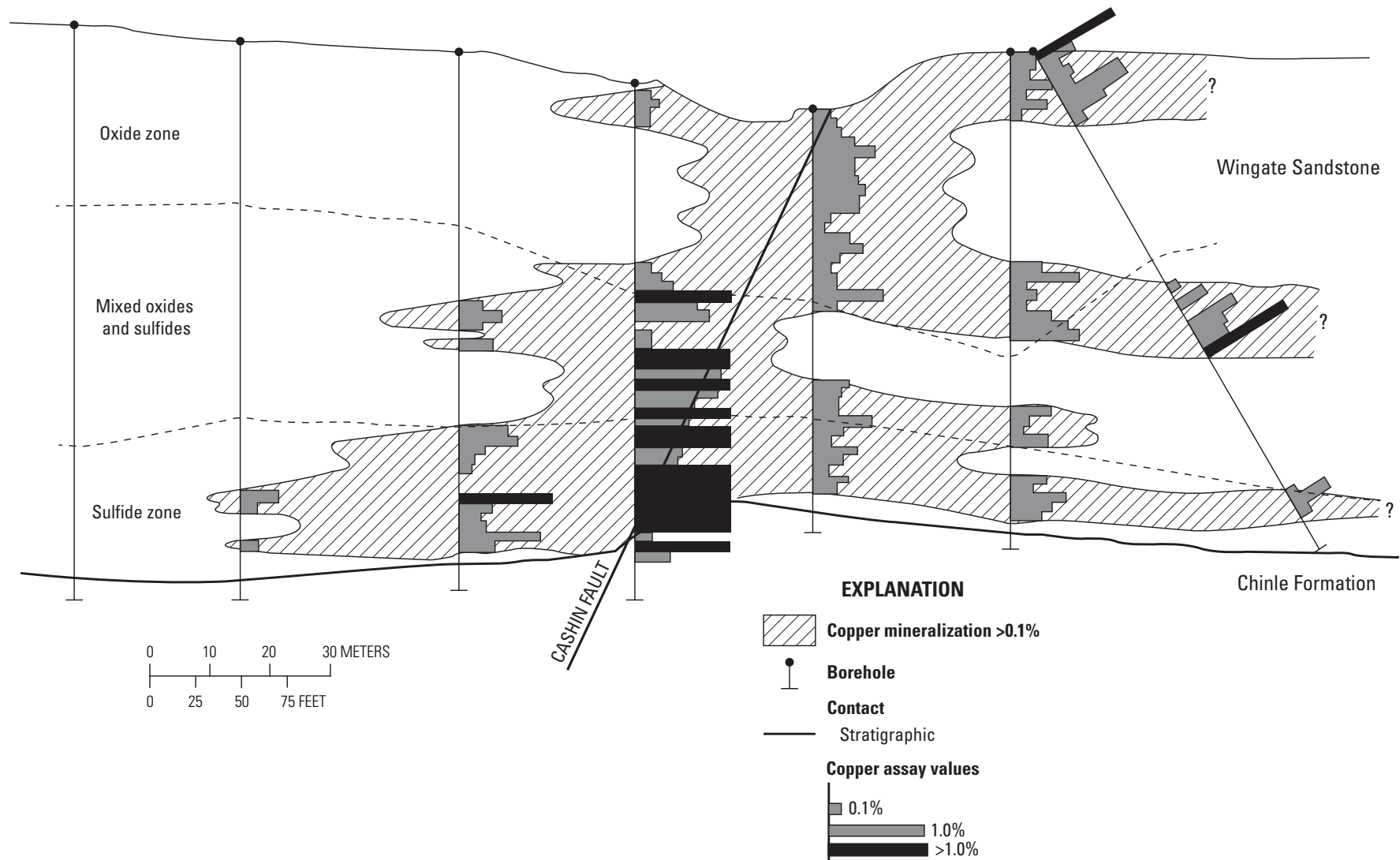


Figure 3.11 Northwest-southeast cross section perpendicular to the Cashin Fault, Colorado, United States, showing the distribution of copper. Histograms for copper show mineralization from 0.1 to 1.0 percent in shaded gray color; the length of the bars is proportional to the assay values. Assays with greater than 1 percent copper are shown as black bars (modified from Thorson and MacIntyre, 2005). %, percent.

surfaces, and thrust faults cause upward displacement and ductile deformation, brecciation, and kink folding, especially at contrasting lithologic contacts such as shale against sandstone or dolomite.

Mineralogy

Chalcopyrite, bornite, chalcocite, digenite, and covellite are the major copper sulfide ore minerals in SCRVR deposits. The major supergene ore minerals are malachite, chrysocolla, and azurite. Gold and silver may be present, as well as pyrite, pyrrhotite, arsenopyrite, sphalerite, tennantite, galena, brannerite, monazite, uraninite, pitchblende, molybdenite, heterogenite, carrollite, and spherocobaltite. Cobalt and arsenic may be present in pyrite. Cobalt, when present as discrete mineral phases, occurs in heterogenite, carrollite, and spherocobaltite. Silver occurs in solid solution in chalcocite and tennantite. Gangue minerals consist of quartz, plagioclase, carbonates (including dolomite, ferroan dolomite, and calcite), potassium feldspar, biotite, muscovite, barite, rutile, hematite, and Mn-oxides including psilomelane and manganite.

Alteration and Weathering

Alteration halos around veins and breccias are ubiquitous in SCRVR deposits and are a product of local sodic and potassic alteration, silicification, and dolomitization of the host rocks. More widespread bleaching, moderate to intense sodic- (calcic) metasomatism, silicification, and dolomitization of the host rocks may also occur. Supergene enrichment and subsequent deep oxidation and weathering can result in complete dissolution of the carbonate rock to produce a distinctive residual silty black material (called *Terre Noir* in the Congolese part of the CACB).

Geochemical Signature

Copper and cobalt may be present in anomalous amounts in surface samples, soils, and stream sediments. Gold, uranium, lead, and zinc may also be present.

Geophysical Signature

Induced polarization and resistivity surveys may identify copper sulfide minerals associated with SCRVR deposits. Airborne and ground gravity, magnetic, and electromagnetic studies may facilitate mapping of structures and define ore controls and trap sites.

Genesis

Distinctions between stratabound and SCRVR deposits are not always clear cut and may in some cases be a matter of scale. The processes required to form an SCRVR deposit are the same as those required for other sediment-hosted copper

deposits (see chapter 1). SCRVR deposits form when oxidized copper-bearing fluids meet a reductant. Four ingredients are required: (1) an oxidized, hematite-stable copper source rock containing ferromagnesian minerals and (or) mafic rock fragments, (2) a source of sulfur, (3) a basinal brine to mobilize and transport the copper and sulfur, and (4) stratigraphic or structural conditions (a physical trap) that cause mixing of the brine with a reductant (chemical trap).

SCRVR deposits commonly cut multiple lithologies, record multiple pulses of mineralization, and may be metamorphosed. Small-scale sulfide-bearing quartz-carbonate veins and veinlets in stratabound deposits have been ascribed to local remobilization of ore during metamorphic, or late diagenetic to synorogenic events that post-date the primary ore deposition. Based on observations of identical sulfide mineral assemblages in disseminations and associated gangue veinlets cutting the same rocks in stratiform copper deposits in the CACB, Sillitoe and others (2010) argued that host rocks must have been competent enough to undergo brittle fracture, where veinlets acted as feeders for disseminated mineralization. Therefore, they concluded that the disseminated ore could not result from passive fluid infiltration during early diagenesis associated with rifting and extension, and emphasized massive brine expulsion by hydraulic fracturing associated with contractural tectonism, basin inversion, uplift, and exhumation. At the Kansanshi SCRVR deposit, early pre- or synorogenic disseminated and veinlet mineralization is present, but the main ores are associated with steep late orogenic veins and hydrothermal breccias formed in the waning stages of the Lufilian orogeny. Similar observations at the Frontier deposit led Sillitoe and others (2010) to conclude that CACB copper was mobilized over a time span that pre- and post-dated peak Lufilian orogeny. At Dikulushi, copper was remobilized from an early polymetallic vein paragenesis to form the higher-grade copper-silver deposit.

Hydrocarbons and organic material in host rocks are the probable reductants in SCRVR deposits. Direct evidence for reductants in SCRVR deposits typically is lacking, although relict pyrobitumen is observed in pre-mineralization chert at Dikulushi and oil-bearing fluid inclusions are present in sandstone at the Cashin deposit.

The model for copper deposits in the Paradox Basin developed by Thorson (2005) requires multiple fluids for formation of the deposits: stage 1 early diagenetic fluids form iron oxides in red beds, stage 2 reducing fluids convert hematite to pyrite, with hydrocarbons as an important source of reductant, and stage 3 epigenetic copper-bearing saline fluids introduced along structural feeder zones where copper precipitates on contact with reductants in bleached beds.

Exploration and Resource Assessment Guidelines for SCRVR Deposits

Structurally disrupted, continental to restricted marine, rift-related sedimentary basins that host stratabound copper

deposits or other associated deposit types are considered permissive sites for SCRVR deposits. The presence of evaporite beds in the sequence and (or) evidence of halokinesis are considered favorable factors, as is the presence of mafic igneous rocks related to extension and rifting. Because SCRVR deposits are epigenetic, and are therefore assumed to form after lithification of the host rocks, evidence of tectonic disruption and faults at high angles to bedding are particularly favorable.

SCRVR-type mineralization is most likely to be developed where structural features intersect (1) carbonaceous and (or) pyritic marine or lacustrine sedimentary rocks interbedded with or occurring up-section or laterally from continental red-bed sedimentary rocks, and (or) (2) continental red-bed sedimentary rocks that exhibit evidence of the presence or former presence of sour gas or hydrocarbons in pore spaces. Indicators of hydrocarbon reductants include, bitumen, dead oil, petroleum and (or) natural gas in fluid inclusions, or non-red (bleached white or gray) areas within continental, hematite-stable (red) siliciclastic rocks.

Several key features of epigenetic SCRVR copper deposits that may have a bearing on exploration targeting and assessment include the following (partly based on Maiden, 2011):

- Exploration guides for SCRVR copper deposits include identification of controlling structures and zones of structural complexity. Structures and rock fabrics resulting from post-lithification deformation provide the primary setting and trap for mineralizing fluids.
- Rock competency is critical because the rheological contrast between lithologic units in a host succession will control the generation and location of porosity in the form of veins and breccias. This may be reflected in the tendency for SCRVR deposits to be developed in clastic units because they are more brittle compared to altered volcanic rocks and shales.
- Identification of reduced and permeable zones adjacent to faults and other possible structures that could channel fluid flow can guide exploration targets.
- Copper concentrates in structurally controlled dilatant zones: fault splays, fault intersections, shear zones, brecciated rock at fault bends, fold axes, kink folding, and in alteration zones.
- Multiple deformation events and (or) multiple hydrothermal events may be involved in formation of SCRVR deposits. Copper may be pumped up along late structures.
- Alteration, especially sodic alteration, as well as veins and breccia zones are characteristic of the

deposit type. Copper veins may represent part of a halo of a larger structurally controlled hydrothermal event related to deformation.

- Supergene minerals (chalcocite, malachite, azurite) may comprise the main ore minerals in oxidized deposits, or oxidized parts of deposits.
- Recognition of structure, rather than stratigraphy, as the primary ore control distinguishes SCRVR from sediment-hosted stratabound deposits.

Grade and Tonnage Models for SCRVR Deposits

Eleven structurally controlled replacement and vein copper deposits in the CACB were used to create preliminary grade and tonnage models (figs. 3-12 and 3-13). Summary statistics for the 11 deposits are given in table 3-3. Median and mean values for ore tonnage are 15 and 76 million metric tons, respectively, and for copper grade are 1.82 and 2.58 percent, respectively. Too few values of silver and cobalt are reported to create frequency distributions for resource modeling.

Goodness of fit analysis using the Shapiro-Wilk test did not result in the rejection of the assumption that log-transformed values for tonnage and copper grades have a normal distribution. Log-transformed values of copper are significantly correlated with log tonnage ($r=-0.72$, $n=11$). The standard deviation of log-transformed value of ore tonnage is less than one (0.75).

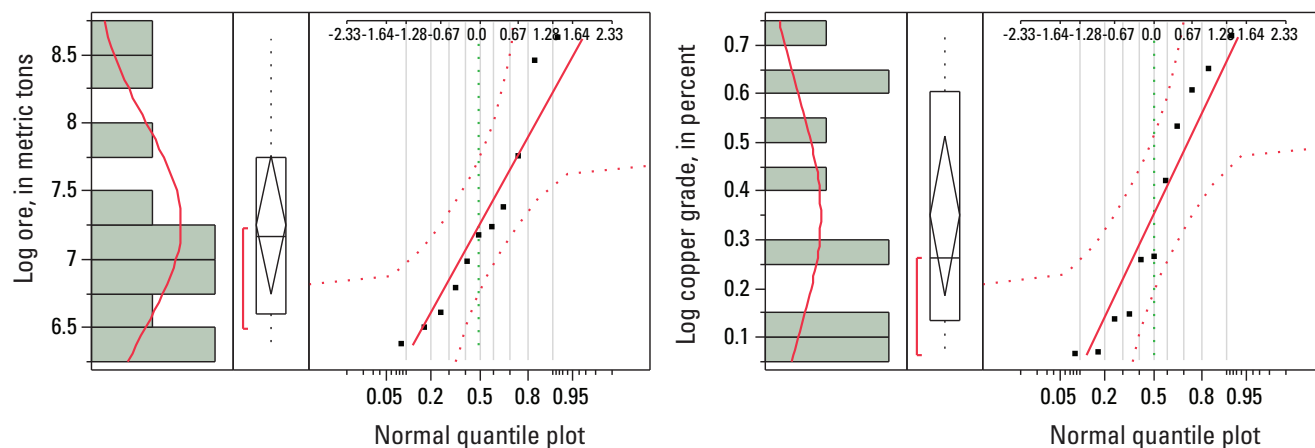
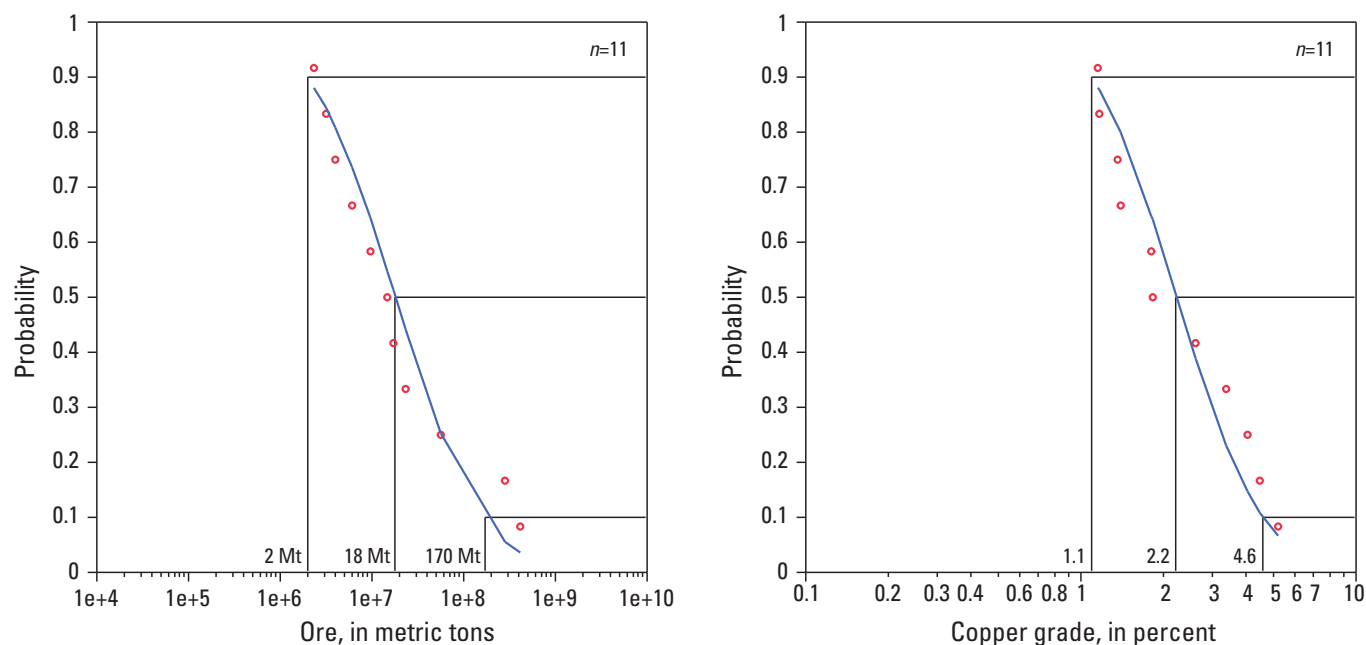
Acknowledgments

Recognition of the need to create descriptive as well as grade and tonnage models for sediment-hosted SCRVR copper deposits grew out of discussions with Murray Hitzman (Colorado School of Mines, Golden, Colorado) regarding the diversity of deposits within the CACB during the data gathering and construction of the database presented in appendix A of this report. The first SCRVR grade and tonnage models were prepared during the CACB assessment workshop in Cape Town during February, 2010 with extensive input from the workshop participants: David Broughton, Michael Christie, Susan Frost-Killian, Murray Hitzman, Douglas Jack, Sharad Master, and Jonathan Woodhead. Their insights, contributions, and participation are gratefully acknowledged. The preliminary grade and tonnage models were provided by Michael Zientek. Hannah Campbell, Kasandra Lindsey, Drew Luders, and Heather Parks created the figures, and reviews by USGS colleagues James Bliss, Pamela Dunlap, and Daniel Mosier substantially improved the report.

Table 3-3. Summary statistics for tonnage and grade of structurally controlled replacement and vein (SCRV) copper deposits.

[g/t, grams per metric ton]

Mineral resource	Number of samples	25th quantile	Median	75th quantile	Mean
Ore, metric tons	11	4,000,000	15,000,000	57,000,000	76,000,000
Copper grade, percent	11	1.36	1.82	4.02	2.58
Silver grade, g/t	3	4.7	10	115	43
Cobalt grade, percent	3	0.08	0.10	0.64	0.27
Contained copper metal, metric tons	11	140,000	210,000	1,000,000	1,000,000

**Figure 3-12.** Histogram, box plot, and normal quantile plot illustrating the distribution of log-transformed values for tonnage and copper grade for 11 structurally controlled replacement and vein copper deposits.**Figure 3-13.** Cumulative frequency plots of grade and tonnage for 11 structurally controlled replacement and vein copper deposits. Each red circle is a data point for a deposit; the blue curve is the calculated lognormal distribution based on the population parameters of the data. Values for tonnage and grade for the 90th, 50th, and 10th probability values of the distribution are illustrated by extending a horizontal line from the vertical axis to the data curve, then drawing a vertical line to the horizontal axis. The value for the point where the vertical line intersects the horizontal axis is labeled. For some deposits, values for some metals are not reported, resulting in a censored or truncated dataset. For these metals, only the probability values for the data points with reported values are illustrated. Mt, million metric tons.

References Cited (Chapters 1, 2, and 3)

- American Association of Petroleum Geologists, 1996, Sedimentary provinces of the world (BG)—Including GIS layer for giant oil and gas fields, a GIS mapping file in ARC/INFO: American Association of Petroleum Geologists Data-pages 52, CD-ROM.
- Abdullah, S., Chmyriov, V.M., and Dronov, V.I., 1980, Geology and mineral resources of Afghanistan: Ministry of Mines and Industries, Afghan Geological and Mines Survey, Republic of Afghanistan Geological and Mineral Survey, 419 p.
- Abramov, B.N., 2008, Petrochemistry of the Paleoproterozoic Udokan copper-bearing sedimentary complex: Lithology and Mineral Resources, v. 43, p. 37–43.
- African Eagle Resources plc, 2009, Ndola project fact sheet: African Eagle Resources plc, 2 p., accessed Mar. 23, 2010, at http://www.africaneagle.co.uk/downloads/Ndola_November_2009.pdf.
- Aleinikoff, J.N., Hayes, T.S., Evans, K.V., Mazdab, F.K., Pillers, R.M., and Fanning, C.M., 2012, SHRIMP U-Pb ages of xenotime and monazite from the Spar Lake red bed-associated Cu-Ag deposit, western Montana—Implications for ore genesis: *Economic Geology*, v. 107, p. 1251–1254.
- Alexander Mining plc, 2005, Alexander Mining plc placing by Evolution Securing Limited of 66,666,667 ordinary shares at 10p each at 30 pence per ordinary share and admission of the whole to the ordinary share capital to trading on AIM: Alexander Mining plc AIM admission document, 24 March 2005, 118 p., accessed September 5, 2011, at http://www.alexandermining.com/files/AXM_Admission_Document.pdf.
- Andritzky, G., 1998, Mineral map of Namibia: Geological Survey of Namibia, 1 map on 2 sheets, scale 1:1,000,000.
- Annels, A.E., 1974, Some aspects of the stratiform ore deposits of the Zambian Copperbelt and their genetic significance, in Bartholomé, P., ed., *Gisements stratiformes et provinces cuprifères [Stratiform copper deposits and provinces]*: Liège, Belgium, La Société Géologique de Belgique, p. 235–254.
- Annels, A.E., 1984, The geotectonic environment of Zambian copper-cobalt mineralization: *Journal of the Geological Society of London*, v. 141, no. 2, p. 279–289.
- Annels, A.E., 1989, Ore genesis in the Zambian Copperbelt, with particular reference to the northern sector of the Chambishi Basin, in Boyle, R.W., Brown, A.C., Jefferson, C.W., Jowett, E.C., and Kirkham, R.V., eds., *Sediment-hosted stratiform copper deposits: Geological Association of Canada Special Paper 36*, p. 427–452.
- Anvil Mining Ltd., 2009, Annual information form for the financial year ended Dec. 31, 2008 [dated March 31, 2009]: Anvil Mining Ltd. Annual Information Form, 67 p., accessed October 4, 2010, at [http://www.anvilmining.com/files/090331%20AIF%202008%20_clean_\(1\).pdf](http://www.anvilmining.com/files/090331%20AIF%202008%20_clean_(1).pdf).
- Arkhangel'skaya, V.V., Bykhovskiy, L.Z., Volodin, R.N., Narkelyun, L.F., Skursky, V.C., Trubachev, A.I., and Chechetkin, V.S., 2004, Udokanskoe mednoe i Katuginskoe redkometall'noe mestorozhdeniya Chitinskoiblasti, Rossiya [Udokan copper and Katuginskoe rare metal deposit Chita Oblast, Russia]: Chita, Russia, Administration of Chita, 519 p. [In Russian.]
- Arthurs, J.W., 1992, Geological map of the Solwezi area, degree sheet 1226, NW quarter, with part of 1126 SW, to accompany report no. 36 by J.W. Arthurs: Zambia Geological Survey, 1 sheet, scale 1:100,000.
- Bakun, N.N., Volodin, R.N., and Krendelev, F.P., 1966, Genesis of the Udokansk cupriferous sandstone deposit (Chitinsk Oblast): *International Geology Review*, v. 8, no. 4, p. 455–466.
- Barron, J.W., Broughton, D.W., Armstrong, R.A., and Hitzman, M.W., 2003, Petrology, geochemistry and age of gabbroic bodies in the Solwezi area, northwestern Zambia, in *Contributions presented at the 3rd IGCP-450 Conference, Proterozoic sediment-hosted base metal deposits of western Gondwana: Conference and Field workshop Lubumbashi 2003*, Lubumbashi, D.R. Congo, p. 75–77.
- Bartholomé, P., 1962, Les minerais cupro-cobaltifères de Kamoto (Katanga-Ouest). I Pétrographie [Minerals of Kamoto copper-cobalt (Katanga West). I Petrography]: *Studia Universitatis "Lovanium," Faculté des Sciences, Léopoldville (Kinsasha)*, v. 14, 40 p.
- Bartholomé, P., 1974, On the diagenetic formation of ores in sedimentary beds with special reference to the Kamoto copper deposit, Shaba, Zaire, in Bartholomé, P., ed., *Gisements stratiformes et provinces cuprifères [Stratiform copper deposits and provinces]*: Liège, Belgium, La Société Géologique de Belgique, p. 203–214.
- Bartholomé, P., Evrard, P., Katekesha, F., Lopez-Ruiz, J., and Ngongo, M., 1976, Diagenetic ore-forming processes at Kamoto, Katanga, Republic of Congo, in Amstutz, G.C., and Barnard, A.J., eds., *Ores in sediments—VIII. International Sedimentological Congress, Heidelberg, August 31–September 3, 1971*: Berlin, Heidelberg, New York, Springer-Verlag, International Union of Geological Sciences, Series A, no. 3., p. 21–42.
- Barton, P.B., Brew, D.A., Ayuso, R.A., Gamble, B.M., John, D.A., Ludington, S.D., Lindsey, D.A., Force, E.R., Goldfarb, R.J., and Johnson, K.M., 1995, Recommendations

- for assessments of undiscovered mineral resources: U.S. Geological Survey Open-File Report 95-82, 139 p.
- Bateman, A.M., 1935, The Northern Rhodesia copper belt: Washington, D.C., XVI International Geological Congress, Copper Resources of the World, v. 2, p. 713–740.
- Bavarian Geological State Office, 2004, Zechstein, verbreitung und tiefenlage der Trias basis [Zechstein, extent and depth of the Triassic base]: Bavarian Ministry of Economic Affairs, Infrastructure, Transport and Technology, Geothermal Atlas of Bavarian geological data and temperature maps, scale 1:500,000, accessed September 9, 2010, at http://www.stmwivt.bayern.de/fileadmin/user_upload/stmwivt/Themen/Energie_und_Rohstoffe/Dokumente_und_Cover/Geothermie/Geothermieatlas_Zechstein.pdf. [In German.]
- Bawiec, W.J., and Spanski, G.T., 2012, Quick-start guide for version 3.0 of EMINERS—Economic Mineral Resource Simulator: U.S. Geological Survey Open-File Report 2009–1057, 26 p., accessed July 15, 2012, at <http://pubs.usgs.gov/of/2009/1057/>. (This report supplements USGS OFR 2004–1344.)
- Beales, F.W., and Hardy, J.L., 1977, The problem of recognition of occult evaporites with special reference to southeast Missouri: *Economic Geology*, v. 72, p. 487–490.
- Bechtel, Achim, Sun Yuzhuang, Püttmann, Wilhelm, Hoernes, Stephan, and Hoefs, Jochen, 2001, Isotopic evidence for multi-stage base metal enrichment in the Kupferschiefer from the Sangerhausen Basin, Germany: *Chemical Geology*, v. 176, p. 31–49.
- Beck, Richard, 1905, The nature of ore deposits: *New York, Engineering and Mining Journal*, v. 1 and 2, 685 p.
- Beitler, Brenda, Chan, J.A., and Parry, W.T., 2003, Bleaching of Jurassic Navajo Sandstone on Colorado Plateau Laramide highs—Evidence of exhumed hydrocarbon supergiants?: *Geology*, v. 31, p. 1041–1044.
- Bekker, A., Holland, H.D., Wang, P.-L., Rumble III, D., Stein, H.J., Hannah, J.L., Coetzee, L.L., and Beukes, N.J., 2004, Dating the rise of atmospheric oxygen: *Nature*, v. 427, p. 117–120.
- Bekker, A., Kaufman, A.J., Kardu, J.A., and Eriksson, K.A., 2005, Evidence for Paleoproterozoic cap carbonates in North America: *Precambrian Research*, v. 137, p. 167–206.
- Bender, Friedrich, 1975, Geology of the Arabian Peninsula—Jordan: U.S. Geological Survey Professional Paper 560-I, 36 p., 3 plates.
- Benson, D.G., 1974, Geology of the Antigonish Highlands and Cape George map areas, Nova Scotia: Geological Survey of Canada Memoir 376, 90 p.
- Bładek, Wiktor, Bryja, Zbigniew, and Paździora, Jan, 2005, Jak powstała potęga Polskiej Miedzi? [How was the might of Polish copper established?], a paper presented at the First Conference—Dziedzictwo i historia górnictwa oraz możliwości wykorzystania pozostałości dawnych robót górniczych [Heritage and history of mining, and the possibilities to use remains of old mining works], Ładek Zdroj, Poland, April 21–23, 2005: Teberia.pl Web Page, accessed September 14, 2010, at http://www.teberia.pl/index_txt.php?id=1969.
- Bliss, J.D., Orris, G.J., and Menzie, W.D., 1987, Changes in grade, volume, and contained gold during the mining life-cycle of gold placer deposits: *Canadian Mining and Metallurgical Bulletin*, v. 80, no. 903, p. 75–80.
- Bogdanov, Yu.V., Bur'yanova, E.Z., Kuttyrev, E.I., Feoktistov, V.P., and Trifonov, N.P., 1973, Stratifitsirovannye mestorozhdeniya medi SSSR [Stratabound copper deposits of the USSR]: Leningrad, Nedra Publishing House, 312 p.
- Bogdanov, Yu.V., Kochin, G.G., Kuttyrev, E.I., Travin, L.V., and Feoktistov, V.P., 1966, Geology, formation conditions and distribution of cupriferous sandstones in northeastern Olekma-Vitim mountain province: *International Geology Review*, v. 8, no. 11, p. 1305–1315.
- Boleneus, D.E., Appelgate, L.M., Stewart, J.H., and Zientek, M.L., 2005, Stratabound copper-silver deposits of the Mesoproterozoic Revett Formation, Montana and Idaho, with a section on databases and spatial-data files for the geology and mineral deposits of the Revett Formation by D.E. Boleneus, L.M. Appelgate, M.H. Carlson, D.W. Chase, and M.L. Zientek: U.S. Geological Survey Scientific Investigations Report 2005-5231, 66 p., 3 plates, Excel spreadsheet, spatial database. (Also available at <http://pubs.usgs.gov/sir/2005/5231/>.)
- Box, S.E., Syusyura, Boris, Hayes, T.S., Taylor, C.D., Zientek, M.L., Hitzman, M.W., Seltmann, Reimar, Chechetkin, Vladimir, Dolgopolova, Alla, Cossette, P.M., and Wallis, J.C., 2012, Sandstone copper assessment of the Chu-Sarysu Basin, Central Kazakhstan: U.S. Geological Survey Scientific Investigations Report 2010–5090–E, 63 p. and spatial data tables, accessed November 6, 2012, at <http://pubs.usgs.gov/sir/2010/5090/e/>.
- Brognon, G.P., and Verrier, G.R., 1966, Oil and geology in Cuanza basin of Angola: *American Association of Petroleum Geologists Bulletin*, v. 50, p. 108–158.
- Brookins, D.G., 1976, Uranium deposits of the Grants, New Mexico, Mineral Belt: United States Energy Research and Development Agency GJBX-16(76), 143 p.
- Broughton, D., and Rogers, T., 2010a, Discovery of the Kamoia Cu deposit, Central African Copperbelt, DRC: PowerPoint and PDF Slide Presentations, Society of Economic Geologists 2010 Conference Keystone, Colo., Oct 2–5, 2010, 19Broughton.pdf, CD-ROM.

- Broughton, D., and Rogers, T., 2010b, Discovery of the Kamao Cu deposit, Central African Copperbelt, D.R.C., in Goldfarb, R.J., Marsh, E.E., and Monecke, Thomas, eds., *The challenge of finding new mineral resources—Global metallogeny, innovative exploration, and new discoveries, Volume I—Gold, silver, and copper-molybdenum*: Society of Economic Geologists Special Publication Number 15, p. 287–297.
- Broughton, D.W., Hitzman, M.W., and Stephens, A.J., 2002, Exploration history and geology of the Kansanshi Cu (-Au) deposit, Zambia, in Goldfarb, R.J., and Nielson, R.L., eds., *Integrated methods for discovery—Global exploration in the twenty-first century*: Littleton, Colorado, Society of Economic Geologists Special Publication 9, p. 141–153.
- Broughton, D.W., Valorose, C.P., Coker, S.A., Spera, S.L., Venendaal, J.F., and Hitzman, M.W., 2004, Congolese-style hypogene and supergene copper mineralization at the Kalengwa deposit, Zambia: Geological Society of America Abstracts with Programs, v. 36, no. 5, Abstract 222-11, p. 517. (Also available at http://gsa.confex.com/gsa/2004AM/finalprogram/abstract_78090.htm.)
- Brown, A.C., 1971, Zoning in the White Pine copper deposit, Ontonagon County, Michigan: *Economic Geology*, v. 66, p. 543–573.
- Brown, A.C., 1986, Marquette District—Lower Proterozoic copper and iron: Geological Association of Canada, Mineralogical Association of Canada, Canadian Geophysical Union, Joint Annual Meeting, Ottawa 1986, Field Trip 1 Guidebook, p. 10–20.
- Brown, A.C., 1992, Sediment-hosted stratiform copper deposits: *Geoscience Canada*, v. 19, no. 3, p. 99–115.
- Brown, A.C., 1997, World-class sediment-hosted stratiform copper deposits—Characteristics, genetic concepts, and metallogenes: *Australian Journal of Earth Sciences*, v. 44, p. 317–328.
- Brown, A.C., 2005, Refinements for footwall red bed diagenesis in the sediment-hosted stratiform copper deposits model: *Economic Geology*, v. 100, no. 4, p. 765–771.
- Brown, A.C., 2009, A process-based approach to estimating the copper derived from red beds in the sediment-hosted stratiform copper deposit model: *Economic Geology*, v. 104, p. 857–868.
- Buffington, D.L., King, N.D., Stevens, M.G., and Tschabrun, D.B., 2005, Technical report of the Lisbon Valley Copper Project, San Juan County, Utah: Pincock, Allen, and Holt Technical Report, prepared for Constellation Copper Corporation, September 22, 2005, 9434.00, 108 p., accessed September 5, 2011, at http://www.pitecreative.com/staging/CCU/art/lisbon/PAH_REVISED_Final_9_27.pdf.
- Bureau of Geology and Mineral Resources of Sichuan Province, comp., 1991, Geologic map of Sichuan Province, People's Republic of China, Map 1 in Bureau of Geology and Mineral Resources of Sichuan Province, Regional geology of Sichuan Province: Beijing, Geological Publishing House, People's Republic of China Ministry of Geology and Mineral Resources Geological Memoirs Series 1, no. 23, 1 map on 4 sheets, scale 1:1,000,000. [In Chinese with English abstract.]
- Bureau of Geology and Mineral Resources of Yunnan Province, comp., 1990, Geologic map of Yunnan Province of the People's Republic of China, Map 1 in Bureau of Geology and Mineral Resources of Yunnan Province, Regional geology of Yunnan Province: Beijing, Geological Publishing House, People's Republic of China Ministry of Geology and Mineral Resources Geological Memoirs Series 1, no. 21, 1 map on 4 sheets, scale 1:1,000,000. [In Chinese with English abstract.]
- Cailteux, J.L.H., Kampunzu, A.B., and Lerouge, C., 2007, The Neoproterozoic Mwashya-Kansuki sedimentary rock succession in the Central African Copperbelt, its Cu-Co mineralization, and regional correlations: *Gondwana Research*, v. 11, no. 3, p. 414–431.
- Cailteux, J.L.H., Kampunzu, A.B., Lerouge, C., Kaputo, A.K., and Milesi, J.P., 2005, Genesis of sediment-hosted stratiform copper-cobalt deposits, central African Copperbelt: *Journal of African Earth Sciences*, v. 42, p. 134–158.
- Cairney, T., and Kerr, C.D., 1998, Geology of the Kabwe area—Explanation of degree sheet 1428, NW quarter: Geological Survey of Zambia Report No. 47, 40 p.
- Canfield, D.E., 2005, The early history of atmospheric oxygen—Homage to Robert M. Garrels: *Annual Reviews of Earth and Planetary Science*, v. 33, p. 1–36.
- Cathles, L.M., III, Oszczepalski, Sławomir, and Jowett, E.C., 1993, Mass balance evaluation of the late diagenetic hypothesis for Kupferschiefer Cu mineralization in the Lubin Basin of southwestern Poland: *Economic Geology*, v. 88, p. 948–956.
- Chandler, F.W., 1988, Diagenesis of sabkha-related, sulphate nodules in the Early Proterozoic Gordon Lake Formation, Ontario, Canada: *Carbonates and Evaporites* v. 3, no. 1, p. 75–94.
- Chartry, G., and Franceschi, G., comps., 2004, Mineral occurrences database and GIS map of the Democratic Republic of [the] Congo: Royal Museum for Central Africa, scale 1:2,000,000, CD-ROM.
- Committee for Mineral Reserves International Reporting Standards, 2006, International reporting template for the reporting of exploration results, mineral resources, and mineral reserves: Committee for Mineral Reserves International Reporting Standards, 53 p., accessed at http://www.criirco.com/crirsco_template_first_ed_0806.pdf.

- Cowley, W.M., Katona, L.F., and Gouthes, G., 2009, Assessment of mineral prospectivity of the northern Flinders Ranges using GIS analysis: Government of South Australia, Primary Industries and Resources, SA Report Book 2009/19, 102 p.
- Cox, D.P., 1986, Descriptive model of sediment-hosted Cu, *in* Cox, D.P., and Singer, D.A., eds., Mineral deposit models: U.S. Geological Survey Bulletin 1693, p. 205.
- Cox, D.P., 2003a, revised 2007, Descriptive model of reduced-facies Cu 30b.2, *in* Cox, D.P., Lindsey, D.A., Singer, D.A., Moring, Barry, and Diggles, M.F., Sediment-hosted copper deposits of the world—Deposit models and database: U.S. Geological Survey Open-File Report 03–107, version 1.3, 10 p. (Also available at <http://pubs.usgs.gov/of/2003/of03-107/>.)
- Cox, D.P., 2003b, revised 2007, Descriptive model of Revett Cu 30b.4, *in* Cox, D.P., Lindsey, D.A., Singer, D.A., Moring, Barry, and Diggles, M.F., Sediment-hosted copper deposits of the world—Deposit models and database: U.S. Geological Survey Open-File Report 03–107, version 1.3, 5 p. (Also available at <http://pubs.usgs.gov/of/2003/of03-107/>.)
- Cox, D.P., 2003c, revised 2007, Descriptive model of sediment-hosted Cu 30b.1, *in* Cox, D.P., Lindsey, D.A., Singer, D.A., Moring, Barry, and Diggles, M.F., Sediment-hosted copper deposits of the world—Deposit models and database: U.S. Geological Survey Open-File Report 03–107, version 1.3, 11 p. (Also available at <http://pubs.usgs.gov/of/2003/of03-107/>.)
- Cox, D.P., and Bernstein, L.R., 1986, Descriptive model of Kipushi Cu-Pb-Zn, *in* Cox, D.P., and Singer, D.A., eds., Mineral deposit models: U.S. Geological Survey Bulletin 1693, p. 227.
- Cox, D.P., and Singer, D.A., 2003a, revised 2007, Grade and tonnage model of sediment-hosted Cu 30b, *in* Cox, D.P., Lindsey, D.A., Singer, D.A., Moring, B.C., and Diggles, M.F., Sediment-hosted copper deposits of the world—Deposit models and database: U.S. Geological Survey Open-File Report 03–107, version 1.3, 5 p. (Also available at <http://pubs.usgs.gov/of/2003/of03-107/>.)
- Cox, D.P., and Singer, D.A., 2003b, revised 2007, Grade and tonnage model of redbed Cu 30b.3, *in* Cox, D.P., Lindsey, D.A., Singer, D.A., Moring, B.C., and Diggles, M.F., Sediment-hosted copper deposits of the world—Deposit models and database: U.S. Geological Survey Open-File Report 03–107, version 1.3, 5 p. (Also available at <http://pubs.usgs.gov/of/2003/of03-107/>.)
- Cox, D.P., and Singer, D.A., 2003c, revised 2007, Grade and tonnage model of reduced-facies Cu 30b.2, *in* Cox, D.P., Lindsey, D.A., Singer, D.A., Moring, B.C., and Diggles, M.F., Sediment-hosted copper deposits of the world—Deposit models and database: U.S. Geological Survey Open-File Report 03–107, version 1.3, 5 p. (Also available at <http://pubs.usgs.gov/of/2003/of03-107/>.)
- Cox, D.P., and Singer, D.A., 2003d, revised 2007, Grade and tonnage model of Revett Cu 30b.4, *in* Cox, D.P., Lindsey, D.A., Singer, D.A., Moring, B.C., and Diggles, M.F., Sediment-hosted copper deposits of the world—Deposit models and database: U.S. Geological Survey Open-File Report 03–107, version 1.3, 4 p. (Also available at <http://pubs.usgs.gov/of/2003/of03-107/>.)
- Cox, D.P., Barton, P.R., and Singer, D.A., 1986, Introduction, *in* Cox, D.P., and Singer, D.A., eds. Mineral deposit models: U.S. Geological Survey Bulletin 1693, p. 1–10.
- Cox, D.P., Carrasco, R., André-Ramos, O., Hinojosa-Velasco, A., and Long, K.R., 1992, Copper deposits in sedimentary rocks, *in* U.S. Geological Survey and Servicio Geológico de Bolivia, Geology and mineral resources of the Altiplano and Cordillera Occidental, Bolivia: U.S. Geological Survey Bulletin 1975, p. 95–108.
- Cox, D.P., Lindsey, D.A., Singer, D.A., and Diggles, M.F., 2003, revised 2007, Sediment-hosted copper deposits of the world—Deposit models and database: U.S. Geological Survey Open-File Report 03–107 version 1.1, 50 p. (Also available at <http://pubs.usgs.gov/of/2003/of03-107/>.)
- Cressman, E.R., 1985, The Prichard Formation of the lower part of the Belt Supergroup (middle Proterozoic) near Plains, Sanders County, Montana: U.S. Geological Survey Bulletin 1553, 64 p.
- Dardir, A.A., editor-in-chief, 1998, Metallogenic map of Arab Republic of Egypt (Metallic and non metallic deposits), Sheet no. 11: Cairo, Egypt, The Egyptian Geological Survey and Mining Authority, scale 1:1,000,000.
- Davidson, D.M., 1931, Geology and ore deposits of Chambishi, Northern Rhodesia: Economic Geology, v. 26, p. 131–152.
- Davis, G.R., 1954, The origin of the Roan Antelope copper deposit of Northern Rhodesia: Economic Geology, v. 49, no. 6, p. 575–615.
- De Putter, Thierry, Mees, Florian, Decrée, Sophie, and Dewaele, Stijn, 2010, Malachite, an indicator of major Pliocene Cu mobilization in a karstic environment (Katanga, Democratic Republic of Congo): Ore Geology Reviews, v. 38, p. 90–100.
- Decrée, Sophie, Deloule, Étienne, Ruffet, Gilles, Dewaele, Stijn, Mees, Florias, Marignac, Christian, Yans, Johan, and De Putter, Thierry, 2010, Geodynamic and climate controls in the formation of Mio-Pliocene world-class oxidized cobalt and manganese ore in the Katanga province, DR Congo: Mineralium Deposita, v. 45, p. 621–629.

- Demesmaeker, G., François, A., and Oosterbosch, R., 1963, La tectonique des gisements cuprifère stratiformes du Katanga, in Lombard, J., and Nicolini, P., eds., *Gisements stratiformes de cuivre en Afrique* [Stratiform copper deposits in Africa]: Paris, Association des Services Géologique Africains [Association of African Geological Surveys], p. 47–115.
- Department of Primary Industries and Resources South Australia, 2006, Neoproterozoic geological provinces: South Australian Resources Information Geoserver, accessed October 5, 2011, at <http://www.pir.sa.gov.au/minerals/sarig>.
- Dewaele, Stijn, Muchez, Philippe, Heijlen, Wouter, Boutwood, Amanda, Lemmon, Terry, and Tyler, Roger, 2006, Reconstruction of the hydrothermal history of the Cu-Ag vein-type mineralisation at Dikulushi, Kundelungu foreland, Katanga, D.R. Congo: *Journal of Geochemical Exploration*, v. 89, p. 376–379.
- Diatchkov, S.A., 1994, Principles of classification of reserves and resources in the CIS countries: *Mining Engineering*, v. 46, no. 3, p. 214217.
- Discovery Minerals Ltd., 2010, Annual Report 2010: Brisbane, Australia, Discovery Minerals Ltd. Annual Report, 79 p., accessed September 2, 2011, at <http://www.discoverymetals.com/annual-reports-7/2010-annual-report-5?y=2010&m=10>.
- Dixon, Roger, 2007, Independent technical report on the assets of Nikanor plc in the Katanga Province, Democratic Republic of Congo: SRK Consulting Project Technical Report No. 385848, prepared for Nikanor plc and Katanga Mining Ltd., November 28, 2007, 185 p. (Also available at <http://www.sedar.com>.)
- Dixon, Roger, Simposya, Victor, Takolia, Ebrahim, Waldeck, Wally, Salter, Henrietta, von Wielligh, Anton, Naismith, Alan, Cilliers, Petrus, and McNeill, R., 2009, An independent technical report on the material assets of Katanga Mining Limited, Katanga Province, Democratic Republic of Congo (“DRC”): SRK Consulting Technical Report, prepared for Katanga Mining Ltd., March 17, 2009, 216 p. (Also available at <http://www.sedar.com>.)
- Doornenbal, J.C., and Stevenson, A.G., eds., 2010, Petroleum geological atlas of the Southern Permian Basin area: TNO Geological Survey of the Netherlands, DVD.
- Dreisinger, D., Shaw, M., Britton, S., Hodson, T., Gluck, T., and Ross, T., 2010, Baja Mining Corp. El Boleo (Boleo) Project, Technical Report update 2, March 2010, Baja California South, Mexico: Baja Mining Corp., March 2, 2010, 206 p., accessed July 16, 2011, at http://www.bajamining.com/static/technical_reports/2010%20MAR%20-%20http://www.bajamining.com/static/technical_reports/2010%20MAR%20-%20Technical%20Report.pdf%20Report.pdf.
- Drexel, J.F., McCallum, Wayne, Reid, Anthony, Preiss, Wolfgang, Cowley, Wayne, Katona, Laszlo, and Gouthas, George, 2009, Review of the Burra Mine Project, 1980–2008—A progress report: Government of South Australia, Primary Industries and Resources SA Report Book 2008/16, 40 p., accessed September 2, 2011, at http://www.minerals.pir.sa.gov.au/__data/assets/pdf_file/0011/92999/RB200800016.pdf.
- Durieux, C.G., and Brown, A.C., 2007, Geological context, mineralization, and timing of the Juramento sediment-hosted stratiform copper-silver deposit, Salta district, north-western Argentina: *Mineralium Deposita*, v. 42, p. 879–899.
- Dyson, I.A., 2004, Geology of the eastern Willouran Ranges—Evidence for earliest onset of salt tectonics in the Adelaide Geosyncline: *MESA Journal*, v. 35, p. 48–56.
- El Desouky, H.A., 2008, Group metallogenesis of stratiform copper deposits in the Lufilian orogen, Democratic Republic of Congo: Geodynamics and geofluids Research Group at K.U. Leuven, accessed August 4, 2011, at <http://geo.kuleuven.be/g&g/hamdy/index.htm>.
- El Desouky, H.A., Muchez, P., and Cailteux, J., 2009, Two Cu-Co sulfide phases and contrasting fluid systems in the Katanga Copperbelt, Democratic Republic of Congo: *Ore Geology Reviews*, v. 36, p. 315–332.
- El Desouky, H.A., Muchez, Philippe, and Tyler, Roger, 2008, The sandstone-hosted stratiform copper mineralization at Mwitapile and its relation to the mineralization at Lufukwe, Lufilian foreland, Democratic Republic Of Congo: *Ore Geology Reviews*, v. 34, p. 561–579.
- Ellis, M.W., and McGregor, J.A., 1967, The Kalengwa copper deposit in northwestern Zambia: *Economic Geology*, v. 62, p. 781–797.
- Elston, W.E., 1967, Summary of the mineral resources of Bernalillo, Sandoval, and Sante Fe Counties, New Mexico: New Mexico Bureau of Mines and Mineral Resources Bulletin 81, 81 p.
- Entwistle, L.P., and Bouin, L.O., 1955, The chalcocite-ore deposits at Corocoro, Bolivia: *Economic Geology*, v. 50, p. 555–570.
- Evans, D.G., and Nunn, J.A., 1989, Free thermohaline convection in sediments surrounding a salt column: *Journal of Geophysical Research*, v. 94, no. B9, p. 1413–1422.
- Evans, H.T., Jr., 1959, The crystal chemistry and mineralogy of vanadium, in Garrels, R.M., and Larsen, E.S., 3rd, comps., *Geochemistry and mineralogy of the Colorado Plateau uranium ores*: United States Geological Survey Professional Paper 320, p. 91–102.

- Federal Institute for Geosciences and Natural Resources, 1993, *Geologische Karte der Bundesrepublik Deutschland* [Geological map of Germany]: Federal Institute for Geosciences and Natural Resources, scale 1:1,000,000. [In German.]
- First Quantum Minerals Ltd., 2010, Annual information form, as of December 31, 2009: First Quantum Minerals Ltd. Annual Information Form, 88 p., accessed March 16, 2011, at <http://www.first-quantum.com/i/pdf/AIF.pdf>.
- Flint, S.S., 1989, Sediment-hosted stratabound copper deposits of the Central Andes, in Boyle, R.W., Brown, A.C., Jefferson, C.W., Jowett, E.C., and Kirkham, R.V., eds., *Sediment-hosted stratiform copper deposits*: Geological Association of Canada Special Paper 36, p. 371–398.
- Folk, R.L., 1959, Practical petrographic classification of limestones: *American Association of Petroleum Geologists Bulletin*, v. 43, p. 1–38.
- Foster, M.D., 1959, Chemical study of the mineralized clays, in Garrels, R.M., and Larsen, E.S., 3rd, comps., *Geochemistry and mineralogy of the Colorado Plateau uranium ores*: United States Geological Survey Professional Paper 320, p. 121–132.
- François, Armand, and Cailteux, Jacques, 1981, La couverture Katangienne, entre les socles de Zilo et de la Kabompo, République du Zaïre - région de Kolwezi. [The Katangian cover between the basements of Zilo and Kabompo, Republic of Zaïre, Kolwezi area]: *Annales Musee Royal de l'Afrique Centrale, Série in-octavo, Sciences Géologiques*, no. 87, 50 p.
- François, Armand, 1973, L'extrémité occidentale de l'arc cuprifère Shabien—Etude géologique [The western end of the Shabien copper arc—Geological study]: [Likasi, Zaïre], Département Géologique de la Gécamines, 65 p.
- François, Armand, 2006, La partie centrale de l'Arc cuprifère du Katanga; étude géologique [The central part of the Katanga Copperbelt; geologic study]: *Musée Royal de l'Afrique Centrale, Tervuren African Geoscience Collection*, v. 109, 61 p.
- Freeman, P.V., comp., 1988, Description of mineral deposits on the Copperbelt (and Kabwe, Nampundwe): Lukasa, Zambia, [Consolidated Copper Mines Ltd. (ZCCM) unpublished company report], 88 p.
- Fugro Robertson, Ltd., 2008, Fugro Tellus sedimentary basins of the world map: AAPG Datapages, accessed November 6, 2009, at <http://www.datapages.com/AssociatedWebsites/GISOpenFiles/FugroTellusSedimentaryBasinsoftheWorldMap.aspx>.
- Gablina, I.F., 1981, New data on formation conditions of the Dzhezkazkan copper deposit: *International Geology Reviews*, v. 23, no. 11, p. 1303–1311.
- Garlick, W.G., and Fleisher, V.D., 1972, Sedimentary environment of Zambian copper deposition: *Geologie en Mijnbouw*, v. 51, no. 3, p. 277–298.
- Garlick, W.G., 1961, Chambishi, in Mendelsohn, F., ed., *The geology of the Northern Rhodesian Copperbelt*: London, Macdonald & Co. (Publishers) Ltd., p. 281–297.
- Garrity, C.P., and Soller, D.R., 2009, Database of the geologic map of North America; adapted from the map by J.C. Reed, Jr. and others (2005): U.S. Geological Survey Data Series 424, accessed April 16, 2012, at <http://pubs.usgs.gov/ds/424/>.
- Garven, G., 1985, The role of regional fluid flow in the genesis of the Pine Point deposit, western Canada sedimentary basin: *Economic Geology*, v. 80, p. 307–324.
- GECO Project, 2009, Mineralogical database of the Katangan Copperbelt: GECO Project Web Page, accessed August 5, 2011, at <http://www.gecoproject.org/?page=minerals&>.
- Geological Survey of Norway, 2008, Fact sheet for deposit 2017–006, deposit area—Repparfjord: Norges geologiske undersøkelse [Geological Survey of Norway], The Ore Database, accessed September 2, 2011, at http://aps.ngu.no/pls/oradb/minres_deposit_fakta.Main?p_objid=766&p_spraak=E.
- GeoPubs, 1998, Geological dataset of the Central African Copperbelt: Essex, England, GeoPubs [dataset purchased from <http://www.geopubs.co.uk/home.htm> and downloaded on December 16, 2009].
- Giusiano, Adolfo, Franchini, M.B., Impiccini, Agnes, and Pons, M.J., 2008, Mineralización de Cu en sedimentitas Mesozoicas del Grupo Neuquén y hábitat de los hidrocarburos en la Dorsal de Huincul Neuquén [Cu mineralization in Mesozoic sediments of the Neuquén Group and habitat of hydrocarbons in the Neuquén Huincul Ridge]: *Salta, 17º Congreso Geológico Argentino, Actas 2* [17th Argentina Geological Congress, Proceedings 2, Summary in full for the Neuquén Basin Symposium], p. 769–770.
- Good, P.I., and Hardin, J.W., 2009, *Common errors in statistics (and how to avoid them)*, third edition: Hoboken, New Jersey, Wiley, 273 p.
- Goossens, Pierre, 2007, Phoenix rising in an uncertain world—New mining activities in Katanga: *Académie Royale des Sciences d'Outre-Mer, Bulletin des séances*, v. 53, no. 3, p. 361–385.
- Gourlay, A.W., 2005, Technical report on the Coates Lake copper deposit, Nahanni Mining District, western Northwest Territories: Lumina Resources Corp. Technical Report, August 15, 2005, 38 p., accessed September 5, 2011, at http://www.westerncoppercorp.com/content/pdfs/technical_reports/Aug1505_Redstone_TechnicalReport.pdf.
- Gray, Anton, 1932, The Mufulira copper deposit, Northern Rhodesia: *Economic Geology*, v. 27, no. 4, p. 315–343.
- Gray, G.G., Pottorf, R.J., Summa, L.L., May, S.R., and Holl, J.E., 1996, Fluid flow and the Cashin fault: *Geological Society of America Abstracts with Programs*, v. 23, p. A254.

- Gregory, J., Hanssen, G., Cameron, A., Thomas, I., Cooper, D., and Broom, M., 2006, Frontier Copper Project, Haut Katanga Province, Democratic Republic of Congo: First Quantum Minerals Ltd. Technical Report, pursuant to National Instrument 43-101 of the Canadian Securities Administrators, December 21, 2006, 118 p. (Also available at <http://www.sedar.com>.)
- Guiraud, René, 1999, Paleozoic geodynamic evolution of the northeastern African epicratonic basins—An outline, *in* Feist, R., Talent, J.A., and Daurer, A., eds., North Gondwana—Mid-Paleozoic terranes, stratigraphy and biota: *Gabhandungen der Geologicshen Bundesanstalt*, v. 54, p. 15–26.
- Gunson Resources Ltd., 2009, Mount Gunson Copper Project preliminary feasibility studies—MG 14 deposit: Gunson Resources Ltd. ASX Release October 12, 2009, 8 p., accessed July 16, 2011, at <http://www.gunson.com.au/files/reports/Preliminary%20Feasibility%20Study%2012%20oct%2009.pdf>.
- Haddon, I.G., comp., 2001, Sub-Kalahari geological map: Council for Geosciences, South Africa, 1 sheet, scale 1:2,500,000.
- Haest, M., Muchez, P., Dewaele, S., Boyce, A.J., von Quadt, A., and Schneider, J., 2009, Petrographic, fluid inclusion and isotopic study of the Dikulushi Cu-Ag deposit, Katanga (D.R.C.)—Implications for exploration: *Mineralium Deposita*, v. 44, p. 505–522.
- Haest, M., Muchez, P., Dewaele, S., Franey, N., and Tyler, R., 2007, Structural control on the Dikulushi Cu-Ag deposit, Katanga, Democratic Republic of Congo: *Economic Geology*, v. 102, p. 1321–1333.
- Haest, M., Muchez, P., Petit, J.C.J., and Vanharcke, F., 2009, Cu isotope ratio variations in the Dikulushi Cu-Ag deposit, D.R.C.—Of primary origin or induced by supergene reworking?: *Economic Geology*, v. 104, no. 7, p. 1055–1064.
- Haest, Maarten, Schneider, Jens, Cloquet, Christophe, Latruwe, Kris, Vanhaecke, Frank, and Muchez, Philippe, 2010, Pb isotopic constraints on the formation of the Dikulushi Cu–Pb–Zn–Ag mineralisation, Kundelungu Plateau (Democratic Republic of Congo): *Mineralium Deposita*, v. 45, no. 4, p. 393–410.
- Hagni, R.D., and Gann, D.E., 1976, Microscopy of copper ore at the Creta mine, southwestern Oklahoma, *in* Johnson, K.S. and Croy, R.L., eds., Stratiform copper deposits of the Midcontinent Region, a symposium: *Oklahoma Geological Survey Circular* 77, p. 40–50.
- Hahn, G.A., and Thorson, J.P., 2006, Geology of the Lisbon Valley sandstone-hosted copper deposits, San Juan County, Utah, *in* Bon, R.L., Gloyn, R.W., and Park, G.M., eds., Mining districts of Utah: *Utah Geological Association Publication* 32, p. 511–533.
- Hammarstrom, J.M., Zientek, M.L., Orris, G.J., and Taylor, C.D., 2010, Global Mineral Resource Assessment—Challenges and opportunities for developing and refining assessment methods [abs.]: Geological Society of America Denver 2010 Annual Meeting Final Program Web Page, accessed November 22, 2010, at http://gsa.confex.com/gsa/2010AM/finalprogram/abstract_178026.htm.
- Harris, D.P., 1984, Mineral resource appraisal—Mineral endowment, resources, and potential supply—Concepts, methods, and cases: Oxford, Clarendon Press, 445 p.
- Hayes, T.S., 1984, Zonation and paragenesis of the Spar Lake stratabound copper-silver deposit in the Belt Supergroup, Montana (abs.): Geological Society of America Abstracts with Programs, v. 16, p. 534.
- Hayes, T.S., 1990, A preliminary study of thermometry and metal sources of the Spar Lake stratabound copper-silver deposit, Belt Supergroup, Montana: U.S. Geological Survey Open-File Report 90-0484, 30 p.
- Hayes, T.S., and Einaudi, M.T., 1986, Genesis of the Spar Lake stratabound copper-silver deposit, Montana—Part I. Controls inherited from sedimentation and pre-ore diagenesis: *Economic Geology*, v. 81, p. 1899–1931.
- Hayes, T.S., Landis, G.P., Whelan, J.F., Rye, R.O., and Moscati, R.J., 2012, The Spar Lake strata-bound Cu-Ag deposit formed across a mixing zone between trapped natural gas and metal-bearing brine: *Economic Geology*, v. 107, p. 1223–1250.
- Hayes, T.S., Rye, R.O., Whelan, J.F., and Landis, G.P., 1989, Geology and sulphur-isotope geothermometry of the Spar Lake stratabound Cu-Ag deposit in the Belt Supergroup, Montana, *in* Boyle, R.W., Brown, A.C., Jefferson, C.W., Jowett, E.C., and Kirkham, R.V., eds., Sediment-hosted stratiform copper deposits: Geological Association of Canada Special Paper 36, p. 319–338.
- Hitzman, M.W., Selley, David, and Bull, Stuart, 2010, Formation of sedimentary rock-hosted stratiform copper deposits through Earth history: *Economic Geology*, v. 105, p. 627–639.
- Hitzman, Murray, Kirkham, Rodney, Broughton, David, Thorson, Jon, and Selley, David, 2005, The sediment-hosted stratiform copper ore system, *in* Hedenquist, J.W., Thompson, J.F.H., Goldfarb, R.J., and Richards, J.P., eds., *Economic Geology—One hundredth anniversary volume 1905-2005*: Boulder, Colorado, Society of Economic Geologists, p. 609–642.
- Hoy, L.D., and Ohmoto, H., 1989, Constraints for the genesis of redbed-associated stratiform Cu deposits from sulphur and carbon mass-balance relations, *in* Boyle, R.W., Brown, A.C., Jefferson, C.W., Jowett, E.C., and Kirkham, R.V., eds., Sediment-hosted stratiform copper deposits: Geological Association of Canada Special Paper 36, p. 135–149.

- Huderek, Richard, 2008a, Katangan Copperbelt: Google Earth KML file, accessed July–September 2009 and October 2010, at <http://maps.google.com/maps/ms?ie=UTF8&hl=nl&oe=UTF8&msa=0&msid=118078989952556264569.00044e1e24afa04af0cca&output=kml>.
- Huderek, Richard, 2008b, *Zambian_copperbelt.kml*: Google Earth KML file, accessed July 8, 2009 and Oct. 2010, at <http://maps.google.com/maps/ms?hl=en&gl=us&ie=UTF8&oe=UTF8&msa=0&msid=118078989952556264569.000451715e9f065a35bbe&output=kml>.
- Isachsen, Y.W., and Evenson, C.G., 1956, Geology of uranium deposits in the Shinarump and Chinle Formations on the Colorado Plateau, in Page, R., Stocking, H.E., and Smith, H.G., comps., *Contributions to the geology of uranium and thorium*: United States Geological Survey Professional Paper 300, p. 263–280.
- Ivanhoe Nickel & Platinum, 2011, Developing Kamao's world-class copper discovery and Platreef's nickel, platinum, palladium, copper & gold: Ivanhoe Nickel & Platinum Brochure, 2 p., accessed February 29, 2012, at <http://www.ivanplats.com/i/pdf/2011-March-Brochure.pdf>.
- Jackson, G.C.A., 1932, The ores of the N'Changa Mine and extensions, Northern Rhodesia: *Economic Geology*, v. 27, no. 3, p. 247–280.
- Jackson, M.P.A., and Talbot, C.J., 1991, A glossary of salt tectonics: Texas Bureau of Economic Geology Geological Circular 91-4, 44 p.
- Jackson, M.P.A., Warin, O.N., Woad, G.M., and Hudec, M.R., 2003, Neoproterozoic allochthonous salt tectonics during the Lufilian Orogeny in the Katangan Copperbelt, central Africa: *Geological Society of America Bulletin*, v. 115, no. 3, p. 314–330.
- Jakubiak, Z., and Smakowski, T., 1994, Classification of mineral reserves in the former Comecon countries, in Whateley, M.K., and Harvey, P.K., eds., *Mineral resource evaluation II—Methods and case histories*: Geological Society, London, Special Publications 79, p. 17–28.
- Japan International Cooperation Agency, and Metal Mining Agency of Japan [JICA and MMAJ], 1996a, Report on the cooperative mineral exploration in the Chambishi southeast area the Republic of Zambia: Japan International Cooperation Agency and Metal Mining Agency of Japan, 53 p., accessed May 27, 2010, at [http://lvzopac.jica.go.jp/external/library?func=function.opacsch.mmindex&view=view.opacsch.toshoshozodsp\(=eng&shoshisbt=1&shoshino=0000088693&volno=0](http://lvzopac.jica.go.jp/external/library?func=function.opacsch.mmindex&view=view.opacsch.toshoshozodsp(=eng&shoshisbt=1&shoshino=0000088693&volno=0).
- Japan International Cooperation Agency and Metal Mining Agency of Japan, 1996b, Report on the cooperative mineral exploration in the Chambishi Southeast area, consolidated report: Japan International Cooperation Agency and Metal Mining Agency of Japan, 69 p. and appendixes.
- Johnson, K.S., 1976, Permian copper shales of southwestern Oklahoma, in Johnson, K.S. and Croy, R.L., eds., *Stratiform copper deposits of the Midcontinent Region, a symposium*: Oklahoma Geological Survey Circular 77, p. 3–14.
- Jowett, E.C., 1986, Genesis of Kupferschiefer Cu-Ag deposits by convective flow of Rotliegendes brines during Triassic rifting: *Economic Geology*, v. 81, p. 1823–1837.
- Jowett, E.C., 1987, Formation of sulfide-calcite veinlets in the Kupferschiefer Cu-Ag deposits in Poland by natural hydrofracturing during basin subsidence: *Journal of Geology*, v. 95, p. 513–526.
- Jowett, E.C., Pearce, G.W., and Rydzewski, Andrzej, 1987, A Mid Triassic paleomagnetic age of the Kupferschiefer mineralization in Poland, based on a revised apparent polar wander path for Europe and Russia: *Journal of Geophysical Research*, v. 92, no. B1, p. 581–598.
- Kalahari Minerals plc, 2006, Placing of 40,000,000 new Ordinary Shares at 15p per share—Admission to trading on AIM: Kalahari Minerals plc, 15 March 2006, 97 p., accessed September 5, 2011, at http://www.kalahari-minerals.com/Investor_Relations/Document_Downloads/Admission_Document/Admission_Document/File.aspx?id=213.
- Kalahari Minerals plc, 2008, Investor roadshow, March 2008: Kalahari Minerals plc, Company Update 11.03.2008, accessed September 5, 2011, at http://www.kalahari-minerals.com/News/Presentations/Company_Update_11_03_2008/File.aspx?id=55.
- Kamitani, Masaharu, Okumura, Kimio, Teraoka, Yoji, Miyano, Sumiko, and Watanabe, Yasusi, 2007, Mineral deposit data of mineral resources map of east Asia: Geological Survey of Japan, DataSheet.xls, accessed September 6, 2011, at http://www.gsj.jp/Map/EN/docs/overseas_doc/DataSheet.xls.
- Kamona, A.F., and Günzel, A., 2007, Stratigraphy and base metal mineralization in the Otavi Mountainland, Northern Namibia—A review and regional interpretation: *Gondwana Research*, v. 11, no. 3, p. 396–413.
- Kampunzu, A.B., Akanyang, P., Mapeo, R.B.M., Modie, B.N., and Wendorff, M., 1998, Geochemistry and tectonic significance of the Mesoproterozoic Kgwebe metavolcanic rocks in northwest Botswana—Implications for the evolution of the Kibaran Namaqua-Natal Belt: *Geological Magazine*, v. 135, p. 669–683.

- Kampunzu, A.B., Cailteux, J.L.H., Kamona, A.F., Intiomale, M.M., and Melcher, F., 2009, Sediment-hosted Zn-Pb-Cu deposits in the Central African Copperbelt: *Ore Geology Reviews*, v. 35, p. 263–297.
- Key, R.M., Liyungu, A.K., Njamu, F.M., Somwe, V., Banda, J., Mosley, P.N., and Armstrong, R.A., 2001, The western arm of the Lufilian arc in NW Zambia and its potential for copper mineralization: *Journal of African Earth Sciences*, v. 33, p. 503–528.
- Key, Roger, 1998, National geologic map of Botswana—Digital format: Botswana Geological Survey, scale 1:1,000,000.
- Khalifa, M.A., Soliman, H.E., and Wanas, H.A., 2006, The Cambrian Araba Formation in northeastern Egypt—Facies and depositional environments: *Journal of Asian Earth Sciences*, v. 27, p. 873–884.
- Kidwell, A.L., and Bower, R.R., 1976, Mineralogy and micro-textures of sulfides in the Flowerpot Shale of Oklahoma and Texas, *in* Johnson, K.S. and Croy, R.L., eds., *Stratiform copper deposits of the Midcontinent Region*, a symposium: Oklahoma Geological Survey Circular 77, p. 51–60.
- Kirkham, R.V., 1989, Distribution, settings, and genesis of sediment-hosted stratiform copper deposits, *in* Boyle, R.W., Brown, A.C., Jefferson, C.W., Jowett, E.C., and Kirkham, R.V. eds., *Sediment-hosted stratiform copper deposits*: Geological Association of Canada Special Paper 36, p. 3–38.
- Kirkham, R.V., 1996a, Sediment-hosted stratiform copper, *in* Eckstrand, O.R., Sinclair, W.D., and Thorpe, R.I., eds., *Geology of Canadian Mineral Deposit Types*: Geological Survey of Canada, *Geology of Canada*, no. 8, p. 223–240.
- Kirkham, R.V., 1996b, Volcanic redbed copper, *in* Eckstrand, O.R., Sinclair, W.D., and Thorpe, R.I., eds., *Geology of Canadian mineral deposit types*: Geological Survey of Canada, *Geology of Canada*, no. 8, p. 241–252. (Also available as Geological Society of America, *The Geology of North America*, v. P-1.)
- Kirkham, R.V., Carrière, J.J., and Rafer, A.B. comp., 2003, World distribution of sediment-hosted, stratiform copper deposits and occurrences: Geological Survey of Canada, unpublished, accessed Sept 26, 2009, at http://apps1.gdr.nrcan.gc.ca/gsc_minerals/index.phtml?language=en-CA.
- Kirkham, R.V., Carrière, J.J., Laramée, R.M., and Garson, D.F., 1994, Global distribution of sediment-hosted stratiform copper deposits and occurrences: Geological Survey of Canada Open File 2915b, 256 p.
- Kirkham, Rodney, and Broughton, David, 2005, Supplement to the sediment-hosted stratiform copper ore system, *in* Hedenquist, J.W., Thompson, J.F.H., Goldfarb, R.J., and Richards, J.P., eds., *Economic Geology—One hundredth anniversary volume 1905-2005*: Littleton, Colorado, Society of Economic Geologists, Inc., p. 609–642.
- Klitzsch, Eberhard, List, F.K., and Pöhlmann, Gerhard, 1987, Geological map of Egypt, Sheet NH 36 SE South Sinai: Cairo, Egypt, Cononco Coral and the Egyptian General Petroleum Company, scale 1:500,000.
- Knitzchke, Gerhard, 1995, Metall- und produktionsbilanz für die Kupferschieferlagerstätte im Südöstlichen Harzvorland [Metal production and balance sheet for the Kupferschiefer deposit in the southeastern Harz foreland], *in* Jankowski, Günter, editor, *Zur geschichte des Mansfelder Kupferschieferbergbaus* [The mining history of the Mansfeld Kupferschiefer]: Clausthal-Zellerfeld, Germany, GDMB-Infomationgesellschaft, p. 270–303.
- Konnikov, A.Z., Kornutova, E.I., Kuteinikov, E.S., Magnushchevski, E.L., Mironyuk, E.P., Shtein, L.F., and Krapivko, S.Y., 1984 [1990], [Geological map of the USSR, new series, sheet O-49(50) Bodaybo, Map of pre-Quaternary rocks]: Leningrad, Ministry of Geology of the USSR, VSEGEI, scale 1:1,000,000. [In Russian.]
- Kopp, Jürgen, Simon, Andreas, and Göthel, Michael, 2006, Die kupfer-lagerstätte Spremberg-Graustein in Südbrandenburg [The copper deposit Spremberg-Graustein in South Brandenburg]: Brandenburgische Geowissenschaftliche Beiträge, Kleinmachnow, v. 13, no. 1/2, p. 117–132., accessed September 5, 2011, at <http://www.zit-bb.de/sixcms/media.php/4055/Ver%25C3%25B6ffKoppSimonG%25C3%25B6thelSpremergnk.pdf>.
- Kulick, Jens, Leifeld, D., and Theuerjahr, A.-K., 1986, Section B: German Kupferschiefer excursion, *in* Jowett, E.C., ed., *Kupferschiefer and other sediment-hosted deposits in central Europe*: Geological Association of Canada, Mineralogical Association of Canada, Canadian Geophysical Union Joint Annual Meeting, Ottawa, Ontario, 1986 Field Trip Guidebook 12, p. 11–34.
- Jackson, M.P.A., and Talbot, C.J., 1991, A glossary of salt tectonics: Texas Bureau of Economic Geology Geological Circular 91-4, 44 p.
- Jackson, M.P.A., Warin, O.N., Woad, G.M., and Hudec, M.R., 2003, Neoproterozoic allochthonous salt tectonics during the Lufilian Orogeny in the Katangan Copperbelt, central Africa: *Geological Society of America Bulletin*, v. 115, no. 3, p. 314–330.
- Laghmouch, M., comp., 2008a, Carte géologique de la République Démocratique Du Congo, L'arc cuprifère du Katanga [Geologic map of the Democratic Republic of the Congo, Katanga Copperbelt]: Royal Museum of Central Africa, scale 1:500,000.
- Laghmouch, M., comp., 2008b, L'Arc cuprifère du Katanga: géologie et minéralisations (2007)—GIS and raster [Katanga copper arc—geology and mineralization]: Tervuren, Belgium, Royal Museum of Central Africa, scale 1:500,000, CD-ROM.

- Lagzdina, G.Yu., Mironyuk, E.P., Mikhaylov, K.V., Nikolaeva, M.G., and Tarasova, V.G., 1978, [Geological map of the USSR, new series, sheet O-(50), 51 Aldan, Map of the pre-Quaternary rocks]: Ministry of Geology of the USSR, VSEGEI, scale 1:1,000,000. [In Russian.]
- Lattanzi, Christopher, 1997, Mining engineer's report: Micon International Ltd., prepared for KGHM Polska Miedź S.A., July 7, 1997, accessed June 22, 2009, at http://www.kghm.pl/_files/File/Gielda/Prospekt-en/Mining%20Engineers%20Report.pdf.
- Le Burn, Steve, and Hayward, Peter, 2011, Kapulo Project, DRC: Coffey Mining Pty Ltd. National Instrument 43-101 Technical Report, prepared for Mawson West Ltd, revised 7 March, 2011, refiled March 18, 2011, 101 p. (Also available at <http://www.sedar.com>.)
- Lefebure, D.V., and Alldrick, D.J., 1996, Sediment-hosted Cu \pm Ag \pm Co, in Lefebure, D.V., and Höy, T, eds., Selected British Columbia mineral deposit profiles, Volume 2—Metallic deposits: British Columbia Ministry of Employment and Investment, Open File 1996-13, p. 13–16.
- Lefebvre, J.J., 1974, Mineralisations cupro-cobaltiferes associees aux horizons pyroclastiques situes dans le faisceau superieur de la Serie de Roan, a Shituru, Chaba Zaire [The cupro-cobaltiferous mineralization associated with pyroclastic horizons in the upper part of Roan series, Shituru, Shaba, Zaire], in Bartholome, P., ed., Gisements stratiformes et provinces cupriferes [Stratiform copper deposits and provinces]: Liège, Belgium, La Société Géologique de Belgique, p. 103–122.
- Liedtke, Maren, and Vasters, Jürgen, 2008, Renaissance des deutschen Kupferschieferbergbaus? [Renaissance of German copper shale mining?]: Bundesanstalt für Geowissenschaften und Rohstoffe, Commodities Top News Number 29, 15 p., accessed September 5, 2011, at http://www.bgr.bund.de/DE/Gemeinsames/Produkte/Downloads/Commodity_Top_News/Rohstoffwirtschaft/29_kupferschieferbergbau.pdf.
- Lindgren, W., Graton, L.C., and Gordon, C.H., 1910, The ore deposits of New Mexico: U.S. Geological Survey Professional Paper 68, 361 p.
- Lindsey, D.A., and Cox, D.P., 2003, revised 2007, Descriptive model of Redbed Cu 30b.3, in Cox, D.P., Lindsey, D.A., Singer, D.A., Moring, B.C., and Diggles, M.F., Sediment-hosted copper deposits of the world—Deposit models and database: U.S. Geological Survey Open-File Report 03–107, version 1.3, 5 p. (Also available at <http://pubs.usgs.gov/of/2003/of03-107/>.)
- Lindsey, D.A., Woodruff, L.G., Cannon, W.F., Cox, D.P., and Heran, W.D., 1995, Sediment-hosted Cu deposits (model 30b; Cox, 1986), in du Bray, E.A., ed., Preliminary compilation of descriptive geoenvironmental mineral deposit models: U.S. Geological Survey Open-File Report 95-0831, p. 214–224. (Also available at <http://pubs.usgs.gov/of/1995/ofr-95-0831/CHAP28.pdf>.)
- Ljunggren, P., and Meyer, H.C., 1964, The copper mineralization in the Corocoro Basin, Bolivia: Economic Geology, v. 59, p. 110–125.
- Lockwood, R.P., 1972, Geochemistry and petrology of some Oklahoma red bed copper occurrences: Norman, University of Oklahoma, Ph.D. dissertation, 125 p.
- Lopatin, N.V., 1971, [Temperature and geologic time as factors in coalification]: Izvestiya Akademii Nauk URSS, Seriya Geologicheskaya, v. 3, p. 95–196. [In Russian.]
- Lur'ye, A.M., and Gablina, I.F., 1972, The copper source in production of Mansfeld-type deposits in the west Ural Foreland: Geochemistry International, v. 9, p. 56–67.
- Mach, Leah, Clarke, Peter, Michael, Nick, and Puspa, Patricia, 2006, Technical report, Cashin copper deposit: SRK Consulting Project Reference No. 162302, prepared for Constellation Copper Corporation, May 2006, 76 p. (Also available at <http://www.sedar.com>.)
- MacIntyre, T.J., Thorson, J.P., and Hitzman, M.W., 2004, Setting the stage for sediment-hosted copper—Fault related hydrocarbon(?) bleaching and copper ore at the Cashin Mine, Montrose County, Colorado: Geological Society of America Abstracts with Programs, v. 36, no. 5, p. 516. (Also available at https://gsa.confex.com/gsa/2004AM/finalprogram/abstract_74076.htm.)
- MacIntyre, T.J., Thorson, J.P., and Hitzman, M.W., 2005, Fault-related bleaching and sediment-hosted copper mineralization around the Paradox Valley, Montrose, Colorado: Window to the World, Geological Society of Nevada Symposium, Program with Abstract, Reno/Sparks, Nevada, May 2005, p. 64.
- MacKevett, Jr., E.M., Cox, D.P., Potter, II, R.W., and Silberman, M.L., 1997, Kennecott-type deposits in the Wrangell Mountains, Alaska—High-grade copper ores near a basalt-limestone contact, in Goldfarb, R.J., and Miller, L.D., eds., Mineral deposits of Alaska: Economic Geology Monograph 9, p. 66–89.
- Maiden, Ken, 2011, Exploration models—You can flirt with a model but you shouldn't marry one: Australian Institute of Geoscientists (AIG) Base Metals Symposium, June 2011, Perth, Australia, accessed July 15, 2011, at <http://aig.org.au/attachments/Ken%20Maiden%20Exploration%20Models.pdf>.
- Marjonen, R., 2000, Geological map of the Kitwe-Mufulira area, quarter degree sheets 1228 SW and part of 1228 NW, to accompany report no. 60 by R. Marjonen: Zambia Geological Survey, scale 1:100,000.
- Marquillas, R.A., del Papa, Cecilia, and Sabino, I.F., 2005, Sedimentary aspects and paleoenvironmental evolution of a

- rift basin—Salta Group (Cretaceous-Paleogene), northwestern Argentina: *International Journal of Earth Sciences*, v. 94, p. 94–113.
- Marston and Marston, Inc., 2011, Resource estimate and NI 43-101 technical report for Copperwood Project, Ironwood Michigan: Marston and Marston, Inc. Technical Report, prepared for Orvana Resources US Corp., March 7, 2011, 135 p., accessed July 27, 2011, at <http://www.orvana.com/projects/pdf/110307-copperwood-technical-report.pdf>.
- Martins-Neto, M.A., and Catuneanu, O., 2010, Rift sequence stratigraphy: *Marine and Petroleum Geology*, v. 27, p. 247–253.
- Master, S., Rainaud, C., Armstrong, R.A., Phillips, D., and Robb, L.J., 2005, Provenance ages of the Neoproterozoic Katanga Supergroup (Central African Copperbelt), with implications for basin evolution, in Robb, L.J., Cailteux, J.L.H., and Sutton, S.J., eds., *Recent advances in the geology and mineralization of the Central African Copperbelt dedicated to the memory and work of Henri Ali Basira Kampunzu*: *Journal of African Earth Sciences*, v. 42, no. 1–5, p. 41–60.
- Mawson West Ltd., 2006, Technical update-Kapulo Copper Project—DRC/Zambia, ASC Release: Perth, Western Australia, Mawson West Ltd., 7 p.
- McCarthy, J.H., and Reimer, G.M., 1986, Advances in soil gas exploration for natural resources: *Journal of Geophysical Research*, v. 91, p. 12327–12338.
- McGowan, R.R., Roberts, S., Foster, R.P., Boyce, A.J., and Collier, D., 2003, Origin of the copper-cobalt deposits of the Zambian Copperbelt—An epigenetic view from Nchanga: *Geology*, v. 31, p. 497–500.
- McKinney, Mark, Brown, Ian, Goldschmidt, Allan, and Lomborg, Ken, 2009, Tschudi copper deposit—Geological modelling and mineral resource estimate: Coffey Mining (SA) (Pty) Ltd., prepared for Weatherly Mining Namibia Ltd., 13 November 2009, 127 p., accessed September 5, 2011, at http://www.weatherlyplc.com/downloads/pdf/Coffey_Tschudi_Resource_Estimate_13112009_Final.pdf.
- Mendelsohn, F., 1989, Central/southern African ore shale deposits, in Boyle, R.W., Brown, A.C., Jefferson, C.W., Jowett, E.C., and Kirkham, R.V. eds., *Sediment-hosted stratiform copper deposits*: Geological Association of Canada Special Paper 36, p. 453–469.
- Metcalf, R., Rochelle, C.A., Savage, D., and Higgo, J.W., 1994, Fluid-rock interactions during continental red bed diagenesis—Implications for theoretical models of mineralization in sedimentary basins, in Parnell, J., ed., *Geofluids—Origins, migration and evolution of fluids in sedimentary basins*: Geological Society, London, Special Publications 78, p. 301–324.
- Michalik, M., 1997, Chlorine containing illites, copper chlorides and other chlorine bearing minerals in the Fore-Sudetic copper deposit (Poland) (extended abstract), in Papunen, H., ed., *Mineral deposits—Research and exploration—Where do they meet?*: Rotterdam, Balkema, p. 543–546.
- Michalik, M., 2001, Diagenesis of the Weissliegend sandstones in the southwest margin of the Polish Rotliegend Basin: Krakow, Poland, Polska Akademia Nauk, Prace Mineralogiczne 91, 176 p.
- Moore, T.A., 1968b, Geological map of the Ndola area (degree sheet 1228 SE quarter) to accompany Report No. 20: Zambia Geological Survey Department, scale 1:100,000.
- Morrison, S.J., and Parry, W.T., 1986, Formation of carbonate-sulfate veins associated with copper ore deposits from saline basin brines, Lisbon Valley, Utah—Fluid inclusion and isotopic evidence: *Economic Geology*, v. 81, no. 12, p. 1853–1866.
- Mosier, D.L., Berger, V.I., and Singer, D.A., 2009, Volcanogenic massive sulfide deposits of the world—Database and grade and tonnage models: U.S. Geological Survey Open-File Report 2009-1034, accessed February 17, 2012, at <http://pubs.usgs.gov/of/2009/1034/>.
- Mosier, D.L., Singer, D.A., and Cox, D.P., 1986, Grade and tonnage model of sediment-hosted Cu, in Cox, D.P., and Singer, D.A., eds., *Mineral deposit models*: U.S. Geological Survey Bulletin 1693, p. 206–208.
- Musée Royal de l’Afrique Centrale, 2006a, Carte géologique de la République Démocratique du Congo, Région de Kolwezi-Kalukundi, Partie ouest de l’arc cuprifère du Katanga [Geological map of the Democratic Republic of Congo, Kolwezi-Kalukundi region-Western Katanga Copper Arc] [GIS and raster]: Tervuren [Belgium], Musée Royal de l’Afrique centrale, scale 1:100,000.
- Musée Royal de l’Afrique Centrale, 2006b, Carte géologique de la République Démocratique du Congo, Région de Likasi, Partie centrale de l’arc cuprifère du Katanga [Geological map of the Democratic Republic of Congo, Likasi Region, central part of the Katangan Copperbelt] [GIS and raster]: Tervuren [Belgium], Musée Royal de l’Afrique Centrale, scale 1:100,000.
- Musée Royal de l’Afrique Centrale, 2008, Carte géologique de la République Démocratique du Congo, Région de Kolwezi-Kalukundi-Likasi, Parties occidentale et centrale de l’arc cuprifère du Katanga [Geological map of the Democratic Republic of Congo, Kolwezi Region-Kalukundi-Likasi Parties of Western and Central Katanga Copper Arc]: Tervuren [Belgium], Musée Royal de l’Afrique Centrale, scale 1:200,000, CD-ROM.
- Nawrocki, Jerzy, 2000, Clay mineralogy, crystallinity, and K-Ar ages of illites within the Polish Zechstein basin—

- Implications for the age of Kupferschiefer mineralization—A discussion: *Economic Geology*, v. 95, p. 241–242.
- Nawrocki, Jerzy, 1997, Permian to Early Triassic magnetostratigraphy from the Central European Basin in Poland—Implications on regional and worldwide correlations: *Earth and Planetary Science Letters*, v. 152, p. 37–58.
- Newton, Joseph, and Wilson, C.L., 1942, *Metallurgy of copper*: New York, John Wiley & Sons, Inc., 539 p.
- Nicholson, S.W., Shirey, S.B., Schulz, K.J., and Green, J.C., 1997, Rift-wide correlation of 1.1 Ga midcontinent rift system basalts—Implications for multiple mantle sources during rift development: *Canadian Journal of Earth Sciences*, v. 34, p. 504–520.
- Nimry, Y.F., ed., 1973, *The copper and manganese prospects of the Wadi Araba: Hashemite Kingdom of Jordan*, Natural Resources Authority, Mining Division, 107 p.
- Notebaart, C.W., and Vink, B.W., 1972, Ore minerals of the Zambian Copperbelt: *Geologie en Mijnbouw*, v. 51, p. 337–345.
- Novachuk, Oleg, 2008, Kazakhmys plc—Strong base for stability and growth: Kazakhmys plc Presentation at Credit Suisse Global Steel and Mining Conference, September 2008, accessed September 5, 2011, at <http://www.kazakhmys.com/en/resources/383/2008%20Global%20Steel%20and%20Mining%20Conference%20Credit%20Suisse.pdf>.
- Nowack, G.J., Speczik, Stanislaw, and Oszczepalski, Sławomir, 2001, Petrographic composition of organic matter in the Kupferschiefer horizon of Poland, in Piastryński, A., and others, eds., *Mineral deposits at the beginning of the 21st century*, Proceedings of the joint sixth biennial SGA-SEG meeting, Kraków, Poland, 26–29 August 2001: Lisse, Belgium, A.A. Balkema Publishers, p. 67–70.
- O’Sullivan, John, 2006, Scott Grant claims, license 06436, Canfield Creek Prospect, Cumberland County, Nova Scotia, NTS 11E/13a, Report on prospecting and compilation of data: [Nova Scotia Department of Natural Resources Mineral Resources Branch] Assessment Report AR2006-083, 16 p., accessed September 5, 2011, at http://www.gov.ns.ca/natr/meb/data/ar/2006/AR_ME_2006-083.pdf.
- Oszczepalski, Sławomir, 1989, Kupferschiefer in southwestern Poland—Sedimentary environments, metal zoning, and ore controls, in Boyle, R.W., Brown, A.C., Jefferson, C.W., Jowett, E.C., and Kirkham, R.V., eds., *Sediment-hosted stratiform copper deposits*: Geological Association of Canada Special Paper 36, p. 571–600.
- Oszczepalski, Sławomir, 1999, Origin of the Kupferschiefer polymetallic mineralization in Poland: *Mineralium Deposita*, v. 34, p. 599–613.
- Oszczepalski, Sławomir, and Speczik, Stanisław, 2011, Rudy miedzi i srebra [copper and silver ore], in Wołkowicz, Stanisława, Smakowskiego, Tadeusza, and Speczika, Stanisława, eds., *Bilans perspektywicznych zasobów kopalin Polski wg stanu na 31 XII 2009 r.* [Balance of Polish prospective minerals resources as of 31 December 2009]: Warsaw, Ministry of Environment, Polish Geological Institute, p. 76–93, accessed September 5, 2011 at http://www.pgi.gov.pl/pl/component/docman/doc_download/218-bilans-zasobow-perspektywicznych-2010.pdf.
- Oszczepalski, Sławomir, Nowak, G.J., Bechtel, A., and Zák, Karel, 2002, Evidence of oxidation of the Kupferschiefer in the Lubin-Sieroszowice deposit, Poland—Implications for Cu-Ag and Au-Pt-Pd mineralization: *Polish Geological Institute Geological Quarterly*, v. 46, p. 1–23.
- Peters, S.G., and Bawiec, W.J., 2007, Sediment-hosted copper, in Peters, S.G., Ludington, S.D., Orris, G.J., Sutphin, D.M., Bliss, J.D., and Rytuba, J.J., eds., and the U.S. Geological Survey-Afghanistan Ministry of Mines Joint Mineral Resource Assessment Team, Preliminary non-fuel mineral resource assessment of Afghanistan: U.S. Geological Survey Open-File Report 2007-1214, p. 274–298, accessed November 9, 2012, at <http://pubs.usgs.gov/of/2007/1214/>.
- Piastryński, Adam, Pieczonka, Jadwiga, and Głuszek, Adam, 2002, Red bed-type gold mineralization, Kupferschiefer, south-west Poland: *Mineralium Deposita*, v. 37, p. 512–528.
- Pinaar, P.J., 1961, Bwana Mkubwa area, in Mendelsohn, F., ed., *The geology of the Northern Rhodesian Copperbelt*: London, Macdonald & Co. (Publishers) Ltd., p. 467–484.
- Polish Geological Institute, 2009, Wykaz złóż rud miedzi [list of copper ore deposits]: Polish Geological Institute, accessed September 16, 2010, at http://www.pgi.gov.pl/surowce_mineralne/PDF-tabele2/Rudy%20miedzi.pdf.
- Pollastro, R.M., Karshbaum, A.S., and Viger, R.J., 1997, Maps showing geology, oil and gas fields and geologic provinces of the Arabian Peninsula: U.S. Geological Survey Open-File Report 97-470B, version 2.0, accessed April 16, 2012, at <http://pubs.usgs.gov/of/1997/ofr-97-470/OF97-470B/>.
- Pretorius, Awie, and Park, Vivian, 2011, Resource estimate update, Hana Mining Ltd., Ghanzi Copper-silver Project, Ghanzi District, Botswana: Sphynx Consulting CC Technical Report for NI 43-101, prepared for Hana Mining Ltd. February 3, 2011, 235 p., accessed July 15, 2011, at http://www.hanamining.com/i/pdf/HanaMining-43-101-Report_Feb%202011_ALL.pdf.
- Prosser, Sarah, 1993, Rift-related linked depositional systems and their seismic expression, in Williams, G.D., and Dobb, A., eds., *Tectonics and seismic sequence stratigraphy*: Geological Society of London Special Publication 71, p. 35–66.
- Rabb’a, Ibrahim, and Nawasreh, Mohammed, 2006, Mineral status and future opportunity—Copper: Hashemite Kingdom of Jordan, Natural Resources Authority, Geological Survey Administration, 21 p., accessed July 16, 2011, at http://www.nra.gov.jo/images/stories/pdf_files/Copper.pdf.

- Rackley, R.I., 1976, Origin of western-states type uranium mineralization, *in* Wolf, K.H., ed., *Handbook of Strata-bound and Stratiform Ore Deposits*, v. 7: Elsevier, New York, p. 89–156.
- Rainbird, R.H., Jefferson, C.W., and Young, G.M., 1996, The early Neoproterozoic sedimentary Succession B of northwestern Laurentia—Correlations and paleogeographic significance: *Geological Society of America Bulletin*, v. 108, p. 454–70.
- Reidy, Paddy, Dorling, Simon, Adams, Patrick (Rick), Brans, Rhett, and deKlerk, Quinton, 2009, Kipoi Copper Project in the Democratic Republic of the Congo, May 29, 2009: CSA Global Pty Ltd. NI 43-101 Technical Report, prepared for Tiger Resources Ltd., May 29, 2009, 214 p. (Also available at <http://www.sedar.com>.)
- Rentsch, A.E., 1974, The Kupferschiefer in comparison with the deposits of the Zambian Copperbelt, *in* Bartholomé, P., ed., *Gisements stratiformes et provinces cuprifères [Stratiform copper deposits and provinces]*: Liège, Belgium, La Société Géologique de Belgique, p. 395–418.
- Riese, W.C., 1980, The Mount Taylor uranium deposit, San Mateo, New Mexico: Albuquerque, New Mexico, University of New Mexico, Unpublished Ph.D. dissertation, 643 p.
- Root, D.H., Menzie, W.D., and Scott, W.A., 1992, Computer Monte Carlo simulation in quantitative resource estimation: *Natural Resources Research*, v. 1, no. 2, p. 125–138.
- Ruan, Huichu, Hua, Renmin, and Cox, D.P., 1991, Copper deposition by fluid mixing in deformed strata adjacent to a salt diapir, Dongchuan area, Yunnan Province, China: *Economic Geology*, v. 86, p. 1539–1545.
- Ruxton, P.A., 1986, Sedimentology, isotopic signature, and ore genesis of the Klein Aub copper mine, South West Africa/Namibia, *in* Anhaeusser, C.R., and Maske, S., eds., *Mineral deposits of southern Africa*: Johannesburg, Geological Society of South Africa, p. 1725–1738.
- Rybakov, Michael, and Segev, Amit, 2004, Top of the crystalline basement in the Levant: G3-Geochemistry, Geophysics, Geosystems, v. 5, no. 9, 8 p. doi: 10.1029/2004GC000690.
- Salisbury Resources, 2011, Cattle Grid—Copper—South Australia, ML 5599: Salisbury Resources Web Page, accessed July 16, 2011, at http://www.salisburyresources.com.au/?page_id=117.
- Sall, John, Creighton, Lee, and Lehman, Ann, 2007, JMP® start statistics, a guide to statistics and data analysis using JMP®, Fourth Edition: Cary, North Carolina SAS Institute Inc., 607 p.
- Schoenike, H.G., and Zeballos, R.A., 1976, The geology, exploration, and development of the stratiform copper deposit located northwest of Crowell, Texas, *in* Johnson, K.S., and Croy, R.L., eds., *Stratiform copper deposits of the Midcontinent region, a symposium*: Oklahoma Geological Survey Circular 77, p. 99.
- Scholtzhauer, S.D., 2007, *Elementary statistics using JMP®*: Cary, North Carolina, SAS Institute Inc., 458 p.
- Schreiber, U.M., comp., 1980, Geological map of Namibia: Geological Survey of Namibia, scale 1:1,000,000.
- Schuenemeyer, J.H., and Drew, L.J., 2011, *Statistics for earth and environmental scientists*: Hoboken, New Jersey, John Wiley & Sons, Inc., 407 p.
- Schulz, K.J., and Briskey, J.A., 2003, The Global Mineral Resource Assessment Project: U.S. Geological Survey Fact Sheet 053-03, accessed February 2, 2011, at <http://pubs.usgs.gov/fs/fs053-03/>.
- Selley, David, 2000, Proterozoic sediment-hosted copper deposits—Geological framework and copper mineralization in South Australia: University of Tasmania, Centre for Ore Deposit Research, AMIRA/ARC Project P544, Meeting 2, December 2000, 42 p., accessed July 16, 2011, at http://www.codes.utas.edu.au/reports/AMIRA_Reports/P544/P544_02_Dec_2000.pdf.
- Selley, David, Broughton, David, Scott, Robert, Hitzman, Murray, Bull, S.W., Large, R.R., McGoldrick, P.J., Croaker, Mawson, Pollington, Nicky, and Barra, Fernando, 2005, A new look at the geology of the Zambian Copperbelt, *in* Hedenquist, J.W., Thompson, J.F.H., Goldfarb, R.J., and Richards, J.P., eds., *Economic Geology—One hundredth anniversary volume 1905-2005*: Society of Economic Geologists, Littleton, Colo., United States, p. 965–1000.
- Servicio Geológico Mexicano, 1997, Carta geologic-minera Santa Rosalía, Baja California Sur: Servicio Geológico Mexicano Map G12-1, Secretaría de Economía, scale 1:250,000. (Also available at http://mapserver.sgm.gob.mx/cartas_impresas/productos/cartas/cartas250/geologia/metadatos/santa_rosalia.html)
- Sillitoe, R.H., Perelló, José, and García, Alfredo, 2010, Sulfide-bearing veinlets throughout the stratiform mineralization of the Central African Copperbelt—Temporal and genetic implications: *Economic Geology*, v. 105, no. 8, p. 1361–1368.
- Simposya, V.M., and Hart, P.C.L., 2008, Technical report on the mineral resources for the Konkola North Copper project, Chililabombwe, Zambia: SRK Consulting Project Number 384408, prepared for TEAL Exploration and Mining Co., March 2008, 78 p. (Also available at <http://www.sedar.com>.)
- Simposya, V.M., Waldeck, H.G., Tagami, M., and McDonald, A.J., comps., 2008, The Shituru Copper Project feasibility study, Katanga Province, Democratic Republic of Congo:

- SRK Consulting Report no. 359212 (October 29, 2008), prepared for International Barytex Resources, Ltd., 125 p. (Also available at <http://www.sedar.com>.)
- Sinclair, A.J., and Blackwell, G.H., 2006, *Applied mineral inventory estimation*: New York, Cambridge University Press, 381 p.
- Singer, D.A., 1992, Grade and tonnage model of Sier-ran kuroko deposits, *in* Bliss, J.D., ed., *Developments in mineral deposit modeling*: U.S. Geological Survey Bulletin 2004, p. 29–32.
- Singer, D.A., 1993, Basic concepts in three-part quantitative assessments of undiscovered mineral resources: *Natural Resources Research*, v. 2, no. 2, p. 69–81.
- Singer, D.A., 1995, World-class base and precious metal deposits—A quantitative analysis: *Economic Geology*, v. 90, no. 1, p. 88–104.
- Singer, D.A., 2011, A lognormal distribution of metal resources: *Earth Science – Journal of China University of Geosciences*, v. 36, no. 2, p. 1–8.
- Singer, D.A., and Menzie, W.D., 2010, *Quantitative mineral resource assessments—An integrated approach*: New York, Oxford University Press, 219 p.
- Singer, D.A., and Mosier, D.L., 1986, Grade and tonnage model of kuroko massive sulfide, *in* Cox, D.P., and Singer, D.A., eds., *Mineral deposit models*: U.S. Geological Survey Bulletin 1693, p. 190–197.
- Singer, D.A., and Page, N.J., 1986, Grade and tonnage model of minor podiform chromite, *in* Cox, D.P., and Singer, D.A., eds., *Mineral deposit models*: U.S. Geological Survey Bulletin 1693, p. 34–38.
- Singer, D.A., Berger, V.I., and Moring, B.C., 2008, Porphyry copper deposits of the world—Database, map, and grade and tonnage models, 2008: U.S. Geological Survey Open-File Report 2008-1155, 45 p., accessed January 15, 2009, at <http://pubs.usgs.gov/of/2008/1155/>.
- Singer, D.A., Berger, V.I., and Moring, B.C., 2009, Sediment-hosted zinc-lead deposits of the world—Database and grade and tonnage models: U.S. Geological Survey Open-File Report 2009-1252, accessed February 17, 2012, at <http://pubs.usgs.gov/of/2009/1252/>.
- Singer, D.A., Briskey, J.A., and Cunningham, C.G., 2008, Grade and tonnage model of giant porphyry copper deposits, *in* Cunningham, C.G., Zappettini, E.O., Vivallo S., Waldo, Celada, C.M., Quispe, Jorge, Singer, D.A., Briskey, J.A., Sutphin, D.M., Gajardo M., Mariano, Diaz, Alejandro, Portigliati, Carlos, Berger, V.I., Carrasco, Rodrigo, and Schulz, K.J., 2008, *Quantitative mineral resource assessment of copper, molybdenum, gold, and silver in undiscovered porphyry copper deposits in the Andes Mountains of South America*: U.S. Geological Survey Open File Report 2008–1253, p. 64–67, accessed October 10, 2011, at <http://pubs.usgs.gov/of/2008/1253/>.
- Singer, D.A., Page, N.J., and Lipin, B.R., 1986, Grade and tonnage model of major podiform chromite, *in* Cox, D.P., and Singer, D.A., eds., *Mineral deposit models*: U.S. Geological Survey Bulletin 1693, p. 38–44.
- Singewald, J.T., Jr., and Berry, E.W., 1922, The geology of the Corocoro copper district of Bolivia: *Johns Hopkins University Studies in Geology*, no. 1, 117 p.
- Sneh, A., Bartov, Y., Weissbrod, T. and Rosensaft, M., 1998, *Geological Map of Israel*: Geological Survey of Israel, 4 sheets, 1:200,000.
- Soulé, J.H., 1956, Reconnaissance of the “red bed” copper deposits in southeastern Colorado and New Mexico: U.S. Bureau of Mines Information Circular 7740, 74 p.
- SRK Consulting, 2006, Resource estimate Centennial Deposit, Lisbon Valley, Utah: SRK Consulting Project no. 162301 (February 2006), prepared for Constellation Copper Corporation, 71 p., accessed September 5, 2011, at <http://www.pitecreative.com/staging/CCU/art/lisbon/LisbonValley.ResourceEstimation.162301.LM.Final.pdf>.
- Stephens, A.J., and Newall, G.C., 2003, The Lonshi copper mine, Katanga Province, Democratic Republic of the Congo: First Quantum Minerals Ltd. Form 43-101F1 Technical Report, March 26, 2003, amending the January 30, 2003 report, 35 p. (Also available at <http://www.sedar.com>.)
- Sutton, S.J., and Maynard, J.B., 2005, A fluid mixing model for copper mineralization at Konkola North, Zambian Copperbelt: *Journal of African Earth Sciences*, v. 42, p. 95–118.
- Sweeney, M., Turner, P., and Vaughan, D.J., 1986, Stable isotope and geochemical studies of the role of early diagenesis in ore formation, Konkola Basin, Zambia Copper Belt: *Economic Geology*, v. 81, p. 1838–1852.
- Sweeney, M.A., and Binda, P.L., 1989, The role of diagenesis in the formation of the Konkola Cu-Co ore body of the Zambian Copperbelt, *in* Boyle, R.W., Brown, A.C., Jefferson, C.W., Jowett, E.C., and Kirkham, R.V., eds., *Sediment-hosted stratiform copper deposits*: Geological Association of Canada Special Paper 36, p. 499–518.
- Sweeney, M.A., and Binda, P.L., 1994, Some constraints on the formation of the Zambian Copperbelt deposits: *Journal of African Earth Sciences*, v. 19, no. 4, p. 303–313.
- Swenson, J.B., Person, M., Raffensperger, J.P., Cannon, W.F., Woodruff, L.G., and Berndt, M.E., 2004, A hydrogeologic model of stratiform copper mineralization in the Midcontinent Rift System, northern Michigan, USA: *Geofluids*, v. 4, p. 1–22.
- Syusyura, B.B., 2008, Copper-bearing sandstones of Kazakhstan, *in* *Ore Provinces of Central Asia*, International Geo-

- logical Congress – IGC-33 Reports of geologists of Central Asia countries: Ministry of Energy and Mineral Resources of Republic of Kazakhstan, Almaty, p. 1–13.
- Syusyura, B.B., Glybovsky, V.O., and Kislitsin, A.V., 1986, Red-colored terrigenous sediments—Specific copper-forming systems, *in* Friedrich, G.H., Genkin, A.D., Nal-drett, A.J., Ridge, J.D., Sillitoe, R.H., and Vokes, F.M., eds., *Geology and metallogeny of copper deposits*: Berlin, Springer-Verlag, Proceedings 27th International Geological Congress, Moscow, 1984, p. 504–512.
- Syusyura, Boris, and Tyugay, Oleg, 2008, Cupriferous sandstones of Kazakhstan: 33rd International Geological Congress, Oslo, August 6–14th 2008, Abstract no. 1342858, accessed April 27, 2012, at <http://www.cprm.gov.br/33IGC/1342858.html>.
- Taylor, H.K., 1972, General background theory of cutoff grades: *Transactions of the Institute of Mining and Metallurgy*, v. 81, section A, p. A160–A179.
- Taylor, Roger, 2011, Gossans and leached cappings—Field assessment: Berlin Heidelberg, Springer-Verlag, 146 p.
- Theys, L.F., and Lee, L.V., 1958, Sulfate roasting copper-cobalt sulfide concentrates: *Journal of Metals*, February 1958, p. 134–136.
- Thieme, J.G., and Johnson, R.L., 1981, Geological map of the Republic of Zambia, second edition: Zambia Geological Survey, 1 map on 4 sheets, scale 1:1,000,000.
- Thorson, J.P., 2004, Paradox basin sandstone-hosted copper deposits generated by two episodes of basinal fluid expulsion: *Geological Society of America Abstracts with Programs*, v. 36, no. 5, p. 517.
- Thorson, J.P., 2005, Introduction and itinerary, *in* Thorson, J.P., and Presnell, Ricardo, eds., *Lisbon Valley sediment-hosted copper deposits and Paradox basin fluids field trip*: Society of Economic Geologists Guidebook Series, v. 37, p. 1–6.
- Thorson, J.P., and MacIntyre, Timothy, 2005, Geology of the Cashin Mine sandstone-hosted disseminated copper deposit, Montrose County, Colorado, *in* Thorson, J.P., and Presnell, Ricardo, eds., *Lisbon Valley sediment-hosted copper deposits and Paradox basin fluids field trip*: Society of Economic Geologists Guidebook Series, v. 37, p. 43–49.
- Timberline Resources, 2012, Other projects—Snowstorm, ID: Timberline Resources Corporation, accessed March 5, 2012, at http://mapserver.sgm.gob.mx/cartas_impresas/productos/cartas/cartas250/geologia/metadatos/santa_rosalia.html.
- Torrealdy, H.I., Hitzman, M.W., Stein, H.J., Markeley, R.J., Armstrong, R., and Broughton, D., 2000, Re-Os and U-Pb dating of vein-hosted mineralization at the Kansanshi copper deposit, northern Zambia: *Economic Geology*, v. 95, p. 1165–1170.
- Trites, A.F., Jr., Chew, R.T., 3rd, and Lovering, T.G., 1959, Mineralogy of the uranium deposit at the Happy Jack mine, San Juan County, Utah, *in* Garrels, R.M., and Larsen, E.S., 3rd, comps., *Geochemistry and mineralogy of the Colorado Plateau uranium ores*: United States Geological Survey Professional Paper 320, p. 185–195.
- U.S. Department of State, 2009, Small-scale digital international land boundaries (SSIB)—Lines, edition 10: Boundaries and Sovereignty Encyclopedia (B.A.S.E.), U.S. Department of State, Office of the Geographer and Global Issues.
- Unrug, R., 1989, Landsat-based structural map of the Lufilian fold belt and the Kundelungu aulacogen, Shaba (Zaire), Zambia, and Angola, and the regional position of Cu, Co, U, Au, Zn, and Pb mineralization, *in* Boyle, R.W., Brown, A.C., Jefferson, C.W., Jowett, E.C., and Kirkham, R.V., eds., *Sediment-hosted stratiform copper deposits*: Geological Association of Canada Special Paper 36, p. 519–524.
- Van Belle, Gerald, 2008, *Statistical rules of thumb*, second edition: Hoboken, New Jersey, John Wiley & Sons, Inc., 272 p.
- van Eden, J.G., 1974, Depositional and diagenetic environment related to sulfide mineralization, Mufulira, Zambia: *Economic Geology*, v. 69, p. 59–79.
- Van Waggoner, J.C., Mitchum, R.M., Campion, K.M., and Rahmanian, V.D., 1990, Siliciclastic sequence stratigraphy in well logs, cores, and outcrops—Concepts for high-resolution correlation of time and facies: *American Association of Petroleum Geologists Methods in Exploration Series*, no. 7, 55 p.
- Vejbæk, O.V., and Britze, Peter, compilers, 1994, Top of the pre-Zechstein rocks—Structural depth map: Geological Survey of Denmark, Map Series no. 45, scale 1:750,000.
- Veselinovic-Williams, M., and Frost-Killian, S., 2003 [2007], Digital international metallogenic map of Africa: Council for Geoscience, South Africa and Commission for the Geologic Map of the World, scale 1:5,000,000, CD-ROM.
- Volodin, R.N., Chechetkin, V.S., Bogdanov, Yu, V., Narkelyun, L.F., and Trubachev, A.I., 1994, The Udokan cupriferous sandstones deposit (Eastern Siberia): *Geology of Ore Deposits*, v. 36, no. 1, p. 1–25.
- Wagner, T., and Lorenz, J., 2002, Mineralogy of the complex Co-Ni-Bi vein mineralization, Bieber deposit, Spessart, Germany: *Mineralogical Magazine*, v. 66, no. 3, p. 385–407.
- Warren, J.K., 2000, Evaporites, brines, and base metals—Low temperature ore emplacement controlled by evaporite diagenesis: *Australian Journal of Earth Sciences*, v. 47, p. 179–208.

- Wedepohl, K.H., 1964, Untersuchungen am Kupferschiefer in Nordwestdeutschland—Ein Beitrag zur Deutung der Genese bituminöser Sedimente [Studies on copper shale in north-western Germany—A contribution to the significance of the genesis of bituminous sediments]: *Geochimica et Cosmochimica Acta*, v. 28, p. 305–364.
- Weed, W.H., 1907, *The copper mines of the world*: New York and London, Hill Publishing Company, 375 p.
- Weisgerber, Gerd, 2006, The mineral wealth of ancient Arabia and its use, I—Copper mining and smelting at Feinan and Timna—Comparison and evaluation of techniques, production, and strategies: *Arabian Archaeology and Epigraphy*, v. 17, p. 1–30.
- Wengen, Chen, and Bin, Xia, 2005, Diagenetic origin of the Luzhou copper deposit, Yunnan Province, China, in Mao, Jingwen, and Bierlein, F.P., eds., *Mineral Deposit Research—Meeting the global challenge*: Berlin, Springer, p. 91–92.
- White, W.S., 1968, The native copper deposits of northern Michigan, in Ridge, J.D., ed., *Ore deposits of the United States, 1933–1967, the Graton-Sales Volume*: New York, American Institute of Mining, Metallurgical, and Petroleum Engineers, p. 303–325.
- White, W.S., 1971, A paleohydrologic model for mineralization of the White Pine copper deposit, northern Michigan: *Economic Geology*, v. 66, p. 1–13.
- Wilbrand, J.T., 1978, The copper resources of northern Michigan: Final report for U.S. Bureau of Mines, Contract No. J0366067, 21 p., accessed April 23, 2012, at http://www.michigan.gov/documents/deq/GIMDL-USBMOFR1978_302972_7.pdf.
- Wilson, J.T., 1966, Did the Atlantic close and then re-open?: *Nature*, v. 211, p. 676–681.
- Wodzicki, A., and Piestrzyński, A., 1994, An ore genetic model for the Lubin-Sieroszowice mining district, Poland: *Mineralium Deposita*, v. 29, p. 30–43.
- Woodward, L.A., Kaufman, W.H., Schumacher, O.L., and Talbott, L.W., 1974, Strata-bound copper deposits in Triassic sandstone of Sierra Nacimiento, New Mexico: *Economic Geology*, v. 69, p. 108–120.
- Yamana Resources Inc., 1997, Annual report 1997: Yamana Resources Inc. Annual Report, 52 p. (Also available at <http://www.sedar.com>.)
- Yan, Guangsheng, Qiu, Ruizhao, Lian, Changyun, Li, Jinyi, Xiao, Keyan, and Mao, Jingwen, 2010, [Quantitative assessment on the resource potential of porphyry and sediment-hosted copper deposits in China]: Beijing, Geological Publishing House, 218 p. [In Chinese.]
- Yikang, Liu, 2002, Geological overview and mining districts of China: PDAC meeting presentation, March 12, 2002, 59 p., accessed January 3, 2011, at <http://www.gl.ntu.edu.tw/joomla/images/Yikang%201995%20Ore%20deposits%20in%20China.pdf>.
- Yi-Ming, Zhao, and Wu, Liangshi, 2006, [China's copper mineral resource map]: China Geological Publishing House, scale 1:5,000,000. [In Chinese.]
- Zhuang, Hanping, Ran, Chongying, He Mingqin, and Lu, Jialan, 1996, Interactions of copper, evaporite, and organic matter and genesis of sandstone-hosted copper deposits in the Chuxiong Basin, Yunnan province: *Acta Geologica Sinica*, v. 9, p. 407–419.
- Zimbabwe Geological Survey, 1985, Provisional geological map of Zimbabwe, seventh edition: Zimbabwe Geological Survey, 1 sheet, scale 1:1,000,000.

Appendixes A–B

Appendix A. Relational Database of Sediment-Hosted Copper Deposits, Resources, and Production in the Central African Copperbelt, Democratic Republic of the Congo and Zambia

By Anna B. Wilson, J. Douglas Causey, Paul D. Denning, Timothy S. Hayes, John D. Horton, Michael J. Kirschbaum, Heather L. Parks, Cliff D. Taylor, and Michael L. Zientek

Introduction

This appendix describes a Microsoft Access® database containing geologic, mineral resource, production, and other economic information for more than 100 sediment-hosted copper deposits in the Central African Copperbelt (CACB), in the Democratic Republic of the Congo (DRC) and Zambia. Deposit types represented include stratabound as well as structurally controlled replacement and vein deposits. The database was designed to be used to estimate the in-situ mineral endowment and to create tonnage and grade models for use in mineral resource assessment studies. In addition, the database needed to be interactive as it would be queried to calculate the total tonnage and weighted average copper and cobalt grades for each deposit and deposit group. Mineral resource estimates and mineral production information are recorded for each site, along with information such as the site name, location, and a geologic categorization of the mineralization according to mineral deposit type, and references. This appendix summarizes the database design, describes the information content, and provides some guidance on how to use the database. Instructions for use of the database, especially understanding the use of queries, revising, or adapting the data, assume the user has a solid working knowledge how to use Microsoft Access® and a reasonable understanding of SQL (Structured Query Language) tools.

The database extends and revises the earlier work of other economic geologists who have summarized the geology and mineral resource endowment of the CACB (Kirkham and others, 1994; Cox and others, 2003, revised 2007; Kirkham and Broughton, 2005). This study benefited from new exploration activity in the region, enhanced reporting requirements for publicly traded mineral exploration companies, the ability to search for and find information using the Internet, the use of GIS technology to understand the spatial context of the data, and access to publicly available high-resolution satellite imagery.

Data are available from both public and private sources, but we are constrained to using only publicly available data. And although this compilation is based on data in the public domain, we did review information that we could not include in the database. Compilations created by colleagues in the mining industry for their clients were extraordinarily

helpful. We also reviewed licensed or copyrighted information available from other scientific organizations and commercial vendors. Their work directed us to primary data sources and gave us a basis on which to evaluate the outcome of our work. Grade and tonnage estimates computed from this database (table A1) are reasonably close to some of the confidential summaries shared by colleagues in the mining industry and to those available through commercial databases.

The Database Design section describes the database tables, queries, forms, and their relationships. The Users' Guide section describes how to open and use the database. The FAQ section poses what we anticipate might be frequently asked questions and answers them. The database, sir2010-5090j_DB.zip, is available on the Internet at <http://pubs.usgs.gov/sir/2010/5090/j/>.

Data Discussion and Methodology

The relational database, CACB_sedCu_deposits.mdb, accompanying this report was created in Microsoft Access® (version 2003).¹ Figures in this report were produced in version 2010. The database describes copper deposits (including mines, properties, or projects) in the CACB and provides production information, resource estimates, total endowment, and references cited. Mineral exploration and production rights in the CACB are associated with tracts of land that were originally subdivided based on social criteria, not geology; the names of these tracts (properties) and the exploration activities on them (projects) are recorded if they differ from the deposit name. To the extent possible, the information was recorded so that each site represents a single style of mineralization (deposit type). The record describes the relation of the deposit to mines and properties/projects. In some cases, a deposit is large enough so that it is, or was, developed by more than one mine, in which case data from multiple mines are aggregated and reported as representing a single deposit. Conversely, a mine may develop more than one deposit, in which case the values are reported for the individual deposits, not the mine.

Multiple values for production and estimated resources may have been reported, therefore a database record may have

¹The database has not been fully tested with older or newer versions of Microsoft Access®.

Table A1. Summary of grade, tonnage, and total endowment (pre-mining) of the sediment-hosted copper deposits of the Central African Copperbelt (CACB).

[DepID, deposit identifier from relational database CACB_SedCu_deposits.mdb; DRC, Democratic Republic of the Congo; –, no data or not applicable.]

Deposit ID	Name	Latitude	Longitude	Country	Ore, metric tons	Copper grade, percent	Cobalt grade, percent	Contained copper, metric tons	Contained cobalt, metric tons
Sediment-hosted stratabound copper, reduced-facies—carbonate écaïlle									
45	Bangwe	–10.7289	26.3839	DRC	240,000	4.30	–	10,320	–
110	Dilala East	–10.695	25.47	DRC	19,100,000	2.92	0.87	557,600	165,780
59	DIMA	–10.7423	25.3785	DRC	280,473,964	2.79	0.19	7,811,973	531,328
44	Disele/Dankeru	–10.7525	26.2544	DRC	4,052,000	2.69	0.07	109,125	2,738
31	Etoile	–11.6354	27.5841	DRC	29,697,862	4.32	0.31	1,283,532	92,597
111	Etoile Extension	–11.6301	27.5597	DRC	3,126,357	0.30	0.61	9,379	19,071
19	Fungurume	–10.6153	26.2966	DRC	64,330,000	4.33	0.36	2,784,075	233,076
54	Fwalu	–10.5807	26.155	DRC	40,265,000	2.46	0.17	990,359	69,480
43	Kababankola	–10.7333	26.4227	DRC	1,887,000	1.62	1.12	30,569	21,134
22	Kabolela North and South	–10.8463	26.4788	DRC	11,699,762	2.31	0.50	270,656	58,568
41	Kakanda East	–10.7365	26.4059	DRC	166,000	4.03	0.46	6,690	764
40	Kakanda North	–10.7316	26.4021	DRC	23,287,000	2.62	0.17	610,119	39,588
42	Kakanda South	–10.7388	26.3993	DRC	8,936,000	3.60	0.20	321,696	17,872
26	Kalongwe	–11.0181	25.2219	DRC	3,000,000	5.00	–	150,000	–
37	Kalukundi	–10.6352	25.9334	DRC	8,277,661	2.39	0.39	198,163	32,448
36	Kalukundi Anticline	–10.6517	25.9271	DRC	4,685,813	2.42	0.57	113,375	26,851
35	Kalukundi Principal	–10.6527	25.923	DRC	9,846,812	2.72	0.78	267,777	77,160
25	Kamatanda	–10.951	26.7727	DRC	400,000	4.90	–	19,600	–
24	Kambove Principal	–10.8863	26.6102	DRC	14,040,000	9.09	–	1,276,236	–
14	Kambove West	–10.8862	26.5986	DRC	32,900,000	5.52	0.30	1,816,000	100,000
21	Kamfundwa	–10.8137	26.5862	DRC	26,800,000	2.72	0.20	728,250	53,650
58	Kamoto Mine	–10.7143	25.4009	DRC	139,376,734	4.48	0.35	6,238,825	493,127
127	Kamoya	–10.878	26.5794	DRC	10,000,000	2.70	0.45	270,000	45,000
128	Kamwale	–11.1431	27.1871	DRC	1,560,000	4.92	1.96	76,752	30,576
62	Kananga	–10.6892	25.4588	DRC	8,100,000	1.80	0.88	146,010	71,590
56	Kansalawile	–10.6202	26.2228	DRC	42,272,000	2.55	0.17	1,077,350	70,571
74	Karavia	–11.6637	27.281	DRC	550,000	3.92	–	21,560	–
1	Karu East	–11.6277	27.2764	DRC	5,500,000	1.80	–	99,000	–
72	Kasonta	–11.5996	27.2749	DRC	1,500,000	5.18	–	77,700	–
6	Kasonta South	–11.6101	27.2718	DRC	4,400,000	1.64	–	72,160	–
12	Kazibizi	–10.8392	26.6004	DRC	1,000,000	3.20	0.60	32,000	6,000
38	Kii	–10.6298	25.9349	DRC	4,492,295	2.49	0.58	112,021	26,008
27	Kimbwe	–11.1454	27.4943	DRC	50,000,000	4.00	–	2,000,000	–
68	Kinsevere	–11.3604	27.5733	DRC	50,215,648	4.09	0.00	2,053,315	426
32	Kipapila	–12.0173	27.9023	DRC	2,600,000	4.40	0.54	114,400	14,040
70	Kipoi North	–11.2448	27.092	DRC	5,274,000	1.36	0.05	71,726	2,637
47	Kiwana II	–10.737	26.3055	DRC	82,000	2.70	0.35	2,214	287

Table A1. Summary of grade, tonnage, and total endowment (pre-mining) of the sediment-hosted copper deposits of the Central African Copperbelt (CACB).—Continued

[DepID, deposit identifier from relational database CACB_SedCu_deposits.mdb; DRC, Democratic Republic of the Congo ; –, no data or not applicable.]

Deposit ID	Name	Latitude	Longitude	Country	Ore, metric tons	Copper grade, percent	Cobalt grade, percent	Contained copper, metric tons	Contained cobalt, metric tons
Sediment-hosted stratabound copper, reduced-facies—carbonate écaïlle									
7	Kolwezi	–10.7259	25.4581	DRC	20,000,000	6.00	–	1,200,000	–
61	KOV	–10.7134	25.4185	DRC	235,900,000	4.87	0.39	11,481,980	928,890
52	Kwatebala	–10.5804	26.1899	DRC	114,741,000	1.95	0.36	2,234,970	415,895
48	Lufomboshi	–10.7521	26.2381	DRC	225,000	1.98	0.06	4,455	135
28	Luishia	–11.1668	27.0087	DRC	49,376,615	3.16	0.40	1,559,171	197,833
15	Luiswishi	–11.5151	27.4391	DRC	8,000,000	2.50	1.10	200,000	88,000
49	Luita	–10.7394	26.286	DRC	438,000	2.90	0.60	12,702	2,628
29	Lukuni	–11.506	27.4207	DRC	2,700,000	4.30	–	116,100	–
30	Lupoto	–11.5993	27.2631	DRC	37,152,000	2.63	–	976,320	–
113	Makala R2	–10.769	25.6685	DRC	1,211,695	2.81	0.27	33,993	3,240
57	Mambilima	–10.62	26.2434	DRC	70,693,000	2.45	0.16	1,729,301	114,553
23	M’Sesa	–10.8503	26.6099	DRC	8,000,000	5.90	0.21	472,000	17,000
39	Mukondo	–10.7244	26.3487	DRC	36,255,529	2.00	1.40	725,111	507,577
9	Mupine	–10.6979	25.404	DRC	10,000,000	2.50	–	250,000	–
60	Musonie T17 West	–10.7135	25.4433	DRC	30,977,200	2.38	0.61	737,910	187,597
123	Mutanda Ya Mukonkoto	–10.7859	25.8134	DRC	299,600,000	1.23	0.59	3,673,910	1,761,040
20	Mutoshi	–10.6817	25.5386	DRC	10,765,000	4.20	0.30	451,770	32,731
124	Mutoshi (breche)	–10.6816	25.5384	DRC	45,460,000	1.75	–	793,609	–
8	Mutoshi Northwest	–10.6726	25.5174	DRC	10,000,000	4.00	–	400,000	–
55	Mwandinkomba	–10.5963	26.2049	DRC	35,430,000	3.16	0.14	1,120,315	48,789
73	Niamumenda	–11.6024	27.2922	DRC	2,600,000	2.25	2.31	58,500	60,000
46	Nundo	–10.7053	26.359	DRC	66,000	0.78	1.00	515	660
64	Ruashi	–11.619	27.5444	DRC	45,843,595	2.81	0.25	1,286,500	112,690
50	Saafi	–10.7401	26.4204	DRC	181,000	2.70	0.30	4,887	543
131	Shamitumba	–10.958	26.6083	DRC	175,000	3.30	0.70	5,775	1,225
13	Shangolowe	–10.7949	26.5684	DRC	25,000	8.00	–	2,000	–
115	Shinkolobwe Signal	–11.0494	26.5706	DRC	125,200	3.17	1.70	3,974	2,125
125	Shituru	–11.0172	26.7709	DRC	7,860,000	4.39	0.07	344,983	5,328
51	Taratara	–10.7245	26.3667	DRC	165,000	1.83	0.92	3,020	1,518
53	Tenke	–10.6015	26.1372	DRC	122,251,000	2.06	0.28	2,517,634	337,463
Sediment-hosted stratabound copper, reduced-facies ore shale									
99	Baluba	–13.0597	28.3399	Zambia	91,800,000	2.41	0.14	2,213,230	128,120
87	Chambishi Main and West	–12.658	28.0426	Zambia	116,223,700	2.53	–	2,940,038	–
10	Chambishi Southeast	–12.7	28.1061	Zambia	177,629,000	2.13	0.07	3,781,032	123,009
83	Chingola	–12.5445	27.8255	Zambia	141,390,000	1.47	–	2,075,438	–
108	Fitwaola	–12.4085	27.8806	Zambia	3,450,000	2.94	–	101,430	–
126	Ichimpe	–12.7351	28.1493	Zambia	3,100,000	1.78	–	55,180	–

Table A1. Summary of grade, tonnage, and total endowment (pre-mining) of the sediment-hosted copper deposits of the Central African Copperbelt (CACB). —Continued

[DepID, deposit identifier from relational database CACB_SedCu_deposits.mdb; DRC, Democratic Republic of the Congo ; –, no data or not applicable.]

Deposit ID	Name	Latitude	Longitude	Country	Ore, metric tons	Copper grade, percent	Cobalt grade, percent	Contained copper, metric tons	Contained cobalt, metric tons
Sediment-hosted stratabound copper, reduced-facies ore shale									
79	Konkola	–12.3449	27.7978	Zambia	662,874,267	3.03	–	20,078,663	–
101	Luanshya	–13.1132	28.3735	Zambia	264,000,000	2.80	–	7,403,360	–
92	Mindola–Nkana N–S	–12.8233	28.1908	Zambia	701,787,416	2.17	0.06	15,209,735	428,602
100	Muliashi	–13.0802	28.3196	Zambia	48,970,000	1.42	0.06	695,374	27,913
33	Musoshi	–12.2719	27.7362	DRC	111,900,000	2.11	–	2,361,090	–
84	Nchanga	–12.5102	27.8539	Zambia	425,730,000	3.24	0.03	13,791,044	130,838
86	Pitanda	–12.6539	27.9886	Zambia	15,000,000	1.70	–	255,000	–
Sediment-hosted stratabound copper, sandstone copper—Roan arenite									
98	Bwana Mkubwa	–13.0315	28.6923	Zambia	8,600,000	3.34	–	287,240	–
95	Chibuluma South	–12.9125	28.0809	Zambia	7,365,766	3.70	–	272,321	–
94	Chibuluma–Chibuluma West	–12.8232	28.0933	Zambia	19,922,000	3.69	0.19	734,766	37,114
96	Chifupu	–12.9307	28.0703	Zambia	1,936,000	3.05	–	59,048	–
88	Fitula	–12.6599	27.8717	Zambia	4,500,000	5.00	–	225,000	–
90	Kasaria–Luansobe	–12.4497	28.1386	Zambia	21,500,000	2.31	–	496,650	–
34	Kinsenda	–12.2614	27.9655	DRC	35,000,000	5.50	–	1,925,000	–
65	Lubembe	–12.3571	28.0949	DRC	47,500,000	2.20	–	1,045,000	–
85	Mimbula	–12.6266	27.8611	Zambia	46,850,000	1.20	–	560,700	–
2	Mokambo North	–12.4262	28.3221	Zambia	3,854,000	1.70	–	65,518	–
81	Mokambo Project	–12.4674	28.373	Zambia	14,900,000	1.22	–	181,780	–
11	Mokambo South	–12.4967	28.3898	Zambia	6,000,000	2.70	–	162,000	–
82	Mufulira	–12.5198	28.2285	Zambia	332,586,652	2.66	–	8,860,079	–
106	Mutundu North	–12.5845	28.3409	Zambia	4,300,000	1.44	–	61,920	–
91	Mwambashi B	–12.7232	27.9687	Zambia	14,210,000	1.78	–	253,626	–
93	Mwerkera	–12.7998	28.5007	Zambia	7,100,000	1.53	–	108,630	–
129	Ndola East	–12.9012	28.6094	Zambia	40,000,000	0.76	–	304,000	–
80	Nsato	–12.4849	28.188	Zambia	8,400,000	1.61	–	135,240	–
89	Pitanda South	–12.6738	27.9612	Zambia	7,060,000	1.58	–	111,548	–
130	Sebembere	–14.3479	28.3347	Zambia	5,700,000	1.90	–	108,300	–
Structurally controlled replacement and vein									
18	Dikulushi	–8.892	28.2743	DRC	3,114,104	4.45	–	138,591	–
67	Frontier	–12.7278	28.4745	DRC	284,247,567	1.17	–	3,313,797	–
102	Kalengwa	–13.4592	24.9989	Zambia	4,000,000	5.20	–	208,000	–
76	Kansanshi	–12.0968	26.433	Zambia	412,472,600	1.16	–	4,767,305	–
71	Kileba	–11.2859	27.1244	DRC	9,502,431	1.40	–	133,034	–
69	Kipoi Central	–11.2551	27.0948	DRC	56,611,535	1.81	0.08	1,023,100	46,430
66	Lonshi	–13.1771	28.9408	DRC	16,935,836	4.02	–	680,838	–
17	Nama A	–12.2662	27.6015	Zambia	43,656,000	0.10	0.06	43,219	24,011

Table A1. Summary of grade, tonnage, and total endowment (pre-mining) of the sediment-hosted copper deposits of the Central African Copperbelt (CACB). —Continued

[DepID, deposit identifier from relational database CACB_SedCu_deposits.mdb; DRC, Democratic Republic of the Congo ; –, no data or not applicable.]

Deposit ID	Name	Latitude	Longitude	Country	Ore, metric tons	Copper grade, percent	Cobalt grade, percent	Contained copper, metric tons	Contained cobalt, metric tons
Structurally controlled replacement and vein									
16	Nama C	–12.1978	27.5155	Zambia	78,218,000	0.01	0.04	9,386	33,634
105	Nama D	–12.1429	27.4913	Zambia	63,909,000	0.04	0.08	22,368	51,127
4	Safari North	–8.3268	29.2374	DRC	1,965,000	2.79	–	54,738	–
5	Safari South	–8.3309	29.238	DRC	392,000	1.80	–	7,056	–
109	Sase Central	–11.4528	27.078	DRC	14,700,000	1.36	0.02	200,400	3,100
3	Shaba	–8.3005	29.2354	DRC	6,014,000	3.38	–	203,192	–
63	Tilwezembe	–10.7998	25.6921	DRC	23,351,600	1.83	0.64	426,757	148,724
Unclassified copper deposits									
78	Chimwungo	–12.2776	25.8854	Zambia	760,900,000	0.64	0.01	4,858,530	68,833
97	Itawa	–12.9617	28.668	Zambia	40,000,000	0.76	–	304,000	–
107	Kalumbila	–12.2601	25.3186	Zambia	340,000,000	0.78	0.03	2,652,000	102,000
114	Kimwehulu	–10.6637	25.589	DRC	3,463,848	0.86	–	29,789	–
75	Lubwe	–12.179	25.9511	Zambia	70,000,000	0.80	–	560,000	–
112	Makala R4	–10.7746	25.672	DRC	17,251,408	0.30	0.33	51,117	56,386
77	Malundwe	–12.2279	25.8119	Zambia	161,700,000	0.89	0.01	1,437,980	23,314
103	Mufumbwe	–13.6799	24.7949	Zambia	5,200,000	2.30	–	119,600	–
104	Samba	–12.735	27.8844	Zambia	14,000,000	1.10	–	154,000	–

more than one value for production and estimated resource. During the process of creating this database, we recorded all the production and resource estimates that were available for a property. Resource estimates are usually reported in different categories (for example, measured, indicated, demonstrated, inferred) based on the quality of information; this information was retained in the database. We reviewed all the information to determine which set of records would give us the best and most comprehensive estimate of pre-mining in-situ resources (resources and (or) reserves, plus production) for the deposit. The data recorded in the database is also available in the Excel spreadsheet, CACB_raw_data.xls; references for this information are included in the Excel file, CACB_database_references.xls. Care was taken to (1) not count any values more than once (in the case of overlapping mine properties), (2) keep track of inclusive versus exclusive resources and reserves, and (3) not count production that was already accounted for in a previous in-ground resource estimate. For complex areas comprising multiple deposits, we were careful to keep track of individual ore bodies. Most data sources reported the tonnage and grade of mineralized rock; however, some reported contained metal and grade (from which total tonnage can be computed by dividing contained metal by grade). Only the records that allowed us to estimate total endowment are included in the database.

Tonnage and grade information for deposits that are contiguous or whose outer limit of the resource estimate tract were within 500 meters (m) of each other were aggregated for the purposes of resource modeling. In a few cases, a company reported combined resources and production for multiple deposits; these aggregated records are categorized as deposit groups.

Total tonnage and weighted average copper and cobalt grades are calculated for each deposit and deposit group using custom queries. Simply put, grade multiplied by tonnage² equals the amount of contained metal.³ If data for grade or tonnage are not provided, the amount of contained metal is used to calculate the missing data, provided either tonnage or grade is available. If neither of these values are present for copper, the value for acid soluble copper (ASCu) is multiplied by the ore tonnage. Use of ASCu values will result in underreporting the in-situ endowment because it does not consider the copper losses during processing.

²Divided by 100 to convert from weight percent.

³Microsoft Access® calculates to a higher precision than is warranted by the data. We formatted the displays to show rounded numbers that may still be too precise, but are closer to the correct significant figures.

Where the calculation of cobalt grade for a deposit uses data records that both include and exclude values for cobalt, the metal tonnage calculation assumes the grade is zero for each record lacking a value for cobalt. In some cases, tonnage, grade, and contained cobalt are reported. In those cases, the contained metal is calculated using the tonnage and grade values. Out of 64 records where this is true, 23 calculated values are either greater than or less than the reported tonnage by more than 1 metric ton. The difference between calculated and reported amounts of cobalt metal range from 233 to 400 metric tons, except for one record in which the calculated amount of cobalt is 79,762 metric tons greater than the reported metal tonnage. This one large discrepancy may be due to several factors, including reporting true recovered metal or estimating possible loss from mining and milling. For most properties, we believe the reported cobalt grade is either lower than the true grade or not even mentioned. Total tonnage of metal is divided by the total tonnage of ore for each deposit and deposit grouping to calculate weighted average grades.⁴

Silver and gold, present in some of these deposits in small quantities, are not economically important commodities in most of the CACB deposits. The number of deposits for which silver and gold grades were reported is small (9 and 5, respectively), and the amounts of contained silver and gold in these deposits is minor. Thus, weighted average grades of silver and gold for those few deposits are not calculated.

Many mineralized surface exposures have historically been worked by individuals and small-scale mining operations (artisanal mining), by high-grading rich pockets of ore. Most of this production has gone unreported; however, the amount mined by this method is assumed to have been minimal.

Comparison of Total Endowment with Previously Published Values

The total pre-mining endowment of copper in the CACB was 166,000,000 metric tons⁵ which is a little more than three times the total production of 50,200,000 metric tons or 47,800,000 metric tons reported by Freeman (1988) and Fortin (2006) (table A2). Considering only the known deposits, there is still more than twice as much copper in the ground as has ever been produced in the CACB. The total endowment of cobalt is 6,500,000 metric tons.

For Zambia, Freeman (1988) reported total production of 29,200,000 metric tons copper. We report total production of 36,500,000 metric tons copper, which means 7.3 million metric tons was produced in the 23 years since Freeman's estimate. Other reasons for discrepancies between our values and

those previously published include: (1) our sources may have included or excluded production from parts of each property, and (2) production reported may actually contain information from several unrelated properties because some processing plants received ore from many mines, even some from the DRC. We strove to include only production information from the individual deposits, not from the total amount of ore put through processing plant.

In the DRC, Gécamines (successor to Union Minière du Haut Katanga) controlled all mining until about 1995; thus we believe that data reported before that date are reasonably accurate. In 1995, the government monopoly was broken up and Gécamines retained only partial control, which is, in part, why there was a drastic decrease in reported production. Our database, on the other hand, reflects higher production in recent years, but is undoubtedly deficient with respect to production prior to 1994.

Fortin (2006) reported cobalt production of about 500,000 metric tons for the DRC, but we were unable to find reliable figures for cobalt production in Zambia. Our estimate for the total cobalt endowment (6.5 million metric tons) in the CACB includes 671,000 metric tons of cobalt already produced (of which 87 percent, or 5.66 million metric tons, came from the DRC).

Sources of Information

Data from both public and proprietary sources were reviewed; however, we compiled only publicly available data from about 130 information sources. We also examined several databases including, but not limited to, those compiled by Cox and others (2003, revised 2007), Kirkham and others (1994), and Kirkham and Broughton (2005), to help us identify the important sediment-hosted copper deposits in central Africa. Compilations created by our colleagues in the mining industry for their clients were extraordinarily helpful, but we do not report those values unless they are in the public domain. We also reviewed licensed or copyrighted information available from other scientific organizations and commercial vendors. All of these products directed us to primary data sources that could be cited.

Complete bibliographic citations for all the publicly available information used to compile the deposits and resources data are stored in a table that is related to both the deposit and resource tables (see Data Tables section). Relations are many-to-many, so junction tables were constructed to provide the necessary links between the deposit and resource tables and the references table.

Database Design

The relational database (CACB_sedCu_deposits.mdb) contains three types (Data, Look-up, and Junction) of tables (12 of them in all, including one, internally generated,

⁴Multiplied by 100 to account for weight percent.

⁵There are several kinds of "tons", but this report only uses metric tons. Metric tons may also be denoted as tonnes and abbreviated as t. No other form of tons can be symbolized tonne or t.

Table A2. Comparison of copper production and total copper endowment with previously reported values.

Location	Data Source	Time Period	Copper (t) ¹
Production			
Zambia	Freeman (1988) ²	To 1988	29,200,000
Zambia	This report	To 2009	36,500,000
DRC	Gecamines (Fortin, 2006) ³	1914–2006	18,600,000
DRC	This report	To 2009	13,700,000
Total endowment			
Zambia	This report	To 2009	96,100,000
DRC	This report	To 2009	69,900,000
Total CACB	This report	To 2009	166,000,000

¹In metric tons.² Production taken from Freeman, 1988, page 18.³ Production interpolated from bar graph and only includes production from Gecamines and its predecessor properties.

“Switchboard Items,” that just holds information for the Switchboard⁶), seven forms, ten queries, and one macro (script or program) (table A3). Forms provide the user with a display for entering, editing, and viewing the information for each deposit. Queries are custom requests. The macro simply opens the switchboard form immediately after the splashscreen closes.

The table relationships are shown in figure A1. We recommend that users read about the tables to understand what data are included, even though most of the users’ interactions will be with the forms.

Some of the queries, described in the Queries section, are used to calculate tonnages and grades of the deposits. Other queries provide selections of related fields from multiple tables so they can be used on the forms. The forms, described in the Forms section, provide the user with reformatted views of the data, in many instances showing multiple tables in a single view. They are mainly used for data input, but also can be used to produce hard-copy printouts. The Switchboard form has three buttons that are used to perform automated actions.

Field names in the tables may be represented by aliases in the forms used to view that same data. Field names in tables and their corresponding alias used on a form are given in table A4.

Tables

There are three types of tables: data tables, look-up tables, and junction tables (fig. A2). Data tables (1_Deposittbl,

2_Resourcestbl, and 3_Referencestbl) contain information acquired from a variety of publicly available sources and categorized for the purposes of determining copper and cobalt endowment of the sediment-hosted copper deposits in the CACB; the table name begins with a number followed by an underscore and ends with the suffix “tbl.” Look-up tables (table name ending with the suffix “_LU”) contain lists and descriptions of terms that are used to populate fields in the data tables. Junction tables (table name ending with the suffix “_MM”) are used to manage many-to-many relationships in order to create joins between data tables. The Switchboard Items table (Switchboard Items) is included among the data tables; it simply holds data for the Switchboard Manager. The tables and relationships between them are shown in figure A1.

Data Tables

1_Deposittbl Table

The mineral deposit data table, 1_Deposittbl table, contains basic information about each deposit. A brief description of each of the 15 fields is provided in table A5.

GroupName identifies a collective name for one or more deposits that are not known to be contiguous, but are within 500 m of another deposit of the same deposit type. Thus, a group may contain several deposits in close proximity. If there is only one such deposit, the group name is the same as the deposit name. Groups are used for grade and tonnage modeling of the different deposit types.

Property is a name for the property or project associated with the deposit(s). A property may contain multiple deposits, but each deposit will have its own DepID. For example, the Konkola/Mushoshi Property contains the Fitwaola, Konkola,

⁶An Access form that facilitates navigation through the database.

Table A3. List and description of files in the database.

File Name	Description
Data tables	
1_Deposittbl	Deposit table, primary table
2_Resourcestbl	Resource data
3_Referencetbl	References
Look-up tables	
DepositSubtype_LU	List of deposit style names for use in Geology portion of 1_Mastertbl_frm
DepositType_LU	Deposit type names
Province_LU	State and Province names
ResourceCat_LU	List of terms used in the Resource_cat field of the 2_Resourcestbl table
ResourceStd_LU	List of mineral evaluation reporting code standards for use in the Resources_std field of the 2_Resourcestbl table
SiteActivity_LU	List of terms for SiteStatus field in 1_Mastertbl table
Junction tables	
DepRef_MM	Table provides one-to-many links between 1_Deposittbl and 3_Referencetbl
ResRef_MM	Table provides one-to-many links between 2_Resourcestbl and 3_Referencetbl
Internally generated table	
Switchboard Items	
Forms	
1_Deposittbl_frm	CACB sediment-hosted copper master form. Use for editing and viewing all related data
2_Resourcestbl_frm	Subform used on 1_Deposittbl_frm to display resources and related references
Deposit_WgtAvg_qry_subform	Form that shows calculated tonnage and grade values. Form used as subform on 1_Deposittbl_frm form
DepRef_MM_subform	Subform uses DepRef_qry to show references related to deposit information on 1_Deposittbl_frm
ResRef_MM_subform	Subform uses ResRef_qry to show references related to resource information on 2_Resourcestbl_frm and 1_Deposittbl_frm
Splashscreen	A form that opens with the database and shows the reference for this report and a disclaimer for 5 seconds
Switchboard	Form that opens after the Splashscreen form closes with buttons for several actions
Queries	
Deposit_SumGradexTons_qry	Query uses the Group_tonsXgrade_qry to sum all the grades times tonnages for each deposit
Deposit_SumTons_qry	Query uses the 1_Mastertbl and 2_Resourcestbl to sum the tonnages for all deposits
Deposit_TonsxGrade_qry	Query uses 1_Mastertbl and 2_Resourcestbl to calculate the tonnage times grade for all deposits
Deposit_WgtAvg_qry	Query calculates tonnage and weighted average copper and cobalt grades for all deposits
DepRef_qry	Query used to join 1_Deposittbl to 3_Referencetbl
Group_SumGradexTons_qry	Query uses the Group_tonsXgrade_qry to sum all the grades times tonnages for each group
Group_SumTons_qry	Query uses the 1_Mastertbl and 2_Resourcestbl to sum the tonnage for all deposit groups
Group_TonsxGrade_qry	Query uses 1_Mastertbl and 2_Resourcestbl to calculate the tonnage times grade for all deposit groups
Group_WgtAvg_qry	Query calculates tonnage and weighted average copper and cobalt grades for all deposit groups
ResRef_qry	Query used to join 2_Resourcestbl to 3_Referencetbl

Table A4. Source tables, queries, and fields for data displayed on the forms, as well as any controls or type of data that should be entered.

[Source Field is the name of the corresponding field in the table]

Form Field Name	Source Table or Query	Source Table Field Name	Controls
1_Deposittbl_frm			
Group Name	1_Deposittbl	GroupName	None—free form
DepID	1_Deposittbl	DepID	Manual entry is not allowed; value is automatically generated
MRDS	1_Deposittbl	MRDS	8-digit integer from the Deposit ID field in the USGS NewMRDS ¹ database
Deposit Name	1_Deposittbl	Name	None—free form
Property	1_Deposittbl	Property	None—free form
Deposit_WgtAvg_qry_subform	Deposit_WgtAvg_qry	Calculated field	Manual entry is not allowed; value is calculated automatically by the query Deposit_WgtAvg_qry
Latitude	1_Deposittbl	Latitude	None—should be an integer between -90 and 90
Longitude	1_Deposittbl	Longitude	None—should be integer between 180 and 180
Country	1_Deposittbl	Country	Limited to countries listed in the look-up table Province_LU
Province	1_Deposittbl	Province	Limited to a province listed in the look-up table Province_LU
Other names	1_Deposittbl	Name_other	None—free form
Includes	1_Deposittbl	Includes	None—free form
Site Activity	1_Deposittbl	SiteActivity	Limited to a term listed in the look-up table SiteActivity_LU
Production	1_Deposittbl	Production	Check box limits entry: box checked for yes, unchecked for no
Deposit Type	1_Deposittbl	DepositType	Limited to terms in the look-up table DepositType_LU
DepositSubtype	1_Deposittbl	DepositSubtype	Limited to terms in the look-up table DepositSubtype_LU
2_Resourcetbl_frm			
ResID	2_Resourcetbl	ResID	Limited to a value in the fieldResID in the table 2_Resourcetbl
Subpart	2_Resourcetbl	Subpart	None—free form
Resource category	2_Resourcetbl	ResourceCat	Limited to term in the look-up table ResourceCat_LU
Resource standard	2_Resourcetbl	ResourceStd	Limited to term in the look-up table ResourceStd_LU
Year(s)	2_Resourcetbl	EstYear	None—free form
ASCu grade	2_Resourcetbl	ASCu_grade	None—free form
Ag grade	2_Resourcetbl	Ag_grade	None—free form
ASCu amount	2_Resourcetbl	ASCu_amt	None—free form
Ag amount	2_Resourcetbl	Ag_amt	None—free form
Ore (mt)	2_Resourcetbl	Ore_MT	None—free form
Cu grade	2_Resourcetbl	Cu_grade	None—free form
Co grade	2_Resourcetbl	Co_grade	None—free form
Cu equivalent	2_Resourcetbl	Cu_equiv	None—free form
Au grade	2_Resourcetbl	Au_grade	None—free form
Cu amount	2_Resourcetbl	Cu_amt	None—free form
Co amount	2_Resourcetbl	Co_amt	None—free form
Cu_cutoff	2_Resourcetbl	Cu_cutoff	None—free form
Au amount	2_Resourcetbl	Au_amt	None—free form
Reference Page	2_Resourcetbl	Reference	None—free form
Deposit_WgtAvg_qry_subfrm			
DepID	Deposit_WgtAvg_qry	DepID	One-to-one link to 1_Deposittbl
Ore (mt)	Deposit_WgtAvg_qry	Ore (mt)	Calculated field
Cu (%)	Deposit_WgtAvg_qry	Cu (%)	Calculated field
Co (%)	Deposit_WgtAvg_qry	Co (%)	Calculated field
DepRef_MM_Subform			
RefNo	4_Referencetbl	RefNo	RefNo field from DepRef_qry
Deposit Reference	4_Referencetbl	Reference	None—free form
ResRef_MM_Subform			
RefNo	4_Referencetbl	RefNo	RefNo field from ResRef_qry
Resources Reference	4_Referencetbl	Reference	None—free form

¹An abbreviated version of Mineral Resources Data System or MRDS (also known as NewMRDS) is available to the public on the Web at <http://tin.er.usgs.gov/mrds/> or at <http://mrdata.usgs.gov/>.

Table A5. Design and table structure of mineral deposits data table, 1_Deposittbl.

Field Name	Data Type	Data Size	Description
DepID	Number	Long Integer	Primary key—Unique deposit identification number.
GroupName	Text	50	Name assigned to one or more deposits that can be grouped because of distance rules.
Property	Text	50	Name of property or lease.
Name	Text	255	Name of deposit.
Name_other	Text	255	Historical names or spelling variations used for deposit.
Includes	Text	255	Names of properties or sites that are subsets of the property.
SiteActivity	Text	50	Description of the exploration or operational activity at time of source publication (active, development, exploration, inactive, mined out, prospect, unknown, and no entry).
Country	Text	50	Country name(s) where deposit is located.
Province	Text	50	Province name where deposit is located.
Latitude	Number	Double	Latitude of center of mine or ore body, in decimal degrees, WGS 84 datum.
Longitude	Number	Double	Longitude of center of mine or ore body, in decimal degrees, WGS 84 datum.
DepositType	Text	75	Deposit type/model associated with deposits in this database (list of values is provided in the look-up table DepositType_LU).
DepositSubtype	Text	50	Deposit subtype/model associated with deposits in this database (list of values is provided in the look-up table DepositSubtype_LU).
MRDS	Number	Long Integer	ID number of property in USGS MRDS database.
Production	Boolean (Yes/No)	N/A	Yes, or check mark = this deposit has produced. No, or blank = no known production or only artisanal mining.

and Mushoshi deposits, each its own separate record. Mineral rights are leased according to previously established (usually surveyed) land parcels. Each parcel will have a formal legal description. However, it is common for companies to refer to these parcels as a property or project.

Name is a unique identifier for the deposit, a site with reported production, or an estimate of the tonnage and grade of mineralized rock.

Name_other and **Includes** contain other names by which the deposit may be known, or the deposit includes (especially useful for larger deposits that include multiple pits or workings which may be listed to eliminate any confusion over what is included in the definition of the deposit).

Latitude and **Longitude** coordinates of the approximate center of a mine or ore body were derived from publications and examination of Google Earth images in comparison with the GIS data (see appendix B). Some of the deposits have been mined and are visible on Google Earth or other satellite imagery. Some reports contained maps, which were georegistered to determine the locations, and in some instances a location was specified in another coordinate system or projection. All the data were converted to geographic coordinates, WGS 84 datum.

DepositType and DepositSubtype (see table A3) use the same terms as the Type and Subtype fields of the Deposit and

Prospects GIS database (see appendix B). MRDS contains the deposit's identifier as used in the USGS global database of mines and prospects known as Mineral Resources Data System or MRDS.⁷ Production contains a check box to indicate whether or not the deposit was mined and has known production. The box is checked to indicate that, yes, the deposit has been mined, and if there is known production those values are given in the resource table, 2_Resourcestbl. The box is not checked (empty) to indicate, no, the deposit is not known to have produced, or if mining was artisanal in nature, or if only small amounts of ore were removed for exploration purposes. This box is unchecked for about three quarters of the deposits because they are in the exploration stage and have never produced ore.

2_Resourcestbl Table

The mineral resources data table, 2_Resourcestbl table, contains published copper, cobalt, silver, and gold resource and production data for sediment-hosted copper deposits in the

⁷An abbreviated version of Mineral Resources Data System or MRDS (also known as NewMRDS) is available to the public on the web at <http://tin.er.usgs.gov/mrds/> or at <http://mrdata.usgs.gov/>.

CACB. A brief description of each of the 20 fields is provided in table A6. All resource and production values are in metric tons (tonnes) for both raw ore and contained metal. Grades are either weight percent (base metals) or grams per metric ton (precious metals). In many cases, the resources were reported in million metric tons or thousand metric tons, so they were converted to metric tons to eliminate potential misinterpretation of the values by many orders of magnitude.

EstYear is the year(s) for which the resource or production was reported. Often a recent publication will cite an estimate made decades ago, thus the year of the reference is not always an accurate indication of when the estimate was really made.

Cu_cutoff contains values for copper cutoff grade, usually reported as an economic cutoff using metal prices at the time of disclosure. In the few instances where a list of resources at various cutoff grades was published for a deposit, we selected the cutoff that the company used for its computations and report discussions, even if a potentially larger tonnage at lower grade was also reported. Cutoff grade is subject to economic filters and may change with time. For example, a deposit for which grade and tonnage was calculated at a cutoff grade of 0.5 weight percent Cu at a time of low metal prices, might be given a lower cutoff grade if and when the price rises substantially. Cutoff grade may also vary as technology changes.

All the fields ending with “_amt” (for Cu, ASCu⁸, Co, Ag, and Au) store data for the amount of contained metal in the ore (Ore_MT). Data were included only if reported in the source publication. It appeared that this was commonly computed in the source publication by multiplying the tons of ore times the grade (and dividing by 100 to account for the grade in percent). Numbers may, or may not be rounded, depending on how they were reported. In some cases, this is the reported recovery from processing the ore. In those cases, the ResourceCat field will be classified as production. Keep in mind that if the value reported is actual production, that would be the amount recovered and does not account for loss or waste in the recovery process, which can be significant. Acid-soluble copper-equivalent amounts (ASCu_amt), were only available for fewer than 10 percent of the deposits.

Subpart lists the specific subarea of the deposit for which values are reported for any resources or production. Some deposits contain or represent several different ore bodies; values for each ore body are reported individually.

3_Referencetbl Table

The reference data table, 3_Referencetbl, contains full citations of sources used for deposit, resource, and production information (table A7). Published (stable) sources are cited

in full USGS bibliographic style. For unpublished (public-domain) sources, we give as much information as possible so that the reader can locate the reference.

Many of the sources were company Web sites (URL and date accessed are provided in the citation). By nature, Web sites may not be permanent. In fact, many have vanished in the short duration of this data compilation, which makes reconfirming some of the data difficult, if not impossible. This is especially true of Web sites for companies that have been bought, sold, merged, changed name, been acquired by other companies, or have failed and cease to exist.

Look-up Tables

Look-up tables provide lists and descriptions of values (terms) used in the data tables; they maintain a one-to-many relationship with the data tables for fields of the same name.

DepositType_LU table

The deposit-type look-up table, DepositType_LU (table A8), contains a list and description of terms in the DepositType field of the 1_Deposittbl data table. This table is related one-to-many to DepositType field in the 1-Deposittbl table (fig. A1).

DepositSubtype_LU table

The deposit-subtype look-up table, DepositSubtype_LU (table A9), contains a list and description of terms in the DepositSubtype field of the 1_Deposittbl data table. This table is related one-to-many to DepositSubtype field in the 1_Deposittbl data table (fig. A1).

Province_LU table

The province and country look-up table, Province_LU (table A10), contains a list of provinces and the countries in which they occur. Although the DRC is in transition from 11 provinces to 25 provinces, the new boundaries were not available, thus the look-up table only contains the 11 original provinces.

ResourceCat_LU table

The mineral resource categories look-up table ResourceCat_LU (table A11) contains a list and description of terms used by workers in the CACB to describe the level of knowledge of the resources and reserves. These terms are based on the standards accepted by most nations for reporting of resources and reserves (described in the next section, ResourceStd_LU table).

ResourceStd_LU table

The resource standard look up table ResourceStd_LU (table A12) provides a list of acronyms for the organizations that defined the standard resources terms used in the

⁸Acid soluble Cu

Table A6. Design and table structure of mineral resources data table, 2_Resource.tbl.

Field Name	Data Type	Data Size	Description
ResID	Number	Long Integer	Primary key ¹ —a unique identification number resource record.
DepID	Number	Long Integer	Foreign key ² —Identification number in the 1_Deposit.tbl table for the deposit to which this resource relates.
EstYear	Text	50	Year of resource estimation, year resource estimation was published, or year(s) of production.
Ore_MT	Number	Double	Metric tons of resources or production (as ore, not metal).
Cu_grade	Number	Double	Grade of copper, in weight percent.
ASCu_grade	Number	Double	Grade of acid soluble copper, in weight percent.
ASCu_amt	Number	Double	Metric tons of acid soluble copper.
Cu_amt	Number	Double	Metric tons of contained copper metal.
Cu_equiv	Number	Double	Copper equivalent, in weight percent.
Cu_cutoff	Number	Double	Cutoff grade for copper used to make resource estimate, in weight percent.
Co_grade	Number	Double	Grade of cobalt, in weight percent.
Co_amt	Number	Double	Metric tons of contained cobalt metal.
Ag_grade	Number	Double	Grade of silver, in parts per million (equals grams per ton).
Ag_amt	Number	Double	Metric tons of contained silver.
Au_grade	Number	Double	Grade of gold, in parts per million (equals grams per ton).
Au_amt	Number	Double	Metric tons of contained gold.
ResourceCat	Text	36	Type of reserve or resource classification.
ResourceStd	Text	20	Standard used to define the resource classification from ResourceStd_LU look-up table.
Subpart	Text	50	Sub-part of a deposit for which resources are reported.
RefPage	Text	50	Page number in reference where resource data came from. Format is RefID (page no.).

¹The primary key is a field that contains a value (can be numeric, alphanumeric, or character) that is unique for each record or row in the table.

²Foreign key is a field containing a value or string that is used to establish relations among tables in a relational database.

Table A7. Design and table structure of reference data table, 3_Reference.tbl.

Field Name	Data Type	Data Size	Description
RefNo	Number	Long Integer	Primary key—A unique reference record identification number.
Reference	Memo	N/A	Complete citation in USGS format.

Table A8. Structure and content of deposit-type look-up table, DepositType LU table.

Field Name	Data Type	Data Size	Description
DepositType	Text	50	Primary Key—Deposit type name from pick-list. Same as Subtype field in GIS (see appendix B).
DepositTypeDesc	Text	255	Description of the DepositType term.
Values for DepositType			
Sediment-hosted stratabound copper deposit			
Structurally controlled replacement and vein			
Unclassified Cu			
Unclassified Cu, supergene enrichment			

Table A9. Structure and content of deposit-subtype look-up table, DepositSubtype_LU.

Field Name	Data Type	Data Size	Description
DepositSubtype	Text	50	Primary key – Deposit subtype name from pick-list. Corresponds to the “type” field in the GIS (see appendix B).
DepositSubtypeDesc	Text	255	Description of the DepositSubtype term.
Values for DepositSubtype			
Reduced-facies, carbonate écaille			
Reduced-facies, ore shale			
Sandstone, Roan arenite			

ResourceStd field of the deposit data table 1_Deposittbl or in the Resource Standard box in the form 1_Deposittbl_frm.

SiteActivity_LU table

The site activity look-up table, SiteActivity_LU (table A13), contains terms that are used to describe the current mining activity at the deposit site.

Junction Tables

In a relational database, it is not possible to directly link tables that are related many-to-many and query them properly. Trying to do this will create a matrix of all possible combinations, which is not what we want to do. In essence, junction tables provide one-to-many links between tables. The deposits table has a one-to-many relation to the junction table and the reference table has a one-to-many relation to the junction table. Similar relationships are also established between the resources data table and the junction table and the reference data table and the junction table (fig. A1). Two junction tables were constructed to link data tables that have a many-to-many relationship. Foreign keys in the junction tables link to primary keys in the data tables.

DepReftbl_MM table

The deposit reference junction table, DepRef_MM (table A14), links the deposit and reference data tables 1_Deposittbl and 3_Referencetbl, respectively (fig. A1).

ResReftbl_MM table

The resource reference junction table, ResRef_MM (table A15), links the resource and reference data tables 2_Resourcestbl and 3_Referencetbl, respectively (fig. A1).

Internally Generated Table for Switchboard

Microsoft Access® automatically generated an internal table, Switchboard Items (table A16), when the Switchboard form was created (see Forms section). It is used by the software to keep track of items used by the form and to invoke custom commands as requested by the user.

Queries

Queries serve two purposes in this database: (1) computation of the total endowment (tonnage, weighted average

Table A10. Structure and content of the province and country look-up table, Province_LU.

Field Name	Data Type	Data Size	Description
Province	Text	50	Name of province from pick-list; field corresponds to Province field in 1_Deposittbl data table.
Country	Text	50	Name of country in which the province occurs. Field corresponds to country field in 1_Deposittbl data table.
Values for Provinces			
Bandundu			Democratic Republic of the Congo
Bas-Congo			Democratic Republic of the Congo
Équateur			Democratic Republic of the Congo
Kasai-Occidental			Democratic Republic of the Congo
Kasai-Oriental			Democratic Republic of the Congo
Katanga			Democratic Republic of the Congo
Kinshasa			Democratic Republic of the Congo
Maniema			Democratic Republic of the Congo
Nord-Kivu			Democratic Republic of the Congo
Orientale			Democratic Republic of the Congo
Sud-Kivu			Democratic Republic of the Congo
Central			Zambia
Copperbelt			Zambia
Eastern			Zambia
Luapula			Zambia
Lusaka			Zambia
Northern			Zambia
North-Western			Zambia
Southern			Zambia
Western			Zambia

Table A11. Structure, content, and description of terms in the mineral resource categories look-up table, ResourceCat_LU.

Field Name	Data Type	Data Size	Description
ResourceCat	Text	75	Primary key—Type of resource, reserve, or production.
ResourceCatDesc	Memo	N/A	Description of the term in the ResourceCat field.
Values for Resource Category			
Indicated	SAMREC—An “Indicated Mineral Resource” is that part of a Mineral Resource for which tonnage, densities, shape, physical characteristics, grade, and mineral content can be estimated with a reasonable level of confidence. It is based on exploration, sampling, and testing information gathered through appropriate techniques from locations such as outcrops, trenches, pits, workings, and drill holes. The locations are too widely or inappropriately spaced to confirm geological and/or grade continuity but are spaced closely enough for continuity to be assumed.		
Indicated +inferred	This is the sum of the indicated and inferred resources.		
Inferred	SAMREC—An “Inferred Mineral Resource” is that part of a Mineral Resource for which tonnage, grade, and mineral content can be estimated with a low level of confidence. It is inferred from geological evidence and assumed but not verified geological and (or) grade continuity. It is based on information gathered through appropriate techniques from locations such as outcrops, trenches, pits, workings, and drill holes that may be limited or of uncertain quality and reliability.		
Measured	SAMREC—A “Measured Mineral Resource” is that part of a Mineral Resource for which tonnage, densities, shape, physical characteristics, grade, and mineral content can be estimated with a high level of confidence. It is based on detailed and reliable exploration, sampling, and testing information gathered through appropriate techniques from locations such as outcrops, trenches, pits, workings, and drill holes. The locations are spaced closely enough to confirm geological and grade continuity.		
Measured+indicated	This is the sum of the measured and indicated resources.		
Measured+indicated+inferred	This is the total mineral resources—the sum of the measured, indicated, and inferred resources.		
Ore reserve	Total reserves if terms proven or probable are not specified.		
Other	Category undefined (leave comment).		
Probable	SAMREC—A “Probable Mineral Reserve” is the economically mineable material derived from a Measured and (or) Indicated Mineral Resource. It is estimated with a lower level of confidence than a Proved Mineral Reserve. It is inclusive of diluting materials and allows for losses that may occur when the material is mined. Appropriate assessments, which may include feasibility studies, have been carried out, including consideration of, and modification by, realistically assumed mining, metallurgical, economic, marketing, legal, environmental, social, and governmental factors. These assessments demonstrate at the time of reporting that extraction is reasonably justified.		
Production	Production—for any year or years. Years may be added parenthetically.		
Proved	SAMREC—A “Proved Mineral Reserve” is the economically mineable material derived from a Measured Mineral Resource. It is estimated with a high level of confidence. It is inclusive of diluting materials and allows for losses that may occur when the material is mined. Appropriate assessments, which may include feasibility studies, have been carried out, including consideration of and modification by realistically assumed mining, metallurgical, economic, marketing, legal, environmental, social, and governmental factors. These assessments demonstrate at the time of reporting that extraction is reasonably justified.		
Proved+Probable	Also called a “mineral reserve,” this is the sum of the proved and probable reserves that meets one of the accepted country coding classifications.		
Reserve	Term generally refers to reserves numbers that predate or are not defined by existing resource codes.		
Resource	Resource is assumed to be some combination of measured, indicated, demonstrated, or inferred.		
Total endowment	Total endowment is the remaining reserve/resource plus historic production combined to estimate the original amount of mineral resources.		

Table A12. Structure, content, and description of terms in the mineral resource standards look-up table, ResourceStd_LU.

Field Name	Data Type	Data Size	Description
ResourceStd	Text	50	Primary key—Acronym for the code used in reporting mineral resources and reserves.
ResourceStdDesc	Text	255	Full name of the ResourceStd code.
Values for ResourceStd			
Acronym	Description		
CIM	NI ¹ 43-101, Canadian Institute of Mining, Metallurgy, and Petroleum Standards and Guidelines for Valuation of Mineral Properties (CIM Standing committee on Reserve Definitions, 2005).		
JORC	Australasian Joint Ore Reserves Committee—Code for Reporting Mineral Resources and Ore Reserves (The Joint Ore Reserves Committee, 2004).		
NA	Not applicable, the data is production, not resources.		
None	No Standard.		
SAMREC	South African Mineral Resource Committee's South African Code for the Reporting of Exploration Results, Mineral Resources and Mineral Reserves (The Southern African Institute of Mining and Metallurgy and Geological Society of South Africa, 2007).		

¹NI stands for National Instrument.**Table A13.** Structure, content, and description of terms in the site activity look-up table, SiteActivity_LU.

Field Name	Data Type	Data Size	Description
SiteActivity	Text	50	Primary key—Term that describes the status mining activity at the site.
SiteActivityDesc	Text	255	Definition of SiteActivity terms.
Values for SiteActivity			
active	The deposit is being mined at the time of information.		
development	The deposit is being prepared for mining. This is a transitory phase between exploration and active.		
exploration	Active exploration is being done. This may include geochemical sampling, geophysics, geologic mapping, and drilling.		
inactive	The deposit was being mined but has stopped before the deposit was mined out.		
mined out	The deposit is considered completely mined out (depleted).		
prospect	Minor exploration has occurred.		
unknown	Status of current activity at the deposit is unknown.		

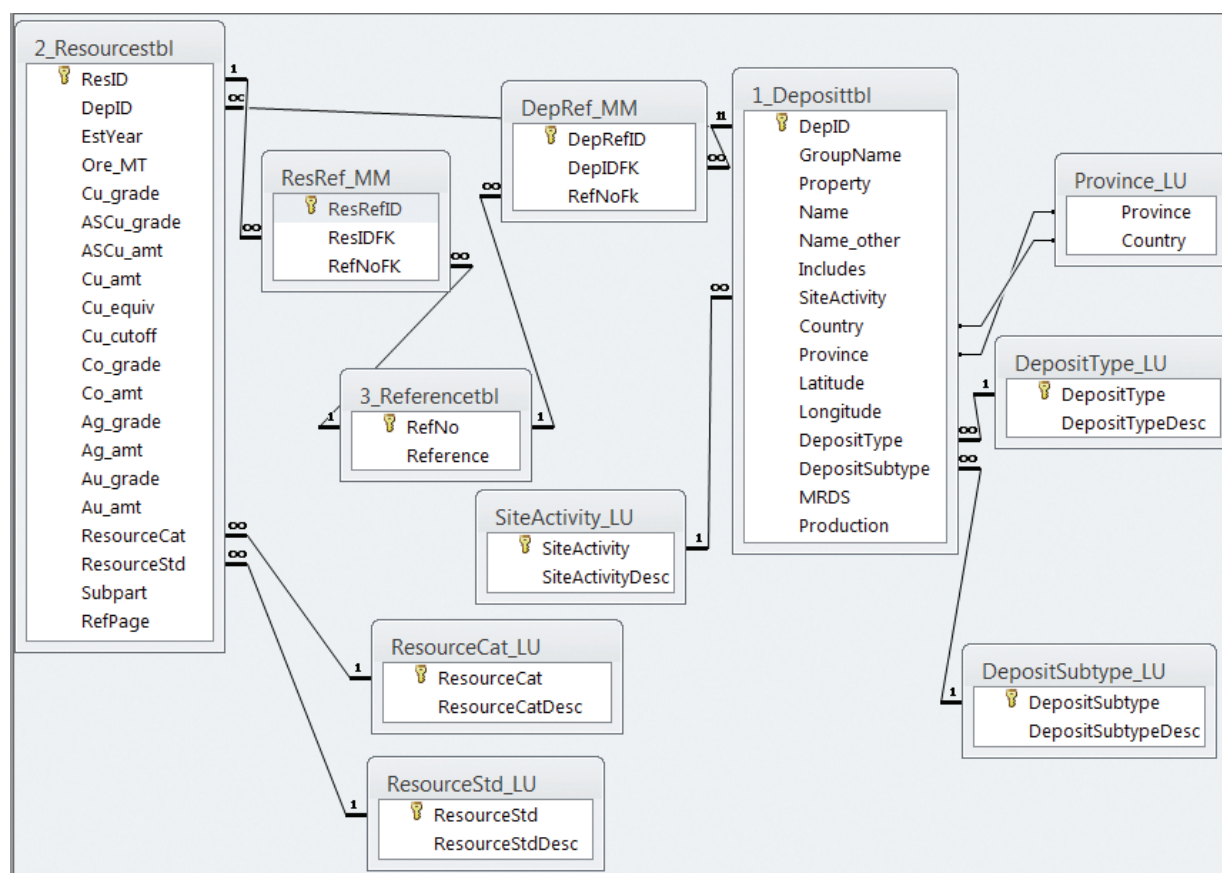


Figure A1. Relations among the 11 Access data tables. (Note that ∞, the symbol for infinity, represents “many” as in one-to-many or many-to-many.)

Table A14. Structure and content of the deposit reference junction table, DepRef_MM.

Field Name	Data Type	Data Size	Description
DepRefID	AutoNumber	Long Integer	Primary key—Unique numeric identifier for associated (paired) foreign keys (DepIDFK and RefNoFk).
DepIDFK	Number	Long Integer	Foreign key—Numeric identifier for each deposit; links to DepID, the primary key field in the deposit data table 1_Deposittbl.
RefNoFk	Number	Long Integer	Foreign key—Numeric identifier for source reference; links to RefNo, the primary field in reference data table 3_Referencestbl.

Table 15. Structure and content of the resource reference junction table, ResRef_MM.

Field Name	Data Type	Data Size	Description
ResRefID	AutoNumber	Long Integer	Primary key—Unique numeric identifier for associated (paired) foreign keys (ResIDFK and RefNoFk).
ResIDFK	Number	Long Integer	Foreign key—Numeric identifier for resources; links to ResID, the primary key field in the resources data table 2_Resourcestbl.
RefNoFK	Number	Long Integer	Foreign key—Numeric identifier for source reference; links to RefNo, primary key field in reference data table 3_Referencestbl.

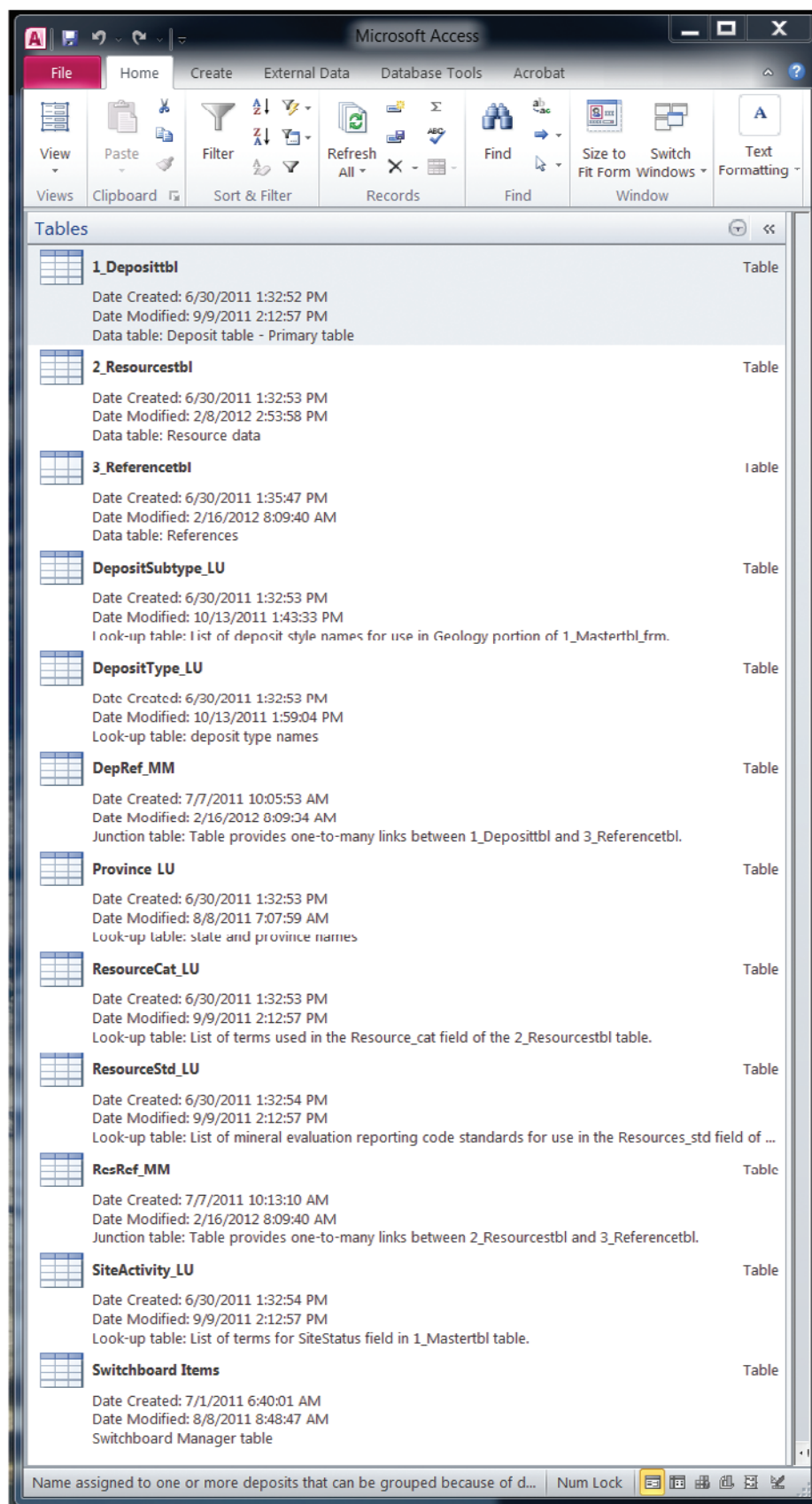


Figure A2. List of tables in the database.

Table A16. Structure and content of the Switchboard Items table.

[Note that this table is not user generated and therefore may not be modified]

Field Name	Data Type	Data Size	Description
SwitchboardID	AutoNumber	Long Integer	Number is automatically generated by Access.
ItemNumber	Number	Integer	Primary key—Row number for items on the Switchboard.
ItemText	Text	255	Text of items on Switchboard form.
Command	Number	Integer	Code that identifies one of the commands available.
Argument	Text	255	Name of the form, report or switchboard to run.

grade, and copper and cobalt content) of the individual deposits and spatially related groups of deposits in the CACB (table A17) and (2) link 3_referencetbl records to 1_deposittbl and 2_resourcestbl tables (DepRef_qry, ResRef_qry). The queries in this database were formed using SQL (Structured Query Language) tools in Microsoft Access®: the built-in GUI (Graphical User Interface) tools were sufficient to create all of the query designs.

The reason tonnages and grades for the deposits and deposit groups are calculated through a series of queries is that Access (database) does not have the same functions as Excel (spreadsheet). The @sumproduct and @sum functions that are available in Excel and could be used to calculate weighted averages are not available in Access®. An alternative is to write code, but as new versions of software are released or upgraded, code can become obsolete. One of the easier ways to make computations in Access® is by using the built-in features to create a series of linked queries (table A17).

In the case of the CACB data, there are resource records in which a total copper grade might not be given, but a tonnage of metal is known. In these cases, the query first checks for a grade (Cu_grade field) and uses it. If no grade is given, it selects the amount of metal (stored in Cu_amt field) and uses that value. If there is only an acid soluble copper grade (ASCu_grade field), then that value is used. Every resource record has at least one value in one of those three fields for copper. The order of selection of the field to use is controlled by our evaluation of which field has the most reliable value. Grades of total copper (Cu_grade) are always the preferred values. Values for cobalt are treated similarly except there is only either a grade (Co_grade field) or amount of metal (Co_amt field), but no acid-soluble equivalent.

The coding used to do the complex selection of data and calculations for both the deposits and groups are the same and are shown below. The complete SQL coding can be viewed by examining the queries in the database using SQL View option when in Design View. Different outputs are due to the differences in selection of records to use. In the case of the deposits, the resources are calculated using information in the 2_Resourcestbl table that is related to the deposit names found in the field called Name in the 1_Deposittbl. For groups, resources are calculated on the group names found in the field

called GroupName. Queries that contain the word “sum” use the simple Access sum function.

The sections below briefly describe each query, provide the SQL code and portray the GUI interface (Design View). See the Users’ Guide section for how to invoke these queries.

Deposit_SumTons_qry Query

The query, Deposit_SumTons_qry (fig. A3), sums the resource and production tonnage records to produce a total tonnage for each deposit.

Deposit_TonsxGrade_qry Query

The query, Deposit_TonsxGrade_qry (fig. A4), calculates the product of tonnage times copper and cobalt grades for each resource record in the 2_Resourcestbl table. If no grade is given, the query checks to see if a value exists for the amount of copper and cobalt. If so, it uses that value. The result is divided by 100 to convert from percent. Output from this query is passed to the query Group_SumGradexTons_qry.

Deposit_SumGradexTons_qry Query

The query Deposit_SumGradexTons_qry (fig. A5) uses output from the Deposit_TonsxGrade_qry query to sum the tonnage of copper and cobalt in a deposit.

Deposit_WgtAvg_qry Query

The query, Deposit_WgtAvg_qry (fig. A6), calculates the weighted average copper and cobalt for each deposit. The query produces a list of deposit names with total tonnage, and average grade of copper and cobalt for each.

Queries and Calculations Performed on Groups of Deposits

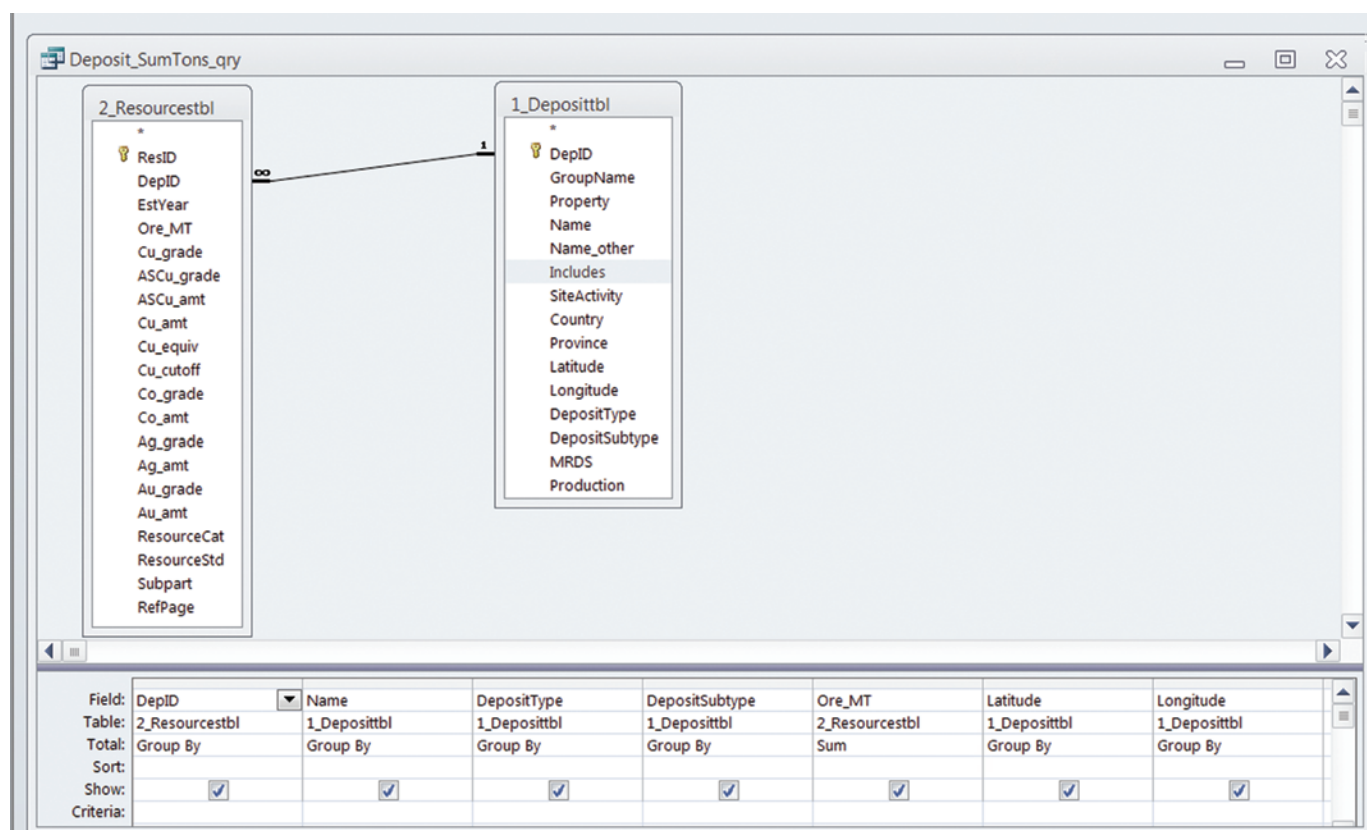
Group_SumTons_qry Query

The query, Group_SumTons_qry (fig. A7), sums the resource and production tonnage records for each deposit group to produce a total tonnage for the deposit group.

Table A17. List of queries and brief description of output and use in other queries.

[NA, not applicable]

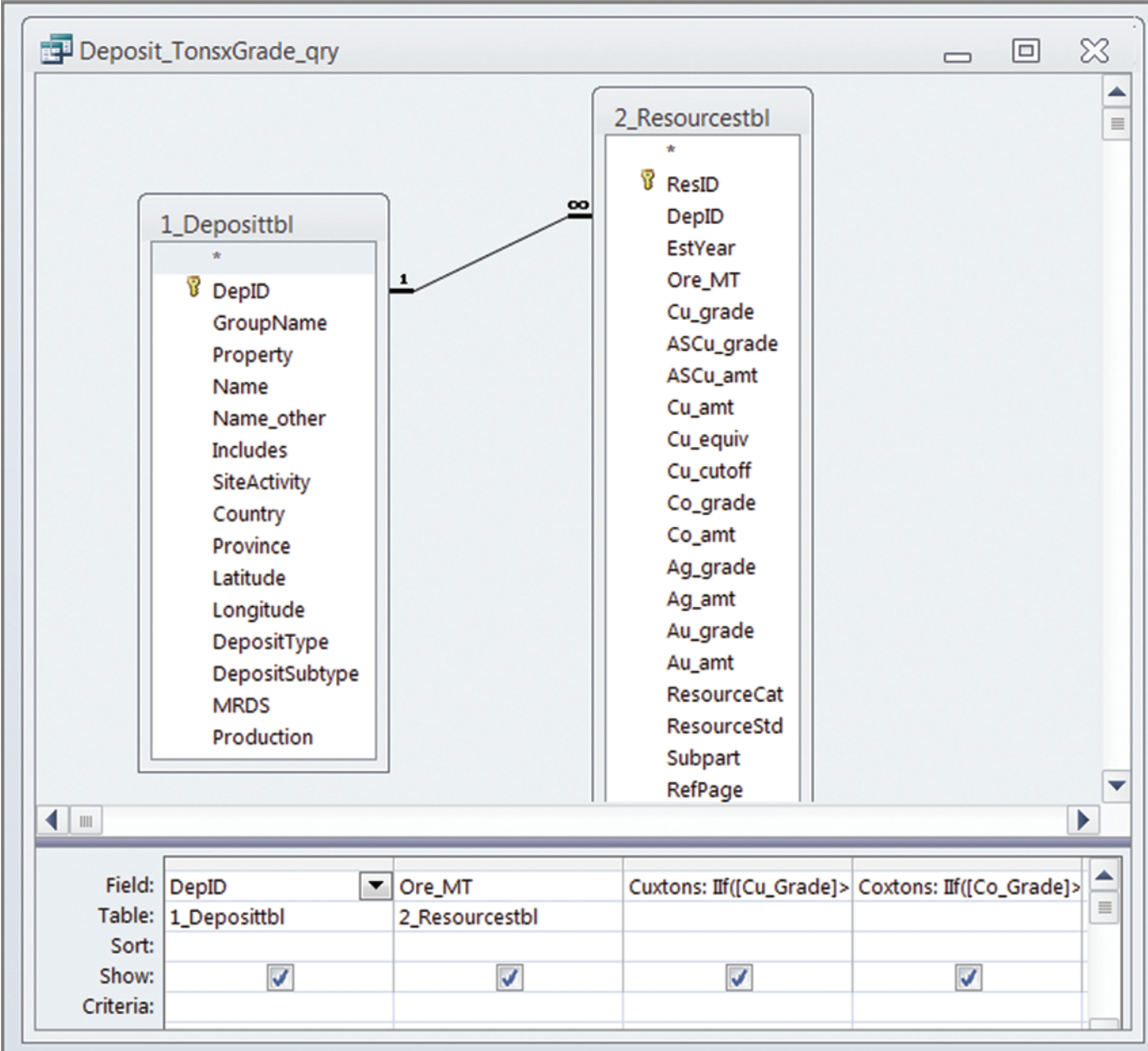
Query	Output	Query in which output is used
Deposit_SumTons_qry	Total tonnage of ore (in metric tons) for each deposit.	Deposit_WgtAvg_qry
Deposit_TonsxGrade_qry	Amount of metal in each resource or production record.	Deposit_TonsxGrade_qry
Deposit_SumGradexTons_qry	Total tonnage (in metric tons) of copper and cobalt metal, for each deposit.	Deposit_WgtAvg_qry
Deposit_WgtAvg_qr	Total tonnage (in metric tons) and weighted average copper and cobalt grades (in percent), for each deposit.	Query run from command button on Switchboard form “Run Deposit grade/ton Query” button.
Group_SumTons_qry	Total tonnage of ore (in metric tons) for each deposit group.	Group_WgtAvg_qry
Group_TonsxGrade_qry	Amount of metal in each resource or production record.	Group_SumGradexTons_qry
Group_SumGradexTons_qry	Total tonnage (in metric tons) of copper and cobalt metal, for each deposit group.	Group_WgtAvg_qry
Group_WgtAvg_qry	Total tonnage (in metric tons) and weighted average copper and cobalt grades (in percent), for each deposit group.	Query run from command button on Switchboard form “Run Group/Deposit grade/ton Query” button.
DepRef_qry	Used to link RefID from 3_Referencetbl table with 1_Deposittbl table.	NA
ResRef_qry	Used to link RefID from 3_Referencetbl table with 2_Resourcestbl table.	NA



SQL code:

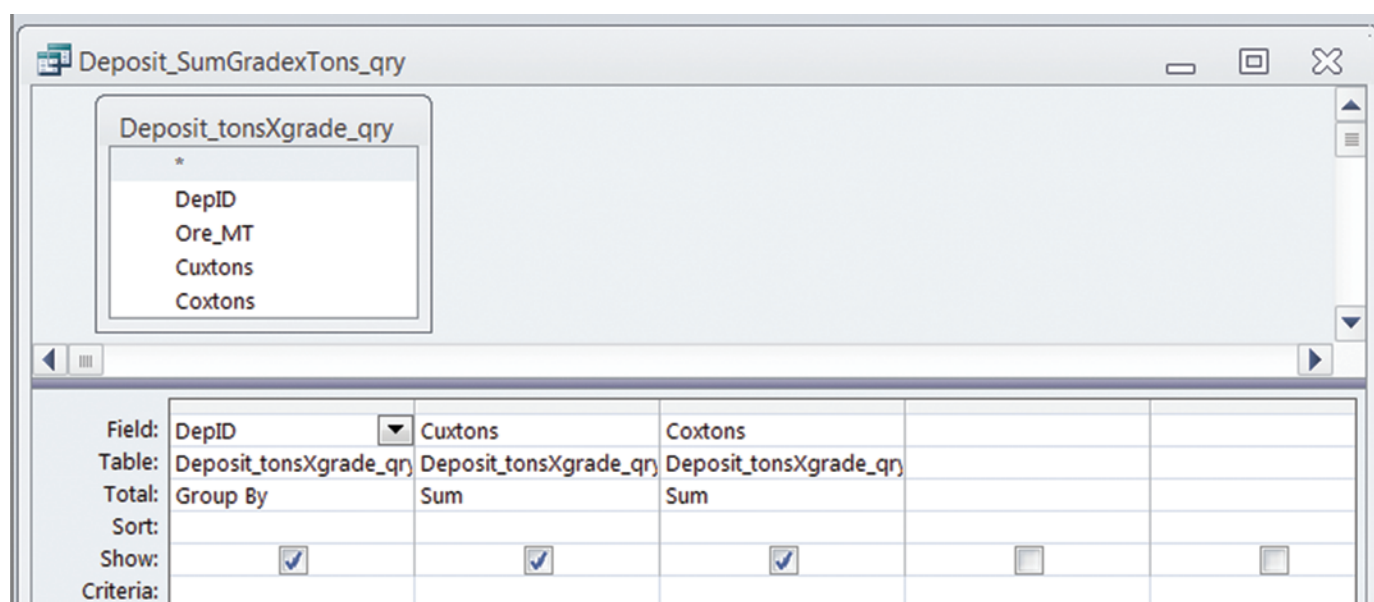
```
SELECT [2_Resourcestbl].DepID, [1_Depositstbl].Name, [1_Depositstbl].DepositType, [1_Depositstbl].DepositSubtype,
       Sum([2_Resourcestbl].Ore_MT) AS SumOfOre_MT, [1_Depositstbl].Latitude, [1_Depositstbl].Longitude
FROM 1_Depositstbl INNER JOIN 2_Resourcestbl ON [1_Depositstbl].DepID=[2_Resourcestbl].DepID
GROUP BY [2_Resourcestbl].DepID, [1_Depositstbl].Name, [1_Depositstbl].DepositType, [1_Depositstbl].DepositSubtype,
         [1_Depositstbl].Latitude, [1_Depositstbl].Longitude;
```

Figure A3. Deposit_SumTons_qry query design view and Structured Query Language (SQL).



SQL code:
SELECT [1_Deposittbl].DepID, [2_Resourcstbl].Ore_MT, If([Cu_Grade]>0,[Cu_Grade]/100*[Ore_MT],If([Cu_amt]>0,[Cu_amt],[ASCu_grade]/100*[Ore_MT]))
AS Cuxtons, If([Co_Grade]>0,[Co_Grade]/100*[Ore_MT],[Co_amt]) AS Coxtons
FROM 1_Deposittbl INNER JOIN 2_Resourcstbl ON [1_Deposittbl].DepID = [2_Resourcstbl].DepID;

Figure A4. Deposit_TonsxGrade_qry query design view and Structured Query Language (SQL).



SQL code:

```
SELECT Deposit_tonsXgrade_qry.DepID, Sum(Deposit_tonsXgrade_qry.Cuxtons) AS SumOfCuxtons, Sum(Deposit_
tonsXgrade_qry. Coxtons) AS SumOfCoxtons
FROM Deposit_tonsXgrade_qry
GROUP BY Deposit_tonsXgrade_qry.DepID;
```

Figure A5. Deposit_SumGradexTons_qry query design view and Structured Query Language (SQL).

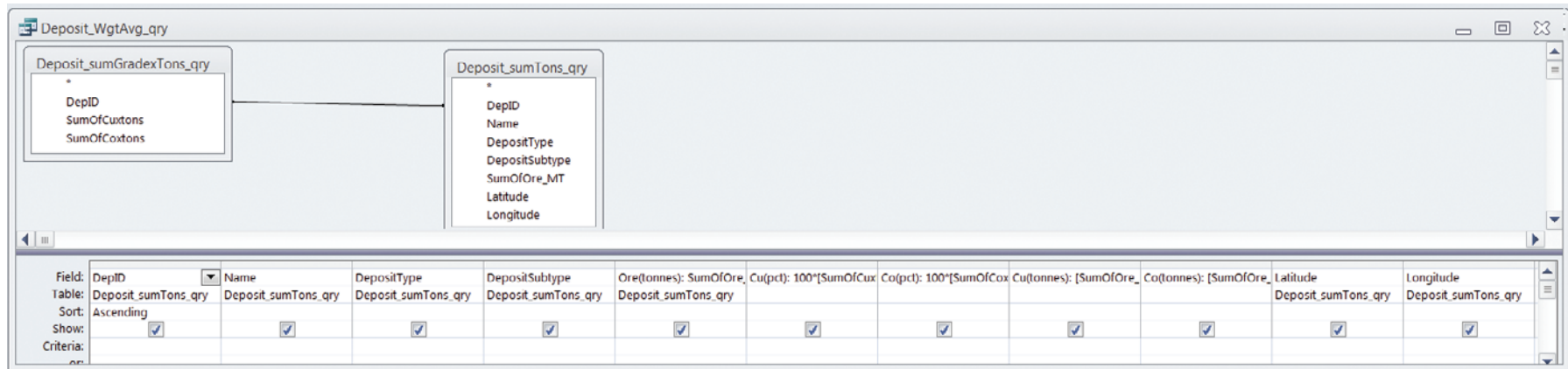


Figure A6. Deposit_WgtAvg_qry query design view and Structured Query Language (SQL).

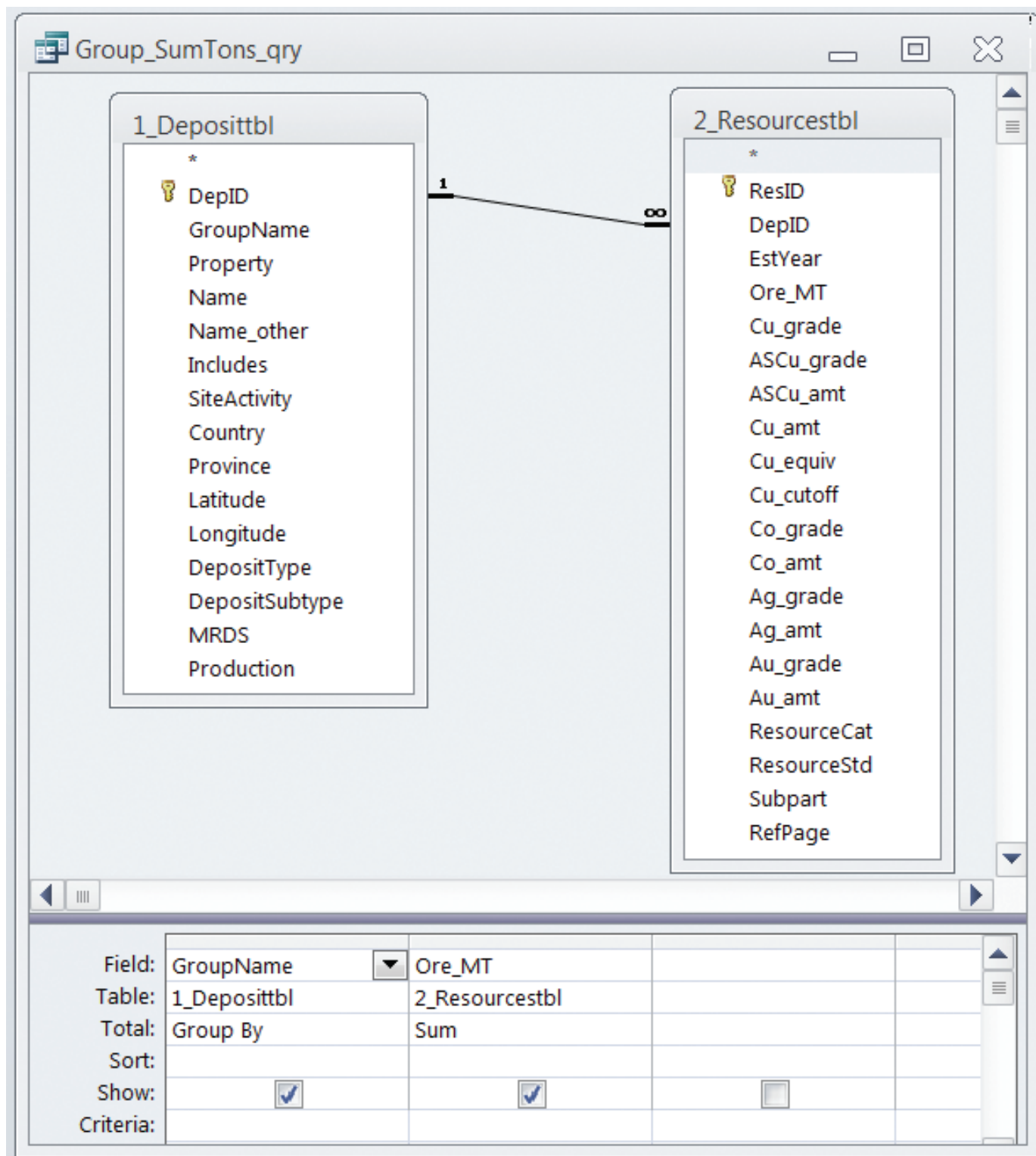


Figure A7. Group_SumTons_qry query design view and Structured Query Language (SQL).

Group_TonsxGrade_qry Query

The query, Group_TonsxGrade_qry (fig. A8), is used in the calculation of grades for each deposit group. It calculates the product of tonnage times copper and cobalt grades for each resource record in the 2_Resourcestbl table. If no grade is given, the query checks if a value exists for the amount of copper and cobalt and divides the result by 100. If no copper grade or amount is given, it uses the acid soluble copper grade to calculate the metal tonnage for each deposit group.

Group_SumGradexTons_qry Query

The query, Group_SumGradexTons_qry (fig. A9), uses output from the Group_TonsxGrade_qry query to add the tonnage of metals for a deposit group.

Group_WgtAvg_qry Query

The query, Group_WgtAvg_qry (fig. A10), calculates the weighted average copper and cobalt for each deposit group. The query produces a list of group names with total tonnage, and average grade of copper and cobalt for each group.

Queries Used to Provide Lists of References

DepRef_qry Query

The query, DepRef_qry (fig. A11), connects the deposit records to their source reference. It is used in the 1_Deposittbl_frm to display the deposit information and the associated references.

ResRef_qry Query

The query, ResRef_qry (fig. A12), is similar to the DepRef_qry, but it links the resource information to its source reference. The 2_Resourcestbl_frm form used the output of this query to display resource and references for each deposit.

Forms

Forms provide a means of identifying the database (Splashscreen), performing user-specified functions (Switchboard), incorporating data provided by the user simultaneously into multiple tables; and viewing snapshots of data by record. The names and brief descriptions of each form are given in table A18. Subforms and some forms are designed to be placed on other forms. 2_Resourcestbl_frm and forms with the suffix “subform” should not be opened independently and resized, or else they will not display properly on the 1_Deposittbl_frm form into which they were made to fit.

Database Identification

Splashscreen Form

The form, Splashscreen (fig. A13), displays briefly (5 seconds) whenever the database is opened. Splashscreen provides the citation for the publication in which this database is included and a standard USGS disclaimer. To read the splashscreen for longer than 5 seconds (in Access version 2003)⁹, go to Forms, highlight Splashscreen, right click, and select Design View.

Switchboard Form

Processing options are accessed through three selection buttons on the Switchboard form. (fig. A14) which opens immediately after the splashscreen. A description of each option is provided in table A19.

1_Deposittbl_frm Form

The form 1_Deposittbl_frm (fig. A15) is the primary data entry form. It contains 44 data entry boxes, some of which reference subforms to display related information from multiple tables. Titles for the data entry boxes correspond (from left to right in the form) to field names in the various data tables as given in table A4.

2_Resourcestbl_frm Form

The form 2_Resourcestbl_frm (fig. A16) can be used for data entry and for viewing resource and production information. It contains 19 data entry boxes and a subform titled Resources Reference. The main entry form, 1_Deposittbl_frm, uses the resources data entry form to display resources and (or) production associated with a single deposit. Do not attempt to resize the form 2_Resourcestbl_frm because it may not display properly on the form 1_Deposittbl_frm.

Deposit_WgtAvg_qry_subform Form

The form, Deposit_WgtAvg_qry_subform (fig. A17), is used to display deposit tonnage and grade values (outlined in pink) on the main data-entry form, 1_Deposittbl_frm. These values are generated by the query Deposit_WgtAvg_qry. Do not resize this form, or it will not display properly within the form 1_Deposittbl_frm.

⁹In Access version 2010, go to View and select Design View.

Table A18. Description of the forms in the Central African Copperbelt (CACB) database.

Form Name	Form Description
Splashscreen	Form displays the reference for this report and a disclaimer.
Switchboard	Form automatically opens after the Splashscreen fades and provides buttons for three custom actions.
1_Deposittbl_frm	Master data entry form, used to edit and view all related data for a deposit.
2_Resourcestbl_frm	Subform used on 1_Deposittbl_frm to display resources and related references.
Deposit_WgtAvg_qry_frm	Form that shows calculated tonnage and grade values. Form used as subform on 1_Deposittbl_frm form.
DepRef_MM_Subform	Subform uses DepRef_qry to show references related to deposit information on 1_Deposittbl_frm.
ResRef_MM_Subform	Subform uses ResRef_qry to show references related to resource information on 2_Resourcestbl_frm and 1_Deposittbl_frm.

Table A19. Description of operations that can be performed using the Switchboard form.

Button Name	Description of Action performed
Open data entry form	Immediately opens the 1_Deposittblfrm form.
Run deposit tonnage and grade query	Runs the Deposit_WgtAvg_qry query, which calculates the total tonnage and weighted average grade for individual deposits.
Run grouped deposits total endowment query	Runs the Group_WgtAvg_qry query, which calculates the total tonnage and weighted average grade for defined groups of deposits that meet the distance rules for the associated deposit model.

Source Reference Forms

DepRef_MM_Subform Form and ResRef_MM_Subform form

The deposit references form, DepRef_MM_Subform (fig. A18), displays reference(s) that are sources of information about the deposit, whereas the resource references form ResRef_MM_Subform (fig. A19) displays reference(s) that are sources of resource information for the deposit. The data appear as subforms (outlined in light blue) on the forms 1_Deposittbl_frm or 2_Resourcestbl_frm, respectively. Do not attempt to resize either reference form or they may not display properly within the deposit or resource forms.

Macros

Access uses macros to automatically perform functions. The simple macro, Macro1 (fig. A20), automatically opens the switchboard form immediately after the splashscreen closes.

Users' Guide

How to use the Access Database

The database property attribute is set to “read-only”. To make any modifications to data or database design, the file property must be changed in Windows. We recommend that you make a copy of

the database, save it with a new name (something like CentralAfricaSedCu_EDITED.mdb or CACBSedCu_REVISED.mdb), and change the property so it is no longer read-only. (After copying the file, highlight the copy in Windows Explorer, right click, select Properties, and click on the “Read-only” box to unselect.) Your copy is now ready for editing.

The following sections will walk you through opening, browsing, and computing resource endowments in the database. In anticipation of commonly asked questions, we have also provided a section for what we anticipate might be the most frequently asked questions (FAQ)

Open Access Database

Open the backup or duplicated file. Do not open the original file unless you have confirmed that it is “read only”. (You may be asked “Do you want to block unsafe expressions?” if the Tools/Macro/Security is not set to “Low.” Answer “No” or parts of the database will not work. This may be followed by “Do you want to open this file or cancel the operation?” Click “Open.”)¹⁰

The splashscreen (fig. A13) will appear (and close after 5 seconds) followed by the startup, or switchboard, form with 3 action buttons (fig. A14).

¹⁰Alternatively, there may be a yellow security warning bar at the top of the page. Click on “Enable Content” to continue.

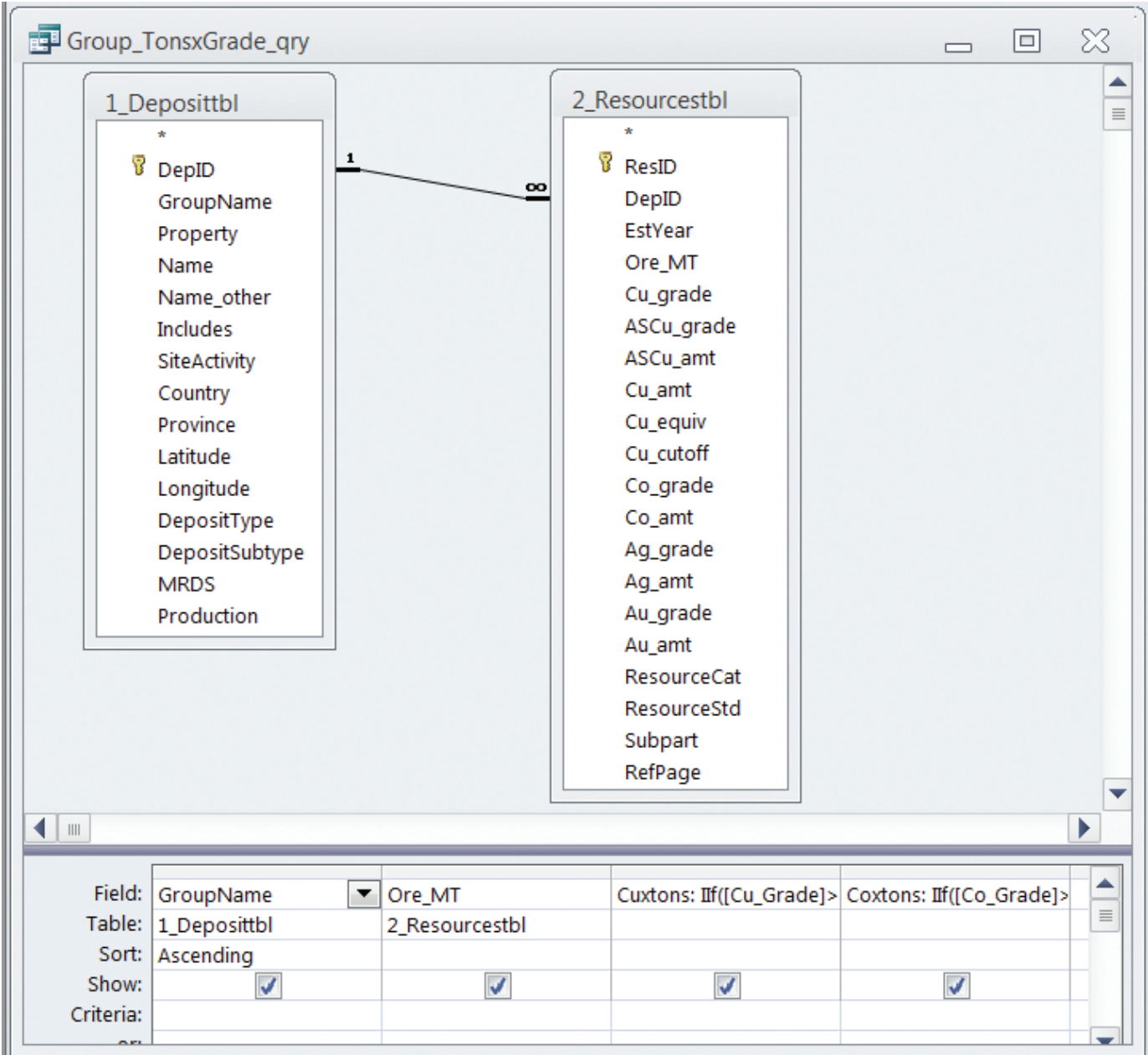


Figure A8. Group_TonsxGrade_qry query design view and Structured Query Language (SQL).

Group_SumGradexTons_qry

Group_tonsXgrade_qry

*

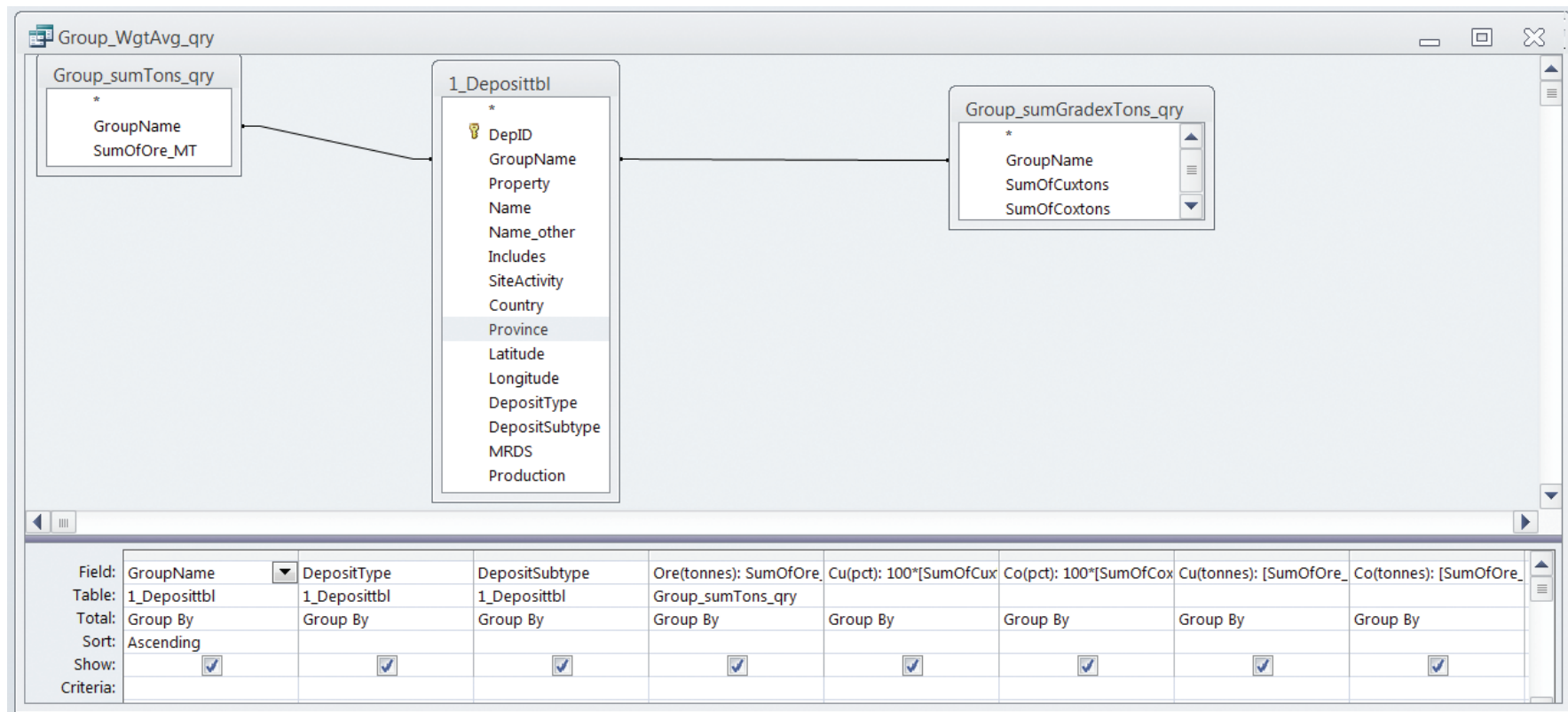
GroupName
Ore_MT
Cuxtons
Coxtons

Field:	GroupName	Cuxtons	Coxtons
Table:	Group_tonsXgrade_qry	Group_tonsXgrade_qry	Group_tonsXgrade_qry
Total:	Group By	Sum	Sum
Sort:			
Show:	<input checked="" type="checkbox"/>	<input checked="" type="checkbox"/>	<input checked="" type="checkbox"/>
Criteria:			

SQL code:

```
SELECT Group_tonsXgrade_qry.GroupName, Sum(Group_tonsXgrade_qry.Cuxtons) AS SumOfCuxtons, Sum(Group_
tonsXgrade_qry.Coxtons) AS SumOfCoxtons
FROM Group_tonsXgrade_qry
GROUP BY Group_tonsXgrade_qry.GroupName;
```

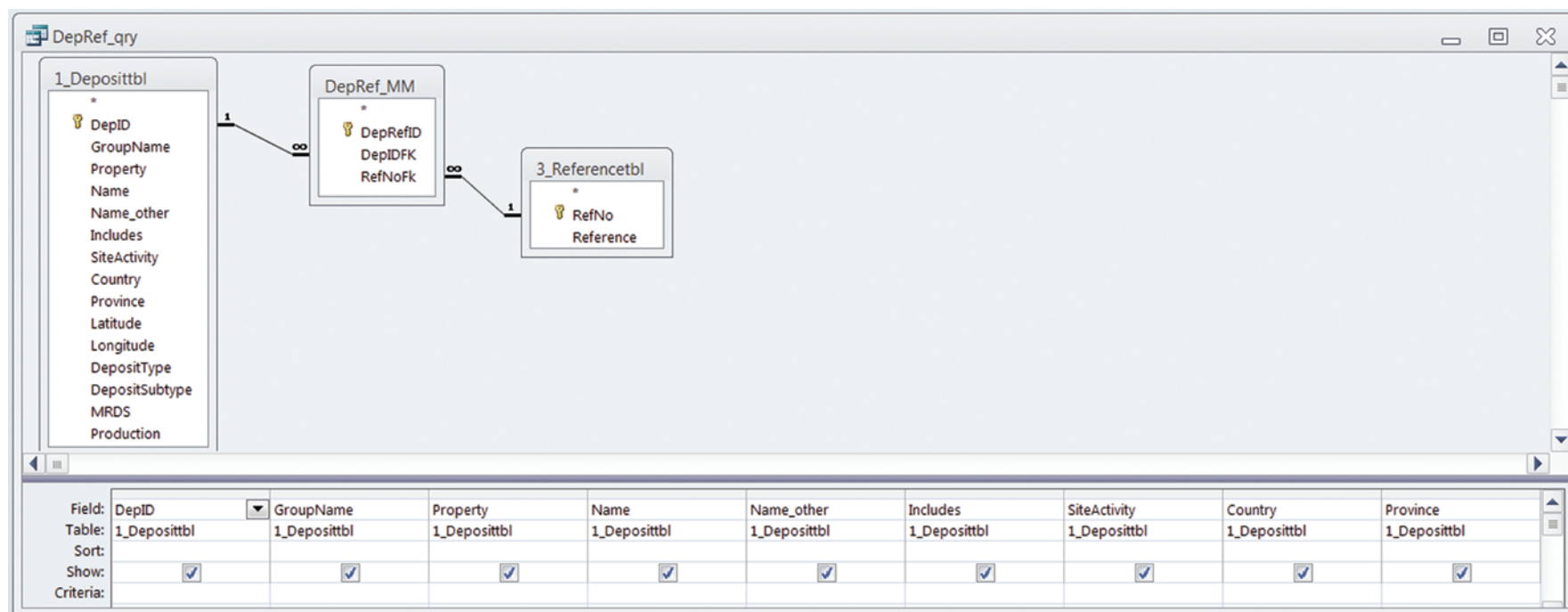
Figure A9. Group_SumGradexTons_qry query design view and Structured Query Language (SQL).



SQL code:

```
SELECT [1_Deposittbl].GroupName, [1_Deposittbl].DepositType, [1_Deposittbl].DepositSubtype, Group_sumTons_
qry.SumOfOre_MT AS [Ore(tonnes)], 100*[SumOfCuxtons]/[SumofOre_MT] AS [Cu(pct)],
100*[SumOfCoxtons]/[SumofOre_MT] AS [Co(pct)], [SumOfOre_MT]*[SumOfCuxtons]/([SumofOre_
MT]*100) AS [Cu(tonnes)], [SumOfOre_MT]*[SumOfCoxtons]/([SumofOre_MT]*100) AS [Co(tonnes)]
FROM (1_Deposittbl INNER JOIN Group_sumTons_qry ON [1_Deposittbl].GroupName = Group_sumTons_qry.GroupName)
INNER JOIN Group_sumGradexTons_qry ON [1_Deposittbl].GroupName = Group_sumGradexTons_qry.
GroupName
GROUP BY [1_Deposittbl].GroupName, [1_Deposittbl].DepositType, [1_Deposittbl].DepositSubtype, Group_sumTons_qry.
SumOfOre_MT, 100*[SumOfCuxtons]/[SumofOre_MT], 100*[SumOfCoxtons]/[SumofOre_MT],
[SumOfOre_MT]*[SumOfCuxtons]/([SumofOre_MT]*100), [SumOfOre_MT]*[SumOfCoxtons]/
([SumofOre_MT]*100)
ORDER BY [1_Deposittbl].GroupName;
```

Figure A10. Group_WgtAvg_qry query design view and Structured Query Language (SQL).



SQL code:

```
SELECT [1_Deposittbl].DepID, [1_Deposittbl].GroupName, [1_Deposittbl].Property, [1_Deposittbl].Name, [1_Deposittbl].Name_other, [1_Deposittbl].Includes,
[1_Deposittbl].SiteActivity, [1_Deposittbl].Country, [1_Deposittbl].Province, [1_Deposittbl].Latitude, [1_Deposittbl].Longitude, [1_Deposittbl].
DepositType, [1_Deposittbl].DepositSubtype, [1_Deposittbl].MRDS, [1_Deposittbl].Production, DepRef_MM.DepIDFK, DepRef_
MM.RefNoFk, [3_Referencetbl].Reference, [3_Referencetbl].RefNo
FROM 3_Referencetbl INNER JOIN (1_Deposittbl INNER JOIN DepRef_MM ON [1_Deposittbl].DepID = DepRef_MM.DepIDFK) ON [3_Referencetbl].RefNo =
DepRef_MM.RefNoFk;
```

Figure A11. DepRef_qry query design view and Structured Query Language (SQL).

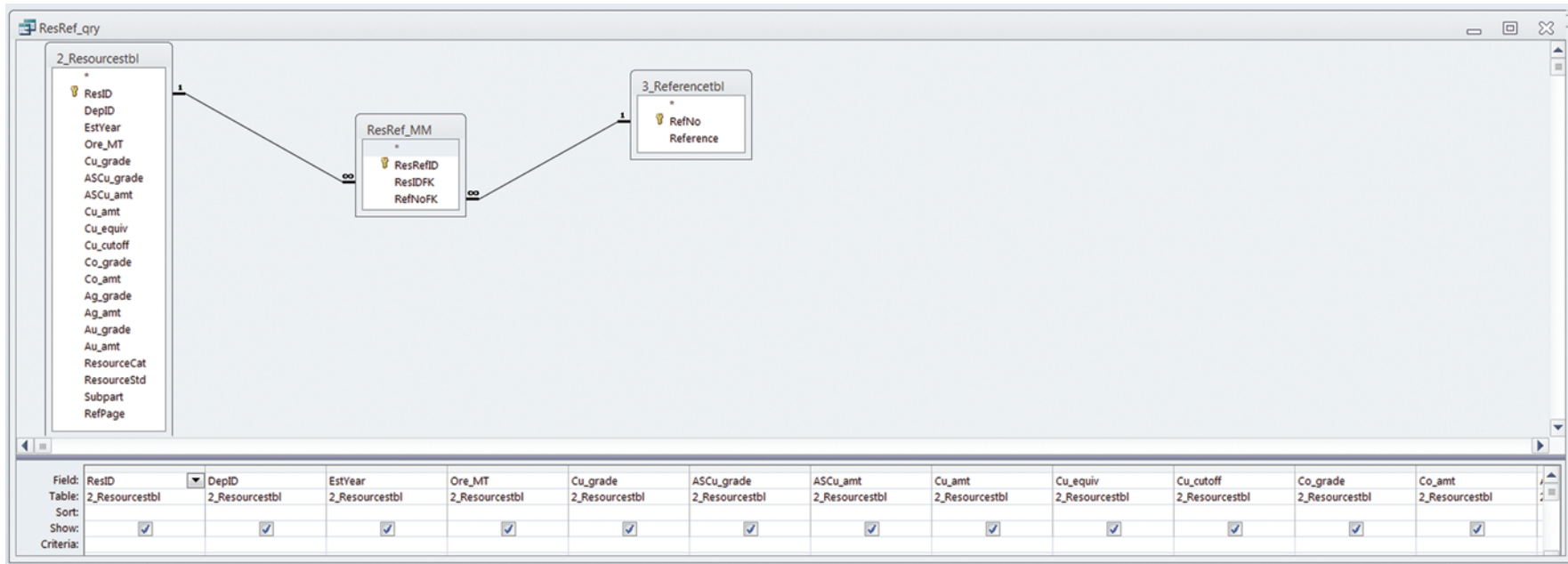


Figure A12. ResRef_qry query design view and Structured Query Language (SQL).

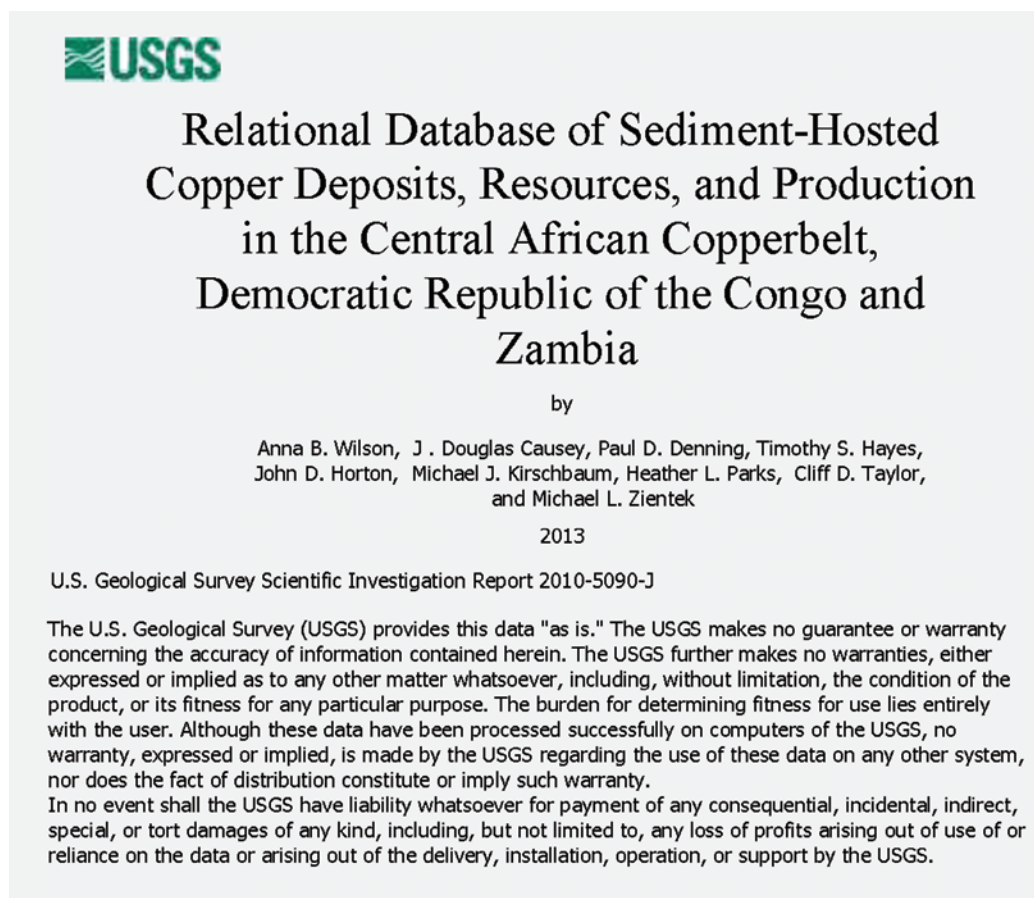


Figure A13. View of the splashscreen form.

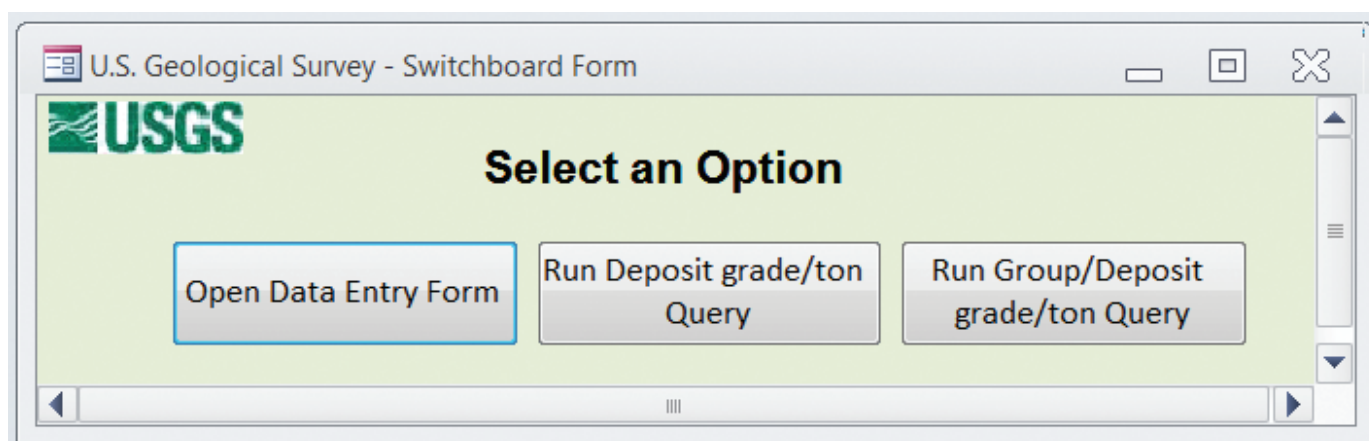


Figure A14. View of the switchboard form showing data entry and query options.

1_Deposittbl1_frm

Group Name: Konkola-Musoshi DepID: 79 MRDS: 10207788

Deposit Name: Konkola Property: Konkola/Mushoshi

DepID	Ore(mt)	Cu(pct)	Co(pct)
79	662,874,267	3.03	

Latitude: -12.3449 Longitude: 27.7978

Country: Zambia Province: Copperbelt

Other Names: Bancroft, Kirila Bombwe(?)

Includes: Musoshi in Shaba Prov., Konkola North, Konkola Deep, Konkola (KCM), Kirila Bomwe orebodies North and South, Saddle Lode, Kaka

Site Activity: active Production: ☒

Deposit Type: Sediment-hosted stratabound copper deposit DepositSubtype: Reduced-facies, ore shale

Deposit Reference

9 Porter GeoConsultancy, 2010, A global database of the World's important mineral deposits: Porter Geoconsultancy Web page accessed October, 2010, at <http://www.portergeo.com.au/database/index.asp>

ResID: 14 DepID: 79 Subpart:

Resource Category: production Resource Standard:

Year(s): 2005 ASCu grade: Ag grade:

Ore (mt): Cu grade: Co grade: ASCu amount: Ag amount:

3,452,341 1.26 Cu equivalent: Au grade:

Cu amount: Co amount: Cu cutoff: Au amount:

43,504 Reference Page: 128 (p. 118)

Resources Reference

128 Vedanta Resources plc, 2005, Annual Report 2005: London, U.K., Vedanta Resources plc, 127 accessed May 26, 2011 at <http://www.vedantaresources.com/uploads/annual20report202005.pdf>

Record: 1 of 19 No Filter Search

Record: 79 of 124 No Filter Search

Figure A15. Form view of the deposit data-entry form for the Konkola deposit, DepID = 79.

2_Resourcestbl_frm

ResID DepID Subpart

Resource Category Resource Standard

Year(s) ASCu grade Ag grade

Ore (mt) Cu grade Co grade ASCu amount Ag amount

Cu amount Co amount Cu equivalent Au grade

Cu cutoff Au amount

Reference Page

Ref Resources Reference

6 Le Burn, Steve, and Hayward, Peter, 2011, Kapulo Project, DRC, National Instrument 43-101 Technical Report, revised 7 March, 2011: Coffey Mining Pty Ltd., 101 p. (Available at www.sedar.com [March 18, 2011]; West Ltd, Technical Report (NI 43-101) - English, refilled March 18, 2011, 5777K).

Record: 1 of 314 No Filter Search

Figure A16. View of the resource data-entry form 2_Resourcestbl_frm for ResID = 1.

Deposit tonnage & grade

DepID	Ore(mt)	Cu(pct)	Co(pct)
1	5,500,000	1.80	

Figure A17. View of the deposit tonnage and grade form, Deposit_WgtAvg_qry_subform.

DepRef_MM_Subform

Refl	Deposit Reference
1	François, Armand, 2006, La partie centrale de l'Arc cuprifère du Katanga: étude géologique: Musée royal de l'Afrique centrale - Belgique, Tervuren African Geoscience Collection v. 109, 61 numbered pages, 130 PDF pages.

Figure A18. View of the deposit references form DepRef_MM_Subform.

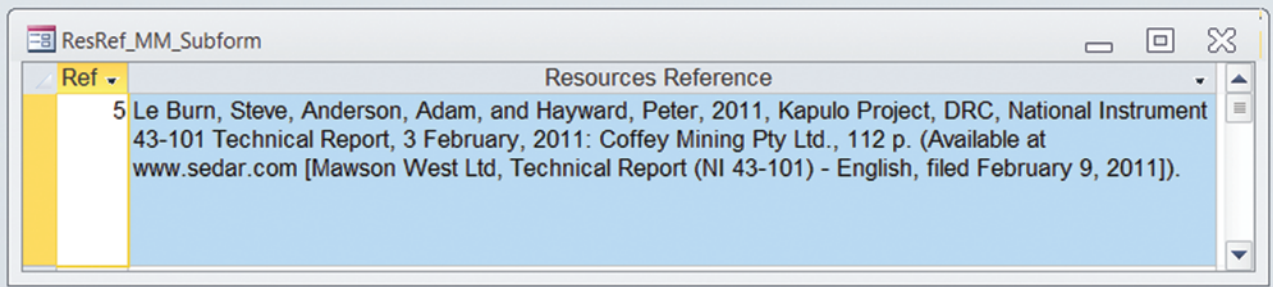


Figure A19. View of the resources references form ResRef_MM_Subform.

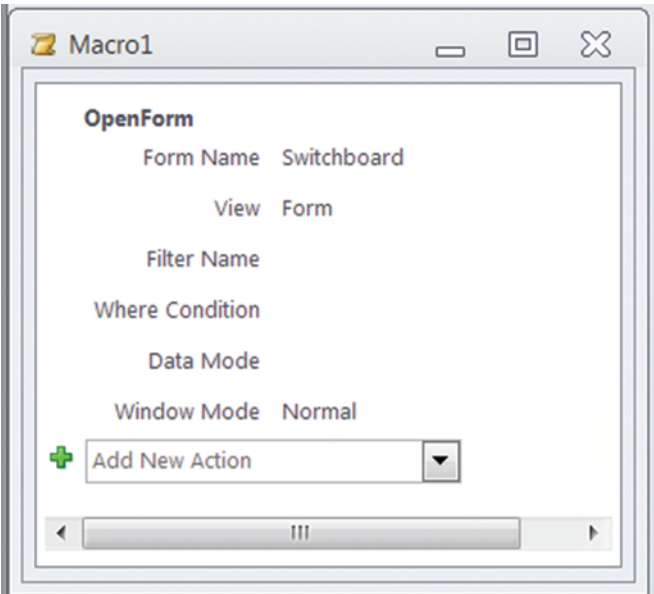


Figure A20. Design View of the macro Macro1.

Browse Database

Select the “Open Data Entry Form” button on the switchboard to browse the database. This opens the master data entry form, 1_Deposit_frm (fig. A21).

The deposits form 1_Deposit_frm displays data that are stored in the three main data entry tables (1_Deposittbl, 2_Resourcecbl, and 3_Referencetbl).

There are two main areas on the deposits form (1_deposit_frm) (fig. A21). The upper part displays identification information (fig. A22), and the lower part (mint-green background) displays resource data (fig. A23). Each part corresponds to a numeric identifier (DepID and ResID, respectively) and an associated list of references. Identification information is stored in the table 1_Deposittbl; the resource data is from the table 2_Resourcecbl. Blue-outlined boxes in each part display the references cited from the master table of references, 3_Referencetbl. Contents of each field are described in the Tables subsection of Database Design (see table A4).

The upper part of the form (fig. A22) contains basic site identification information for the entire deposit such as its name, identification, location, and other details. Contents of each field (table A5) are described in the previous section of this chapter.

The lower part of the form (fig. A23) displays the resource and production records for the deposit. Only one resource record is viewed at a time on this form; how to view all of the records will be discussed a little later.

Note that two record numbers are displayed at the bottom left corners of both the lower frame (2_Resourcecbl_frm) and at the lower left of the outer frame (1_Deposit_frm). These are circled on figs. A22 and A23. When viewing the entire 1_Deposit_frm, the lowermost represents a unique numeric identifier within the deposits table, the upper represents an identifying number in the resources table. Be extremely careful to not confuse these numbers with those for DepID and (or) RefID, because the record number can change when the data tables are sorted or filtered. Therefore, do not assume,

for example, that deposit record 1 (of 124) will always be the Karu East deposit. But Karu East will always correspond to DepID = 1. Similarly, resource record 1 (of n) generally will not correspond to ResID = 1. You can scroll through the records in either frame by navigating with the arrows on the lower left or typing the record number directly into the white box (blank space). Click on the symbol “|<” (vertical bar followed by arrowhead pointing to the left) to view the very first record, or on “>|” (vertical bar followed by arrowhead pointing to the right) to view the very last record. Click on the symbol “>*” (greater than symbol followed by an asterisk) to append a new blank record at the end of the file (you must be in write mode to add records). Again, be very careful not to confuse record number with the value in DepID or ResID.

Identification Information in 1_Deposittbl_frm

The file is automatically numbered (currently 1-131, missing some numbers that were assigned to records that have been merged or deleted) in the DepID field (second from left in the green RESOURCE area of the form). The record number for each deposit may change depending on how the file is sorted, but the DepID (upper right, green circle on fig. A22) will never vary.

Also embedded in this upper form, outlined in pink (fig. A22), is the computation of the overall grade and tonnage, or total endowment of the individual deposit (not the Group). This is a computed field, described in the previous section. We'll describe how it is derived after the resource information discussion that follows.

Resource Information in 2_Resourcestbl_frm and 1_Deposits_frm

The lower part of the main form (mint-green background) displays resource data for the deposit which is stored in the table 2_Resourcestbl: We'll refer to these data as the Resource Records. Each deposit can have many Resource Records, although most have only one or two. These are numbered similarly to the overall deposit records (Record count at lower left of frame, but each has a unique ResID number) and can be thought of as subrecords. All of the resource (and production) values included in the database are used to compute the total endowment of each deposit. Total endowment is reported as a single grade and tonnage in the embedded, pink-outlined box in the upper part of the identification form (figs. A21 and A22).

For example, the record for the Konkola deposit, (DepID 79) lists 19 resource subrecords (circled in red on fig. A24), all of which are used to compute the endowment (fig. A24). Many of these records list production for specific time periods, or resources for different parts of the deposit (scroll through Records 1 through 19 using the arrows at lower left and look at the Resource Category field. For example, you will see that resources are categorized as “production” for ResID

14, “inferred resource” for ResID 208 (for a subpart of the deposit, Konkola North--South Limb), and “inferred” for ResID 209 (for another subpart, Konkola North--East Limb). Most deposits have many fewer subrecords because the production and resource data are not as well documented.

Reference Information

References cited are listed at the base of each of the two parts of the entry form 1_Deposittbl_frm within boxes outlined in light blue. Due to space constraints, only one reference can be viewed in the Form View. However, there is a scroll bar on the right edge of each box (outlined in blue) that indicates that more data exists in the database and the user should scroll to view the other references. Another way to see all the references at once is to print them (see next section).

Calculating Resource Endowments

The “how” of this computation is described in the first part of this chapter. Endowment may be recomputed by using the second button on the Switchboard (fig. A14): “Run Deposit grade/ton Query.”

Print Records

All the records can be printed from the form 1_Deposittbl_frm. The fields will expand, if necessary (for example to show all the references), and multiple resource records will also print. Open 1_Deposittbl_frm in Access. Select “File”, then “Print” then “All.” To print a subset of the records, run a filter, then print “All.” To print only one record, view it, and select Print/Selected Records(s).

Frequently Asked Questions (FAQs)

What happens when a query button I selected is on the switchboard screen?

The Switchboard form (fig. A14) provides three options. The left-most button opens a form that includes a view of all data table records associated with a single deposit from which a user can enter new data, delete or replace existing data, or add a new deposit record. The middle button runs a query which shows the deposit record number, deposit name, deposit type, deposit subtype, total tonnage, weighted average copper and cobalt grades, latitude, and longitude for each deposit record in a spreadsheet format. This is not editable, but can be copied to a spreadsheet program (for example, the Excel file CACB_deposits.xls included with this report). The right-most button runs a query that does the same thing (minus the latitude and longitude) for deposit groups, which are used for the development of the associated CACB sediment-hosted copper deposit models. The results of this query are given in the Excel file CACB_groups.xls that is included with this report.

1_Deposittbl1_frm

Group Name: Karu East DepID: 1 MRDS: 10400610

Deposit Name: Karu East Property: Karu East

DepID	Ore(mt)	Cu(pct)	Co(pct)
1	5,500,000	1.80	

Latitude: -11.6277 Longitude: 27.2764

Country: Democratic Republic of the Congo

Province: Katanga

Other Names:

Includes:

Site Activity: exploration Production: ☐

Deposit Type: Sediment-hosted stratabound copper deposit DepositSubtype: Reduced-facies, carbonate ecaille

Ref: Deposit Reference

10 African Rainbow Minerals, 2010, Mineral resources and reserves 2010: African Rainbow Minerals, 31 p., accessed May 13, 2011, at http://www.arm.co.za/im/files/annual/2010/f/ARM_resources_reserves_2010.pdf

ResID: 280 DepID: 1 Subpart: Karu East

Resource Category: inferred Resource Standard:

Year(s): 2010 ASCu grade: Ag grade:

Ore (mt): 5,500,000 Cu grade: 1.8 Cu amount: Co amount:

ASCu amount: Ag amount:

Cu equivalent: Au grade:

Cu cutoff: Au amount:

Reference Page: 10 (p. 29)

Ref: Resources Reference

10 African Rainbow Minerals, 2010, Mineral resources and reserves 2010: African Rainbow Minerals, 31 p., accessed May 13, 2011, at http://www.arm.co.za/im/files/annual/2010/f/ARM_resources_reserves_2010.pdf

Record: 1 of 1 No Filter Search

Record: 1 of 124 No Filter Search

Figure A21. Deposit entry form, 1_Deposittbl1_frm, opens when "Open Data Entry Form" button is selected from switchboard.

1_Deposittbl1_frm

Group Name: Karu East

Deposit Name: Karu East

Property: Karu East

Latitude: -11.6277 Longitude: 27.2764

Country: Democratic Republic of the Congo

Province: Katanga

DepID	Ore(mt)	Cu(pct)	Co(pct)
1	5,500,000	1.80	

Other Names:

Includes:

Site Activity: exploration ☐ Production ☐

Deposit Type: Sediment-hosted stratabound copper deposit DepositSubtype: Reduced-facies, carbonate ecaille

Deposit Reference:

10 African Rainbow Minerals, 2010, Mineral resources and reserves 2010: African Rainbow Minerals, 31 p., accessed May 13, 2011, at http://www.arm.co.za/im/files/annual/2010/f/ARM_resources_reserves_2010.i

Record: 1 of 124

Figure A22. Upper part of data entry form, 1_Deposit_frm. (Window was resized by dragging the lower right corner upwards to hide lower part of the form but still retain the record count in the bottom of the frame. Note the record number circled in red at the lower left and DepID circled in green at upper right.)

2_Resourcestbl1_frm

ResID: 210 DepID: 33 Subpart: Musoshi

Resource Category: reserve Resource Standard:

Year(s): 1996 ASCu grade: Ag grade:

Ore (mt): 111,900,000 Cu grade: 2.11 Co grade: ASCu amount: Ag amount:

Cu equivalent: Au grade:

Cu amount: Co amount: Cu cutoff: Au amount:

Reference Page: 77, 82

Resources Reference:

77 Kirkham, Rodney, and Broughton, David, 2005, Appendix, Supplement to the sediment-hosted stratiform copper ore system, in J.W. Hedenquist, J.W., J.F.H. Thompson, J.F.H., Goldfarb, R., J.P. Richards, J.P., eds., Economic Geology 100th Anniversary Volume, 1905-2005: Littleton, Colorado, Society of Economic Geologists, p. 609-642.

Record: 210 of 314

Figure A23. Lower part of the main 1_Deposittbl1_frm is 2_Resourcestbl1_frm (treated like a subform). (Note the record number circled at the lower left.)

1_Deposittbl1_frm

Group Name: Konkola-Musoshi DepID: 79 MRDS: 10207788

Deposit Name: Konkola Property: Konkola/Mushoshi

Latitude: -12.3449 Longitude: 27.7978

Country: Zambia Province: Copperbelt

DepID	Ore(mt)	Cu(pct)	Co(pct)
79	662,874,267	3.03	

Other Names: Bancroft, Kirila Bombwe(?)

Includes: Musoshi in Shaba Prov., Konkola North, Konkola Deep, Konkola (KCM), Kirila Bombwe orebodies North and South, Saddle Lode, Kakc

Site Activity: active Production: ☒

Deposit Type: Sediment-hosted stratabound copper deposit DepositSubtype: Reduced-facies, ore shale

Ref: Deposit Reference

9 Porter GeoConsultancy, 2010, A global database of the World's important mineral deposits: Porter Geoconsultancy Web page accessed October, 2010, at <http://www.portergeo.com.au/database/index.asp>

ResID: 14 DepID: 79 Subpart:

Resource Category: production Resource Standard:

Year(s): 2005 ASCu grade: Ag grade:

Ore (mt): 3,452,341 Cu grade: 1.26 Co grade: ASCu amount: Ag amount:

Cu amount: 43,504 Co amount: Cu cutoff: Au amount:

Reference Page: 128 (p. 118)

Ref: Resources Reference

128 Vedanta Resources plc, 2005, Annual Report 2005: London, U.K., Vedanta Resources plc, 127 accessed May 26, 2011 at <http://www.vedantaresources.com/uploads/annual20report202005.pdf>

Record: 1 of 19

Record: 79 of 124

Figure A24. Record for the Konkola Deposit showing 19 resource subrecords (red circle), all of which are combined to compute the endowment (pink outline). (Scroll bar to view additional Deposit References is circled in blue.)

How do I navigate through the deposit table form?

Navigation through the 1_DepositTbl_frm (figs. A15, A21, A24) can be done by using the tab key or a mouse. The tab order is left to right, top to bottom. Dropdown menus in selected fields provide a list of acceptable terms. To search on any field, simply click the cursor in the field, use Edit/Find on the upper tool bar (or Ctrl F), and type what it is you wish to find (not case sensitive). To jump to another record or subrecord, use the Record number field or arrows on the lower right. If more references are available than fit on the screen, a scroll bar will appear on the far right edge of the References part of the form. Simply drag the scroll bar, or use the Page Up or Page Down button on the keyboard. This database works the same way as most other databases. (And as long as the database is set “Read-only” you can’t accidentally mess it up.)

How do I find a record for a particular site or all the sites for a particular property?

The form can be “filtered” to view specific information. In Access 2000 - 2003, from the menu select Records/Filter/Filter By Form. (In Access 2010, the Filter By Form command is found under the Home tab, in Sort & Filter, Advanced). Type the information you want to filter in the appropriate box. Wildcards are permitted by starting the filter term with “like” followed by the term and wildcard characters (asterisk * for multiple characters, question mark ? for single characters) all in quotes (for example, in the Deposit Name box the string [like “bal*”] (without the brackets) will find the Baluba deposit record). Access is not case sensitive.

How do I print the data for all the deposits, a set of deposits, or a specific deposit?

All the records can be printed from the 1_DepositTbl form. Open the form and select File/Print/All. The fields will expand, if necessary, so that all the resource records and references will print. Printing to Adobe PDF printer, if available, will create an easily searchable PDF document (for example, the PDF file Data Entry Form.pdf included with this report). The form is designed to print records on a letter size, portrait view page. The pages will break on individual records. In some cases, multiple pages are necessary to print one record.

To print a subset of records, run a filter (see FAQ 3, above) and select File/Print/All. This will print only the filtered results. To print only one record, make sure that is the record you are viewing, then select File/Print/Selected Record(s). Printing has been tested only with two HP printers

and an Adobe PDF printer: there are no guarantees that this will work with all printers.

Why doesn't the form look the way I expect it to look?

Most of the forms are meant to be used on other forms, not by themselves. It is possible for the user to open any form and make changes in the size of that form (in design view mode). If this happens and you save the changes, that form might then be larger than the space reserved on the form that it was designed to be embedded in and may not display or print correctly. The main form is designed to allow the user to print records on 8.5 × 11 paper (with only 0.5 in. margins right and left and 1 in. top and bottom) and a change, especially if the subform is wider, may cause a partial print page for any part of the form that is wider than maximum width allowed by the printer. Every printer is different. Check that the output for only one record is acceptable before attempting to print many records.

What do I need to do to update a record?

Any record may be updated or changed if the file is not set for “read only”. Values for DepID, ResID, and RefNo are automatically assigned when data is entered into the tables (or forms) 1_DepositTbl, 2_ResourceTbl, or 3_ReferenceTbl, respectively; therefore, these fields cannot be edited. Most fields can be modified or updated directly on the 1_DepositTbl_frm. New records can be added using the data entry form, but it is preferable to revise existing records. Records should be deleted through the tables, not from the forms, because cascading deletes are set for any record in 1_DepositTbl so as to remove associated 2_ResourceTbl records. Do not keep any resource records that you do not want, because statistics are computed assuming that all resource records are necessary and correct.

Acknowledgments

The authors are grateful to our colleagues in academia and industry to encouraging us to prepare this compilation, directing us to relevant information, and sharing unpublished data with us. In particular, we acknowledge David Broughton (Ivanplats Limited), Murray W. Hitzman (Colorado School of Mines), and Jonathan Woodhead (Colorado School of Mines).

Jane Hammarstrom of the USGS in Reston provided comments on an early version of this report. USGS colleagues Daniel Mosier, James Bliss, and Pamela Dunlap, with the USGS, provided helpful and timely technical reviews of the final report.

References Cited

- Cox, D.P., Lindsay, D.A., Singer, D.A., Moring, B.C., and Diggles, M.F., 2003, revised 2007, Sediment-hosted copper deposits of the world—Deposit models and database: U.S. Geological Survey Open-File Report 03-107, v. 1.3, 53 p. (Also available at <http://pubs.usgs.gov/of/2003/of03-107/>.)
- Fortin, Paul, 2006, Gécamine future prospects: accessed 9 February, 2010, at <http://www.canaccordadams.com/NR/rdonlyres/AA6A5FD-19EA-4A36-8D2D-A217ECC2C2D7/0/Gecaminespresnetation.pdf>, 32 p.
- Freeman, P.V., comp., 1988, Description of mineral deposits on the Copperbelt (and Kabwe, Nampundwe): Lukasa, Zambia, [Consolidated Copper Mines Ltd. (ZCCM) unpublished company report], 88 p.
- Kirkham, R.V., Carriere, J.J., Laramée, R.M., and Garson, D.F., 1994, Global distribution of sediment-hosted stratiform copper deposits and occurrences: Geological Survey of Canada Open File 2915b, 256 p.
- Kirkham, Rodney, and Broughton, David, 2005, Supplement to the sediment-hosted stratiform copper ore system, *in* Hedenquist, J.W., Thompson, J.F.H., Goldfarb, R.J., and Richards, J.P., eds., Economic Geology—One hundredth anniversary volume 1905-2005: Littleton, Colorado, Society of Economic Geologists, Inc., p. 609–642.

Appendix B. Spatial Databases for Sediment-Hosted Stratabound and Structurally Controlled Replacement and Vein Copper Deposits and Prospects, Central African Copperbelt, Democratic Republic of the Congo and Zambia

By Heather L. Parks, J. Douglas Causey, Paul D. Denning, Timothy S. Hayes, John D. Horton, Michael J. Kirschbaum, Cliff D. Taylor, Anna B. Wilson, Niki E. Wintzer, and Michael L. Zientek

Introduction

Databases and maps of the location, size, and geologic type of known mineral deposits and occurrences are essential components of mineral resource assessment studies. Three spatial databases provide data for use in an assessment of undiscovered sediment-hosted copper resources in the Central African Copperbelt (CACB) in the Democratic Republic of the Congo (DRC) and Zambia. The CACB is a large ore-system that formed sediment-hosted stratabound and structurally controlled replacement and vein (SCRV) copper deposits. Aboriginal cultures produced copper from this region as early as the 7th century; European companies started producing copper in the early 1900s.

The spatial databases are presented as Esri shapefiles, which contain spatial and descriptive data for deposits and prospects, ore bodies, and open pits. These databases can be queried in a geographic information system (GIS) to portray the distribution, geologic setting, and resource potential of copper deposits and to model grade and resource tonnage in the region. Examples of maps that can be created from the three shapefiles are shown on figures B1, B2, and B3.

Overview of Spatial Databases

The spatial databases are briefly described in table B1. They are provided in vector format as Esri shapefiles and packaged with a look up table for unit descriptions, a meta-data file, list of references cited, and a brief descriptive ASCII text file in the compressed archive file `sir2010-5090j_GIS.zip` which is available on the Internet at <http://pubs.usgs.gov/sir/2010/5090/j/>.

Deposits and Prospects

The spatial database for deposits and prospects, `CACB_deposits_prospects`, is an Esri point shapefile that contains spatial and descriptive data for 529 deposits and prospects and 21 group sites which represent sediment-hosted copper

and structurally controlled replacement and vein deposits and prospects in the CACB. It provides locations of deposits and prospects, in addition to descriptive information for use in a GIS and for estimating undiscovered mineral resource endowments.

The dataset was created, in part, from pre-existing compilations, reports, and maps of copper deposits and prospects. Descriptive data from digital files were normalized and combined into a single shapefile; data for sites with multiple records then were resolved to provide a single record for each site. Information for tonnage and grade were derived from the Microsoft Access® database `CACB_sedCu_deposits.mdb` (see appendix A). Group sites were created to represent multiple sites that have been grouped together using a 500-meter aggregation distance for the purposes of grade and tonnage modeling. These sites can be identified using the “SiteStatus” field in the attribute table. Examples of group sites are shown in figures B1 and B3.

The positional accuracy of the location for each site was checked against mineral occurrence maps and figures from reports. Locations of many sites were derived from coordinates provided in reports and databases; some were manually digitized from figures and maps in reports. Deposit and prospect locations were corrected using the highest resolution data available. For example, a 1:100,000-scale map took precedence over a 1:1,000,000-scale map for the site location. Some locations of developed sites were compared against mines visible on satellite imagery on Google Earth¹ and were shifted accordingly. The maps and satellite images used different datums; we converted all reference material to the same datum (WGS, 1984) when we corrected locations.

We investigated a variety of data: published and unpublished, open access and licensed, public and proprietary. Sites that could not be verified using publicly available data were excluded from the compilation. Examples of the types of

¹<http://www.google.com/earth/index.html>.

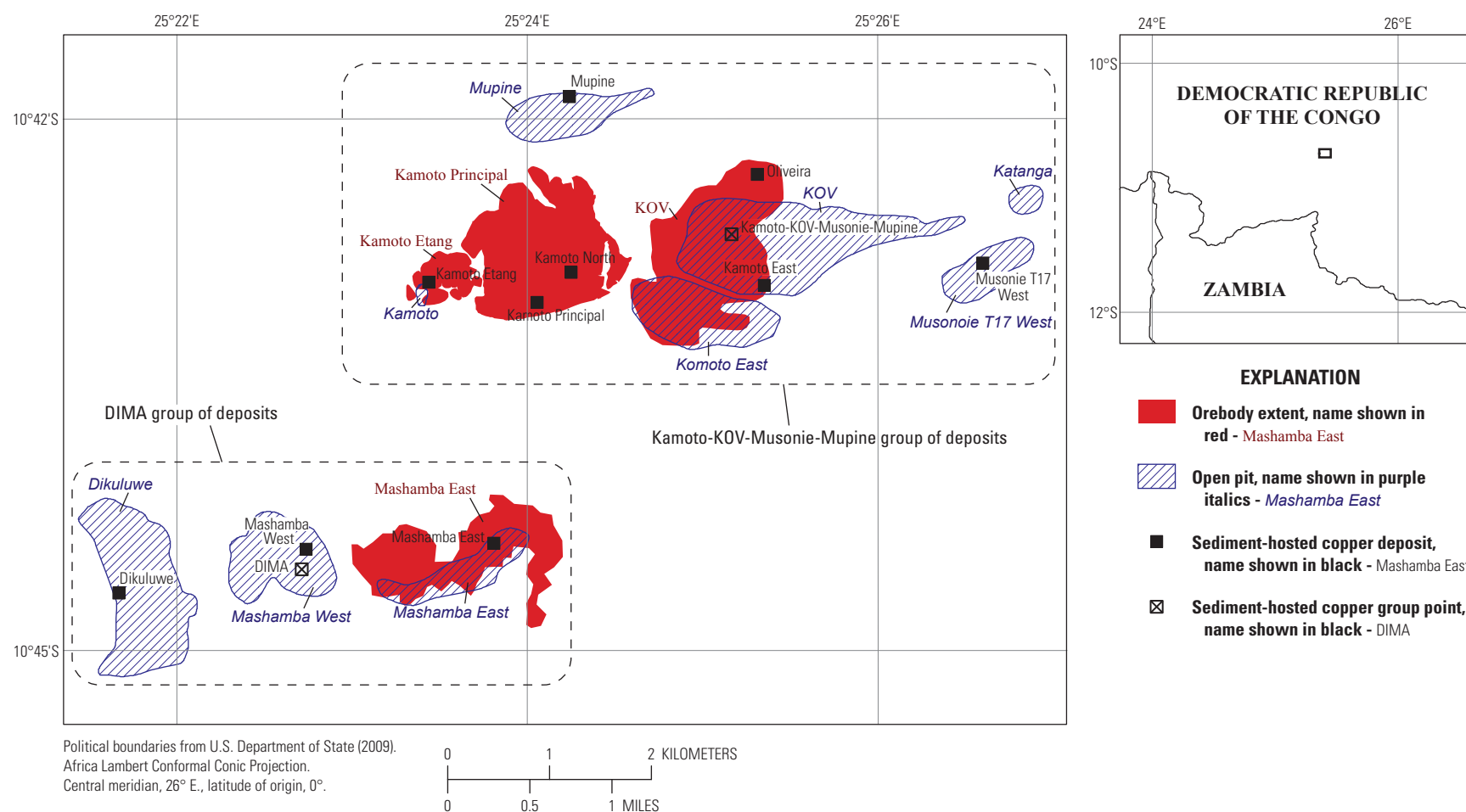


Table B1. Map showing points for deposits, points for grouped deposits, the areal extent of ore bodies, and open pits in the northwestern part of the Central African Copperbelt in the Democratic Republic of the Congo (ore body outlines modified from Dixon and others, 2009). Dashed boxes show the clusters of deposits that are grouped for tonnage and grade modeling.

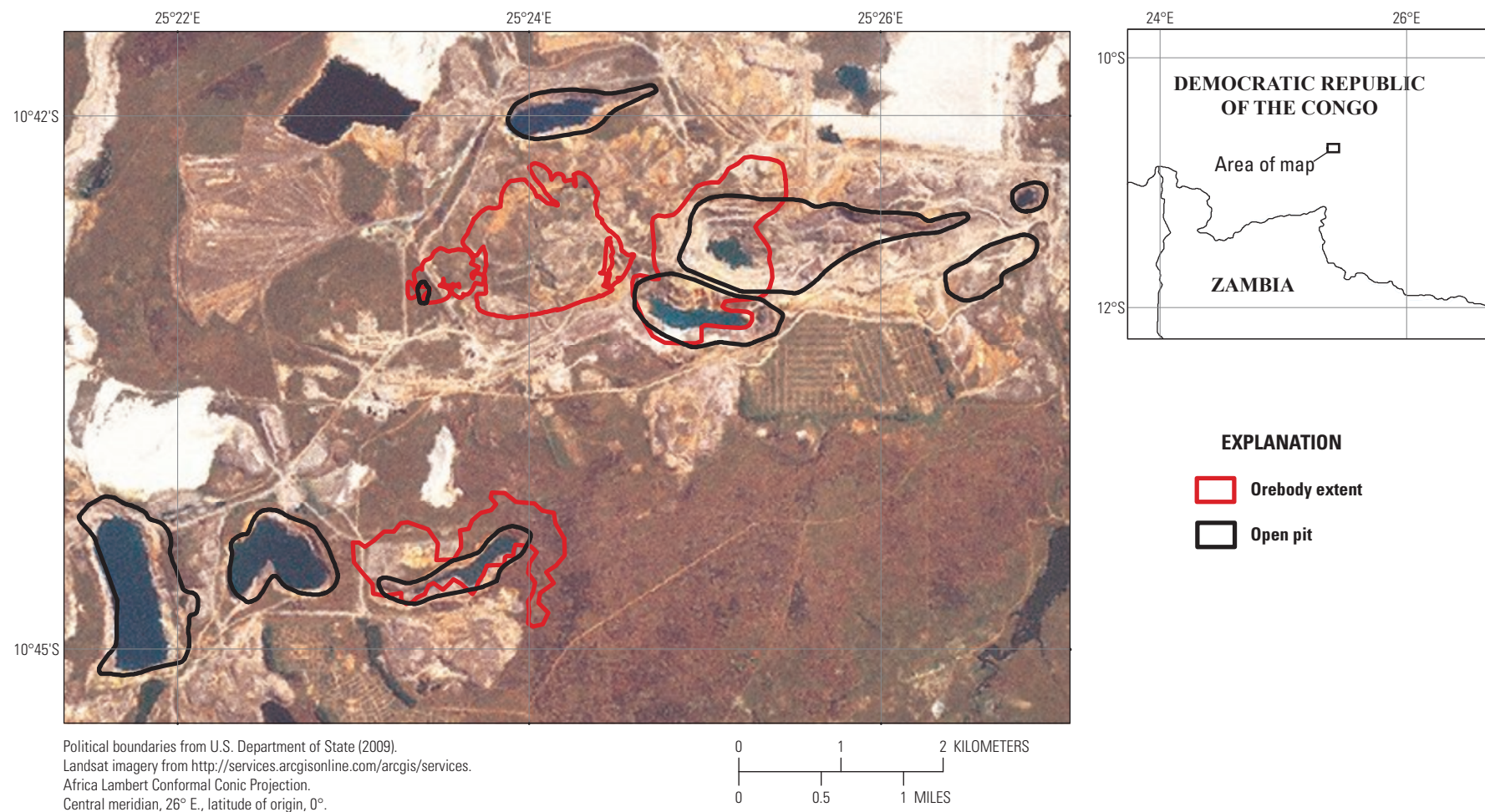


Table B2. Landsat image showing the areal extent of ore bodies and open pits in the northwestern part of the Central African Copperbelt in the Democratic Republic of the Congo (ore body outlines modified from Dixon and others, 2009).

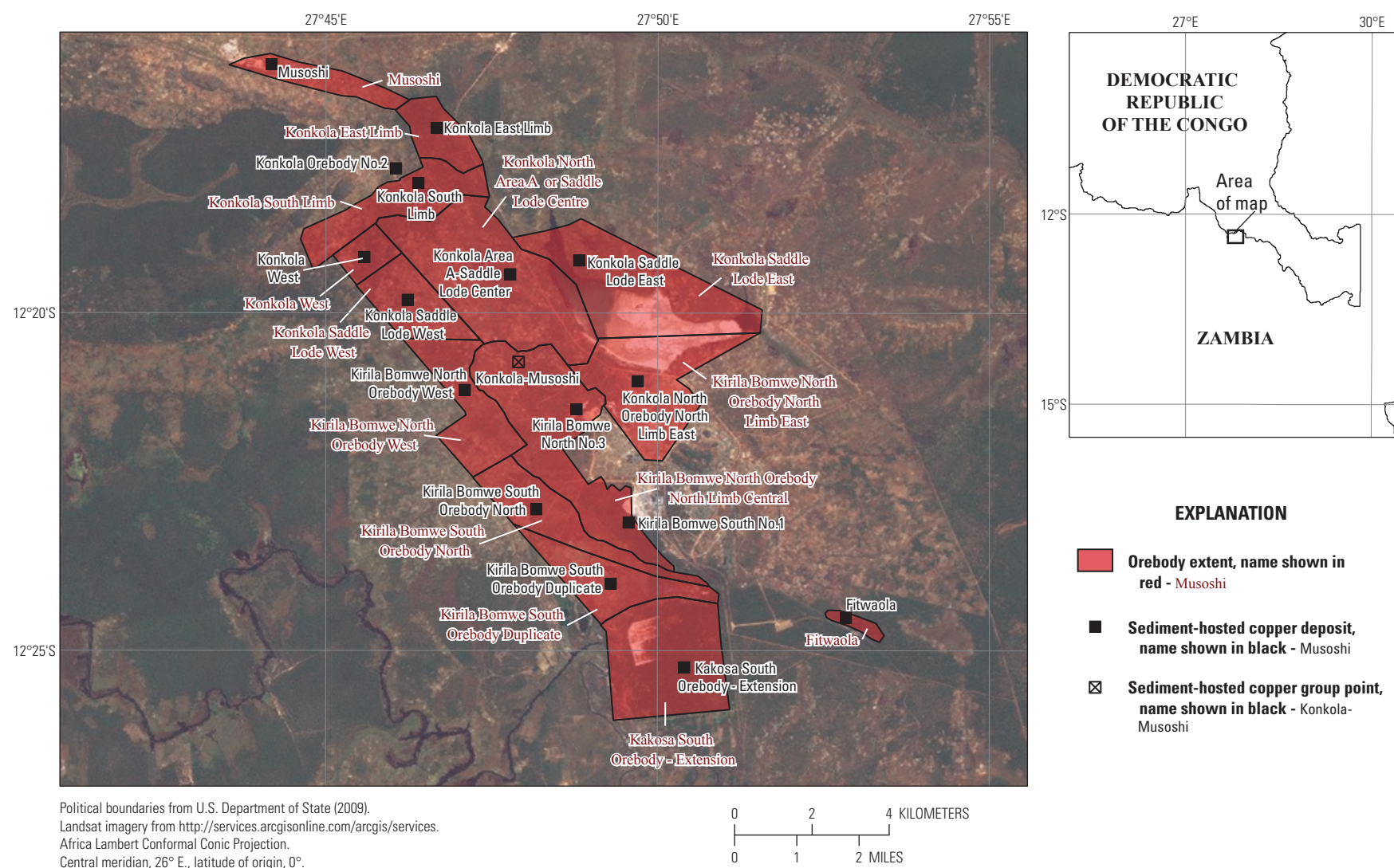


Table B3. Landsat image showing deposits, grouped deposit, and areal extent of ore bodies for the Konkola-Mutushi area in the Central African Copperbelt in the Democratic Republic of the Congo and Zambia (ore body outlines modified from Wolf, 1976; Chileshe and Kulkarni, 1992; and Simposya and Hart, 2008).

Table B1. Description of digital data files for spatial databases (geographic information systems, GIS).

File Name	File Description
Compressed archive file containing spatial databases, associated metadata files, references, and readme.txt	
sir2010-5090j_GIS.zip	GIS and associated files: Esri shapefiles, metadata (*.xml), references (*.xlsx, and *.txt), and readme.txt (ASCII text).
Esri shapefiles	
CACB_deposits_prospects.shp	Sediment-hosted (stratabound and SCRv) Cu deposits and prospects.
CACB_open_pits.shp	Sediment-hosted Cu deposit open pits.
CACB_orebodies.shp	Sediment-hosted Cu deposit ore bodies.
Relational table	
Unit_look_up_table.xlsx	Table with unit names and descriptions that can be joined to the Unit field in the shapefile CACB_deposits_prospects.shp.
Metadata –eXtensible markup language (XML) format (*.xml) files	
CACB_deposits_prospects_metadata.xml	Metadata for shapefile of deposits and prospects.
CACB_open_pits_metadata.xml	Metadata for shapefile of open pits.
CACB_orebodies_metadata.xml	Metadata for shapefile of ore bodies.
List of full references	
GIS references.txt	List of short references used in shapefiles and complete references.
GIS references.xlsx	Table listing short references used in shapefiles and complete references.

information used are summarized in table B2; a complete list of sources used can be found in the references file provided with the databases.

Table B3 lists the fields in the database and the information contained in each. The site name (listed in the field “Name”) is based upon the most frequent usage in publicly available sources. Codes in the field “Unit” are based on Cailteux and others (2007) correlation of units in Zambia and the Democratic Republic of the Congo. A look up table has been included and can be joined with the “Unit” field in a GIS to obtain definitions of the unit codes. Table B4 shows the Katangan Supergroup stratigraphic unit lithologic descriptions and the correlation between Zambian and DRC units.

Ore Bodies

The spatial database for copper ore bodies, CACB_orebodies, is an Esri polygon shapefile that contains spatial and descriptive information for 101 polygons representing 95 copper deposits hosted in sedimentary rocks which have been defined by exploration. Its purpose is to document the areal extent (as projected to the surface) of known ore bodies in the Central African Copperbelt and to constrain estimates of mineral resource endowment for the region. The extents of several ore bodies are shown in plan view in figures B1, B2, and B3.

Areal extents of ore bodies were manually digitized from plan-view maps that were georeferenced for use in a GIS. The shape of an ore body can reflect geologic contacts, economic cutoff limits, and (or) property boundaries. Table B5 lists the fields in the database and the information contained in each. Ore bodies were given the name of the deposit to which it belonged.

Open-Pit Mines

The spatial database for open pits, CACB_open_pits, is an Esri polygon shapefile that contains spatial and descriptive information for 85 polygons representing 76 open-pit mines of sediment-hosted copper deposits in the CACB. It provides the areal extent of open pit mining and was designed for use in mineral assessments to constrain estimates of mineral resource endowment. The extents of several open pits are shown in plan view in figures B1 and B2.

Surface extents of open pits were manually digitized from Google Earth satellite imagery and the data were then imported into an Esri shapefile format. The open pits were given the same name as that of the corresponding mine seen in Google Earth or corresponding deposit or prospect. Table B6 lists the fields in the database and the information contained in each.

Table B2. Examples of the types of sources used to compile the CACB_deposits_prospects shapefile.

Data type	Citation
Information in the public domain	
Report	Guernsey (1952)
Report with map	François (1974)
Report with spatial database	Kirkham and others (1994)
Spatial databases	Cox and others (2003); Kirkham and others (2003); Huderek (2008a,b, 2010)
Licensed and proprietary information	
Proprietary minerals database	Infomine ¹ , Intierra ² , Metals Economic Group ³
Spatial databases	GeoPubs (1998); Veselinovic-Williams and Frost-Killian (2003); Chartry and Franceschi (2004); Zambia Geological Survey Department, written commun., 2006; Musée Royal de l'Afrique Centrale (2008); Laghmouch (2008b)
Unpublished minerals reports	Freeman (1988); Armand François, written commun., 1996

¹<http://www.infomine.com/>.²<http://www.intierra.com/Homepage.aspx>.³<http://www.metalseconomics.com/default.htm>.

Table B3. Definitions of user-defined fields in the attribute table for the shapefile CACB_deposits_prospects.

Field name	Description
Deposit_ID	Unique numeric identifier for site.
DepID	Numeric identifier which correlates to DepID in the data table 1_Deposittbl in the Microsoft Access database CACB_sedCu_deposits.mdb (see appendix A).
Group_name	Name for cluster of deposits which are grouped together (and for which resource data are aggregated) in order to describe and model grade and tonnage; correlates to GroupName in the data table 1_Deposittbl in the Microsoft Access database CACB_sedCu_deposits.mdb (see appendix A).
Name	Name of site.
Name_other	Other names used for the site.
Includes	Names of deposits that were grouped based on proximity (see use of the 500 meter rule in appendix A); list may overflow into the field “Includes2.”
Includes2	Continuation of list of names of deposits that were grouped based on proximity (see use of the 500 meter rule in appendix A).
Katangan	Entry identifies if site is located in the Katangan Supergroup or not; “yes” for hosted in the Katangan Supergroup, “no” for not located in Katangan Supergroup.
Type	Mineral deposit type.
Subtype	Sediment-hosted copper subtype.
SiteStatus	Status of site; prospect – grade and tonnage values are not provided, deposit – grade and tonnage values are provided, and group – represents multiple deposits within 500 m of each other that have been grouped together due to 500 meter aggregation rule.
Latitude	Latitude in decimal degrees, –90.00000 to 90.00000. Negative south of the equator.
Longitude	Longitude in decimal degrees, –180.00000 to 180.00000. Negative west of the Greenwich meridian.
Country	Country in which the site is located.
State_Prov	State or province in which the site is located.
Age_range	Age of host rock in standard divisions of geologic time.
Comm_major	Major commodities in decreasing order of economic importance.
Tonnage_Mt	Ore tonnage in millions of metric tons; zero indicates no data.
Cu_pct	Average copper grade in weight percent; zero indicates no data.
Co_pct	Average cobalt grade in weight percent; zero indicates no data.
Con_Cu_t	Contained copper in million metric tons; zero indicates no data.
Comments	Miscellaneous comments.
HostRocks	Simplified lithologic description of host rocks.
Unit	Geologic map unit label in which site is located; see table 3 for detailed information relating label to rock unit description.
Footwall	Lithology of footwall rocks.
Hangwall	Lithology of hangingwall rocks.
Mineralogy	Ore and gangue minerals in approximate order of abundance.
Ref_short	Short reference; abbreviated citation for reference; full reference is provided in references file.
Tctnic_set	Tectonic setting; entry describes the type of associated structural feature.
Complex	Tectonic complex; name of the associated structural feature.

Table B4. Description of Katangan lithologies used in the “Unit” field (modified from Cailteux and others, 2007).

[Note: Descriptions of units younger and older than the Katangan Supergroup are not included in this table]

SUPER-GROUP	GROUP	SUBGROUP	FORMATION	LITHOLOGY			
Katangan	Kundelungu – Ku (formerly Upper Kundelungu - Ks)	Biano - Ku 3		arkoses, conglomerates, argillaceous sandstones			
		Ngule - Ku 2	Sampwe - Ku 2.3	dolomitic pelites, argillaceous to sandy siltstones			
			Kiubo - Ku 2.2	dolomitic sandstones, siltstones and pelites			
			Mongwe - Ku 2.1	dolomitic pelites, siltstones and sandstones			
			Lubudi - Ku 1.4	pink oolitic limestone and sandy carbonate beds			
		Gombela - Ku 1	Kanianga - Ku 1.3	carbonate siltstones and shales			
			Lusele - Ku 1.2	pink to grey micritic dolomite			
			Kyandamu - Ku 1.1	Petit Conglomérat (glacial diamictite)			
	Nguba – Ng (formerly Lower Kundelungu - Ki)	Bunkeya - Ng 2	Monwezi - Ng 2.2	dolomitic sandstones, siltstones and pelites			
			Katete - Ng 2.1	dolomitic sandstones, siltstones and shales in northern areas; alternating shale and dolomite beds (“Série Récurrente”) in southern areas			
		Muombe - Ng 1	Kipushi - Ng 1.4	dolomite with dolomitic shale beds in southern areas			
			Kakontwe - Ng 1.3	carbonates; Zn-Cu-Pb			
			Kaponda - Ng 1.2	carbonate shales and siltstones; “Dolomie Tigrée” at the base			
			Mwale - Ng 1.1	Grand Conglomérat (glacial diamictite)			
	CONGO				ZAMBIA		
	GROUP	SUBGROUP	FORMATION	LITHOLOGY	LITHOLOGY	FORMATION	SUBGROUP
	Roan R	Mwashya (formerly Upper Mwashya) - R4	Kanzadi - R 4.3	sandstones or alternating siltstones and shales	dolomitic shales, grey to black carbonaceous shales, quartzites		Mwashia Mw 1.1
			Kafubu - R 4.2	carbonaceous shales			
			Kamoya - R 4.1	dolomitic shales, siltstones, sandstones, including conglomeratic beds and cherts in variable position			
		Dipeta - R 3	Kansuki - R 3.4	(formerly Lower Mwashya): dolomites including volcaniclastic beds; Cu-Co	dolomites to arenitic dolomites interbedded with dolomitic shales; intrusive gabbros (formerly Carbonate Unit or Upper Roan)	Bancroft Kanwangungu RU 1 and RU 2	Kirilabombwe
			Mofya - R 3.3	dolomites, arenitic dolomites, dolomitic siltstones			
			R 3.2	argillaceous dolomitic siltstones with interbedded sandstone or white dolomite; intrusive gabbros			
				R.G.S. - R 3.1			
		Mines - R 2	Kambove - R 2.3	stromatolitic, laminated, shaly or talcose dolomites; locally sandstone at the base; interbedded siltstones in the upper part; Cu-Co	dolomite, argillite beds at top	Chingola RL 4	Kitwe
			Dolomitic shales - R 2.2	R 2.2.2 and 3: dolomitic shales containing carbonaceous horizons; occasional dolomite or arkose	arkoses, sandy to dolomitic argillites	Pelito-arkosic RL 5	
				R 2.2.1: arenitic dolomite at the top and dolomitic shale at the base; pseudomorphs after evaporite nodules and concretions; Cu-Co	arenites, argillaceous dolomites, argillites, dolomites, evaporites; Cu-Co	Ore Shale RL 6	
			Kamoto - R 2.1	stromatolitic dolomite (R.S.C.), silicified/arenitic dolomites (R.S.F./D.Strat.), grey argillaceous dolomitic siltstone at the base (Grey R.A.T.); pseudomorphs after evaporites at the contact with RAT.; Cu-Co			
		R.A.T. - R 1	red argillaceous dolomitic siltstones, sandstones and pelites (“Roches Argilo-Talqueuses”)		conglomerates, coarse arkoses and argillaceous siltstones	Mutonda	Mindola - RL 7
		base of the R.A.T. sequence - unknown			quartzites	Kafufya	
		< 900 Ma basal pebble and cobble conglomerate				pebble and cobble conglomerate	Chimfunsi
	± 2,050 Ma KIBARAN and PRE-KIBARAN						

Table B5. Definitions of user-defined attribute fields in the shapefile CACB_orebodies.shp.

Field name	Description
Orebody_ID	Unique numeric identifier for ore body.
Name	Name of deposit to which ore body belongs; correlates to Name in the shapefile CACB_deposits_prospects and to Name in the shapefile CACB_open_pits. (Multiple ore bodies can exist for one deposit.)
DepID	Numeric identifier which correlate to DepID in the data table 1_Deposittbl in the Microsoft Access database CACB_sedCu_deposits.mdb (see appendix A).
Group_name	Name of group to which ore body belongs. Groups represent clusters of deposits which are grouped together (and for which resource data are aggregated) in order to describe and model grade and tonnage; correlates to GroupName in the data table 1_Deposittbl in the Microsoft Access database CACB_sedCu_deposits.mdb (see appendix A).
Area_km2	Area of the areal extent (as projected to the surface) of the ore body, in square kilometers.
Ref_short	Short reference; abbreviated citation for reference; full reference is provided in references file.

Table B6. Definitions of user-defined attribute fields in the shapefile CACB_open_pits.shp.

Field name	Description
OpenPit_ID	Unique numeric identifier for open pit.
Name	Name of deposit to which open pit belongs; correlates to Name in the shapefile CACB_deposits_prospects and to Name in the shapefile CACB_orebodies.
DepID	Numeric identifier which correlate to DepID in the data table 1_Deposittbl in the Microsoft Access database CACB_sedCu_deposits.mdb (see appendix A).
Group_name	Name of group to which open pit belongs. Groups represent clusters of deposits which are grouped together (and for which resource data are aggregated) in order to describe and model grade and tonnage; correlates to GroupName in the data table 1_Deposittbl in the Microsoft Access database CACB_sedCu_deposits.mdb (see appendix A).
Area_km2	Area of open pit, in square kilometers.
Ref_short	Short reference; abbreviated citation for reference; full reference is provided in references file.

Acknowledgments

The authors are grateful for helpful and constructive technical reviews provided by USGS colleagues James Bliss, Pamela Dunlap, and Daniel Mosier.

References Cited

- Cailteux, J.L.H., Kampunzu, A.B., and Lerouge, C., 2007, The Neoproterozoic Mwashya-Kansuki sedimentary rock succession in the Central African Copperbelt, its Cu-Co mineralization, and regional correlations: *Gondwana Research*, v. 11, no. 3, p. 414–431.
- Chartry, G., and Franceschi, G., comps., 2004, Mineral occurrences database and GIS map of the Democratic Republic of [the] Congo: Royal Museum for Central Africa, scale 1:2,000,000, CD-ROM.
- Chileshe, B.C., and Kulkarni, R.V., 1992, Konkola Deep mining project—Concept and planning: *Mine Water and the Environment*, v. 11, no. 3, p. 1–15.
- Cox, D.P., Lindsey, D.A., Singer, D.A., and Diggles, M.F., 2003, revised 2007, Sediment-hosted copper deposits of the world—Deposit models and database: U.S. Geological Survey Open-File Report 03–107 version 1.1, 50 p. (Also available online at <http://pubs.usgs.gov/of/2003/of03-107/>.)
- Dixon, Roger, Simposya, Victor, Takolia, Ebrahim, Waldeck, Wally, Salter, Henrietta, von Wielligh, Anton, Naismith, Alan, Cilliers, Petrus, and McNeill, R., 2009, An independent technical report on the material assets of Katanga Mining Limited, Katanga Province, Democratic Republic of Congo (“DRC”): SRK Consulting Technical Report, prepared for Katanga Mining Ltd., March 17, 2009, 216 p. (Also available at <http://www.sedar.com>.)
- François, Armand, 1974, Stratigraphie, tectonique et minéralisations dans l’arc cuprifère du Shaba (République du Zaïre) [Stratigraphy, tectonics and mineralizations in the Shaba copper-bearing arc (Republic of Zaire)] in Bartholomé, Paul, ed., *Gisements stratiformes et provinces cuprifères* [Stratiform deposits and cupriferous provinces]: Liège, Belgium, La Société Géologique de Belgique, p. 79–101.
- Freeman, P.V., comp., 1988, Description of mineral deposits on the Copperbelt (and Kabwe, Nampundwe): Lukasa, Zambia, [Consolidated Copper Mines Ltd. (ZCCM) unpublished company report], 88 p.
- GeoPubs, 1998, Geological dataset of the Central African Copperbelt: Essex, England, GeoPubs [dataset purchased from <http://www.geopubs.co.uk/home.htm> and downloaded on December 16, 2009].
- Guernsey, T.D., 1952, A prospector’s guide to mineral occurrences in Northern Rhodesia: Salisbury, Charter House, 91 p.
- Huderek, Richard, 2008a, Katangan Copperbelt: Google Earth KML file, accessed July–September 2009 and October 2010, at <http://maps.google.com/maps/ms?ie=UTF8&hl=nl&oe=UTF8&msa=0&msid=118078989952556264569.00044e1e24afa04af0cca&output=kml>.
- Huderek, Richard, 2008b, *Zambian_copperbelt.kml*: Google Earth KML file, accessed July 8, 2009, and October 2010, at <http://maps.google.com/maps/ms?hl=en&gl=us&ie=UTF8&oe=UTF8&msa=0&msid=118078989952556264569.000451715e9f065a35bbe&output=kml>.
- Huderek, Richard, 2010, *Katangan copperbelt.kml*: Google Earth KML file, accessed July 6, 2011, at <http://maps.google.nl/maps/ms?ie=UTF8&oe=UTF8&msa=0&msid=118078989952556264569.00044e1e24afa04af0cca&output=kml>.
- Kirkham, R.V., Carrière, J.J., and Rafer, A.B. comp., 2003, World distribution of sediment-hosted, stratiform copper deposits and occurrences: Geological Survey of Canada, unpublished, accessed Sept 26, 2009, at http://apps1.gdr.nrcan.gc.ca/gsc_minerals/index.phtml?language=en-CA.
- Kirkham, R.V., Carrière, J.J., Laramée, R.M., and Garson, D.F., 1994, Global distribution of sediment-hosted stratiform copper deposits and occurrences: Geological Survey of Canada Open File 2915b, 256 p.
- Laghmouch, M., comp., 2008, *L’Arc cuprifère du Katanga: géologie et minéralisations* (2007)—GIS and raster [Katanga copper arc - geology and mineralization]: Tervuren, Belgium, Royal Museum of Central Africa, scale 1:500,000, CD-ROM.
- Musée Royal de l’Afrique Centrale, 2008, Carte géologique de la République Démocratique du Congo, Région de Kolwezi-Kalukundi-Likasi, Parties occidentale et centrale de l’arc cuprifère du Katanga [Geological map of the Democratic Republic of Congo, Kolwezi Region-Kalukundi-Likasi Parties of Western and Central Katanga Copper Arc]: Tervuren [Belgium], Musée Royal de l’Afrique Centrale, scale 1:200,000, CD-ROM.
- Simposya, V.M., and Hart, P.C.L., 2008, Technical report on the mineral resources for the Konkola North Copper project, Chililabombwe, Zambia: SRK Consulting Project Number 384408, prepared for TEAL Exploration and Mining Co., March 2008, 78 p. (Also available at <http://www.sedar.com>.)
- U.S. Department of State, 2009, Small-scale digital international land boundaries (SSIB)—Lines, edition 10: Boundaries and Sovereignty Encyclopedia (B.A.S.E.), U.S. Department of State, Office of the Geographer and Global Issues.
- Veselinovic-Williams, M., and Frost-Killian, S., 2003 [2007], Digital international metallogenic map of Africa: Council for Geoscience, South Africa and Commission for the Geological Map of the World, scale 1:5,000,000, CD-ROM.
- Wolf, K.H., ed., 1976, Handbook of strata-bound and stratiform ore deposits: Amsterdam, Elsevier, 585 p.

